Novel Group 6 Complexes of Cyclopentadienylidene Ylides

by

JOHN HUGH BROWNIE

A thesis submitted to the Department of Chemistry

in conformity with the requirements for

the degree of Doctor of Philosophy

Queen's University

Kingston, Ontario, Canada

September, 2007

Abstract

Methyldiphenylphosphonium cyclopentadienylide, $C_5H_4PMePh_2$ (**II**), has been synthesized and characterized spectroscopically and crystallographically, and has been found to exhibit properties consistent with the zwitterionic structure **IIb**. New group 6 complexes, $(\eta^5\text{-}C_5H_4PMePh_2)M(CO)_3$, have been synthesized and fully characterized. Comparisons of ν(CO) of these complexes with those of the isoelectronic $(\eta^6\text{-}C_6H_6)M(CO)_3$ and $[(\eta^5\text{-}C_5H_5)M(CO)_3]^-$ suggest that the electron donating ability of the ylide is between that of the cyclopentadienyl anion (Cp^-) and benzene, but closer to Cp^-. The electronic structures of **II** and of $(\eta^5\text{-}C_5H_4PMePh_2)Cr(CO)_3$ have been investigated using *ab initio* methodologies. Thermal and photochemical substitutions of the CO ligands of $(\eta^5\text{-}C_5H_4PMePh_2)M(CO)_3$ (M = Cr, Mo) by equimolar amounts of PMe_3 and PPh_3 were not observed, but the ylide is displaced photochemically from $(\eta^5\text{-}C_5H_4PMePh_2)Mo(CO)_3$ by excess PMe_3 to form *fac*-$Mo(CO)_3(PMe_3)_3$ while $(\eta^5\text{-}C_5H_4PMePh_2)Mo(CO)_3$ reacts with I_2 to form $[(\eta^5\text{-}C_5H_4PMePh_2)Mo(CO)_3I]I$.

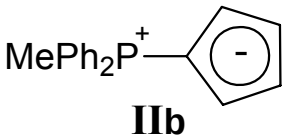

IIb

One electron oxidations of $(\eta^5\text{-}C_5H_4PMePh_2)M(CO)_3$ (M = Cr, Mo, W) have been performed to give the cationic radicals $[(\eta^5\text{-}C_5H_4PMePh_2)M(CO)_3]^+$, which undergo dimerization to give dicationic metal-metal bonded dimers $((\eta^5\text{-}C_5H_4PMePh_2)M(CO)_3)_2^{2+}$ in the solid state. These complexes have been fully characterized spectroscopically and crystallographically. It has been determined that the chromium dimer $((\eta^5\text{-}C_5H_4PMePh_2)Cr(CO)_3)_2^{2+}$ undergoes dissociation extensively in solution to the persistent radical cation monomer $(\eta^5\text{-}C_5H_4PMePh_2)Cr(CO)_3^+$, but that the heavier metal analogues

$((\eta^5\text{-}C_5H_4PMePh_2)M(CO)_3)_2^{2+}$ (M = Mo, W) dissociate very little, if at all. The Cr-Cr bond distance of the chromium complex is 3.3509(7) Å, which is the longest Cr-Cr bond distance known for a compound not containing some type of ligand bridging the metal-metal bond.

The hitherto unknown indenyl-derived ylide, $C_9H_6PMePh_2$, has been synthesized and characterized spectroscopically and crystallographically. The chromium tricarbonyl complex of this ligand, $(\eta^5\text{-}C_9H_6PMePh_2)Cr(CO)_3$, has been synthesized and characterized spectroscopically and crystallographically. This complex is a mixture of two isomers exhibiting planar chirality generated upon coordination of the ligand. This complex represents the first structurally characterized phosphorus non-cyclopentadienylide coordinated in an η^5 manner. The spectroscopic and crystallographic behaviour of $C_9H_6PMePh_2$ demonstrates that this ylide behaves much like the related cyclopentadienylides.

Acknowledgements

I would like to thank my supervisor, Professor Michael Baird for his discussions and advice throughout my time at Queen's University. Mike's passion for chemistry is contagious and has been a constant source of inspiration. In addition, as a supervisor Mike has taken our welfare as people, not just as graduate students, into account and due in part to this, I have deeply appreciated the time I have spent in his lab.

My girlfriend Lisa has helped me through the good times and the bad times of graduate school. Her constant love and support have helped me to complete my studies. Through all times of writing up she was there to help edit and to offer encouragement or a push to keep working. I am forever indebted to her.

Without my parents I would not have been able to undertake this journey. Their constant support and encouragement have helped to push me to become who I am today. At every turn of my life they have offered helpful advice that has helped to ease any obstacles in my way. Thank you.

Finally, I would like to thank all of the members of the Baird Group who have cohabitated the lab with me in the past and the present. The people of the Baird Lab have always been a 'stand-up' bunch that have made the time I spent at Queen's fun and enjoyable.

Claims To Originality

The work presented in this thesis is that of the author. The author, to the best of his knowledge, believes the work an original contribution to organometallic chemistry.

The original contributions include the synthesis and characterization of the various group 6 (Cr, Mo, W) complexes of the ligand, methyldiphenylphosphonium cyclopentadienylide ($C_5H_4PMePh_2$), first reported by Mathey *et al.* in the literature. The synthesis of this ligand is a modified procedure from that used by Mathey. The characterization of the compound was incompletely in the literature and this work corrects this deficiency.

In addition, the synthesis and characterization of the hitherto unknown ylide, methyldiphenylphosphonium indenylide was also completed. The chromium complex of this ligand, $(\eta^5\text{-}C_9H_6PMePh_2)Cr(CO)_3$, was synthesized and characterized and, to the author's knowledge, represents the first transition metal complex of an indenyl derived cyclopentadienylide phosphorus ylide.

Molecular orbital calculations on the ligand $C_5H_4PMePh_2$ and the complex $(\eta^5\text{-}C_5H_4PMePh_2)Cr(CO)_3$ were performed by Hartmut Schmider of The High Performance Computing Virtual Laboratory, Queen's University. Electrochemical studies on the complexes $(\eta^5\text{-}C_9H_6PMePh_2)M(CO)_3$ (M = Cr, Mo, W) were performed by Derek Laws under the supervision of Prof. William Geiger of the Department of Chemistry, University of Vermont. The synthesis and characterization (^1H, ^{13}C, ^{31}P NMR, VT NMR, 2D NMR, IR, X-ray structures, ESI-MS, elemental analysis and magnetic susceptibility) of these complexes was performed by the author. All crystal structure data was collected and solved by Ruiyao Wang of the Department of Chemistry, Queen's University.

Table of Contents

List of Tables

List of Figures

List of Abbreivations

Ar’	Substituted aryl
br	Broad
Bu	Butyl
Bz	Benzyl
°C	Degrees Celsius
d	Doublet
δ	Chemical shift
η	Hapticity
COD	1,5-cyclooctadiene
COSY	Correlation Spectroscopy
COT	cyclooctatetraene
dppm	bis(diphenylphosphino)methane
ESI-MS	Electrospray Ionization Mass Spectroscopy
Et	Ethyl
FT	Fourier Transform
Fv	Fulvalene
h	Hour
HMBC	Heteronuclear multiple bond coherence
HOMO	Highest occupied molecular orbital
HSQC	Heteronuclear single quantum coherence
i	iso
ind	indenyl (C_9H_7)
IR	Infrared
LUMO	Lowest unoccupied molecular orbital
m	Multiplet (NMR), medium (IR)
m	meta
Me	Methyl
mg	milligram
min	minute
mmol	millimole
μmol	micromole
mL	millilitre
NMR	Nuclear Magnetic Resonance
NOESY	Nuclear overhauser effect spectroscopy
p	Para
Ph	Phenyl
Pr	Propyl
ppm	Parts per million
o	ortho
R	Alkyl substituent
s	Singlet (NMR), strong (IR)
sh	shoulder
t	Triplet

t	Tert
THF	Tetrahydrofuran (C_4H_8O)
Trityl	Triphenylmethyl
vs	Very strong
VT	Variable Temperature
vw	Very weak
w	Weak

1. Introduction

1.1 The Ramirez Ylide

Triphenylphosphonium cyclopentadienylide (cyclopentadienylidene triphenylphosphorane) (**I**) (Figure 1-1) was first reported in 1956 by Ramirez and Levy[1] who also explored its chemistry.[2-6] They found *inter alia* that **I** is unusually inert, for instance being unreactive with ketones, unlike typical ylides. They attributed this unusual stability to the charge delocalization implied by resonance structure **Ib**, consistent with the relatively high dipole moment of 7.0 D.[3]

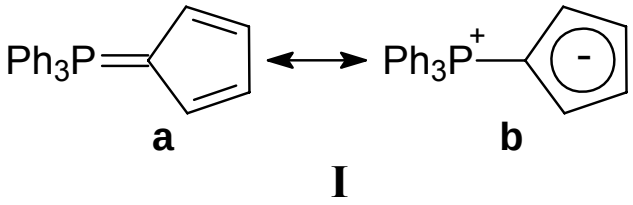

Figure 1-1. The Resonance forms of the Ramirez Ylide (I).

Further evidence for extensive delocalization of the π electron density was found in the crystal structure, which showed significant shortening of the P-C_5 bond,[7] and in the ^{13}C NMR spectrum, which showed an unusually high field chemical shift for the ylide carbon and a P-C(ylide) coupling constant typical of an aliphatic carbon-P bond.[8] A much more thorough examination of the crystal structure of **I** can be found in the discussion section of this thesis.

The interesting features of this compound, from an organometallic point of view, become apparent when resonance structure **Ib** is examined. This resonance form is structurally akin to the Cp ligand that is ubiquitous in organometallic chemistry and catalysis. This class of ligands, with significantly different steric and electronic properties

from those of Cp, would lend itself to the tuning of catalyst properties to give unique reactivities. In addition a number of potential modes of coordination exist (η^{1-5}), with two modes already demonstrated (η^5 and η^1). [9-32] With these potential applications, it is surprising that this class of ligand has 'fallen by the wayside' and virtually no publications dealing with the coordination chemistry of **I** have appeared in over two decades.[9-32]

1.1.1 $C_5H_4PR_3$ Synthesis

One of the major limitations to the utilization of this class of compounds is the lack of a general synthesis for $C_5H_4PR_3$ and other similar ylides. Only a few synthetic methods exist to produce 'Cp' ylides, each with its own drawback. The lack of a general synthesis means that very few C_5H_4 phosphorus ylides are known and very few metal complexes have been prepared beyond those of $C_5H_4PPh_3$. The following sections detail the different preparations for 'Cp' phosphorus ylides that have been reported.

1.1.2 The Ramirez Preparation

The Ramirez ylide, **I**, was synthesized using the method shown in Figure 1-2.[3] The first step in this scheme reported by Ramirez *et al.* was the reaction of two equivalents of triphenylphosphine with dibromocyclopentene, which was prepared by the *in situ* reaction of cyclopentadiene and bromine. After reaction with triphenylphosphine, the diphosphonium salt was produced and then converted into the cyclopentadienyl ylide by reaction with two equivalents of NaOH. Two processes occurred during this step. First, one equivalent of phosphine was displaced during the deprotonation of the ring,

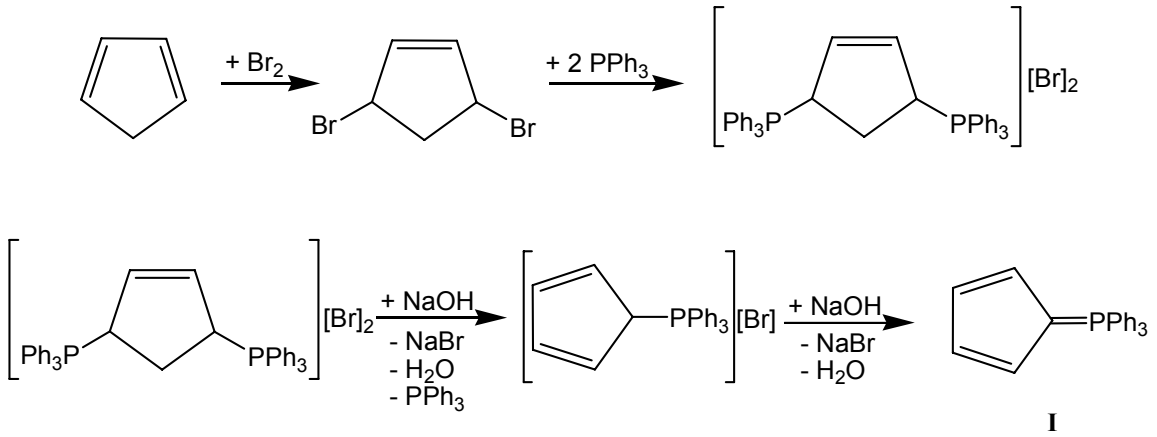

Figure 1-2. The synthesis of the Ramirez Ylide, $C_5H_4PPh_3$ (I).

although the product was not isolated during the reaction. Second, the C_5 ring was deprotonated by the second equivalent of NaOH to yield the ylide (41%).

Ramirez did not extend his method to prepare other similar ylides.[3] One other report extends this method to the synthesis of the tri-*n*-propyl derivative,[33] but this is the only extension of this methodology with PPh_3 to other derivatives of this class of compound. Attempts in our laboratory to extend this method to other phosphines provided black tars, which were presumed to be polymeric materials.[34] Although the Ramirez preparation provides the ylide, **I**, in reasonable yield, it does not provide a general route into cyclopentadienyl phosphorus ylides.

In an attempt to synthesize chelating-cyclopentadienyl phosphorus ylides, the Ramirez methodology was extended to the synthesis of the bis(diphenylphosphino)methane derivative shown in Figure 1-3.[35] As in the first step of the Ramirez synthesis, dibromocyclopentadiene was prepared *in situ* before being added to the phosphine. After deprotonation, the resulting ylide was collected in poor yield (14%). The resulting ylide was unstable and underwent polymerization, probably by a Diels-Alder process, due to tautomerization of the ylide (Figure 1-3).[35]

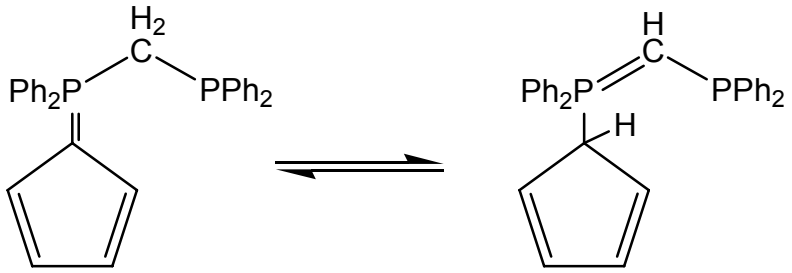

Figure 1-3. The chelating bis(diphenylphosphino)methane derived ylide and its tautomerization.

1.1.3 The Mathey Preparation

We began looking for a different synthetic route into this class of ylides and envisioned that we could synthesize new ylides by the method shown in Equations 1-1 to 1-3.

$$PClPh_2 + NaCp \rightarrow CpPPh_2 + NaCl \quad (1\text{-}1)$$

$$CpPPh_2 + MeI \rightarrow [CpPMePh_2]I \quad (1\text{-}2)$$

$$[CpPMePh_2]I + BuLi \rightarrow C_5H_4PMePPh_2 \ (\mathbf{II}) + LiI + BuH \quad (1\text{-}3)$$

It was quickly determined that a similar route had been reported by Mathey *et al.*, in which they used TlCp in place of NaCp in equation 1-1.[36] Mathey explored the reaction chemistry of this ylide, but did not use it as a ligand in coordination chemistry. This synthetic method begins with the synthesis of cyclopentadienyl diphenylphosphine from chlorodiphenylphosphine. This is one of the few disubstituted chlorophosphines available commercially at a reasonable cost. The phosphine was then treated with MeI to provide the phosphonium iodide as shown in equation 1-2. The last step was the deprotonation of the phosphonium iodide by *n*-butyllithium. Mathey reported the yield of the final step to be 70%.[36]

The Mathey synthetic route requires the use of a chloro-disubstituted phosphine, of which few are commercially available. In addition, most of the commercially available phosphines are expensive and therefore impractical for use in large-scale reactions. Secondly, $CpPR_2$ compounds are generally unstable at room temperature, presumably due to Diels-Alder dimerization and must be converted into phosphonium salts immediately.[37] These two limitations prevent this method from being a general route into cyclopentadienyl phosphorus ylides. However, different alkyl halides can be used to generate a number of complexes with substituents other than methyl, although this extension has not been reported for the phosphine $CpPPh_2$.

Prior to Mathey's report on the synthesis of **II**, Lloyd and coworkers published the preparation of the tetraphenylcyclopentadienylidene derivative of the Ramirez ylide, shown in Figure 1-4.[38] In this synthesis, PPh_3 is added to 5-bromo-

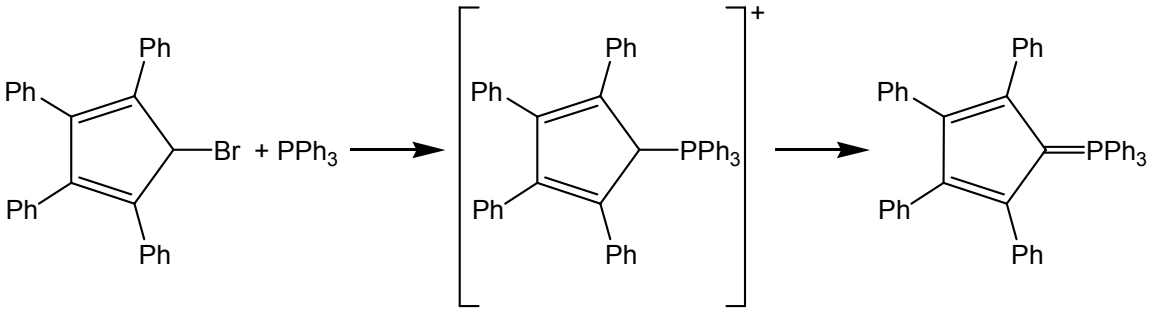

Figure 1-4. The synthesis of $(C_5Ph_4)PPh_3$.

1,2,3,4-tetraphenylcyclopentadiene to yield the phosphonium bromide. The bromide was then exchanged for perchlorate, ClO_4^-, to yield the perchlorate salt. This was then deprotonated with NaOH to give the ylide in excellent yield. The use of the bulky substituents on the bromocyclopentadiene gives this molecule much greater stability than bromocyclopentadiene, C_5H_5Br, or other Cp halides. For this reason, it seems unlikely

that this very reactive molecule would be useful in developing a general route into cyclopentadienyl ylides. Triphenylphosphonium 2,3,4-triphenylcyclopentadienylide was also synthesized by the same group using this methodology.[39]

1.1.4 Phenyl Substituted 'Cp'-Ylides Through Diazocyclopentadienes

One final report details the use of diazocyclopentadienes to generate 'Cp'-ylides by reaction with phosphines. Ramirez initially tried to use this method to generate his ylide, **I**, shortly after his initial report on its synthesis.[40] Diazocyclopentadiene was treated with triphenylphosphine, yielding the phosphazine shown in Figure 1-5. All attempts to thermally decompose the phosphazine failed and Ramirez abandoned this method as a route into 'Cp' phosphorus ylides.[40]

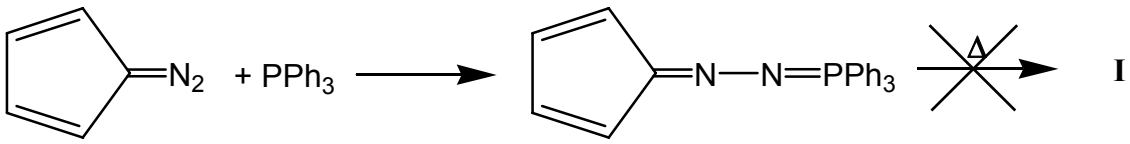

Figure 1-5. The attempted synthesis of I using diazocyclopentadiene.

Lloyd *et al.* revived this methodology and succeeded in generating a number of substituted cyclopentadienyl derivatives of **I**.[41, 42] The reaction was performed by grinding the diazo-compound and triphenylphosphine together and then heating (150-160 °C) the resulting mixture under an inert atmosphere until the evolution of gas ceased (10-60 minutes) (Figure 1-6).[41] Yields ranged from 26-68% depending upon the diazo-compound used.[41] This method is useful in preparing some C_5 ring substituted derivatives

of **I**, but the failure of Ramirez *et al.* demonstrates that this is not a general route into these ylides.[40]

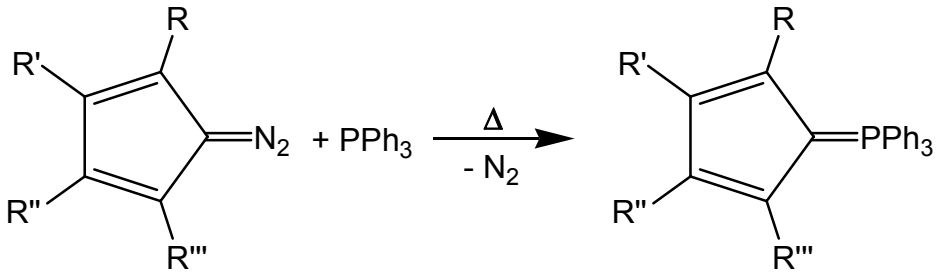

R = R'' = Ph, R' = R''' = H
R = R' = R'' = Ph, R''' = H
R = R' = R''' = Ph, R'' = H
R = Me, R' = R'' = R''' = Ph
R = Bz, R' = R'' = R''' = Ph
R = R' = R'' = Ph, R''' = *p*-MeC$_6$H$_4$

Figure 1-6. The synthesis of ylides from substituted diazocyclopentadienes.

1.1.5 The Preparation of $C_9H_6PPh_3$ – Indenyl Derivatives

In 1967, Crofts and Williamson reported the synthesis of $C_9H_6PPh_3$ – the 'indenyl' derivative of the Ramirez ylide.[43] In this synthesis, C_9H_7Br was added to PPh_3 to give the phosphonium salt $[C_9H_6PPh_3][Br]$, which was subsequently deprotonated to furnish the ylide $C_9H_6PPh_3$ in modest yield. This method was not extended to other phosphines and, before a recent report in 2004, was one of the very few known indenyl derived phosphorus ylides.[44]

1.1.6 The Preparation of $IndPR_2Bz$ (R = Ph or C_6F_5, Bz = Benzyl)

The method developed by Mathey has been extended to the indenyl derivatives of phosphorus ylides in a 2004 report by Rufanov *et al*.[44] However, the authors appeared to

be unaware of Mathey's report 30 years earlier.[36] In this work, $IndPR_2$ (where R = Ph or C_6F_5) was alkylated with ($ClCH_2Ph$) to provide the corresponding phosphonium salts, $[IndPR_2CH_2Ph][Cl]$. This salt was then deprotonated using NaH to give the ylides, $C_9H_6PR_2CH_2Ph$ (Figure 1-7).

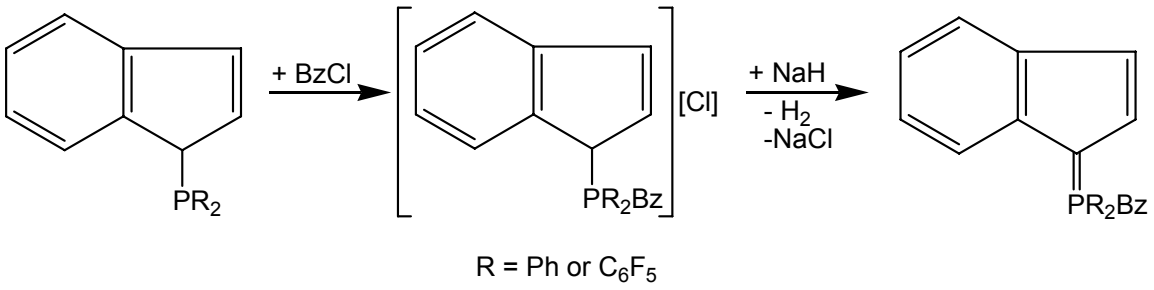

Figure 1-7. The synthesis of indenyl derived phosphorus ylides.

The use of indenyl in place of Cp has the advantage that $IndPR_2$ is stable and can be stored without the decomposition observed in $CpPR_2$ derivatives. However, the complexity of the ^1H NMR spectrum of the 'indenyl' group does cause problems with characterization, which are absent in the relatively simple spectra of the C_5H_4 derivatives.

1.1.7 Fluorenyl Derived Ylides

In addition to the indenyl derivatives, many fluorenyl derivatives are also known for this class of compounds.

The first successful synthesis of triphenylphosphoniumfluorenylide was reported in 1947 by Pinck and Hilbert.[45] They found that when 9-bromofluorene was treated with triphenylphosphine, the desired phosphonium salt was recovered in nearly quantitative

yield. The fluorenyl phosphonium salt was then deprotonated with NH_4OH to give the desired ylide. The synthesis is shown in Figure 1-8.[45]

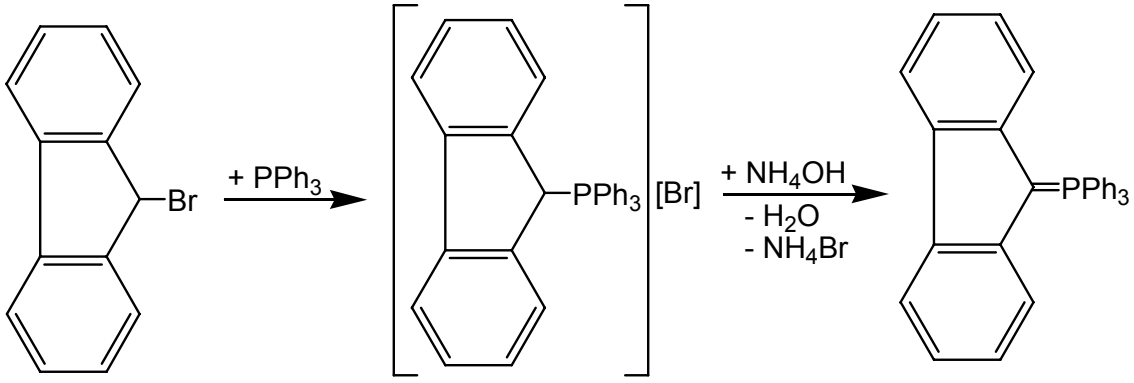

Figure 1-8. The synthesis of the fluorenyl derived triphenylphosphine ylide.

Due to the availability of 9-bromofluorene, many derivatives of this ylide have been synthesized using the same methodology reported by Pinck and Hilbert.[46] A variety of fluorenyl phosphorus ylides, with substitution of the phosphorus R groups, have been generated. In addition, 9-bromofluorene derivatives with substituents on the aryl rings have been used to give even more variety for this class of ligand.[46] The use of bromo-derived 'Cp'-like precursors has thus been demonstrated as an excellent route into the direct precursors for 'Cp'-derived ylides and would be a potentially useful route into Cp ylides if a useable source of CpX (X = halide) could be found.

Beyond those ylides reported above, Schmidbaur *et al.* reported the synthesis of several chelating phosphine fluorenylidene ylides.[35, 47] These structures are shown in Figure 1-9. The addition of 9-bromofluorene to the phosphines gave the desired phosphonium bromide salts. These salts were then deprotonated using methyltriphenylphosphorane, $Ph_3P{=}CH_2$.[35, 47]

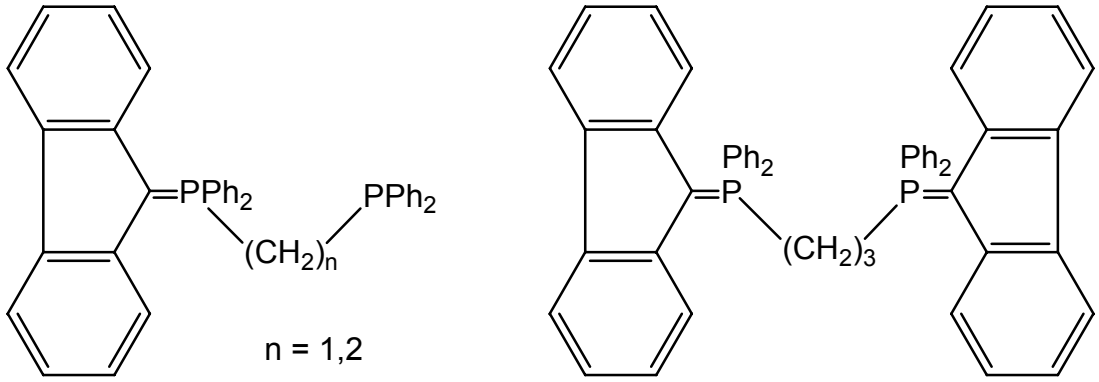

Figure 1-9. Chelating fluorenyl derived ylides and the fluorenyl bis-ylide.

When ethyl and propyl bridged diphosphines were used, bis-salt formation was observed. With the ethyl derivative, the formation of the bis-salt was minimized (<20%) by short reaction times and an excess of the diphosphine. The bis-salt yield was increased with long reaction times. The synthesis of the bis-salt could be achieved with the methylene diphosphine, but only under severe conditions. Deprotonation of the ethyl bridged bis-salt did not afford the desired bis-ylide; a highly insoluble solid was formed. Deprotonation of the ethyl bridge to form a vinylphosphorane, which could then polymerize, was presumed to be occurring.[35]

For the propyl derivative, reaction mixtures always contained the bis-salt as the major product under all reaction conditions, preventing the isolation of the pure mono-salt and mono-ylide. In contrast to the methylene and ethyl bridged diphosphines, the propyl bridged bis-ylide was easily generated in good yield (85%) from the bis-salt by deprotonation with Na_2CO_3.[35]

1.2 Metal Complexes

A number of metal complexes of cyclopentadienyl ylides have been reported. This discussion will cover work done on each transition metal group, as well as work done on main group complexes.

1.2.1 Group 4 Complexes

Very little work has been reported on the synthesis of complexes of the group 4 metals. The first report of group 4 complexes was made in 1977 by Holy *et al*. and describes the reaction of **I** with the group 4 metal halides.[30] The general reaction scheme is presented in the reaction:

$$n\ C_5H_4PPh_3 + MCl_x \rightarrow (C_5H_4PPh_3)_nMCl_x \quad (M = Ti, Zr, Hf, n = 1,2\ x = 3,4) \quad \text{(eq. 1-4)}$$

The reaction with $TiCl_4$ gives a tan coloured precipitate that was characterized by m.p., IR, ^1H NMR and elemental analysis. The product was identified as $[(\eta^5\text{-}C_5H_4PPh_3)_2TiCl_2][Cl]_2$ based upon spectroscopic evidence. The ^1H NMR showed resonances at δ 6.30-6.65 for the C_5H_4 ring protons.[30] Based upon previous reports for Ti-Cp complexes, the authors concluded that the ylide was bound in an η^5 manner. The elemental analysis agrees with the formulation of the proposed complex. No crystals suitable for X-ray analysis were obtained. When $TiCl_3$ was stirred with one equivalent of **I**, a product identified as $(C_5H_4PPh_3)TiCl_3{\cdot}4H_2O$ was obtained. This formulation agrees with the elemental analysis. IR stretching frequencies are also provided, but do not give evidence for the type of bonding in the complex. All attempts to prepare the Ti(II) complex failed.[30]

$ZrCl_4$ was treated with **I** to produce the mono-ylide complex, $[C_5H_4PPh_3ZrCl_3][Cl]$. The product was poorly soluble in most solvents except for DMSO, which limited its characterization by NMR and prevented its recrystallization. The elemental analysis for this compound did not agree well with the reported composition. $HfCl_4$ was also treated with **I** to provide a 1:1 complex, which exhibited similar solubility characteristics to the Zr complex. Again, the elemental analysis results were in poor agreement with the proposed structure, apparently due to combustion problems.[30]

In general, these complexes were poorly soluble in a number of solvents and decomposed when recrystallization was attempted. The complexes were poorly characterized due to the solubility issues and, therefore, no definitive information on the bonding of the cyclopentadienyl to the metal was presented.[30]

One final paper described group 4 complexes of cyclopentadienyl phosphorus ylides. In 2000, Shin *et al.* reported the synthesis of *ansa*-zirconocene and hafnocene complexes of phosphonium bridged permethylcyclopentadienyl ligands.[48] These complexes are shown in Figure 1-10. The zirconocene and hafnium chloro-complexes were characterized by X-ray crystallography.

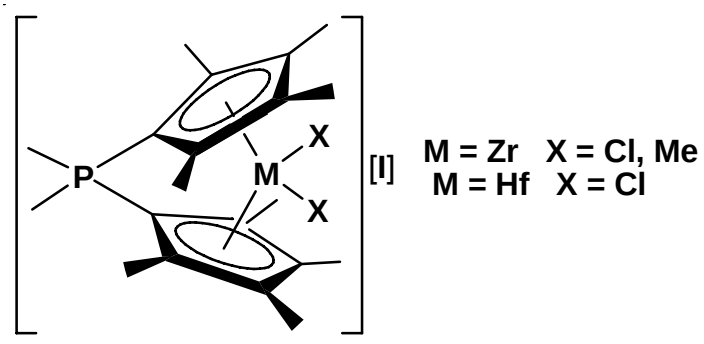

Figure 1-10. The ansa-zirconocene and hafnocene complexes of the phosphonium bridged permethylcyclopentadienyl ligand.

This paper draws no parallel between this research and the Ramirez ylides. However, if the ligand is examined, it in fact belongs to this class of compound. Figure 1-11 shows

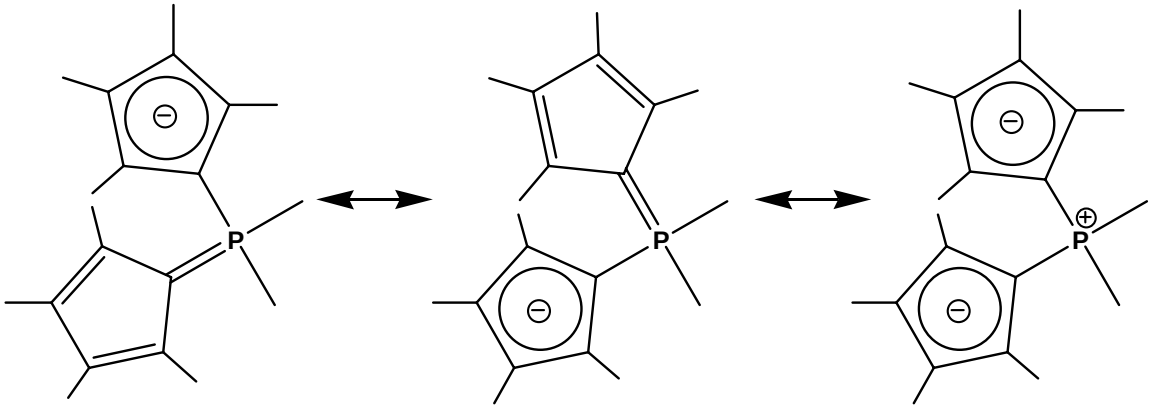

Figure 1-11. The resonance structures of the phosphonium bridged permethylcyclopentadienyl ligand.

the ligand and its resonance structures. When drawn like this, it is easy to see the similarity to the Ramirez ylide. In the crystal structures, the P-C_5Me_4 bonds were equivalent and are 1.800(2) Å for the Zr complex and 1.792(2) Å in the Hf complex.[48] These lengths are considerably longer than observed in other complexes of the Ramirez ylide, indicating that the true structure of the ligand in these complexes is somewhere between a P-C single bond and P-C double bond, but closer to the single bond. This is probably due in part to the resonance of the double bond between the two C_5 rings in the ligand, in addition to the resonance between the single and double bond forms of the P-C_5 bond, akin to resonance structures **Ia** and **Ib**.

The zirconocene dichloride complex was converted to the dimethyl complex by reaction with MeMgI (Figure 1-12). The dimethyl complex was then reacted with CO, which inserted into one of the metal-alkyl bonds to provide the acyl C(O)-Me complex.[48]

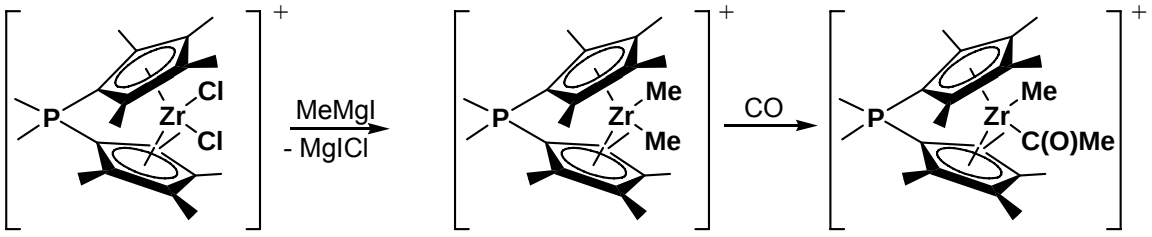

Figure 1-12. The reaction to provide the dimethyl and CO insertion products.

1.2.2 Group 6 Complexes

Complexes of the group 6 metals are the most thoroughly investigated group of complexes of the Ramirez class of ligands. Wilkinson noted soon after the initial Ramirez report that, since **Ib** is isoelectronic with benzene, the ylide might be expected to form compounds of the type $(\eta^5\text{-}C_5H_4PPh_3)M(CO)_3$ (M = Cr, Mo, W), analogous to the known arene compounds $(\eta^6\text{-}C_6H_6)M(CO)_3$.[9] Successful attempts to prepare the group 6 compounds were carried out and the molybdenum compound was obtained analytically pure,[9] although the structures and chemistry of these compounds were only explored many years later.

Kotz and Pedrotty first reported the synthetic procedure to generate the Group 6 tricarbonyls,[10] which had not been reported by Wilkinson *et al*.[9] An excess of the metal hexacarbonyls, $Cr(CO)_6$ and $Mo(CO)_6$, were refluxed in diglyme with **I** to provide the metal complexes in good yields (60-80%).[10] For tungsten, the tris-acetonitrile tricarbonyl, $W(CO)_3(CH_3CN)_3$, was heated to 110°C with **I** to generate the tungsten complex. When $W(CO)_6$ was used, little or no product was isolated.[10] The general reaction scheme is shown in Figure 1-13. The tetraphenylcyclopentadienylidene derivative of molybdenum, $(\eta^5\text{-}C_5Ph_4PPh_3)Mo(CO)_3$, was also synthesized by heating an excess of

$Mo(CO)_3(CH_3CN)_3$ with the ylide, $(C_5Ph_4)PPh_3$, in refluxing THF.[12] This gave the desired product in 60% yield.[12]

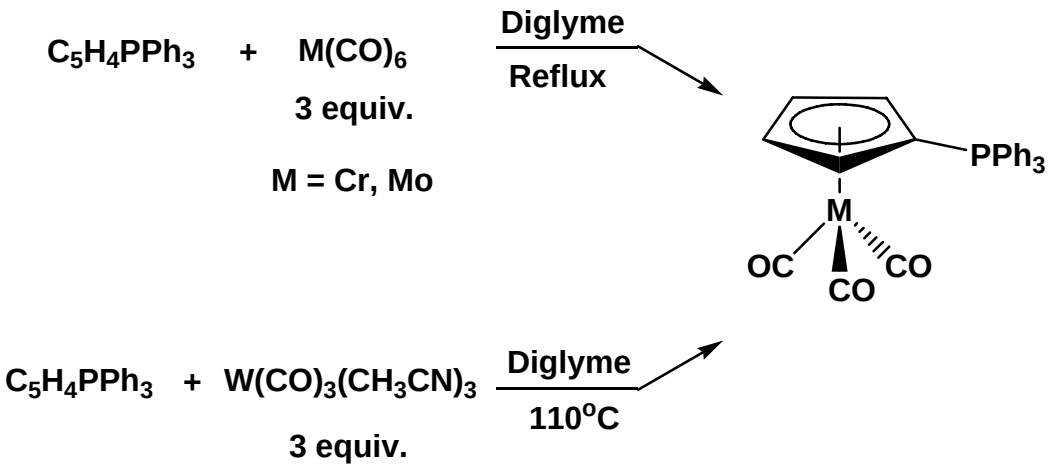

Figure 1-13. The synthesis of the group 6 tricarbonyl complexes of I.

Kotz and Pedrotty reacted the tricarbonyl complexes with trifluoroacetic acid to generate the protonated cationic metal complexes (Figure 1-14).[10] ^1H NMR spectra showed a highly shielded resonance (δ -5 to -8) consistent with the bonding of the hydrogen to the metal. Further evidence of this was demonstrated with the observation of ^{183}W-H coupling, which clearly showed that the hydrogen was bonded directly to the metal. IR spectroscopy also showed the expected increase in CO stretching frequencies, but the ν(M-H) was not observed.[10]

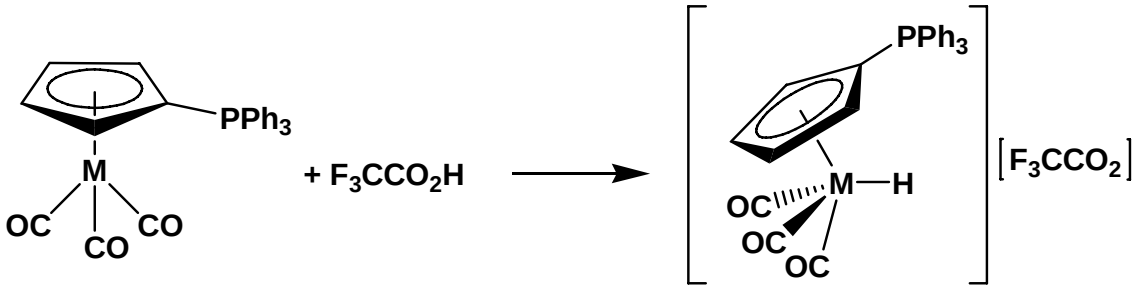

Figure 1-14. The reaction of Group 6 tricarbonyl complexes with F_3CCO_2H (M = Cr, Mo, W).

Further reactions of the metal complexes with BF_3 were performed (Figure 1-15). It was determined that the coordination of BF_3 was reversible (tensimetric titrations) as no change in vapour pressure occurred when more than one equivalent of BF_3 had been added.[10] In addition, removal of the volatile materials from the reaction mixture always showed that unreacted starting material was present (IR) even though the reaction stiochiometry was 1:1 (BF_3:metal complex). IR spectra of these reactions showed a new broad band at 1050 cm^{-1}, consistent with coordinated BF_3 or BF_4^-.[10] The Mo and W adducts analyzed well for this formulation, but the Cr complex could not be obtained due to loss of BF_3 upon workup.[10]

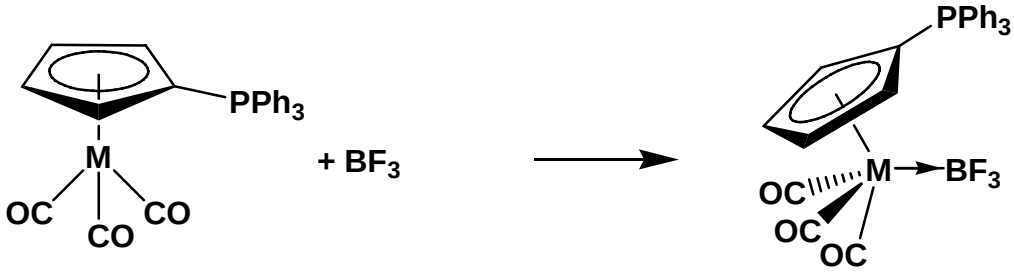

Figure 1-15. The formation of the Lewis acid-base adducts of BF_3 and the group 6 tricarbonyl complexes of I.

In contrast to the metal centre acting as the Lewis base, when the Mo complex was treated with Al_2Me_6, a Lewis acid-base complex was formed in which $AlMe_3$ was coordinated to the oxygen atom of a carbonyl ligand (Figure 1-13).[49] Although no crystal structure was reported to substantiate this, other spectroscopic information provided evidence to support this structural assignment. IR spectroscopy showed CO stretching frequencies at 1932, 1845 and 1665 cm^{-1}.[49] The last peak is much lower in frequency than terminally bound carbonyls and is consistent with the reported carbonyl stretching

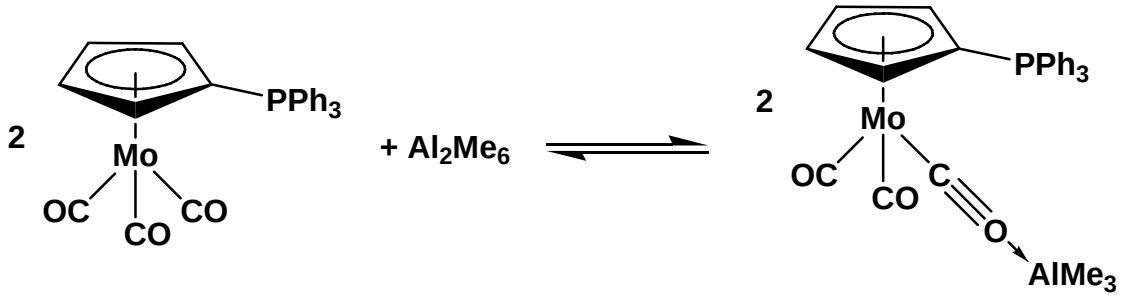

Figure 1-16. The reaction of Al_2Me_6 with $(\eta^5\text{-}C_5H_4PPh_3)Mo(CO)_3$ to form the carbonyl oxygen bound Lewis acid-base adduct.

frequency of $Cp_2Fe_2(CO)_4{\cdot}2AlEt_3$ (1682 cm^{-1}), which was shown by X-ray crystallography to have the aluminum alkyls bound to the carbonyl oxygens.[49] It was suggested that equilibrium between free Al_2Me_6 and bound $AlMe_3$ existed in solution and prevented the isolation and structural characterization of the pure complex. The Mo complex underwent complete dissolution in toluene only when an excess of Al_2Me_6 was present.

The Mo and W complexes were also reacted with HgX_2 (X = Cl, Br and I), CdI_2, $GaBr_3$ and $InBr_3$ (Figure 1-17).[11, 12] In each of these examples, the Lewis acids were shown to bind to the metal and not to the carbonyl oxygen. In all cases a 1:1 complex was formed, even in the presence of excess Lewis acid.[12] Satisfactory elemental analyses were

obtained for most compounds. However, neither the Mo adduct of $GaBr_3$ nor the W adduct of $HgCl_2$ showed the correct analysis. In the case of the Mo-$GaBr_3$ adduct, starting material was present in the IR spectrum and all attempts to separate it from the acid-base adduct failed.[12] The IR spectra of these complexes were similar to the complexes reported by Kotz and Pedrotty, with CO stretching frequencies observed in the 2000-1870 cm^{-1} region.[10] Bonding of the Lewis acids to the CO oxygen was ruled out due to the absence of any strong absorptions in the 1600 cm^{-1} region of the IR spectra.[12]

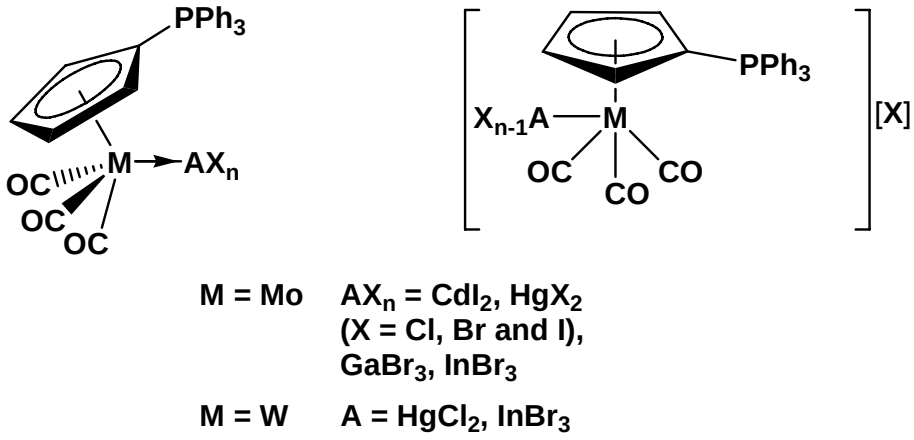

Figure 1-17. The general structure of the Lewis acid-base adducts and the potential ionic complexes formed from these adducts.

For this group of Lewis acid-base adducts, the species could either be the neutral complexes or ionic complexes as shown in Figure 1-17. Conductivity experiments carried out on the Mo complex of HgI_2 showed a molar conductance higher than expected for the neutral complex, but lower than that expected for a 1:1 electrolyte. In addition, when $NaPF_6$ was added to the Mo:$InBr_3$ complex in an attempt to generate the PF_6^- salt, no

reaction occurred.[12] Therefore, some ambiguity remains concerning the structural assignment of these complexes.

The group 6 complexes were treated with halogens and halogenating agents by Cashman and Lalor.[11, 12] The Cr complex was reacted with Br_2 in CH_2Cl_2, which gave a deep red solution at -70 °C that turned green upon warming to -25 °C. Attempts to isolate the PF_6^- salt (by reaction with $NaPF_6$) resulted in the isolation of the PF_6^- salt of the protonated ligand. Reaction of the Mo complex with Cl_2, Br_2 and I_2 gave complexes that were stable at room temperature and could be isolated as red solids. These were then converted to the PF_6^- salts by reaction with $NaPF_6$.[12] Only the PF_6^- salt of the Mo-I_2 reaction analyzed well for the structure shown in Figure 1-18. The Cl and Br complexes gave poor results for elemental analysis.[12]

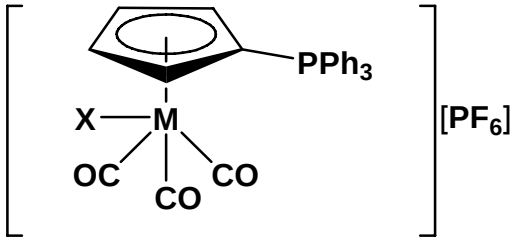

M = Mo X = Cl, Br, I
M = W X = Br

Figure 1-18. The product of the reaction of the Group 6 complexes by either direct halogenation or using a halogenting agent (i.e. CCl_4 or CBr_4).

The halogenated complexes exhibited three strong carbonyl bands in the IR spectra. In many cases ion exchange, to yield PF_6^- salts, was performed to provide material more amenable to purification. Ring halogenation was ruled out by quantitatively converting

the Mo bromine complex back into the Mo complex starting material by reaction with $NaBH_4$.[12]

In order to obtain elementally pure samples of the halide adducts, the Mo and W complexes were treated with trifluoroaceteic acid to provide the hydrido-metal complexes, which were then treated with CCl_4 (Mo only) and CBr_4 (Mo and W). With the Mo complex, this procedure, after ion exchange with $NaPF_6$, yielded materials of analytical purity and identical IR spectra to those obtained from the reaction of the Mo tricarbonyl complex with the elemental halides (Figure 1-18).[12] The tungsten tricarbonyl complex did not give satisfactory results for elemental analysis, but did display the expected IR carbonyl stretches. In addition to this preparation, the reaction of the Mo tricarbonyl complex with $SbCl_5$ also afforded the chlorine complex.[12]

The group 6 tricarbonyl complexes of **I** and the Mo tricarbonyl complex of the tetraphenyl derivative of the Ramirez ylide, $(C_5Ph_4)PPh_3$, were treated with *p*-anisyldiazonium hexafluorophosphate (Figure 1-19).[11, 12] The reaction with Cr resulted in complete decomposition and gave the protonated ylide as the only characterizable product.

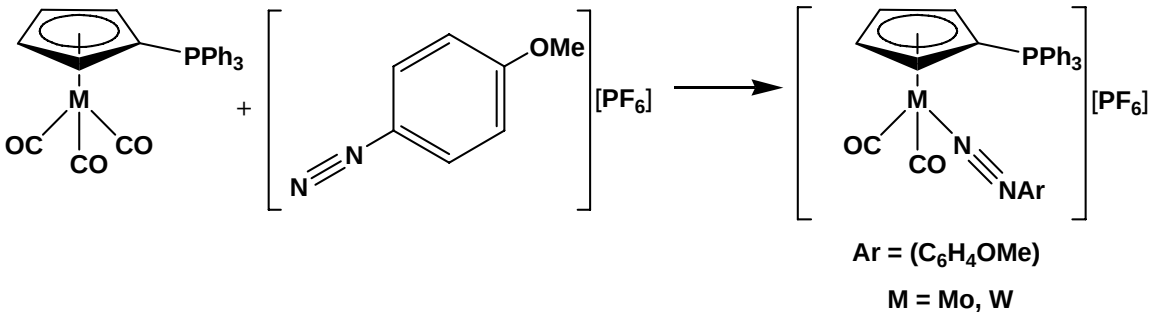

Figure 1-19. The reaction of the group VI complexes with *p*-anisyldiazonium hexafluorophosphate.

.

The Mo and W complexes provided the arylazodicarbonyl metal complexes in greater than 90% yield. Reaction of the Mo complex with PPh_3 in refluxing THF resulted in the substitution of one CO by PPh_3 to give the mono-carbonyl complex (Figure 1-20).[12]

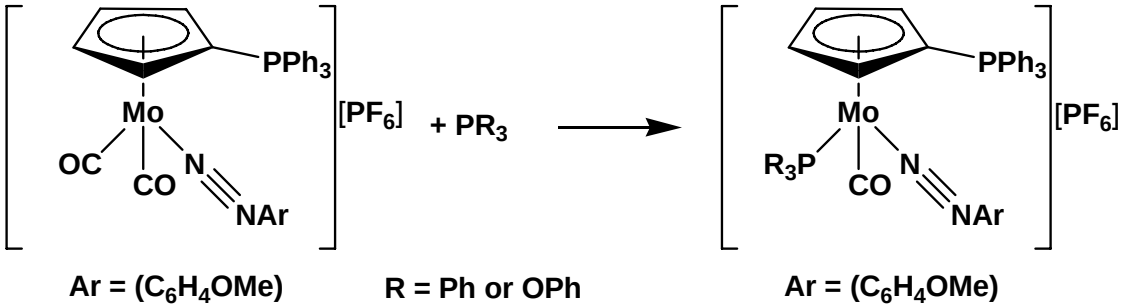

Figure 1-20. CO displacement from the Mo-azo complex by PR_3.

Based upon the oxidation chemistry of the group 6 cyclopentadienyl tricarbonyl anions, $CpM(CO)_3^-$, the reaction of the Mo tricarbonyl complex with the oxidant, tris(*p*-bromophenyl)amminium hexachloroantimonate was examined by Cashman and Lalor.[12] An instantaneous reaction was shown to occur, after which the resulting product was then treated with $NaPF_6$ to give $[(C_5H_4PPh_3)Mo(CO)_3Cl][PF_6]$.[12] Performing the same reaction using the perchlorate amminium salt yielded the dimeric complex shown in Figure 1-21, but due to the explosive nature of the perchlorate salt, elemental analysis could not be performed.[12] The poor solubility of this salt also prevented anion exchange. The IR spectrum of the perchlorate dimer showed four carbonyl stretches (2058 (w), 2027 (m), 1981 (s) and 1930 cm^{-1} (s)) consistent with this assignment.[12] A complex with an almost identical IR spectrum was isolated when the Mo complex was treated with nitrosonium hexafluorophosphate in an attempt to give the nitrosyl complex.

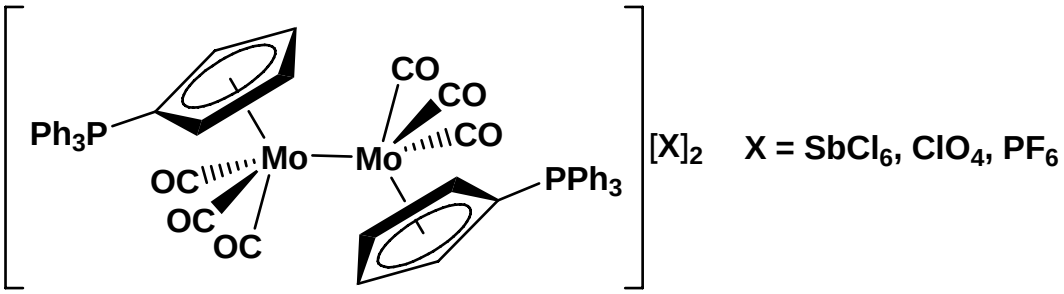

Figure 1-21. The Mo-Mo bound dimer from the oxidation of the Mo complex.

The analytical data for this complex indicate that it has the same formula expected for the dimer (Figure 1-21).[12] The reaction of the oxidized complex (generated from the nitrosonium salt) with $NaBH_4$, regenerated the tricarbonyl starting complex. Therefore, the nitrosonium salt was behaving as a one-electron oxidant.[12]

Reaction of the Mo complex with liquid SO_2 or with SO_2 dissolved in CH_2Cl_2 gave deep red solutions that decomposed on standing to yield amorphous brown carbonyl-free products.[12] Removal of the solvent from these reactions yielded a red solid which quickly turned yellow, providing the tricarbonyl starting complex. An IR spectrum was determined before complete decomposition occurred giving peaks at 2028, 1988 and 1968 cm^{-1} (in addition to peaks from the starting material). The presumed product of this reaction is the Lewis acid-base adduct of SO_2 with the reported structure shown in Figure 1-22.[12]

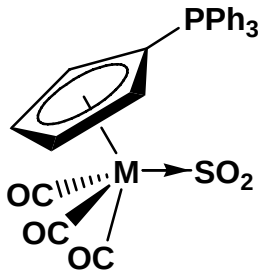

Figure 1-22. The Lewis acid-base adduct of (η^5-$C_5H_4PPh_3$)$Mo(CO)_3$ and SO_2.

The reaction of the Ramirez ylide with the group 6 metals in higher oxidation states was reported by Nalesnik *et al*., who treated the ylide with halides of the group 6 metals.[31] The reaction of **I** with WCl_6 gave a complex with a stoichiometry of $(C_5H_4PPh_3)_2WCl_6$. The proposed structure of this complex is shown in Figure 1-23. ^1H NMR of the reaction product revealed that the resonances for the C_5 ring protons had

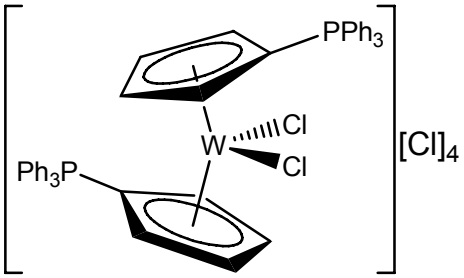

Figure 1-23. The proposed structure of the compound obtained from the reaction of I with WCl_6.

shifted downfield from a multiplet centred at δ 6.20 to a multiplet centred δ 8.57. In addition, the phenyl resonances had also shifted to lower field, but to a much lesser extent than the C_5 ring protons. This deshielding would be expected for the binding of the ylide to a metal in such a high oxidation state. ^{13}C NMR shows a similar trend of downfield shifts for the C_5 ring and phenyl carbons. No crystal structure was obtained to substantiate this structure.[31]

$MoCl_5$ was also reacted with **I** to give a compound that gave an elemental analysis consistent with the formulation $(C_5H_4PPh_3)MoCl_3(OH)_2$.[31] The hydroxides most likely resulted from traces of water in the solvents.[31] This complex was collected in a yield of only 12%. A broad multiplet appears at δ 7.7 in the ^1H NMR spectrum. IR spectroscopic data are also reported, but these do not provide any information on the bonding present in

this complex.[31] Also reported was the reaction of **I** with $CrCl_2$, but this apparently did not produce the desired complex and no other information about this reaction was presented.[31]

Using the chelating fluorenyl derived ylide described above, and shown in Figure 1-9, $Cr(CO)_6$ or $W(CO)_3(CH_3CN)_3$ were treated with the ylide as shown in Figure 1-24.[35] The reaction with W gave $((\eta^1\text{-}C_{13}H_8)\text{-}CH_2\text{-}\eta^1\text{-}PPh_2)W(CO)_3$, shown in Figure 1-24.[35] The product gave an IR spectrum with four CO stretching bands that are similar to the

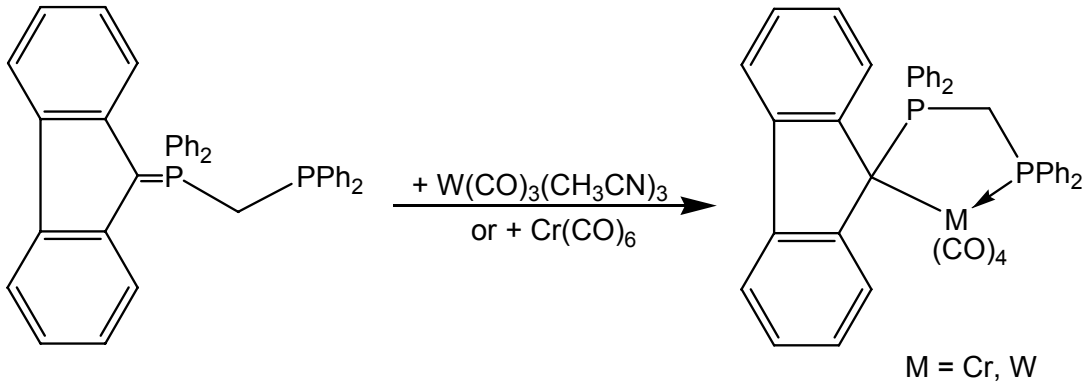

Figure 1-24. The reaction of the chelating fluorenyl derived ylide with the group 6 metal starting materials $Cr(CO)_6$ and $W(CO)_3(CH_3CN)_3$.

previously reported complex, $(Phen)W(CO)_4$.[35] Further evidence of this bonding situation was given by the ^{31}P NMR, which revealed that the two phosphorus resonances had shifted significantly downfield versus the free ligand, consistent with bonding at both the ylidic carbon and the pendant $-PPh_2$ phosphorus. This is the first tungsten complex which had a cyclopentadienyl moiety bound in a monohapto manner.[35] In the case of the Cr reaction, a different result was obtained. Two products were obtained after chromatographic separation. One proved to have an IR spectrum and ^{31}P NMR spectrum similar to those obtained in the case of the tungsten complex. In addition, mass spectroscopy gave a molecular ion peak corresponding to this structural assignment. The

second complex was a tricarbonyl derivative, which had three CO bands in the IR spectrum. The ^{31}P NMR data showed that neither phosphorus resonance was greatly shifted from the free ligand. This indicated that the likely structure was the complex in which the $Cr(CO)_3$ is bound to one of the phenyl rings of the 'fluorenyl' group (Figure 1-25).[35]

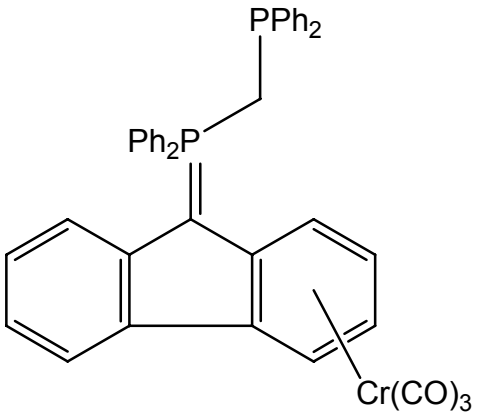

Figure 1-25. The structure of the Cr complex with the metal bound to the fluorenyl phenyl ring.

1.2.3 Group 7 Complexes

Two literature reports detail the synthesis of group 7 metal complexes. In 1976, Nesmeyanov *et al.*[16] reported the synthesis of the cationic Mn tricarbonyl complex of the Ramirez ylide. When **I** was stirred for one day at room temperature with $[Mn(CO)_3(CH_3CN)_3][PF_6]$ in either THF or diglyme, the Mn complex, $[(\eta^5\text{-}C_5H_4PPh_3)Mn(CO)_3][PF_6]$ was obtained as shown in Figure 1-26.[16] This complex is

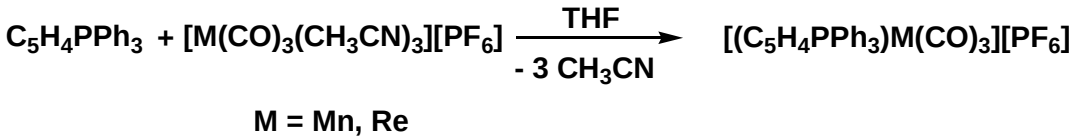

Figure 1-26. The synthesis of $[(C_5H_4PPh_3)M(CO)_3][PF_6]$ (M = Mn, Re).

isoelectronic to the Group VI complexes. It is stable in air as a solid and is soluble in polar solvents such as acetone, THF, methanol and ethanol. Characterization of this complex was performed using IR, ^{1}H NMR, MS and elemental analysis. Two IR stretching modes of the carbonyls are seen at 1963 and 2040 cm^{-1}, which are consistent with this structure.[16] The ^{1}H NMR in acetone-d_6 showed one resonance for the C_5 ring protons at δ 5.83 and a resonance at δ 8.11 for the phenyl protons.[16] Using EI-MS, no peak for the molecular ion was observed at an ionization voltage of 30 eV.[16] The parent ion resulted from the ionized ylide (m/z = 326). Fragmentation of the Mn complex seems reasonable under the high-energy ionization conditions reported. In addition, to achieve sufficient volatilization of the sample, heating was required which may have resulted in thermal degradation. Elemental analysis was in excellent agreement with the expected formulation.

In a separate report by the same group, the synthesis of the Re tricarbonyl derivative of $C_5H_4PPh_3$ was reported.[17] The synthesis of the Re complex required refluxing the THF reaction mixture to ensure substitution. The ^{1}H NMR spectrum showed two resonances, one at δ 6.27 (C_5 protons) and one at δ 7.92 (phenyl protons). The IR spectrum had two carbonyl stretching bands at 2038 and 1950 cm^{-1}.[17] These are

similar to the frequencies seen with the similar Cp tricarbonyl complexes. As with the Mn complex, the MS spectrum of the rhenium complex did not exhibit a molecular ion peak. Again, most likely due to thermal degradation, only a peak for the free ligand was observed at 326 m/z. ^{13}C NMR data were collected for both the Mn and Re complexes. For both complexes, the P-C carbon of the C_5 ring shows only minor shielding versus the free ligand upon complexation.[17] A much more dramatic shift was seen for the other carbons of the C_5 ring, which were shifted upfield by more than δ 20 for both complexes.[17] As expected, little change was noted in the phenyl carbon resonances.

No investigation into the reactivity of these complexes has been reported, leaving a large hole in understanding the behaviour of such species. In addition, while the spectroscopic data clearly indicate successful syntheses of the desired complexes, no structural information was presented. Both compounds were reported as being highly crystalline[16, 17] and X-ray structures of these complexes would add to the understanding of bonding in the complexes.

1.2.4 Group 8 Complexes

The syntheses of iron complexes of phosphorus cyclopentadienyl ylides have been reported using two distinctly different methodologies. Like other complexes, the direct reaction of **I** with several iron precursors has been reported, while a completely new synthetic pathway using the quaternization of phosphorus has been developed.

The reaction of **I** with $Fe(CO)_5$ was initially reported by Cashman and Lalor.[12] When $Fe(CO)_5$ was refluxed with **I** in dimethoxyethane in an attempt to synthesize the complex shown in Figure 1-27, 65% of the unreacted ligand was recovered. After chromatography, a trace of a yellow crystalline iron carbonyl product was obtained with

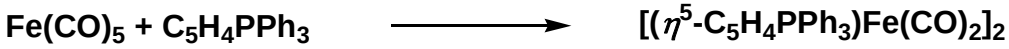

Figure 1-27. The attempted reaction of I with $Fe(CO)_5$.

four IR stretches in the 1900-2100 cm^{-1} region, but the limited quantity of material generated was insufficient to allow further characterization.[12] No other information was reported for this reaction. Alper *et al.*[50] reported the reaction of $Fe_2(CO)_9$ with **I** and found that an unstable red product was generated that had IR peaks in the same region as the complex reported by Cashman and Lalor.[12] Alper *et al.* reported IR peaks at 2049, 1993, 1970 and 1934 cm^{-1}.[50] No further examination of the product was reported. Alper *et al.* also treated the fluorenyl derived ylide of triphenylphosphine (Figure 1-8) with $Fe(CO)_5$, $Fe_2(CO)_9$ and $Fe_3(CO)_{12}$ but did not obtain any organometallic product – only the olefin, bis-fluorenylidine was isolated in a 10% yield.[50]

When **I** was stirred with $FeCl_2$ in THF for several days, a brown precipitate appeared, which was collected via filtration. This material had a stoichiometry of (**I**)Fe_2Cl_4 – a formulation which "appears unique in metallocene chemistry."[32] The complex was stable at room temperature, slightly air-sensitive and soluble only in coordinating solvents such as DMF and DMSO. ^{31}P NMR of the material in DMF gave one sharp resonance at δ 25.9. The sharpness of the peak was given as evidence of the diamagnetism of the complex.[32]

When pentane was added to the filtrate from the same reaction, a second product was obtained from this reaction. A dark red, highly air-sensitive complex was obtained that was insoluble in non-polar solvents.[32] The ^{31}P NMR spectrum in THF-d_8 showed only one resonance at δ 13.2. This is nearly identical to that of the starting ylide (δ 13.1 in

$CDCl_3$). Elemental analysis revealed that the complex had a stoichiometry of $(\mathbf{I})_3Fe_2Cl_4$. For both complexes, although ^{31}P NMR data were reported, no ^{1}H NMR spectrum was provided.[32] Furthermore, the melting/decomposition points are values with >10°C ranges suggesting that the materials may not have been pure. Therefore, the stoichiometric assignments made from the elemental analyses may be incorrect.

A second synthetic route into iron-'Cp'-phosphorus ylides was reported in 1963.[51] In this method, methyl iodide was added to ferrocenes containing phosphine substituted Cp rings as shown in Figure 1-28, to quaternize the phosphine and give ionic complexes. The products were characterized by elemental analysis and IR spectroscopy. However, no yields were reported. The resulting Fe(II) salts are structurally akin to the complexes of **I**. However, much like the report on zirconium and hafnium complexes by Shin *et al.* in 2000,[48] no parallels were drawn between these complexes and the Ramirez ylide complexes.

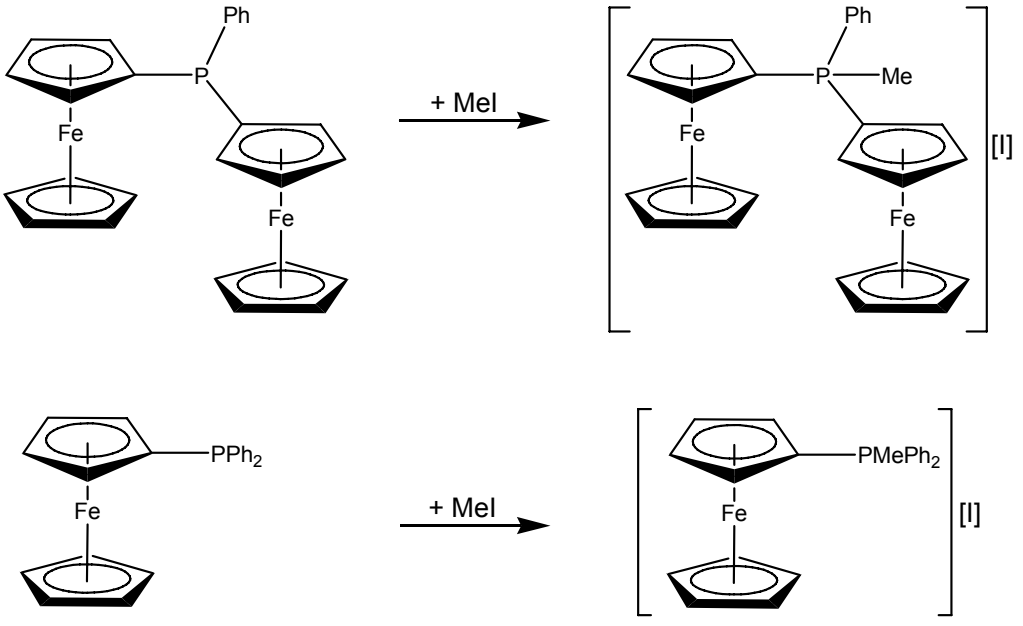

Figure 1-28. Synthesis of iron ylide complexes by quaternization of ferrocenyl phosphines.

Other reports described similar protocols to generate phosphonium salts of ferrocene derivatives. In 1976, in the course of an examination of the kinetics of quaternization of phosphines and arsines, several Ramirez ylide-type complexes were synthesized by the same methodology as reported by Sollott *et al.*[51, 52] The benzyl derivatives of the ferrocenes were synthesized by McEwen *et al.* by the addition of benzyl chloride to the ferrocenyl phosphines as shown in Figure 1-29 to give benzyldiphenylferrocenylphosphonium chloride and benzylphenyldiferrocenylphosphonium chloride.[52] In 1983, the first crystal structure of benzyldiphenylferrocenylphosphonium chloride was reported by McEwen et al.[53] The P-C_5 bond length of 1.768(3) Å is similar to other coordination complexes of Ramirez type ylides and is shorter than a P-C single bond.[53]

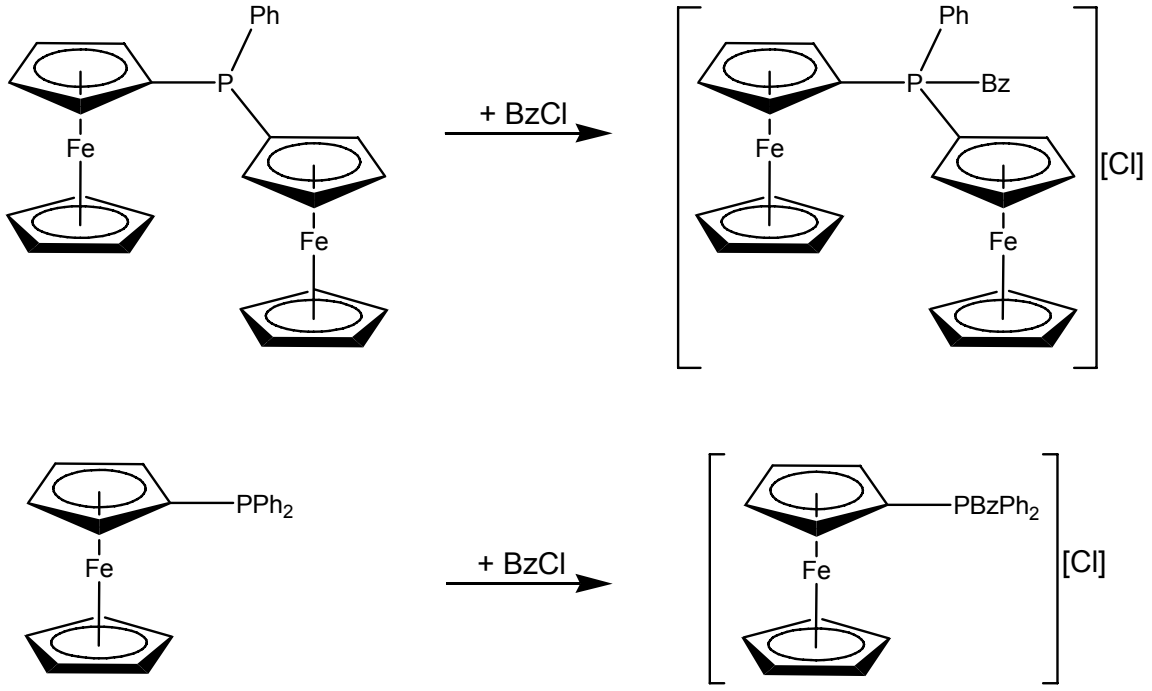

Figure 1-29. Synthesis of iron ylide complexes by quaternization of ferrocenyl phosphines using benzyl chloride.

A much later report, published in 1994, thoroughly described the synthesis of benzyldiphenylferrocenylphosphonium salts from the reaction of benzyl halides with diphenylferrocenylphosphine, followed by conversion to the BF_4^- salts, to yield a series of *para*-substituted benzyl complexes (Figure 1-30).[54] The crystal structure of the methoxy derivative was reported.[54] Full spectroscopic characterization of these complexes was reported, including ^1H and ^{31}P NMR, MS and elemental analysis, making these some of the most well characterized examples of this class of compounds. The crystal structure mirrors the structure obtained for benzyldiphenylferrocenylphosphonium chloride, with a similar bond length for the P-C_5 bond.[54]

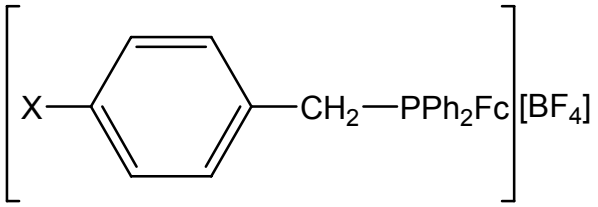

X = H, OMe, F, CN
Fc = ferrocenyl

Figure 1-30. Various *para*-substituted benzyl derivatives of diphenylferrocenylphosphonium.

Several examples of ruthenium complexes have also been reported for the Ramirez ylide. In 1995, the reaction of the cluster compound $[Ru_6C(CO)_{17}]$ with trimethylamine *N*-oxide and **I** to give the complex $[(\eta^5\text{-}C_5H_4PPh_3)Ru_6C(CO)_{14}]$ was reported (the structure is shown in Figure 1-31).[20] This complex was collected in moderate yield (64%) and was characterized by ^1H and ^{31}P NMR, MS, IR and X-ray crystallography. The crystal structure revealed that the ylide was bound to the apical Ru atom in the cluster in an η^5 manner.[20] The P-C_5 bond length of 1.793(12) Å is

considerably longer than in **I** (1.718(2) Å) and is more akin to a P-C single bond. The P-C_5 ring bond is bent significantly out of the plane of the C_5 ring by 19.4(6)°.[20] The IR spectrum showed the main CO stretching band lower in energy by 17 cm^{-1} than that of $[(\eta^6\text{-}C_6H_6)Ru_6C(CO)_{14}]$, indicating that, as expected, **I** is a better donor than benzene.[20] Similar to other coordination complexes of **I**, the ^{31}P NMR resonance moved downfield upon coordination, while the ^1H NMR C_5H_4 proton resonances move upfield.[20]

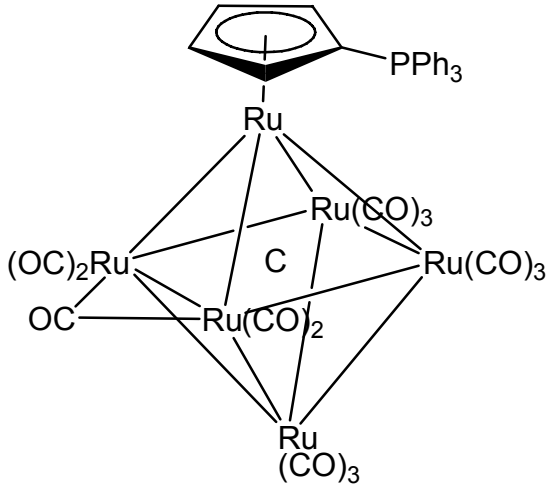

Figure 1-31. The structure of $[(\eta^5\text{-}C_5H_4PPh_3)Ru_6C(CO)_{14}]$.

Two other interesting reports detail the reactivity of Ru complexes, which resulted in the formation of 'Cp'-phosphorus ylide complexes. The first report details the reaction of the complex $[Ru(\eta^5\text{-}C_5H_5)(\eta^4\text{-}C_5H_4O)]_2[PF_6]_2$ with a variety of nucleophiles, which included several phosphines.[55] When this complex was treated with various phosphines the products shown in Figure 1-32 were isolated. The products were obtained in 50-60% yield for the phosphines PR_3 (R = Me, Cy, Ph), but the yields appeared to be quantitative when performed on an NMR scale.[55] A crystal structure of the tricyclohexylphosphine derivative was obtained with a P-C_5 bond length of 1.790(3) Å, which is typical of other

complexes with similar ylide ligands.[55] Identical complexes are obtained for PMe_3 and PCy_3 when $[Ru(\eta^5\text{-}C_5H_5)(\eta^4\text{-}C_5H_4O)(CH_3CN)][PF_6]$ is used as the starting material.[55]

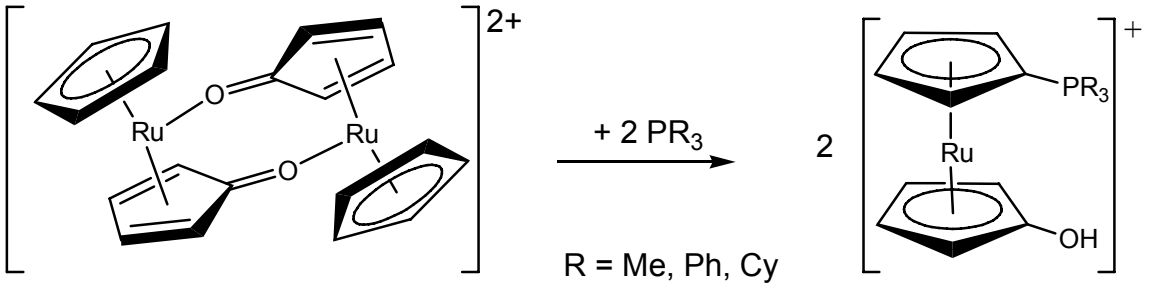

Figure 1-32. Reaction of phosphines with $[Ru(\eta^5\text{-}C_5H_5)(\eta^4\text{-}C_5H_4O)]_2[PF_6]_2$.

However, when PPh_3 was treated with this complex, substitution occurred at the cyclopentadienone to give the complex $[(\eta^5\text{-}C_5H_3OH\text{-}2\text{-}PPh_3)Ru(\eta^5\text{-}C_5H_5)][PF_6]$, shown in Figure 1-33.[55] This complex underwent oxidation by Br_2, I_2, and Ag^+ in CH_3CN to yield the phosphine substituted cyclopentadienone Ru complex. Ferrocenium cation did not undergo reaction with this compound.[55]

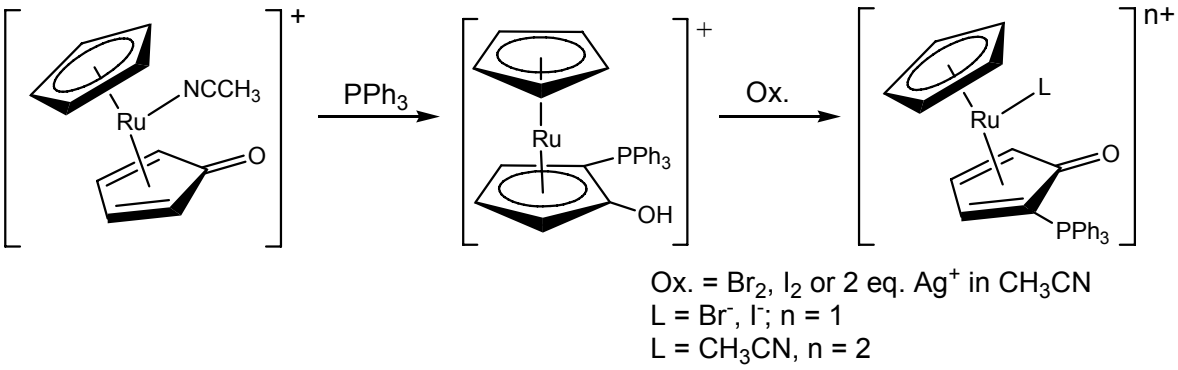

Figure 1-33. The reaction of $[Ru(\eta^5\text{-}C_5H_5)(\eta^4\text{-}C_5H_4O)(CH_3CN)][PF_6]$ with PPh_3 and the resulting product's oxidation.

When [CpRuFvRuCp][BF_4]$_2$ (Fv = fulvalene) was treated with an excess of PPh_3, the 1'-substituted biruthenocene was generated as the major product (87%) (Figure 1-34).[56] The X-ray crystal structure of this complex was reported. The P-C_5 bond length is 1.769(3) Å, longer than in **I**, but shorter than a P-C single bond.[56] The ^{31}P NMR resonance occurred at δ 25.08, which is in the region expected for the coordination complex of **I**.[56] Again, there was no parallel made between this complex and the Ramirez ylide work.

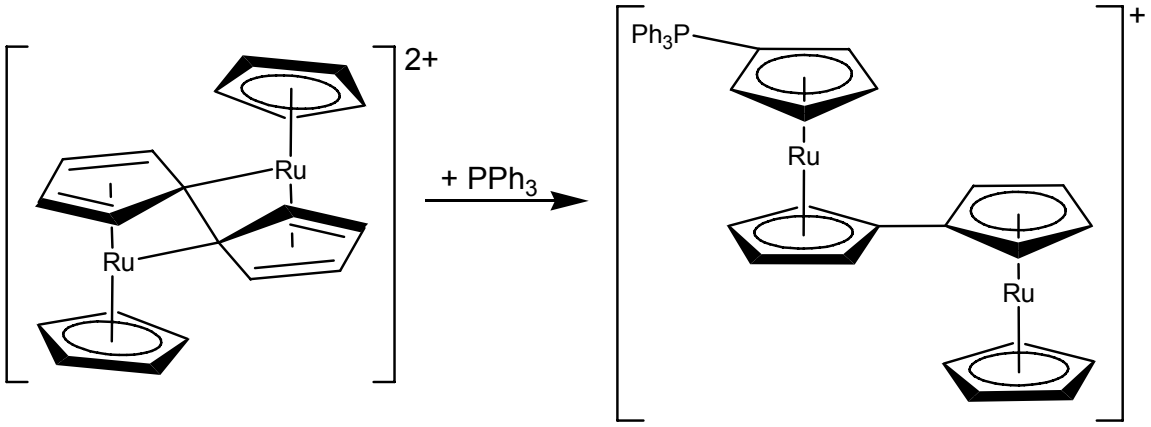

Figure 1-34. The reaction of [CpRuFvRuCp][BF_4]$_2$ with PPh_3.

One final paper details the reaction of **I** with [$Os_3(CO)_{10}(MeCN)_2$].[57] In this reaction, the ylide oxidatively added to the cluster compound to yield a complex in which the C_5 ring was bound to two osmium atoms through a single carbon atom.[57] The synthesis and structure of this complex is shown in Figure 1-35. In this reaction, one of the C_5 ring C-H bonds has been cleaved to yield a σ-bound C_5 ring and a bridging hydrogen atom.

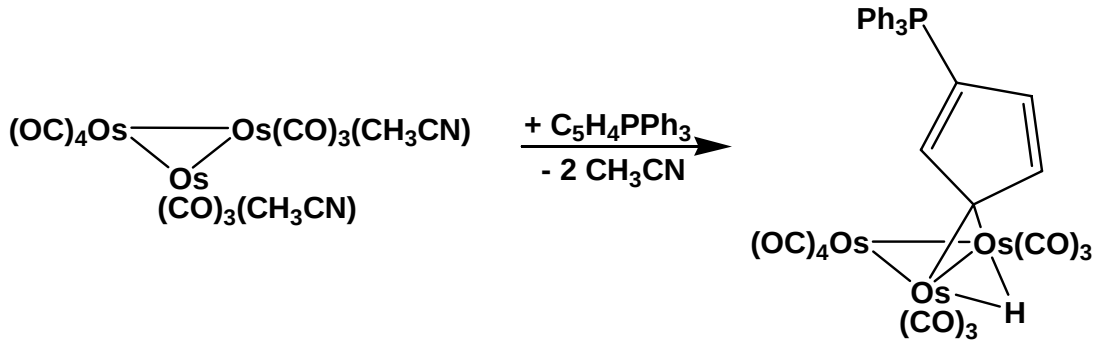

Figure 1-35. The reaction of $[Os_3(CO)_{10}(MeCN)_2]$ with I.

When treated with unsaturated hydrocarbons, $[Os_3(CO)_{10}(MeCN)_2]$, had been reported to undergo oxidative addition of the hydrocarbon by C-H bond cleavage which is similar to the reactivity demonstrated in the reaction shown in Figure 1-35.[57] The reaction occurs within seconds at room temperature in CH_2Cl_2 to give $[(\mu\text{-}C_5H_3PPh_3)Os_3(\mu\text{-}H)(CO)_{10}]$ in 61% yield.[57] The structural assignment of the complex was made using the X-ray crystal structure obtained for **A**. The crystal structure reveals a P-C_5 bond length of 1.74(2) Å, which is just slightly longer than in **I**.[57] Again, this is an indication that the dominant contribution to the bonding situation is made by the zwitterionic resonance structure.[57]

Isomerization of this complex occurred in solution to give the product **B** as the minor product (~40% after several days in chloroform), shown in Figure 1-36.[57]

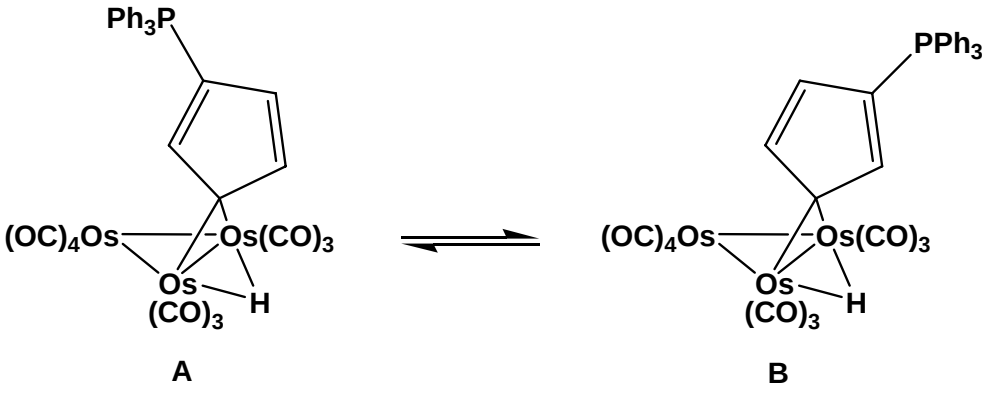

Figure 1-36. Isomerization of $[(\mu\text{-}C_5H_3PPh_3)Os_3(\mu\text{-}H)(CO)_{10}]$.

The pure isomer **B** was isolated by chromatography and, when left to stand in solution, the same end point equilibrium was reached (60% **A**, 40% **B**) as seen when starting from isomer **A**.[57] The IR spectra of the isomers were indistinguishable and ^{1}H NMR data gave similar splitting patterns and chemical shifts, but the coupling constants differ for the two isomers. A mechanism of isomerization was proposed, but experiments to support the mechanism did not yield conclusive results.[57]

When **A** or mixtures of **A**:**B** were thermolized in refluxing toluene, the decarbonylation product, [(μ_3-$C_5H_3PPh_3$)Os_3(μ-H)$(CO)_9$], was obtained in 70% yield.[57] The crystal structure of this complex revealed that the C_5H_3 ring had adopted a μ_3 configuration, bridging the three osmium atoms of the cluster. The ligand can be thought of as donating four electrons through two sigma bonds and two electrons through one η^2 bond of a C_5 ring double bond. Isomerization of this species was also proposed due to peaks in the ^{1}H NMR, but this was not conclusively confirmed. The two isomers are shown in Figure 1-37. [57]

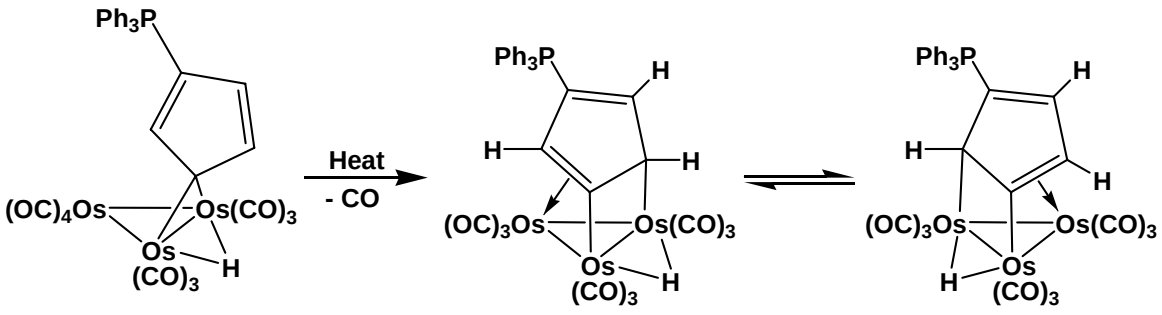

Figure 1-37. The product and isomerization of the decarbonylation of [(μ-$C_5H_3PPh_3$)Os_3(μ-H)$(CO)_{10}$].

1.2.5 Group 9 Complexes

The first report of group 9 metal ylide complexes appeared in 1978. Holy *et al.*[18] reported the synthesis and structure of the complex $[(\eta^5\text{-}C_5H_4PPh_3)Co(CO)_2][Co(CO)_4]$, and the use of this complex in the catalysis of the cyclotrimerization of alkynes. This complex was synthesized by adding $Co_2(CO)_8$ to a solution of **I** in THF and stirring for 30 minutes (Figure 1-38).[18] The resulting complex was collected in 65% yield after precipitation by petroleum ether. The crystal structure of this complex was determined and shows similarities to other structures of this class of compound.[18, 19]

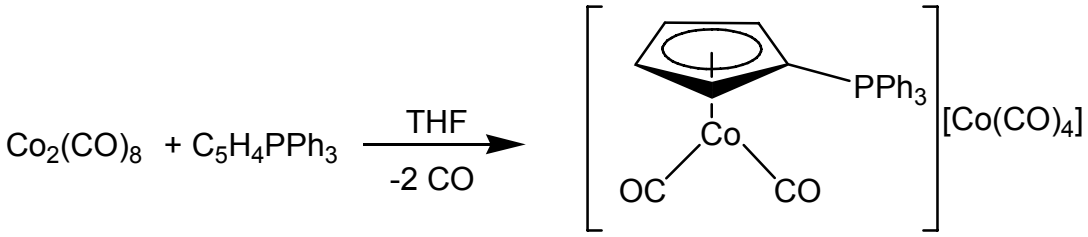

Figure 1-38. The synthesis of $[(\eta^5\text{-}C_5H_4PPh_3)Co(CO)_2][Co(CO)_4]$.

The C_5 ring was bound in an η^5 manner. The C_5 bond distances of the ring were not greatly perturbed from that of the free ligand and showed only slight elongation of the ring bonds. The P-C_5 bond showed the prototypical elongation (1.765(6) Å) upon coordination to the Co atom.[19] This complex was used to catalyze the cyclotrimerization of alkynes to give benzene derivatives in good yield.[18] When it was refluxed with 4-octyne for 3 days, hexa-n-propylbenzene was obtained in 63% yield. No other octyne-derived products were found, but other products must have been generated as only a total of 68% of the alkyne was converted (63% to n-propylbenzene and 5% into other products).[18] When used with diphenylacetylene, this complex catalyzed the formation of

hexaphenylbenzene in 96% yield, with no other diphenylacetylene products detected.[18] A further paper on the catalysis was reported to have been submitted to the *Journal of Organometallic Chemistry*, but was never published.[19]

A cobalt(III) complex of a Ramirez type ylide was obtained as the unexpected product of the reaction of $[CpCo(PEt_3)_2][BF_4]$ with one equivalent of $AgBF_4$, followed by the addition of one equivalent of PEt_3 (Figure 1-39).[58] The product, $[(C_5H_4PEt_3)CoH(PEt_3)_2][BF_4]_2$, was obtained in 88% yield. Confirmation of this formulation was given by ^1H NMR, which showed two multiplets for the C_5H_4 ring protons (at δ 6.3 and δ 5.6) and a hydride resonance with a chemical shift of δ -15.4.[58]

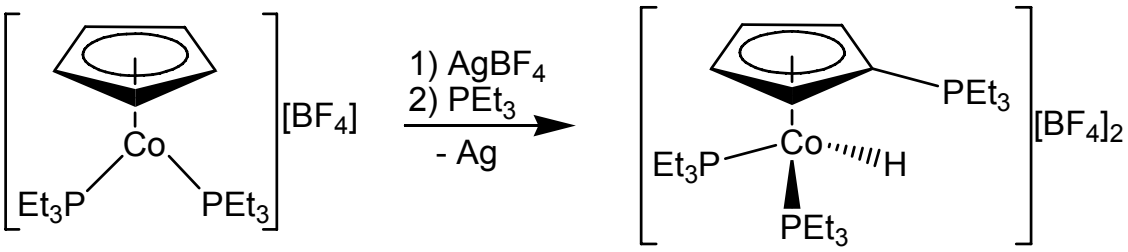

Figure 1-39. The synthesis of $[(C_5H_4PEt_3)CoH(PEt_3)_2][BF_4]_2$.

Elemental analysis agreed with this assignment. The author also noted that similar reactivity was observed on mixing $CpCo(PMe_3)_2$ and alkyl halides (R-X), which also undergo addition on the C_5H_5 ring and give the complexes, $[(RC_5H_4)CoH(PMe_3)_2][X]$.[58]

The first reports of Rh complexes of **I** appeared in 1981.[21] Tresoldi *et al*.[21] synthesized a series of Rh(I) and Rh(III) complexes. The reaction of $[Rh(CO)_2Cl]_2$, $[(1,5\text{-}COD)RhCl]_2$ and $[(nbd)RhCl]_2$ (nbd = norbornadiene, C_7H_8) with $AgPF_6$ followed by addition of **I**, resulted in the syntheses of $[(\mathbf{I})Rh(CO)_2][PF_6]$, $[(\mathbf{I})Rh(1,5\text{-COD})][PF_6]$ and $[(\mathbf{I})RhC_7H_8][PF_6]$, respectively (as shown in Figure 1-40).[21] **I** was found to be a poor

nucleophile towards these rhodium complexes, as it would not split the chloro-bridged dimers used as starting materials.[21] The silver salt, $AgPF_6$ (as well as $AgBF_4$), was used to generate solvated species in solution, which then underwent reaction rapidly with **I** to furnish the desired complexes in good yields. These complexes showed good solubility in acetone and DMSO, were slightly soluble in CH_2Cl_2 and MeOH and were insoluble in non-polar solvents such as benzene.[21]

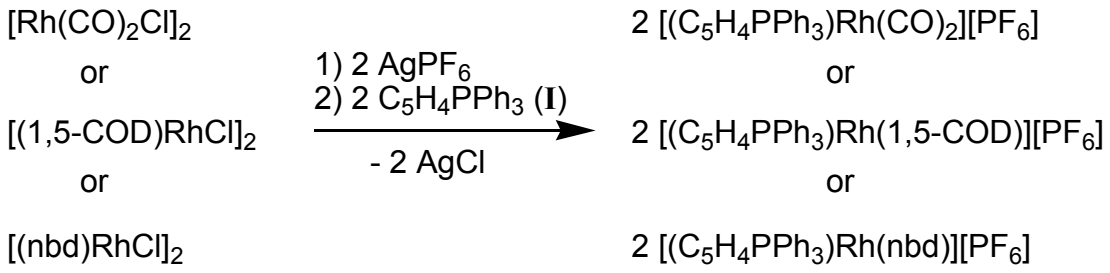

Figure 1-40. The synthesis of rhodium complexes of I.

^1H and ^{13}C NMR data clearly demonstrated the syntheses of the desired complexes, with chemical shifts that are consistent with other complexes of **I**.[21] The IR spectrum of [(**I**)$Rh(CO)_2$][PF_6] showed carbonyl stretches at higher frequencies than the corresponding Cp complex, providing further evidence that **I** is not as good a donor as Cp.[21] A crystal structure of the tetraphenylborate salt of [(**I**)Rh(1,5-COD)]$^+$ was reported later by the same group.[27] The crystal structure revealed that, as expected, **I** was bound in an η^5 manner, with Rh-C_5 bond lengths of 2.22(1)-2.29(1) Å. The P-C_5 bond length is 1.76(1)Å.[27]

The reaction of [(**I**)$Rh(CO)_2$][PF_6] with a series of compounds was also examined by this group.[21] When [(**I**)$Rh(CO)_2$][PF_6] was treated with [$AsPh_4$][Cl] and TlCp,

$[Rh(CO)_2Cl_2][AsPh_4]$ and $[Rh(Cp)(CO)_2]$ were obtained, respectively, by the displacement of **I** from the Rh atom (Figure 1-41).[21] Reaction of $[(\mathbf{I})Rh(CO)_2][PF_6]$ with PPh_3 resulted in the displacement of one carbonyl by the phosphine to yield $[(\mathbf{I})Rh(CO)PPh_3][PF_6]$.[21] The mechanism and kinetics of the CO displacement by PPh_3 in this complex were further studied by Rerek and Basolo,[59] who found that CO substitution occurred ~100 times faster than in the corresponding Cp complex. In addition to PPh_3, the reactions of bridging diphosphines, $Ph_2P(CH_2)_nPPh_2$ (n = 1 (dppm), 2 (dppe), 4 (dppb)), with $[(\mathbf{I})Rh(CO)_2][PF_6]$ were also studied.

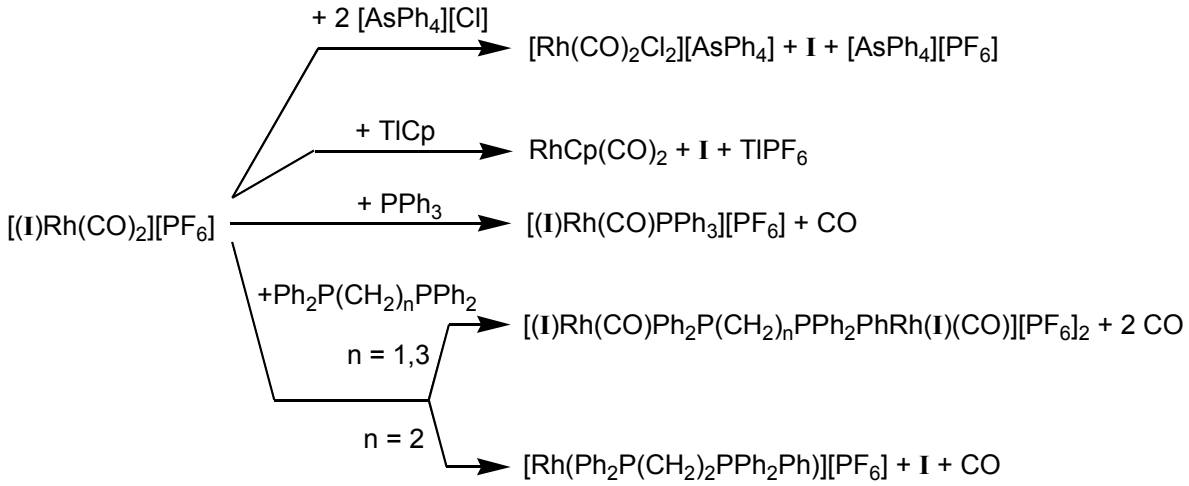

Figure 1-41. The reactions of $[(\mathbf{I})Rh(CO)_2][PF_6]$.

When the phosphines dppm and dppb were added to $[(\mathbf{I})Rh(CO)_2][PF_6]$, the phosphine-bridged dimeric dicationic complexes, $[(\mathbf{I})Rh(CO)(\mu\text{-dppm})Rh(\mathbf{I})(CO)][PF_6]_2$ and $[(\mathbf{I})Rh(CO)(\mu\text{-dppb})Rh(\mathbf{I})(CO)][PF_6]_2$ were obtained (Figure 1-41).[21] An excess of ligand must be avoided in order to isolate these complexes. However, when dppe was treated

with [(**I**)Rh(CO)$_2$][PF$_6$], both **I** and the carbonyl ligands were displaced to give [Rh(dppe)$_2$][PF$_6$].[21]

The reaction of [(Cp*)Rh(acetone)$_3$][PF$_6$]$_2$ with **I** provided the sandwich complex, [(**I**)Rh(Cp*)][PF$_6$]$_2$, in 78% yield as shown in Figure 1-42.[21] The ^{1}H and ^{13}C NMR spectra confirm this assignment. In contrast to the other complexes of rhodium discussed above, the ^{1}H NMR spectrum of this sandwich complex had only one chemical shift for the C_5H_4 ring protons of **I**.[21]

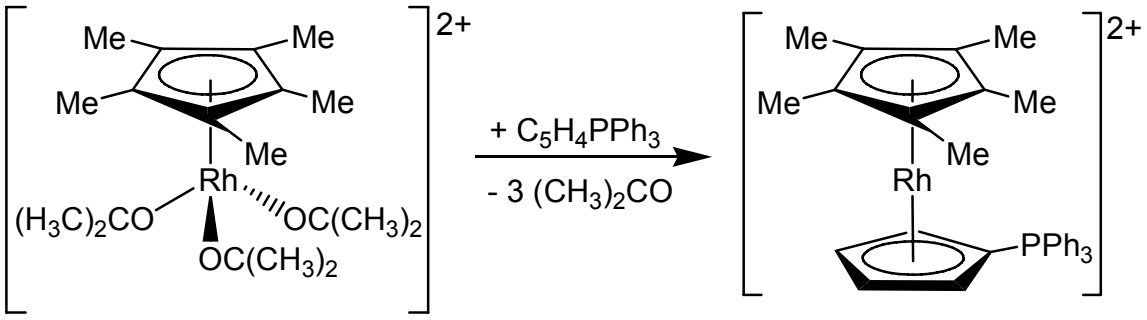

Figure 1-42. The synthesis of the sandwich complex [(I)Rh(Cp*)][PF$_6$]$_2$.

As part of a study on the cyclotrimerization of acetylenes catalyzed by various (η^5-Cp)Rh complexes, the complex, [(**I**)Rh(CO)$_2$][PF$_6$], was examined for its catalytic prowess in this reaction.[60] Dimethylacetylenedicarboxylate (DMAD) and 3-hexyne were used as the alkynes in this study. In the catalysis of the trimerization of DMAD, it was determined that a potential reaction of the catalyst with the acetylene was occurring based upon deviation from first order behaviour; however, this postulate was not confirmed.[60] The rate of cyclotrimerization of DMAD occurred in the following order: [(**I**)Rh(CO)$_2$][PF$_6$] < [(η^5-Cp)Rh(CO)$_2$] < [(η^5-Cp*)Rh(CO)$_2$].[60] All rates were in the same order of magnitude. In the trimerization of 3-hexyne, [(**I**)Rh(CO)$_2$][PF$_6$] again

proved to have the lowest rate of catalysis when compared to the same catalysts mentioned above. No side reaction appeared to be occurring between the catalyst and the monomer in this trimerization.[60] Yields and conversions were not reported for the cyclotrimerizations with [(**I**)Rh(CO)$_2$][PF$_6$].

This group of metals provides the first and, to date, only examples of the use of Ramirez ylide-derived metal complexes in catalysis.[18, 60] With the importance of metallocene catalysts in a variety of applications, it is surprising that so few reports of catalysis using Ramirez-derived complexes exist.

1.2.6 Group 10 Complexes

Only one report in the literature details the synthesis of nickel complexes, while several other papers detail the syntheses of palladium and platinum complexes.

Booth and Smith[23] reported the synthesis of two nickel complexes of the Ramirez ylide. When nickelocene and **I** were refluxed in chloroform in a 1:1 ratio followed by addition of NH_4PF_6, the nickelocene ylide analogue $[Ni(C_5H_4PPh_3)_2][PF_6]_2$, shown in Figure 1-43, was obtained in 37% yield; if the ratio of **I** to nickelocene is increased to 2:1, the complex was recovered in 86% yield.[23] In the ^{1}H NMR, only one multiplet, centred at δ 7.72, was observed.

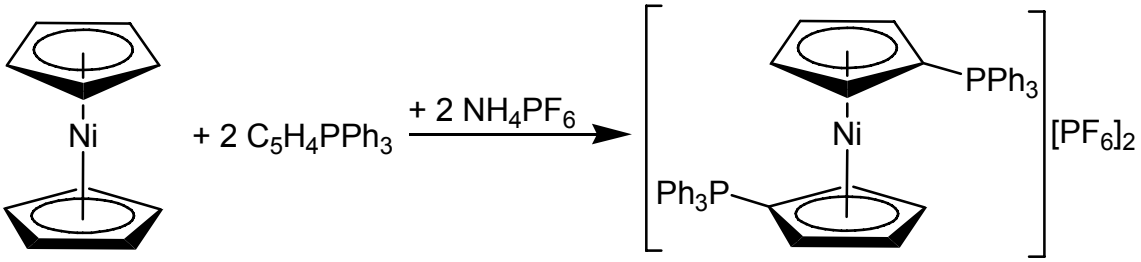

Figure 1-43. Reaction of paramagnetic nickelocene with I.

The C_5H_4 hydrogens may lie in this region of the spectrum, overlapped by the phenyl resonances, as witnessed in other complexes of **I**.[21] However, the solubility of the complex was very poor and peaks may not have been observed due to low concentration. Three peaks were observed in the ^{31}P NMR spectrum. Two singlets were seen: an intense peak at δ -15.6 and a very weak signal, at δ 11.7.[23] The second peak was explained as resulting from a rotamer of the ylide group, but his explanation seems unreasonable as hindered rotation is unlikely for this molecule. A septet resonance was also observed for the counter anion, PF_6^- (δ 144.7).[23] The material analyzed well for the reported formulation. The same complex could also be obtained by the reaction of $NiBr_2$ with **I**, followed by the addition of NH_4PF_6.[23] There are several problems with the report of this complex. Firstly, nickelocene is paramagnetic and the reported product of this reaction would also be paramagnetic; both complexes are 20 electron species. This would be a potential cause for the observation of the lack of the expected ^1H NMR peaks for the C_5H_4 protons in the ^1H NMR spectrum. However, the resolution observed in the ^{31}P NMR suggests that the reported product was not paramagnetic as the resolution of the spectrum of a paramagnetic species would most likely prevent the multiplicity of peaks to be observed. Secondly, if the signals in the ^{31}P NMR are so easily observed, the solubility of the compound was most likely not an issue in the lack of ^1H NMR signals for the C_5H_4 ring. Although the elemental analysis agrees with the formulation presented in the paper, the structural assignment of the product is probably incorrect.

In addition to the reaction of **I** with nickelocene, the reactions of **I** with $NiX_2(PPh_3)_2$ (X = Br, I) were examined.[23] $NiX_2(PPh_3)_2$ (X = Br, I) and **I** were stirred in chloroform, which generated a deep violet solution to which NH_4PF_6 was added. This

resulted in the precipitation of violet microcrystals which gave elemental analyses corresponding to the complex, $[(C_5H_4PPh_3)Ni(PPh_3)_2][PF_6]_2$.[23] The ^1H NMR again showed only a multiplet centred at δ 7.44.[23] No ^{31}P NMR data were provided.

The first report of palladium complexes of **I** appeared in 1976.[24] If the ylide, **I**, was treated with the oligomeric $(PdC_4(CO_2Me)_4)_n$, the monomeric complex $(C_5H_4PPh_3)Pd(C_4(CO_2Me)_4)$ (Figure 1-44) was collected in 79% yield.[24] ^1H NMR data and X-ray crystallography were provided to support this assignment.

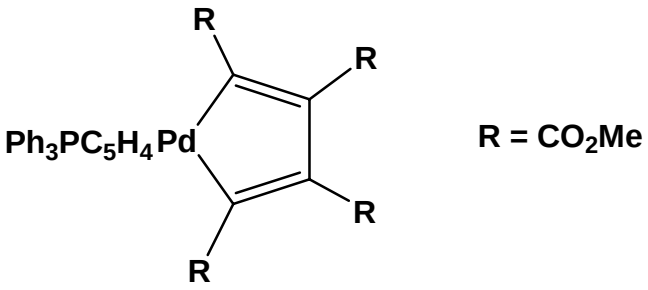

Figure 1-44. The structure of the complex $(C_5H_4PPh_3)Pd(C_4(CO_2Me)_4)$.

The ^1H NMR spectrum shows two sextets at δ 5.58 and δ 6.15. The difference between the shifts is greater than that observed in the Group VI tricarbonyl complexes. Pierpont *et al.* interpreted this shift difference to be due to the fact that the coordination of the C_5 ring was not consistent with η^5 bonding.[24] Variable temperature NMR of this complex was performed (25 °C and -97 °C) and showed that a decrease in the shift difference for the signals of the C_5 ring protons occurred, which indicated potential fluxionality of the bound ylide in the complex. However, the change observed in the ^1H NMR spectrum was minor and did not prove conclusive. The P-C_5 bond length (1.776(9) Å) showed elongation versus that of the free ylide.[24] The crystal structure of this complex also revealed that the Pd atom was bound asymmetrically to the C_5 ring of the ylide; the ylidic

carbon atom and the adjacent carbon have longer bond distances (2.447(6) and 2.429(6) Å) to the palladium atom than the other three carbons of the C_5 ring (2.399(6), 2.334(6) and 2.340 (6) Å).[24] The bond lengths of the C_5 ring are elongated versus the ylide **I**. The C_5 ring bond lengths also indicate some localization of single and double bond character, with some bond lengths approaching that of a C-C single bond (C(2)-C(3) = 1.47(1) Å, C(1)-C(5) = 1.46(1) Å).[24] This was taken to indicate a degree of localized coordination.[24] However, similar bond elongation and localization behaviour is seen in other complexes in which the C_5 ring is bound in an η^5 coordination mode.[15, 19] The values presented here seem to fall within the data presented for the other complexes.[15, 19] Steric interaction of the ylide Ph rings and the methyl carboxylate substituents of the palladacyclopentadiene are most likely related to the asymmetrical bond lengths seen in this structure.[24] These data were presented to suggest that this complex was the first in which the ylide **I** was bound in an η^3 manner. However, the Pd-C_5 ring distances are all close enough to indicate some type of bonding interaction with all carbons of the C_5 ring and the differences in Pd-C_5 bond lengths may be an artefact of steric interactions with the other palladium ligand.

Several palladium ylide complexes were subsequently reported by Hirai *et al.* in two papers which appeared in 1979.[25, 26] Cationic palladium diene (1,5-COD or nbd) complexes were prepared *in situ* by the reaction of (diene)$PdCl_2$ with two equivalents of $AgBF_4$ (or other similar silver salts).[26] These cationic complexes were then treated with **I** to furnish the complexes $[(\eta^5\text{-}C_5H_4PPh_3)Pd(diene)][BF_4]_2$ (53% yield for 1,5-COD and 64% for nbd) (Figure 1-45).[26] For these complexes, the ^1H NMR spectra revealed a much

smaller difference in the chemical shift for the C_5 ring protons (δ 0.22 for 1,5-COD and δ 0 for nbd) than was observed in the complex $(C_5H_4PPh_3)Pd(C_4(CO_2Me)_4)$.[26]

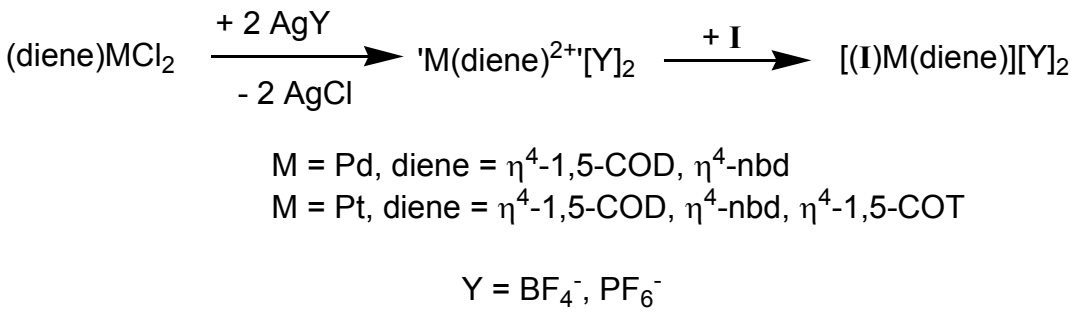

Figure 1-45. The synthesis of cationic palladium and platinum diene complexes of I.

The PF_6^- salts of these identical complexes were also later reported by Tresoldi *et al.*[22] This method was also extended by Hirai *et al.* to allylic phosphorus ylide and allylic complexes shown in Figure 1-46.[25] Moderate to good yields (53-79%) were obtained for all complexes. ^{1}H NMR data and elemental analyses support the synthesis of these complexes.[25]

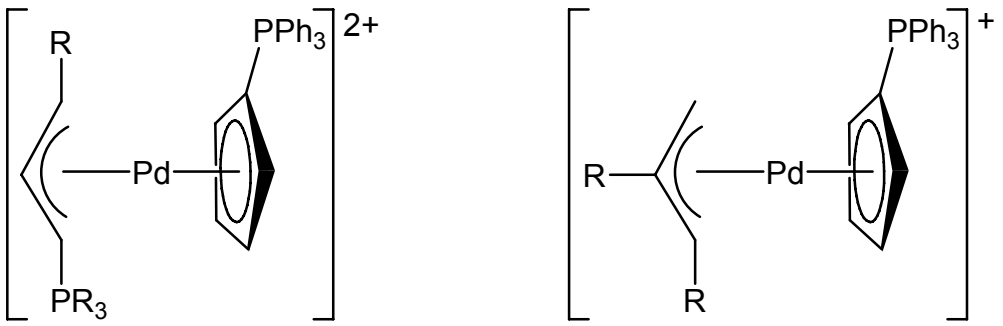

Figure 1-46. Palladium allyl ylide and allyl complexes of I.

Tresoldi *et al.*, also reported the synthesis of platinum diene complexes of **I**.[22] Using an identical procedure to that of Hirai *et al.*,[26] the solvated $[Pt(diene)][PF_6]_2$ species (diene = 1,5-COD, nbd and 1,5-cyclooctatetraene (COT)) were prepared *in situ*

and reacted with **I** (Figure 1-45).[22] The resulting complexes, [(η^5-$C_5H_4PPh_3$)Pt(diene)][PF_6]$_2$, were obtained in yields ranging from 58 to 72%. Based upon ^{1}H NMR chemical shifts, all three complexes have **I** bound to the Pt in an η^5 manner.[22] In solution, these complexes slowly lose diene. Attempts to prepare the methoxy derivative of the Pd or Pt complexes by reaction of **I** with [M(diene-OCH_3)(acetone)$_2$]$^+$, or by the treatment of the dicationic complexes with base in the presence of methanol, failed.[22]

Reactions of $Pd(PPh_3)_2Cl_2$ with the chelating 'fluorenyl' phosphorus ylides shown in Figure 1-9 (n = 1,2) were reported by Holy *et al*.[35] When n = 1, a complex with a structure similar to that reported for the Cr and W complexes (Figure 1-24) was obtained and is shown in Figure 1-47. IR, ^{1}H NMR and ^{31}P NMR were reported for the complex, substantiating the structure depicted in Figure 1-47. The ^{31}P NMR shows similar shifts for the two phosphorus atoms as seen in other complexes (Cr and W) with similar coordination modes.[35] The IR spectrum had two broad bands at 368 and 292 cm^{-1}, which are typical for *cis*-$PdCl_2$ units.[35] This work was also extended to platinum; $PtCl_2$ was reacted with the chelating 'fluorenyl' phosphorus ylide (n = 1) to provide the complex shown in Figure 1-47. This structural assignment was supported by the ^{31}P NMR spectrum which was similar to that of the palladium derivative.[35]

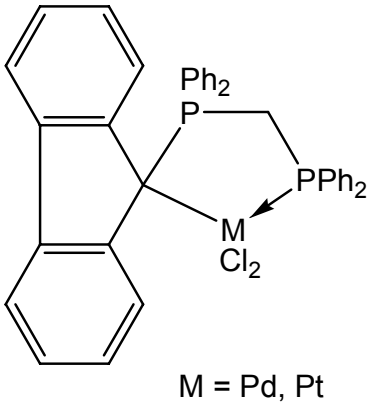

Figure 1-47. Palladium and platinum complexes of the chelating fluorenyl yilde.

When the ligand is changed to the ethylene bridged chelating 'fluorenyl' phosphorus ylide (Figure 1-9, n =2), a bis-ylide containing complex was obtained with the structure shown in Figure 1-48.[35] The IR spectrum of this complex had only one Pd-Cl band (352 cm^{-1}) which is virtually identical to that observed for K_2PdCl_4, indicating that the product most likely had a $PdCl_4^{2-}$ anion present.[35] The ^{31}P NMR spectrum revealed two triplet resonances.[35]

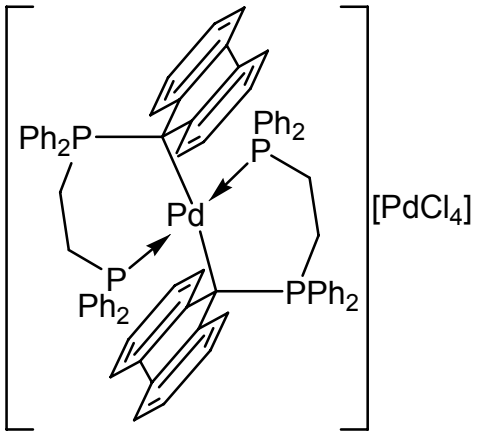

Figure 1-48. The palladium complex of the ethylene bridged chelating fluorenyl ylide.

1.2.7 Group 11 Complexes

The only report of phosphorus 'Cp' ylide complexes of Group 11 metals details the synthesis of the gold complex of the chelating propylene bridged bis-ylide (shown in Figure 1-9).[35] When Me_3PAuCl and this ylide were treated in a 1:1 ratio, the resulting gold complex, shown in Figure 1-49, was obatined in a yield of 30%. No absorption for the Au-Cl bond (usually found between 250-400 cm^{-1}) was observed in the IR spectrum.[35]

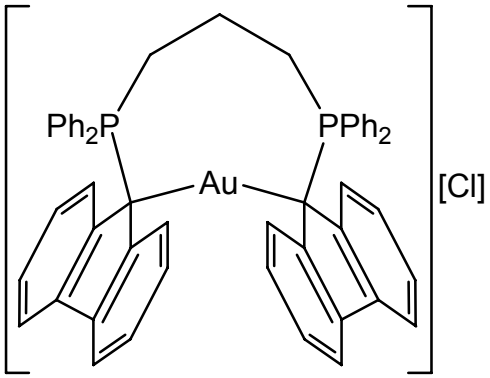

Figure 1-49. The proposed structure of the cationic gold chelating bis-ylide complex.

The ^{31}P NMR spectrum had only one resonance at δ 32.29, which is consistent with this structural assignment.[35] Elemental analysis was in agreement for the carbon content, but the hydrogen analysis was off by ~1%. In addition, no ^{1}H NMR data were provided, which is surprising because ^{31}P NMR data were collected for the complex. It is also reported that conductivity measurements support this assignment, but again, no data for these measurements were provided.[35] In summary, although this structural assignment is plausible, the information provided to substantiate it is incomplete.

1.2.8 Group 12 Complexes

Much like many of the other transition metal groups, there are few reports of phosphorus 'Cp' ylide complexes of the group 12 metals. In 1976, Holy *et al.* reported the synthesis and structure of mercury halide complexes of **I**.[28] When HgX_2 (X = Cl, Br, I) was stirred with **I** in THF, a precipitate was isolated in a yield of 55% (X = I) (Figure 1-50). The X-ray structure of the iodide was determined. In this complex, the C_5 ring is bound to the mercury atom in an η^1 coordination mode through a σ-bond to the β-carbon.

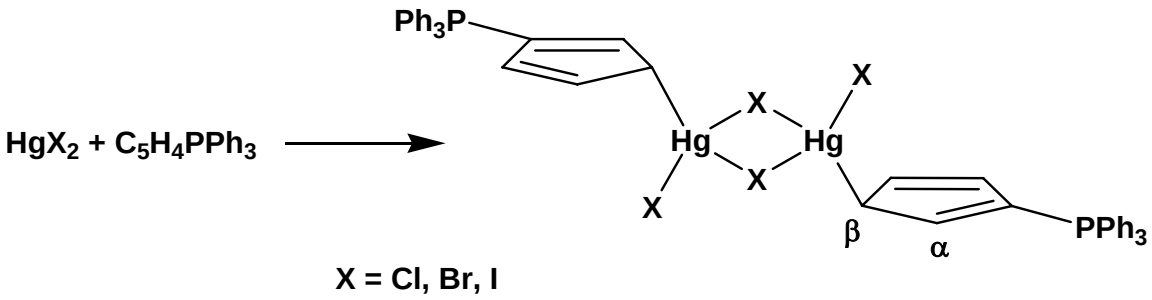

Figure 1-50. The synthesis of the η^1-$C_5H_4PPh_3$ mercury halide dimer complex.

The full structural data were reported in 1978.[61] This was the first report of **I** being bound in this coordination mode. The P-C_5 bond distance (1.748(7) Å) in this complex is elongated versus that of the P-C_5 bond distance in **I** (1.718(3) Å).[7, 28, 61] The C_5 ring bond distances are only nominally shorter than in the free ligand.[28, 61] The bonding at the β-carbon (see Figure 1-50 for labelling) was concluded to be due to potential steric interactions of the triphenylphosphonium group with the metal halide.[28] The α and β carbon peaks of the C_5 ring were broadened in the ^{13}C NMR spectrum of these complexes, giving evidence of fluxional bonding in solution.[28] These complexes represent the potential of this class of ligand to provide interesting structures by coordination in different bonding modes. A later report by Roberts detailed similar

reactions of **I** with mercuric halides followed by quenching of the solutions with KBr, but no conclusive spectroscopic or structural information was obtained.[29]

The reaction of one equivalent of $HgCl_2$ with two equivalents of the methylene bridged chelating fluorenyl ylide (Figure 1-9) was examined by Holy *et al*. who were able to isolate two products from the reaction; one product was soluble in THF, while the other precipitated out of solution.[35] The THF insoluble product was found to have an ylide:$HgCl_2$ ratio of 1:1.5, while the soluble product had a ratio of 1:2 (as determined by elemental analysis).[35] ^{31}P NMR was collected for the 1:2 complex and showed two peaks at δ 35.4 and –12.9. These resonances are similar to those observed for the group 6 complexes of this ligand and indicated that mercury was coordinated to both the pendant phosphorus and ylidic functions as shown in Figure 1-51. Conductivity measurements on this complex indicated that it was non-ionic and a cryoscopic molecular weight determination showed that the complex was monomeric (as opposed to the complex discussed above). Based upon this information, the proposed structure is shown in Figure 1-51.[35] ^{31}P NMR of the 1:1.5 complex showed a phosphine phosphorus shift substantially upfield from the shift in the 1:2 complex. Conductivity measurements showed that the complex was not ionic. Low solubility prevented the determination of the complex molecular weight. No structure of this complex was proposed.[35]

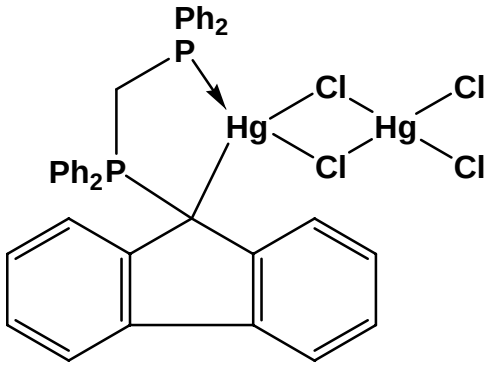

Figure 1-51. The proposed structure of the 1:2 mercury complex of the chelating methylene bridged fluorenyl ylide.

1.2.9 Thallium(III) Complexes

Roberts reported the reaction of **I** and $Tl(OCOCF_3)_3$ in trifluoroacetic acid (CF_3CO_2H).[29] It was determined that when **I** was dissolved in CF_3CO_2H, a product was obtained with the formula of $C_5H_4PPh_3 \cdot 2CF_3CO_2H$, for which the structure is unknown.[29] After 48 hours, a product was obtained which was identified by ^1H NMR spectroscopy to be represented by the structure shown in Figure 1-52.[29] The NMR data agree with coordination of thallium at this carbon. This structure was also consistent with the reaction of HgX_2 with **I** discussed above.[29] As with the mercury complexes, fluxional behaviour was observed as peak broadening was seen in the ^1H NMR spectrum.

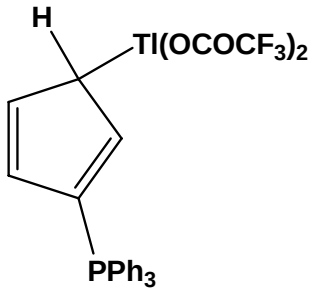

Figure 1-52. The thallium complex obtained from the reaction of I with $Tl(OCOCF_3)_3$.

1.3 Summary

A number of studies have been reported detailing the synthesis of ylide complexes of the Ramirez ylide and other related ylides. These works demonstrate that the ylide, upon coordination to a metal, generally adopts a structure most closely related to the resonance structure **Ib** (Figure 1-1). The few crystal structures available in the literature show that the P-C_5 bond length increases in length to approach that of a P-C single bond. In addition, the complexes of **I** mirror some of the chemistry seen in related Cp complexes. The ligand has also been shown to coordinate in a number of different modes with η^5 and η^1 coordination clearly demonstrated, η^3 potentially demonstrated, and η^2 and η^4 possible. The donor properties of **I** seem to fall between those of benzene and Cp^-.

In part, perhaps, because of difficulties in characterizing many of the compounds obtained, research in this area stagnated and virtually no publications dealing with the coordination chemistry of **I** have appeared in over two decades. This fact has been compounded by the lack of awareness in the community about this class of compound, which has resulted in some potentially interesting interpretations going unrealized. In addition, the reactivities of most of these compounds remain largely unexplored and the effects of ligand substitution on metal complex structures and reactivities have not been examined. This lack of exploration may have potentially arisen from the lack of a general synthetic preparation for this class of ligand. Given the enormous importance of Cp^- and related transition metal complexes, this lack of interest seems quite surprising.

Although significant contributions on this subject have been made, much interesting chemistry remains to be examined and discovered using this class of ligand. If

the weight of modern spectroscopic techniques is brought to bear on the some of the structural questions that have appeared in the literature, new insights may be garnered.

1.4 Other Cyclopentadienyl Ylides

Described above is a detailed review of the literature pertaining specifically to the phosphorus ylides of 'Cp' and 'Cp'-like compounds. Many other group 15 and 16 ylides have been reported including those of sulphur, arsenic and antimony.[12] Studies detailing their reactivities and their coordination chemistry have also been reported.[12, 16, 17, 29] Although these ylides are related to the phosphorus ylides, it is beyond the scope of this thesis to detail the unique chemistry of these ligands. The references cited in section 1.4 are but a few of the examples of the ylides themselves and some of their coordination chemistry.

1.5 Aims of the Current Research

Hoping to avoid the solubility problems apparently limiting development of the chemistry of **I**, we have chosen to investigate the mixed alkyl-aryl cyclopentadienylidene derivative **II** (Figure 1-53), which would also be more amenable to characterization by NMR spectroscopy. The free ylide, **II**, had been neither thoroughly characterized nor investigated with respect to its coordination chemistry.

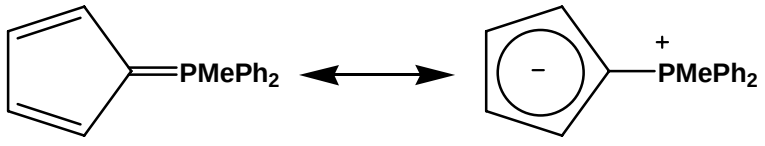

a **b**

II

Figure 1-53. The resonance structures of methyldiphenylcyclopentadienylide (II).

We have also undertaken the syntheses and characterization, and some chemistry of the group 6 compounds (η^5-$C_5H_4PMePh_2$)$M(CO)_3$ (M = Cr, Mo, W). This series was chosen for our study because the group 6 tricarbonyl complexes of **I** are known and we wished to be able to make direct comparisons of the coordination chemistry of **I** and **II**. We have also investigated, via *ab initio* calculations, the nature of the bonding in **II** and of its complex, (η^5-$C_5H_4PMePh_2$)$Cr(CO)_3$. Furthermore, electrochemical behaviour of the group 6 compounds (η^5-$C_5H_4PMePh_2$)$M(CO)_3$ (M = Cr, Mo, W) has been examined. Finally, we have also initiated a study on indenyl derived phosphorus ylides, which have yet to be used to synthesize any transition metal complexes. We report our results herein.

2 Experimental

2.1 General Conditions

All syntheses were carried out under a dry, deoxygenated argon atmosphere using standard Schlenk line techniques. Argon was deoxygenated by passage through a heated column of BASF copper catalyst, and then dried by passing through a column of 4Å molecular sieves. Handling and storage of air-sensitive organometallic compounds was done using an MBraun Labmaster glove box. NMR spectra were recorded using Bruker AV 300, AV 500 and AV 600 spectrometers. All ^{1}H and $^{13}C\{^{1}H\}$ NMR were referenced to carbons or residual protons present in the deuterated solvents with respect to TMS at δ 0. ^{31}P NMR was referenced to external 85% H_3PO_4. IR spectra were acquired on a Perkin Elmer Spectrum One FT-IR spectrometer at a spectral resolution of 4 cm^{-1}. Elemental analyses were conducted by Canadian Microanalytical Service Ltd. of Delta, BC.

Anhydrous methylene chloride, THF, diethyl ether, hexanes and toluene were purchased from Aldrich in 18 L reservoirs packaged under nitrogen, and were dried by passage through columns of activated alumina (Innovative Technology Solvent Purification System). THF, Et_2O and CH_2Cl_2 were then stored over 4Å molecular sieves to result in residual water concentrations that were lower than 20 ppm (Fischer Titration). NMR solvents used for organometallic compounds were degassed under vacuum and dried by passage through a small column of activated alumina before being stored over 4Å molecular sieves. All deuterated solvents were purchased from Cambridge Isotope Laboratories, Inc. or CDN Isotopes. Most chemicals were obtained from Aldrich or Strem and were used as received or purified by established procedures.

2.2 Crystal Structure Determination

X-ray crystal structure determinations were performed by Dr. Ruiyao Wang in the X-ray Crystallography Laboratory at Queen's University. Crystals were mounted on glass fibers with epoxy glue, and data collection was performed on a Bruker smart CCD 1000 X-ray diffractometer with graphite-monochromated Mo K_α radiation (λ = 0.71073 Å) controlled with Crysostream Controller 700. No significant decay was observed during data collections. Data were processed on a Pentium PC using the Bruker AXS Crystal Structure Analysis Package, Version 5.10.[62] Neutral atom scattering factors were taken from Cromer and Waber.[63] The raw intensity data were converted (including corrections for scan speed, background and Lorentz and polarization effects) to structure amplitudes and their esds using the program SAINT, which corrects for *L*p and decay. Absorption corrections were applied using the program SADABS. All non-hydrogen atoms were refined anistropically. The positions for all hydrogen atoms were calculated (unless otherwise stated) and their contributions were included in the structure factors and calculations.

In the case of $[Cr(\eta^5\text{-}C_5H_4PMePh_2)(CO)_3]_2[B(C_6F_5)_4]_2$, the hydrogen atoms on one of the dichloromethane molecules were located from the difference Fourier map but all of the other hydrogen atoms were calculated and their contributions were included in the structure factor calculations. For $[Mo(\eta^5\text{-}C_5H_4PMePh_2)(CO)_3]_2[B(C_6F_5)_4]_2$, the positions of all non-hydrogen atoms were refined anisotropically. The positions for all hydrogen atoms were calculated and their contributions were included in the structure factor calculations. However, the structure can only be refined to R1~13% with a THF molecule disordered. ROTAX[64] was thus used to find the twin law. The twin law [1 0 0 0 -1 0 -

0.252 0 –1] of merit (f.o.m.) 2.48 for 180° rotation was applied to the refinement and the R1 dropped to ~10%. The crystal was thus considered to be merohedrally twinned. SQEEZE[65] was then applied to squeeze out the 1.5 THF molecule, which lead to R1~8.8%. For $[W(\eta^5\text{-}C_5H_4PMePh_2)(CO)_3]_2[B(C_6F_5)_4]_2$, the disordered THF solvent molecule was refined with DFIX, EADP and PART.

In $(\eta^5\text{-}C_9H_6PMePh_2)Cr(CO)_3$, difference electron density maps revealed the presence of disordered lattice solvate molecules, which were ultimately modeled through the use of the SQUEEZE subroutine of the PLATON software suite.[65] Two solvent accessible voids per lattice were found, comprising an equal volume of 203.1 $Å^3$ and contributing a total of 38.8 electrons. The voids were thus assigned to two disordered CH_2Cl_2 molecules. Each CH_2Cl_2 has 42 electrons, and occupies about 60 $Å^3$ in space theoretically. The larger volume of the void in the crystal may be a result of the disorder. The contributions have been included in all derived crystal quantities although the precise composition of the lattice solvate is somewhat speculative.

2.3 The Evans Method

To perform measurements using the Evans method,[66-70] the procedure described below was used. A sample of dried and degassed cyclohexane was weighed into a vial and the volume of sample was determined from its density. To this was added a measured volume of the NMR solvent (~1 mL of either CD_2Cl_2 or THF-d_8). The v/v amount of cyclohexane was approximately 1-5%. This solvent mixture was used for both dissolving the sample and for use in the capillary tubes. The analyte was weighed into the NMR tube (~30-40 mg of $[(\eta^5\text{-}C_5H_4PMePPh_2Cr(CO)_3]_2[B(C_6F_5)_4]_2$). The sample was then dissolved

in the solvent mixture (~0.5 mL). Two capillary tubes were filled with the solvent mixture and placed in the NMR tube (using one capillary did not give a strong enough reference signal). The capillary tubes and the volume of solvent in the tubes extended well above the analyte solution and were not sealed; samples were not inverted after this point. The NMR tube was then capped and the ^{1}H NMR spectrum was recorded and the difference between the reference peaks of the solution and the reference peaks of the capillary solution were calculated and used in further calculations.

2.4 Ab Initio Calculations

All molecular calculations were performed by Hartmut Schmider of the High Performance Computing Virtual Laboratory at Queen's University. To gain information on the electronic structures of $C_5H_4PMePh_2$ (**II**) and (η^5-C_5H_4)$PMePh_2Cr(CO)_3$ (**III**), and also to compare the ylide-metal bonding in **III** with the (η^6-C_6H_6)-metal bonding in (η^6-C_6H_6)$Cr(CO)_3$, a series of *ab initio* calculations was performed on **II** and **III**, employing the Gaussian 03 suite of programs.[71] Using the crystal structures as initial starting points, optimized structures were obtained with the B3LYP[72-74] functional on a self-consistent hybrid-DFT level of calculation in a standard "split valence" 6-31G* basis.[75-78] Using these structures, we then obtained further results at three levels of computation: B3LYP, restricted Hartee-Fock (RHF), and second-order Mollar-Plesset Perturbation Theory (MP2); as well as in two basis sets: the "split valence" 6-31G* basis, and Dunning's correlation consistent double-zeta basis[79, 80] with the chromium atom represented in a Wachters-Hay basis.[81, 82]

2.5 Syntheses involving the Ligand, $C_5H_4PMePh_2$ (II)

2.5.1 Synthesis of $C_5H_4PMePh_2$ (II)

A suspension of 20.0 g of TlCp (0.074 mol) in 200 mL of ether was treated drop wise with 13.3 mL of Ph_2PCl (0.073 mol). As the reaction proceeded, the flask warmed and the solution turned slightly yellow. After stirring for 1 h, the reaction was filtered to remove TlCl, and the phosphine, $P(C_5H_5)Ph_2$, was immediately treated *in situ* with 4.5 mL of MeI (0.072 mol). As the alkylation reaction proceeded, a colourless product precipitated. The reaction mixture was stirred for 3 h and 22.9 g of the colourless phosphonium salt ($[PMe(C_5H_5)Ph_2]I$) was collected by filtration in 81% yield. The product was impure (NMR), but attempts to purify it proved fruitless and the salt was therefore used as obtained in the next step.

To prepare **II**, a suspension of 10.1 g of $[PMe(C_5H_5)Ph_2]I$ (0.026 mol) in 150 mL of THF was cooled in an ice bath and treated drop wise with 17.7 mL of 1.6 M *n*-BuLi in hexanes (0.028 mol). As the *n*-BuLi was added, the solution warmed and the solid disappeared, generating a deep orange-red solution. The reaction was stirred until no solid remained, at which point the reaction was hydrolyzed by the addition of 20 mL of H_2O. This caused the formation of a colourless solid, while the solution turned yellow. The organic layer was decanted and the aqueous layer was washed with 3×75 mL of toluene. The organic layers were combined and the solvent was removed *in vacuo* to yield an orange solid which was extracted with 200 mL of ethyl acetate and passed through a silica column using ethyl acetate as the eluant. The yellow band was collected and the solvent was removed under reduced pressure to yield 2.1 g (30% based upon phosphonium salt) of $C_5H_4PMePh_2$ (**II**) as a yellow powder. X-ray quality crystals and

were obtained by crystallization from CH_2Cl_2 solution at –30° C by layering with hexanes. This procedure has been repeated 20 times with yields ranging from 20-35%. ^{1}H NMR of **II** ($CDCl_3$, 500 MHz): δ 7.64-7.59 (6H, m, Ph), 7.52-7.49 (4H, m, Ph), 6.44 (2H, m, P-C-CH-C*H*), 6.29 (2H, m, P-C-C*H*-CH), 2.37 (3H, d, $^2J_{H-P}$ 13.2 Hz, Me). ^{13}C NMR ($CDCl_3$, 125 MHz): δ 132.6 (d, $^4J_{P-C}$ 2.1 Hz, *p*-Ph), 132.3 (d, J_{P-C} 10.6 Hz, Ph), 129.0 (d, J_{P-C} 11.5 Hz, Ph), 127.5 (d, $^1J_{P-C}$ 88.3 Hz, *ipso*-Ph), 114.9 (d, $^2J_{P-C}$ 16.3 Hz, P-C-*C*H-CH), 114.3 (d, $^3J_{P-C}$ 17.3 Hz, P-C-CH-*C*H), 79.2 (d, $^1J_{P-C}$ 114.2 Hz, P-*C*), 12.6 (d, $^1J_{P-C}$ 63.3 Hz, Me). ^{31}P NMR ($CDCl_3$, 121 MHz): δ 7.95. Anal: Found C 80.76, H 6.56. Calculated C 81.80, H 6.48.

2.5.2 Synthesis of (η^5-$C_5H_4PMePh_2$)$M(CO)_3$ (M = Cr (III), Mo (IV) and W (V))

A solution of 0.39 g of **II** (1.5×10^{-3} mol) and 0.96 g of $Cr(CO)_6$ (4.4×10^{-3} mol) in 30 mL of diglyme was refluxed under argon for 3 h, during which time the solution developed a black-green colour. The reaction was cooled and filtered, and the solid residue was washed with 3×10 mL of diglyme. The resulting filtrate was then treated with 200 mL of hexanes to precipitate a yellow solid that was collected and washed with hexanes (3×10 mL). The solid was dried *in vacuo* to yield 0.35 g (61%) of yellow product. X-ray quality crystals and analytically pure material were obtained by crystallization from CH_2Cl_2 solution at –30°C by layering with hexanes. ^{1}H NMR (CD_2Cl_2, 500 MHz): δ 7.75-7.63 (10H, m, Ph), 4.90 (2H, br, P-C-CH-C*H*), 4.71 (2H, br, P-C-C*H*-CH), 2.55 (3H, d, $^2J_{H-P}$ 13.2 Hz, Me). ^{13}C (CD_2Cl_2, 125 MHz): δ 241.8 (Cr-*C*O), 134.8 (d, $^4J_{P-C}$ 2.2 Hz, *p*-Ph), 133.3 (d, J_{P-C} 11.1 Hz, Ph), 130.2 (d, J_{P-C} 12.3 Hz, Ph), 123.1 (d, $^1J_{P-C}$ 90.2 Hz, *ipso*-Ph), 89.9 (d, $^2J_{P-C}$ 13.4 Hz, P-C-*C*H-CH), 87.5 (d, $^3J_{P-C}$ 13.4

Hz, P-C-CH-*C*H), 65.8 (d, $^{1}J_{P-C}$ 111.4 Hz, P-C), 12.8 (d, $^{1}J_{P-C}$ 65.7 Hz, Me). ^{31}P (CD_2Cl_2, 121 MHz): δ 19.54. Anal: Found C 62.51, H 4.17. Calculated C 63.01, H 4.28. IR (CH_2Cl_2): 1915, 1812 cm^{-1}.

The compound (η^5-$C_5H_4PMePh_2$)$Mo(CO)_3$ (**IV**) was prepared and purified similarly using 0.40 g of **II** (1.5×10^{-3} mol) and 1.21 g of $Mo(CO)_6$ (4.6×10^{-3} mol). The yellow product was obtained in 60 % yield (0.41 g). ^{1}H NMR (CD_2Cl_2, 500 MHz): δ 7.77 (2H, t, $^{3}J_{H-H}$ 7.1 Hz, Ph), 7.71-7.62 (8H, m, Ph), 5.48 (2H, m, P-C-CH-C*H*), 5.29 (2H, m, P-C-C*H*-CH), 2.55 (3H, d, $^{2}J_{H-P}$ 13.6 Hz, Me). ^{13}C (CD_2Cl_2, 125 MHz): δ 231.2 (Mo-*C*O), 135.0 (d, $^{4}J_{P-C}$ 2.9 Hz, *p*-Ph), 133.4 (d, J_{P-C} 10.6 Hz, Ph), 130.2 (d, J_{P-C} 12.5 Hz, Ph), 122.5 (d, $^{1}J_{P-C}$ 90.2 Hz, *ipso*-Ph), 94.5 (d, $^{2}J_{P-C}$ 14.4 Hz, P-C-*C*H-CH), 92.1 (d, $^{3}J_{P-C}$ 12.5 Hz, P-C-CH-*C*H), 71.8 (d, $^{1}J_{P-C}$ 109.4 Hz, P-*C*), 14.4 (d, $^{1}J_{P-C}$ 66.2 Hz, Me). ^{31}P (CD_2Cl_2, 121 MHz): δ 18.25. Anal: Found C 56.81, H 3.76. Calculated C 56.77, H 3.86. IR (CH_2Cl_2): 1918, 1812 cm^{-1}.

The tungsten analogue (η^5-$C_5H_4PMePh_2$)$W(CO)_3$ (**V**) was prepared by reacting 0.11 g of **II** (4.1×10^{-4} mol) and 0.40 g of $W(MeCN)_3(CO)_3$ (1.0×10^{-3} mol) in 20 mL of diglyme at 110 °C for 40 h. The solution turned a black-green colour and a black precipitate formed. The reaction was cooled, the solvent was removed under reduced pressure, and the resulting grey-green solid was dissolved in degassed $CHCl_3$ and passed through an alumina column under an argon atmosphere. The yellow band was collected and the solvent was removed *in vacuo* to yield 0.15 g (70%) of yellow product. X-ray quality crystals and analytically pure material were obtained by crystallization from CH_2Cl_2 solution at –30° C by layering with hexanes. ^{1}H NMR (CD_2Cl_2, 500 MHz): δ 7.78 (2H, t, $^{3}J_{H-H}$ 7.0 Hz, Ph), 7.71-7.62 (8H, m, Ph), 5.46 (2H, m, P-C-CH-C*H*), 5.21

(2H, m, P-C-C*H*-CH), 2.56 (3H, d, $^{2}J_{H-P}$ 13.6 Hz, Me). ^{13}C (CD_2Cl_2, 125 MHz): δ 221.1 (W-*C*O), 135.1 (d, $^{4}J_{P-C}$ 2.1 Hz, *p*-Ph), 133.6 (d, J_{P-C} 10.7 Hz, Ph), 130.3 (d, J_{P-C} 12.9 Hz, Ph), 121.9 (d, $^{1}J_{P-C}$ 90.3 Hz, *ipso*-Ph), 91.4 (d, $^{2}J_{P-C}$ 14.0 Hz, P-C-*C*H-CH), 89.6 (d, $^{3}J_{P-C}$ 11.8 Hz, P-C-CH-*C*H), 70.5 (d, $^{1}J_{P-C}$ 109.6 Hz, P-*C*), 14.5 (d, $^{1}J_{P-C}$ 65.5 Hz, Me). ^{31}P (CD_2Cl_2, 121 MHz): δ 18.58. Anal: Found C 48.34, H 3.14. Calculated C 47.40, H 3.22. IR (CH_2Cl_2): 1912, 1808 cm^{-1}.

2.5.3 Synthesis of $[(\eta^5\text{-}C_5H_4PMePh_2)Mo(CO)_3I][I]$ (VI)

A solution of 0.040g of I_2 (1.6×10^{-4} mol) in 10 mL of CH_2Cl_2 was slowly added to a solution of 0.070 g of **IV** (1.6×10^{-4} mol) in 10 mL of CH_2Cl_2; on addition of the I_2, the yellow solution became bright orange. The reaction mixture was stirred for 30 min and then filtered, and the solvent was removed from the filtrate *in vacuo* to give 0.059 g of red product (54%). X-ray quality crystals and analytically pure material were obtained by crystallization from CH_2Cl_2 solution at –30° C by layering with hexanes. ^{1}H NMR (CD_2Cl_2, 300 MHz): δ 7.87-7.67 (10H, m, Ph), 6.43 (2H, m, P-C-CH-C*H*), 6.04 (2H, m, P-C-C*H*-CH), 3.12 (3H, d, $^{2}J_{H-P}$ 13.6 Hz, Me). ^{13}C NMR (CD_2Cl_2, 125 MHz): δ 229.3 (Mo-*C*O), 216.3 (Mo-*C*O), 136.4 (d, $^{4}J_{P-C}$ 3.8 Hz, *p*-Ph), 133.5 (d, J_{P-C} 11.5 Hz, Ph), 131.2 (d, J_{P-C} 13.4 Hz, Ph), 119.6 (d, $^{1}J_{P-C}$ 91.1 Hz, *ipso*-Ph), 104.1 (d, $^{2}J_{P-C}$ 11.5 Hz, P-C-*C*H-CH), 97.5 (d, $^{3}J_{P-C}$ 8.6 Hz, P-C-CH-*C*H), 87.0 (d, $^{1}J_{P-C}$ 95.0 Hz, P-*C*), 11.7 (d, $^{1}J_{P-C}$ 58.5 Hz, Me). ^{31}P NMR (CD_2Cl_2, 121 MHz): δ 21.08. Anal: Found C 35.58, H 3.12. Calculated C 36.13, H 2.45. IR (CH_2Cl_2): 2055, 1979 cm^{-1}.

2.5.4 Attempted Reactions of IV with MeI and H_2

To a solution of 0.24 g of **IV** (5.3×10^{-4} mol) in 20 mL of THF was added 0.75 g of MeI (5.3×10^{-4} mol). The solution was stirred for 22 h, with neither colour change nor change in the IR spectrum being observed. Similarly, no reaction was observed on bubbling H_2 through a solution of **IV** in THF for 6 h.

2.5.5 Attempted thermal and photochemical reactions of III and IV with PPh_3

Solutions of either **III** or **IV** and 1 equiv of PPh_3 in 20 mL of THF were refluxed for 20 h while being monitored by IR spectroscopy. Similarly, solutions of **IV** and either 1 or 3.5 equiv of PPh_3 in 20 mL of CH_2Cl_2 were photolyzed with UV light from a Hanovia lamp for 20 h during which time the experiments were monitored by IR. No changes in the IR spectra were observed. A similar photochemical experiment with 1 equiv of PMe_3 had the same result.

2.5.6 Photochemical reaction of IV with 3.5 equivalents of PMe_3

A solution of **IV** and 3.5 equivalents of PMe_3 in 20 mL of CH_2Cl_2 was photolyzed with UV light from a Hanovia lamp while being monitored by IR spectroscopy. After 18 h, the IR spectrum showed that the peaks of **IV** had disappeared and had been replaced by new peaks at 1830 cm^{-1} and 1930 cm^{-1}. After removal of the solvent, the residue was dissolved in CD_2Cl_2 and the ^1H and ^{31}P NMR spectra were recorded. Free ligand peaks of **II** were observed in both the ^1H and ^{31}P NMR spectra while a new peak in the ^{31}P NMR spectrum corresponds to the resonance of the previously reported *fac*-$Mo(PMe_3)_3(CO)_3$ complex (δ –17 ppm).[83]

2.5.7 Synthesis of $[Cr(\eta^5\text{-}C_5H_4PMePh_2)(CO)_3]_2[B(C_6F_5)_4]_2$ ($[III_2][B(C_6F_5)_4]_2$)

A solution of 0.110 g of **III** (1.3×10^{-4} mol) and 0.051 g of $[FeCp_2][B(C_6F_5)_4]$ (1.3×10^{-4} mol) in 5 mL of CH_2Cl_2 was stirred for 30 min during which time it changed from deep green to yellow-brown. The solution was then layered with 30 mL of hexanes and cooled to –30°C to give green crystals which were filtered and washed with 3 × 20 mL of hexanes. Yield 0.104 g (76 %). Anal: found C 46.90, H 1.57; calc for $C_{90}H_{34}B_2F_{40}P_2O_6Cr_2{\cdot}3CH_2Cl_2$ 47.45, H 1.64. IR data are given in Table 4. ^{1}H NMR (CD_2Cl_2, 298 K, 600 MHz): δ 28.80 (2H, br s, C_5H_4), 13.65 (2H, br s, C_5H_4), 7.85-7.60 (10H, br, *Ph*), 1.18 (3H, br, *Me*). ^{1}H NMR (THF-d_8, 298 K, 600 MHz): δ 26.08 (2H, br, C_5H_4), 13.62 (2H, br, C_5H_4), 8.07-7.66 (10H, *Ph*), 2.34 (3 H, br s, *Me*). ^{1}H NMR (THF-d_8, 213 K, 600 MHz): δ 7.95-7.75 (10H, m, *Ph*), 6.12 (1H, br, C_5H_4), 5.96 (1H, br, C_5H_4), 5.85 (1H, br, C_5H_4), 5.65 (1H, br, C_5H_4), 2.89 (3H, br, *Me*). High Res. ES-MS (THF): found 400.0320 m/z; calc 400.0348 (diff 6.8926 ppm) MS-MS experiments showed that the peak at 400 m/z (target ion) was responsible for the fragment at 316 m/z (loss of 84 amu = loss of 3CO).

2.5.8 Synthesis of $[Mo(\eta^5\text{-}C_5H_4PMePh_2)(CO)_3]_2[B(C_6F_5)_4]_2$ ($[IV_2][B(C_6F_5)_4]_2$)

In a procedure similar to that described above, a solution of 0.096 g of **IV** (2.2×10^{-4} mol) and 0.186 g of $[FeCp_2][B(C_6F_5)_4]$ (2.2×10^{-4} mol) in 10 mL of THF was stirred for 30 min, turning from reddish-green to red. The resulting solution was layered with 30 mL of hexanes and cooled to –30°C to yield a red oil which slowly solidified. The oil was washed with 3 × 15 mL of hexanes and dried *in vacuo* to give a red solid in a yield of 0.207 g (86%). X-ray quality crystals were grown from a solution of the red material in a

1:4 mixture of CH_2Cl_2:THF layered with hexanes and kept at -30°C. Anal: found C 47.30, H 1.67; calc for $C_{90}H_{34}B_2F_{40}P_2O_6Mo_2$ 48.12, H 1.53. IR data are given in Table 4. ^{1}H NMR (THF-d_8, 298 K, 600 MHz): δ 7.87-7.72 (10 H, m, *Ph*), 6.10-6.04 (2H, br m, C_5H_4) and 5.91 (2H, br m, C_5H_4), 2.88 (3H, d, *Me*, $^2J_{P-H}$ 11.0 Hz). ^{31}P NMR (THF-d_8, 121 MHz): δ 19.88. ^{13}C NMR (THF-d_8, 150 MHz): δ 231.5 (*C*O), 224.8 (*C*O), 149.4 (m, *o*-C_6F_5), 139.4 (m, *p*-C_6F_5), 138.3 (m, *m*-C_6F_5), 136.7 (br s, *p*-Ph), 133.7 (d, J_{P-C} 11.0 Hz, Ph), 131.5 (d, J_{P-C} 13.2 Hz, Ph), 125.6 (br m, *ipso*-C_6F_5), 121.7 (d, J_{P-C} 90.0 Hz, *ipso*-Ph), 103.0 (d, J_{P-C} 8.8 Hz, PC*C*HCH), 97.2 (d, J_{P-C} 11.0 Hz, PCCH*C*H), 86.1 (d, J_{P-C} 94.4 Hz, P*C*CHCH), 8.4 (d, J_{P-C} 60.4 Hz, Me). High Res. ES-MS (THF): found: 445.9969 m/z; calc 445.9988 (diff 4.1748 ppm).

2.5.9 Synthesis of $[W(\eta^5\text{-}C_5H_4PMePh_2)(CO)_3]_2[B(C_6F_5)_4]_2$ ($[V_2][B(C_6F_5)_4]_2$)

A solution of 0.088 g of **V** (1.7×10^{-4} mol) and 0.143 g of $[FeCp_2][B(C_6F_5)_4]$ (1.7×10^{-4} mol) in 10 mL of THF was stirred for 30 min. The resulting solution was layered with 30 mL of hexanes and cooled to –30°C to yield a red oil which slowly solidified. The oil was washed with 3 × 15 mL of hexanes and dried *in vacuo* to give a red solid in a yield of 0.155 g (77%). X-ray quality crystals were grown from a dilute THF solution (~20 mg in 1.5 mL of THF) layered with hexanes and kept at room temperature. Anal: found C 44.67, H 1.94; calc for $C_{90}H_{34}B_2F_{40}P_2O_6W_2$ 44.62, H 1.41. IR data are given in Table 4. ^{1}H NMR (THF-d_8, 298 K, 600 MHz): δ 7.80-7.71 (10H m, *Ph*), 6.05 (4H, br m, C_5H_4), 2.86 (3H, br d, $^2J_{P-H}$ 12.8 Hz, Me). ^{13}C NMR (THF-d_8, 150 MHz): δ 218.5 (s, *C*O), 211.7 (s, *C*O), 149.4 (m, *o*-C_6F_5), 139.4 (m, *p*-C_6F_5), 137.3 (m, *m*-C_6F_5), 136.8 (d, J_{P-C} 2.8 Hz, *p*-Ph), 133.8 (d, J_{P-C} 12.5 Hz, Ph), 131.5 (d, J_{P-C} 13.9 Hz, Ph), 125.6 (br m, *ipso*-

C_6F_5), 121.4 (d, J_{P-C} 90.2 Hz, *ipso*-Ph), 102.8 (d, J_{P-C} 8.3 Hz, PC*C*HCH), 94.4 (d, J_{P-C} 11.1 Hz, PCCH*C*H), 84.3 (d, J_{P-C} 97.1 Hz, P*C*CHCH), 8.4 (d, J_{P-C} 59.6 Hz, Me). ^{31}P NMR (THF-d_8, 121 MHz): δ 20.76. High Res. ES-MS (THF): found 532.0424 m/z; calc 532.0406 (diff 3.5448 ppm).

2.5.10 Oxidation of III with $[Ph_3C][B(C_6F_5)_4]$

A solution of 0.400 g of **III** (9.99×10^{-4} mol) and 0.968 g of $[Ph_3C][B(C_6F_5)_4]$ (1.05×10^{-3} mol) in 15 mL of THF was stirred for 30 min, the green solution slowly turning yellow. The solution was then layered with ~100 mL of hexanes and cooled to –30° C, and a green solid precipitated and was separated from the supernatant. The solid was washed 4 × 10 mL of hexanes before being dried *in vacuo* to yield 0.917 g (85%) of $[Cr(\eta^5\text{-}C_5H_4PMePh_2)(CO)_3]_2[B(C_6F_5)_4]_2$. This material had an IR spectrum to identical to that of the material prepared using $[FeCp_2][B(C_6F_5)_4]$ as oxidant.

2.5.11 Oxidation of III with $[FeCp_2][PF_6]$

A solution of 0.130 g of **III** (3.25×10^{-4} mol) and 0.108 g of $[FeCp_2][PF_6]$ (3.25×10^{-4} mol) in 10 mL of THF was stirred for 1.5 h, turning to a deep brownish-yellow-green colour. As the reaction proceeded, it was monitored by IR spectroscopy which showed the growth of peaks at 2030, 1941 and 1906 cm^{-1}, identical to those of the $[Cr(\eta^5\text{-}C_5H_4PMePh_2)(CO)_3]_2[B(C_6F_5)_4]_2$ obtained using $[FeCp_2][B(C_6F_5)_4]$, and a new set of peaks (already present after 5 min) at 1917, 1821 and 1808 cm^{-1}.

2.5.12 Attempted Synthesis of $[(C_5H_4PMePh_2)_2TiCl_2][Cl]_2$

A 1.0 M solution of $TiCl_4$ in toluene (0.17 mL, 1.69×10^{-4} mol) was added to a stirred solution of **II** (0.122 g, 4.24×10^{-4} mol) in 5 mL of THF resulting in the formation of a red solution from the initial yellow colouration of **II** in THF. The solution was stirred for 30 minutes, during which no further observable change was noted. The solution was then layered with 15 mL of hexanes and stored at -30°C. This resulted in the precipitation of a red precipitate. ^{1}H and ^{31}P NMR spectra were recorded in CD_2Cl_2. The NMR spectra showed that several products had formed, with several prominent resonances in the ^{31}P spectrum.

2.5.13 Attempted Synthesis of $[(C_5H_4PMePh_2)_2TiCl_2][I]_2$

$(C_5H_4PPh_2)_2TiCl_2$ was synthesized by the addition of two equivalents of $LiC_5H_4PPh_2$ to $TiCl_4$ according to the preparation of Leblanc *et al.*.[84] 0.253 g of $(C_5H_4PPh_2)_2TiCl_2$[84] (4.10×10^{-4} mol) and 1.16 g of MeI (0.51 mL, 8.20×10^{-3} mol) was dissolved in 20 mL of THF and refluxed for 20 hours. As the reaction proceeded, a precipitate formed from the red solution. The reaction was allowed to cool before the solvent was decanted from the precipitate. The red precipitate was washed further with Et_2O (3×10 mL) before being dried *in vacuo* resulting in the collection of 0.264 g of solid. ^{1}H NMR and ^{31}P NMR were collected in CD_2Cl_2. The NMR spectra showed that several products had formed, with three prominent resonances in the ^{31}P spectrum. Attempts to purify the resulting mixture by recrystallization from a CH_2Cl_2 solution layered with hexanes at -30°C resulted in the formation of a red oil.

2.5.14 Attempted Synthesis of $[(C_5H_4PBzPh_2)_2TiCl_2][Cl]_2$

0.2766 g of $(C_5H_4PPh_2)_2TiCl_2$[84] (4.48×10^{-4} mol) and 0.567 g of $PhCH_2Cl$ (0.52 mL, 4.48×10^{-3} mol) were dissolved in 20 mL of toluene and refluxed for 20 hours. As the reaction proceeded, a precipitate formed from the red solution. The reaction was allowed to cool before the solvent was decanted from the precipitate. The red precipitate was washed further with Et_2O (3×10 mL) before being dried *in vacuo* resulting in the collection of a red solid. ^1H NMR and ^{31}P NMR spectra were collected in CD_2Cl_2. The NMR spectra showed that several products had formed, with three prominent resonances in the ^{31}P spectrum. No further attempt to purify the material was made due to observing a number of peaks in the ^1H and ^{31}P NMR spectra.

2.6 Syntheses involving the Indenyl Derived Ligand, $C_9H_6PMePh_2$ (VII)

2.6.1 Synthesis of $[IndPMePh_2][I]$ (Ind = C_9H_7)

$IndPPh_2$[85] was synthesized by the addition of LiC_9H_6 to Ph_2PCl according to the preparation of Fallis *et al.*. A solution of $IndPPh_2$ (5.14 g, 1.71×10^{-2} mol) in 20 mL of THF was treated with 1.0 mL MeI (1.61×10^{-2} mol), and the reaction mixture was stirred for 2 days while a precipitate formed slowly. The resulting colourless solid was filtered, washed with ether (3 × 10 mL) and dried under reduced pressure to give 5.55 g of white phosphonium salt (75 % yield). ^1H and ^{31}P NMR were collected. ^1H NMR ($CDCl_3$, 300 MHz): δ 8.10-6.90 (m, Ph), 6.7-6.15 (m, olefinic), 3.18 (d, $^2J_{P-H}$ = 13.3 Hz), 2.85 (d, $^2J_{P-H}$ = 13.3 Hz). ^{31}P NMR ($CDCl_3$, 121 MHz): δ 26.04, 13.52.

Two methyl doublets were visible near 3 ppm in the ^{1}H NMR and two ^{31}P NMR resonances for the two isomers of indenyl were observed. Deprotonation of this salt (described in the next step) confirmed that it was indeed the two phosphonium salt isomers. The ratio of the integrations of the two methyl resonances match with the ratio of the integrations of the two phosphorus peaks in the ^{31}P NMR spectrum. The aromatic region and olefinic regions are extremely complicated and have a number of overlapping peaks due to the two isomers of the phosphonium salt that result from the two isomers of $IndPPh_2$.[85] There is close agreement between the number of protons expected (integration) in the aromatic/olefinic region and the methyl region of the ^{1}H NMR spectrum. The aromatic/olefinic region of the ^{1}H NMR spectrum is shown below in Figure 2-1.

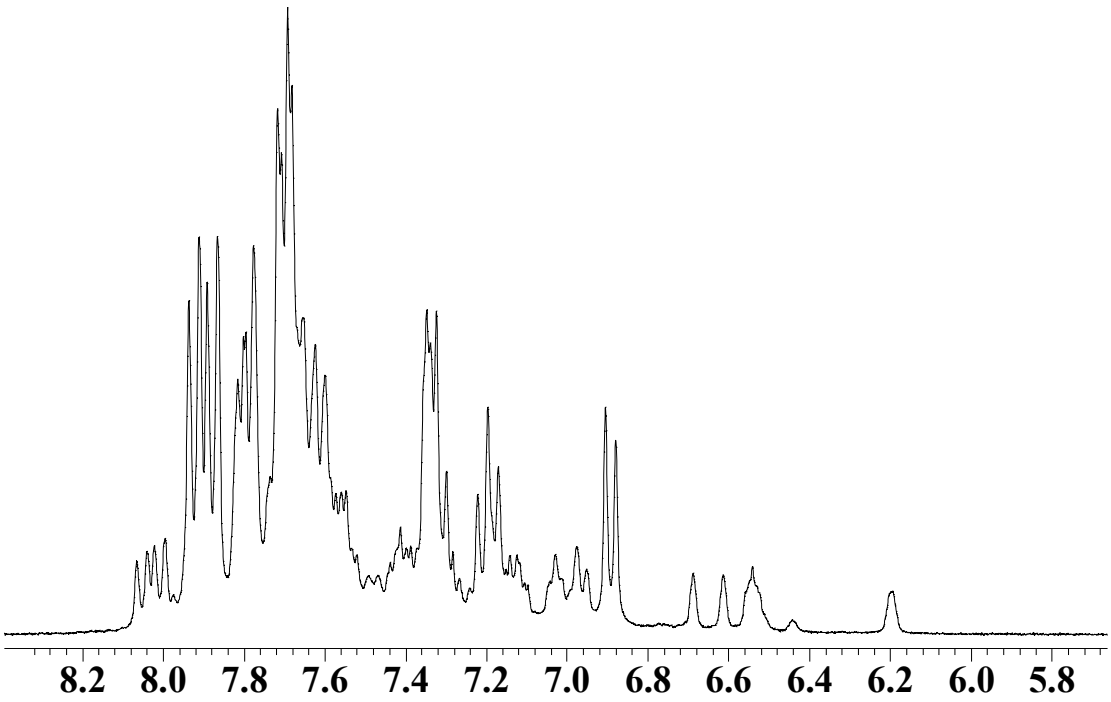

Figure 2-1. The aromatic and olefinic region of the ^{1}H NMR spectrum of [IndPMePh$_2$][I].

2.6.2 Synthesis of $C_9H_6PMePh_2$ (VII)

Synthesis of $C_9H_6PMePh_2$. A mixture of [$IndPMePh_2$][I] (1.30 g, 2.94×10^{-3} mol) and NaH (0.126 g, 5.25×10^{-3} mol) in 20 mL of THF was stirred for 4 days and then filtered. The solid residue was washed 3 × 5 mL of THF, and the combined solutions were concentrated to ~20 mL and then layered with 50 mL of hexanes and cooled to –30 °C to give a light green solid. This was filtered, washed with 3 × 20 mL of hexanes, redissolved in 20 mL of $CHCl_3$ and then taken to dryness under reduced pressure again to yield 0.80 g (87 %) of a green solid that was used without further purification. X-ray quality crystals and analytically pure material were obtained by crystallization from a CH_2Cl_2 solution layered with hexanes and kept at –30 °C. ^1H and ^{13}C NMR data (600 MHz in $CDCl_3$) are listed in the Results and Discussion section in Table 3-12. ^{31}P NMR ($CDCl_3$, 121 MHz): δ 5.69. Anal for $C_{22}H_{19}P$: Found, C 84.38, H 6.35; calc C 84.06, H 6.09. ^{31}P NMR ($CDCl_3$, 121 MHz): δ 5.69. Elemental Analysis for $C_{22}H_{19}P_1$: Found: C 84.38, H 6.35. Calculated: C 84.06, H 6.09.

2.6.3 Synthesis of (η^5-$C_9H_6PMePh_2$)$Cr(CO)_3$ (VIII)

A solution of **VII** (0.435 g, 1.38×10^{-3} mol) and $Cr(CO)_6$ (0.692 g, 3.46×10^{-3} mol) in 25 mL diglyme was refluxed for 3 h before being cooled and filtered through Celite. The Celite was washed with 3 × 10 mL of diglyme, and the resulting orange-red solution was combined with 175 mL of hexanes to give a red-brown product which was collected and redissolved in ~15 mL of CH_2Cl_2. Addition of 40 mL of hexanes and cooling of this solution to –30 °C resulted in the precipitation of 0.25 g of orange-brown product (40% yield). Analytically pure and X-ray quality crystals were obtained by

recrystallization from a CH_2Cl_2 solution layered with hexanes at –30 °C. ^{1}H and ^{13}C NMR data are listed in the Results and Discussion section in Table 3-13. ^{31}P NMR (CD_2Cl_2, 121 MHz): δ 19.84. IR (CH_2Cl_2): 1916 (s), 1816 (s), 1802 (sh). Anal for $C_{25}H_{19}Cr_1O_3P_1 \cdot 0.5\ CH_2Cl_2$: Found, C 61.90, H 4.04; calc C 62.14, H 4.09.

3 Results and Discussion

3.1 The Synthesis and Characterization of $C_5H_4PMePh_2$

Although the synthesis of the title compound was first reported by Mathey *et al*. in 1975 with the intention of studying the reactivity of this molecule in a variety of reactions, Mathey *et al*. did not intend to use this molecule as a ligand as in the work reported for the Ramirez ylide.[36] The synthesis of the title ylide follows a three-step protocol starting from $PClPh_2$ as previously discussed in the Introduction (Equation 1-1 – 1-3).[36] In addition, $C_5H_4PMePh_2$ was poorly characterized with only a low field ^1H NMR spectrum being reported.

3.1.1 The Synthesis of $C_5H_4PMePh_2$

The first step of the synthesis involves the exchange of the chloride of the starting chlorophosphine with Cp^- in a metathesis using TlCp (Figure 3-1). This step generates three isomers of the Cp ring attached to the phosphorus as shown in Figure 3-2.

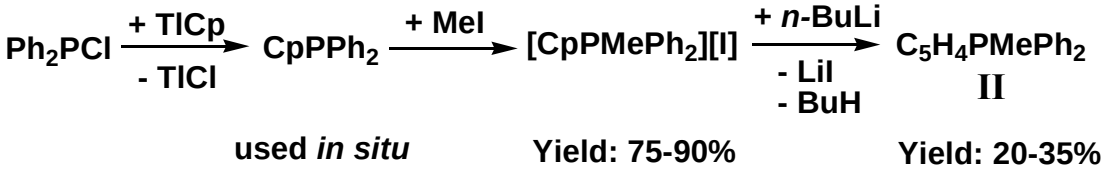

Figure 3-1. The three-step synthesis of the ylide $Ph_2MeP(C_5H_4)$.

^1H NMR and ^{31}P NMR of the crude reaction mixture indicated that we had complete conversion of the chlorophosphine to the desired product and that the three isomers were present in similar amounts to those reported by Mathey.[36]

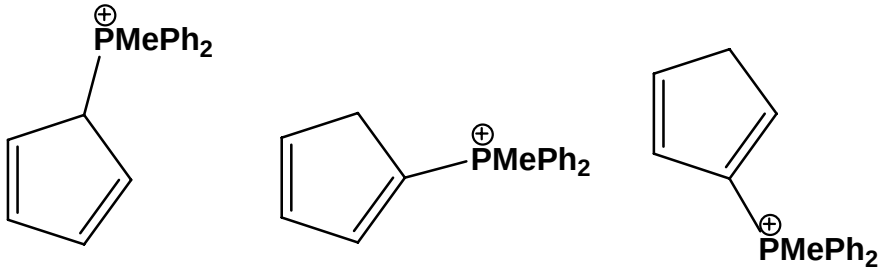

Figure 3-2. The three isomers of the phosphonium salt, [CpPMePh$_2$][I].

In several reaction attempts to synthesize CpPPh$_2$, we determined that it was necessary to use TlCp as our Cp$^-$ source. Experiments using NaCp at various reaction temperatures did not yield pure CpPPh$_2$ (^{1}H and ^{31}P NMR), with resonances observed other than those expected for the three desired Cp isomers. A report by Casey *et al.* details the use of NaCp·DME in the synthesis of CpPPh$_2$, but we did not attempt the synthesis using NaCp·DME as TlCp gave us acceptable results.[37] When CpPPh$_2$ was synthesized, it had to be used immediately because it decomposes on standing, presumably through Diels-Alder dimerization of the Cp group.[36, 37]

In the second step of the synthesis, CpPPh$_2$ was converted into the phosphonium salt, [CpPMePh$_2$][I], by the addition of MeI. Mathey *et al.* reported that, after stirring the reaction mixture for three hours, [CpPMePh$_2$][I] was obtained in a yield of 55%.[36] We found that we obtained higher yields (~80%) of the phosphonium iodide than reported, but the material we recovered was never pure and all attempts to purify it failed. Although the phosphonium iodide was impure, it was used successfully in the final step of the synthesis.

The final step of the ylide synthesis involves the deprotonation of the Cp ring with *n*-BuLi. The reported yield for this step was 70%,[36] but we have attained yields ranging from only 20-35% in over 20 reaction attempts. We have also used the bases MeLi, $KN(SiMe_3)_2$, ^tBuLi, $LiN(^iPr)_2$ and NaOH, but these did not improve the yields obtained using *n*-BuLi. Although the yield of the resulting ylide is relatively low, the product is easily separated from impurities by column chromatography and the starting materials can be made in large scale, making this synthesis an effective route to this ylide.

3.1.2 Characterization of $C_5H_4PMePh_2$ (II)

As part of our study and to make comparisons to the Ramirez ylide, we have characterized **II** by ^1H, ^{31}P, $^{13}C\{^1H\}$ NMR spectroscopy and X-ray crystallography. The ^1H and $^{13}C\{^1H\}$ NMR data are presented in Table 3-1, and will be discussed below. Note that all spectral and structural parameters of free and coordinated cyclopentadienylidenes are presented in terms of the general labelling scheme shown as in Figure 3-3; to facilitate comparisons, the atom numbering for the carbon and hydrogen atoms of the C_5H_4 ring corresponds to the crystallographic labelling schemes.

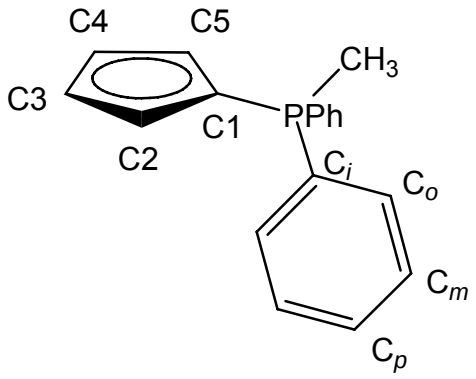

Figure 3-3. The general labelling scheme of the ligand, II, and the complexes III-VI.

Position	**II** ($CDCl_3$)	**III** (CD_2Cl_2)	**IV** (CD_2Cl_2)	**V** (CD_2Cl_2)	**VI** (CD_2Cl_2)
^{1}H: δ					
2,5	6.29 (m)	4.71 (m)	5.29 (m)	5.21 (m)	6.04 (m)
3,4	6.44 (m)	4.90 (m)	5.48 (m)	5.46 (m)	6.43 (m)
Me	2.37 (d, $^{2}J_{P\text{-}H}$ = 13.2)	2.55 (d, $^{2}J_{P\text{-}H}$ = 13.2)	2.55 (d, $^{2}J_{P\text{-}H}$ = 13.6)	2.56 (d, $^{2}J_{P\text{-}H}$ = 13.6)	3.12 (d, $^{2}J_{P\text{-}H}$ = 13.6)
^{13}C: δ					
1	79.2 (d, $^{1}J_{P\text{-}C}$ = 114.2)	65.8 (d, $^{1}J_{P\text{-}C}$ = 111.4)	71.8 (d, $^{1}J_{P\text{-}C}$ = 109.4)	70.5 (d, $^{1}J_{P\text{-}C}$ = 109.6)	87.0 (d, $^{1}J_{P\text{-}C}$ = 95.0)
2,5	114.9 (d, $^{2}J_{P\text{-}C}$ = 16.3)	89.9 (d, $^{2}J_{P\text{-}C}$ = 13.4)	94.5 (d, $^{2}J_{P\text{-}C}$ = 14.4)	91.4 (d, $^{2}J_{P\text{-}C}$ = 14.0)	104.1 (d, $^{2}J_{P\text{-}C}$ = 11.5)
3,4	114.3 (d, $^{3}J_{P\text{-}C}$ = 17.3)	87.5 (d, $^{3}J_{P\text{-}C}$ = 13.4)	92.1 (d, $^{3}J_{P\text{-}C}$ = 12.5)	89.6 (d, $^{3}J_{P\text{-}C}$ = 11.8)	97.5 (d, $^{3}J_{P\text{-}C}$ = 8.6)
Me	12.6 (d, $^{1}J_{P\text{-}C}$ = 63.3)	12.8 (d, $^{1}J_{P\text{-}C}$ = 65.7)	14.4 (d, $^{1}J_{P\text{-}C}$ = 66.2)	14.5 (d, $^{1}J_{P\text{-}C}$ = 65.5)	11.7 (d, $^{1}J_{P\text{-}C}$ = 58.5)
C_i	127.5 (d, $^{1}J_{P\text{-}C}$ = 88.3)	123.1 (d, $^{1}J_{P\text{-}C}$ = 90.2)	122.5 (d, $^{1}J_{P\text{-}C}$ = 90.2)	121.9 (d, $^{1}J_{P\text{-}C}$ = 90.3)	119.6 (d, $^{1}J_{P\text{-}C}$ = 91.1)
C_o, C_m	132.3 (d, $J_{P\text{-}C}$ = 10.6)	133.3 (d, $J_{P\text{-}C}$ = 11.1)	133.4 (d, $J_{P\text{-}C}$ = 10.6)	133.6 (d, $J_{P\text{-}C}$ = 10.7)	133.5 (d, $J_{P\text{-}C}$ = 11.5)
	129.0 (d, $J_{P\text{-}C}$ = 11.5)	130.2 (d, $J_{P\text{-}C}$ = 12.3)	130.2 (d, $J_{P\text{-}C}$ = 12.5)	130.3 (d, $J_{P\text{-}C}$ = 12.9)	131.2 (d, $J_{P\text{-}C}$ = 13.4)
C_p	132.6 (d, $^{4}J_{P\text{-}C}$ = 2.1)	134.8 (d, $^{4}J_{P\text{-}C}$ = 2.2)	135.0 (d, $^{4}J_{P\text{-}C}$ = 2.9)	135.1 (d, $^{4}J_{P\text{-}C}$ = 2.1)	136.4 (d, $^{4}J_{P\text{-}C}$ = 3.8)
M-CO	-	241.8 (s)	231.2 (s)	221.1 (s)	229.3 (s), 216.3 (s)
^{31}P: δ	7.95	19.54	18.25	18.58	21.08

Table 3-1. Selected NMR data for the compounds II-VI. Full listings of NMR data are given in the experimental section listed after the syntheses for each compound. Refer to Figure 3-3 for the atom labeling scheme. Coupling constants are in Hz.

The ^{1}H NMR spectrum, shown in Figure 3-4, of **II** exhibits two broad multiplets, which appear at δ 6.29 and δ 6.44 and are assigned as the C_5H_4 ring protons as shown in Table 3-1. Assignments of the C_5H_4 proton resonances of **II** were made via a NOESY experiment, which showed a strong NOE correlation between the resonance at δ 6.29 and both the Me and the Ph resonances. Thus the resonance at δ 6.29 is to be assigned to the protons attached to carbons 2,5 (refer to Figure 3-3 for labelling scheme) since the proton of carbons 3,4 would be expected to exhibit much less significant NOE correlations. The assignment of the individual ring protons had not been made for any of the ylide ligands or complexes previously reported. A doublet for the P-Me protons appears at δ 2.37 with splitting resulting from coupling to the phosphorus atom.

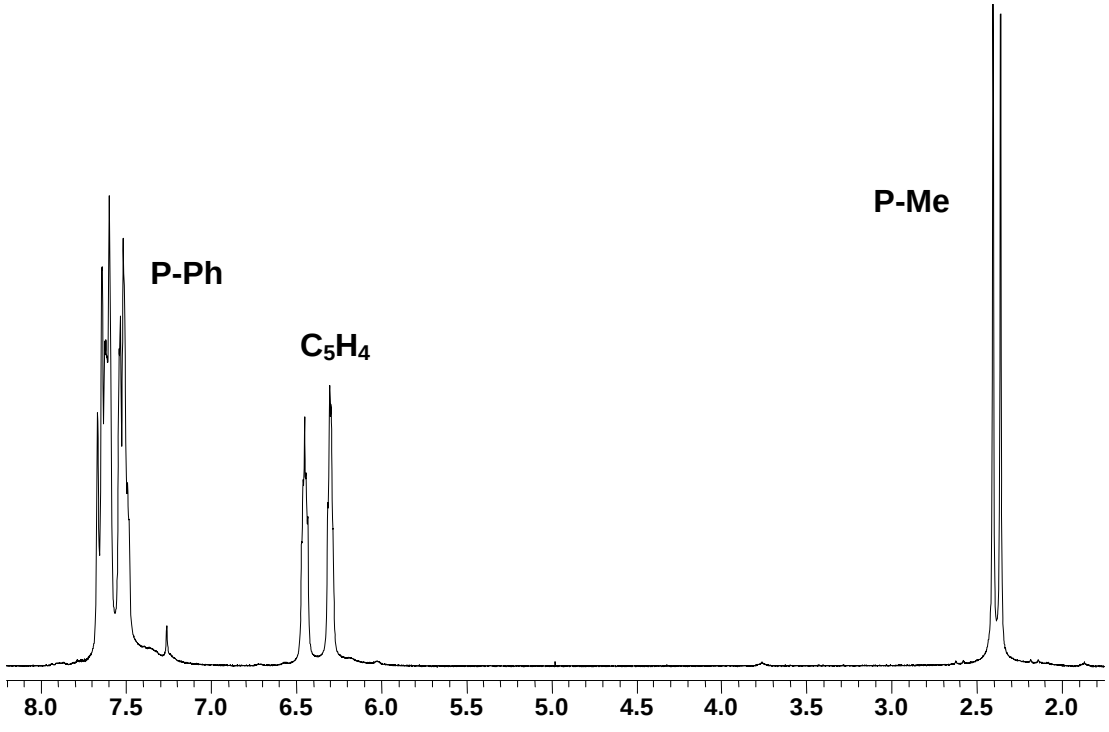

Figure 3-4. The ^{1}H NMR spectrum of $C_5H_4PMePh_2$ (II) in $CDCl_3$.

Once the ring protons had been assigned with the NOESY experiment, carbon assignments were made in part via an HSQC experiment. The resonances of the *ipso* and

para carbons of the phenyl ring were assigned based upon their carbon-phosphorus coupling constants, although the corresponding *ortho* and *meta* carbon resonances could not be assigned unambiguously using HSQC because of overlap in the ^{1}H NMR spectrum (see Table 3-1 for ^{13}C NMR data). Assignment of these carbons by use of the P-C coupling constants was also impossible because of the similarity in magnitudes of the two coupling constants, 10.6 and 11.5 Hz. The P-C(1) carbon has a chemical shift of δ 79.2 and a $^{1}J_{P\text{-}C}$ of 114.2 Hz.

The crystal structure of **II** was obtained for purposes of comparison to the structure of **I**, which was reported previously.[7] The structure of **II** contains two independent molecules (molecules 1 and 2) in the unit cell, and selected bond lengths and angles for **I** and **II** are given in Table 3-2. Crystallographic data for **II** and the coordination complexes, prepared here and to be discussed below, are listed in the Appendix; complete tables of bond lengths and angles may also be found in the Appendix.

The most important structural parameters for assessing the relative contributions of the resonance structures **IIa** and **IIb** (Figure 3-5) to the overall electronic structure involve the bond lengths and angles of the P-C_5H_4 moiety.

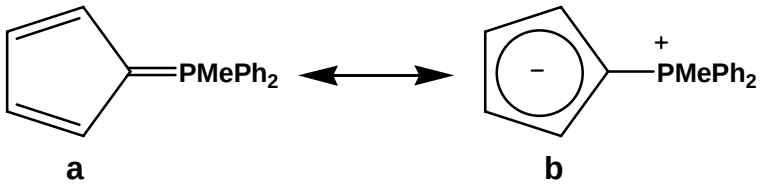

II

Figure 3-5. The resonance structures of methyldiphenylcyclopentadienylide (II).

The crystal structure of **II** is shown in Figure 3-6. The P-C_5H_4 bond length of **I** is 1.718(2) Å,[7] while those of the two molecules of **II** are 1.7277(17) Å and 1.7268(17) Å. The slight elongation of the P-C_5H_4 bond distances in **II** may be the result of having substituted a phenyl group for the better donating methyl group but, more to the point, these P-C_5H_4 bonds are all significantly *shorter* than the P-Ph bonds in **I** and **II** (which fall within the typical range for this type of C-P single bond in phenyl phosphonium ylides[86]) but significantly *longer* than the P=CH_2 bond in Ph_3P=CH_2 (1.66 Å).[86] The latter compound is a typical example of a non-resonance stabilized ylide, and its P=CH_2 bond is believed to contain considerable double bond character.[86] Thus the P-C_5H_4 bond lengths of **I** and **II** are consistent with very significant contribution from both the uncharged and the zwitterionic resonance structures, **Ia** and **Ib**, **IIa** and **IIb**.

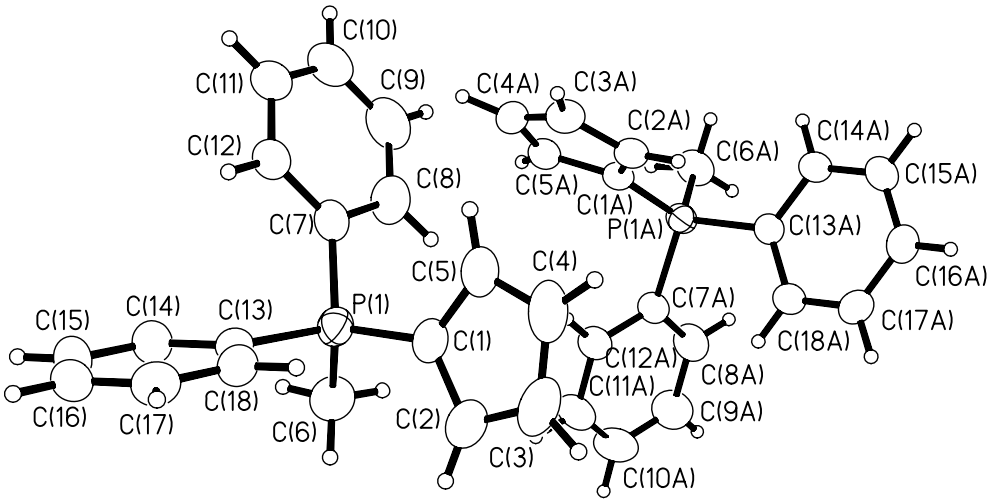

Figure 3-6. Molecular structures of the two molecules in the unit cell of $C_5H_4PMePh_2$.

Interestingly, although the C-C-C bond angles within the five-membered rings of both ylides are all very close to the 108° of a regular pentagon, the C-C bond lengths seemingly also provide evidence for a degree of localization of π bond electron density.

Thus, while the structures of both molecules exhibit long (C_1-C_2), short (C_2-C_3), long (C_3-C_4), short (C_4-C_5), long (C_5-C_1) alternating patterns of bond lengths, as in **Ia** and **IIa**, the "long" bonds are much shorter than a typical C-C single bond length and all bonds are similar to those of benzene (1.3894 Å) for example.[87] Thus again there is evidence for a very significant contribution from both the uncharged and the zwitterionic resonance structures of **I** and **II**.

Compound	**II** (Molecule 1)	**II** (Molecule 2)	**I**[7]
Bond		Bond lengths (Å)	
P(1)-C(1)	1.7277(17)	1.7268(17)	1.718(2)
P-Me	1.799(2)	1.7921(19)	-
P-Ph (av)	1.810	1.802	1.806
C(1)-C(2)	1.429(3)	1.413(2)	1.430(3)
C(1)-C(5)	1.414(3)	1.429(2)	1.419(3)
C(2)-C(3)	1.374(3)	1.384(2)	1.392(4)
C(4)-C(5)	1.384(3)	1.383(3)	1.376(4)
C(3)-C(4)	1.405(3)	1.407(3)	1.401(4)
Bond Angle		Degrees	
C(1)-P(1)-Me	111.46(9)	111.96(9)	-
C(1)-P-Ph (av)	111.44	110.64	111.4
Me-P-Ph (av)	106.96	108.44	-
Ph(1)-P(1)-Ph(2)	108.37(8)	106.55(7)	107.5 (av)
C(1)-C(2)-C(3)	107.42(19)	108.36(16)	106.8(2)
C(2)-C(3)-C(4)	108.85(18)	108.16(18)	108.9(2)
C(3)-C(4)-C(5)	108.74(18)	108.87(15)	108.8(2)
C(4)-C(5)-C(1)	107.47(18)	107.50(17)	108.0(2)
C(5)-C(1)-C(2)	107.51(16)	107.11(16)	107.4(2)

Table 3-2. Selected bond distances and angles for I and II. Refer to Figure 3-3 for the atom labeling scheme.

3.2 The Group 6 Tricarbonyl Compounds of $C_5H_4PMePh_2$

Herein the synthesis, characterization and reactivity of the group 6 compounds $(\eta^5\text{-}C_5H_4PMePh_2)M(CO)_3$ (M = Cr, Mo, W) are described. This series was chosen for study because the group 6 tricarbonyl complexes of $C_5H_4PPh_3$ are known and we wished to be able to make direct comparisons of the coordination chemistry of $C_5H_4PPh_3$ and $C_5H_4PMePh_2$. The group 6 tricarbonyl complexes of $C_5H_4PMePh_2$ and $C_5H_4PMePh_2$ have also been investigated, via *ab initio* calculations, to ascertain the nature of the bonding in **II** and of its complex, $(\eta^5\text{-}C_5H_4PMePh_2)Cr(CO)_3$, **III**.

3.2.1 The Synthesis of the Group 6 Tricarbonyl Compounds $(\eta^5\text{-}C_5H_4PMePh_2)M(CO)_3$ (M = Cr (III), Mo (IV), W (V))

The group 6 tricarbonyl complexes **III**, **IV** and **V** were synthesized using procedures similar to those reported by Kotz *et al.* in the syntheses of the corresponding complexes of **I**.[10] An excess (2 to 3 equivalents) of $M(CO)_6$ (M = Cr, Mo) was refluxed in diglyme with **II** to give the resulting chromium and molybdenum complexes in ~60% yield for both complexes (Figure 3-7). However, the tungsten derivative required the use of $W(CO)_3(CH_3CN)_3$ (also in an excess of 2 to 3 equivalents) to ensure ligand substitution.[10] An excess of $W(CO)_3(CH_3CN)_3$ was heated with **II** in diglyme at 110°C to provide the tungsten complex in 70% yield. **III** and **IV** are easily purified by crystallization from a dichloromethane solution layered with hexanes and kept at -30°C. This treatment affords material suitable for both X-ray crystallography and elemental analysis. In the case of **V**, the crude reaction product was first passed through an alumina column before crystals were grown from the same conditions as used for **III** and **IV** to obtain crystals suitable for X-ray crystallography and elemental analysis.

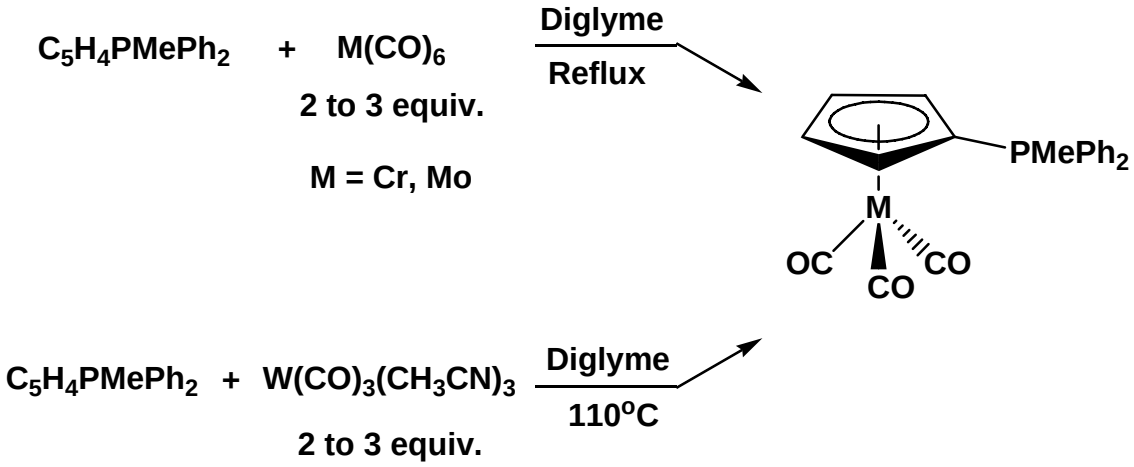

Figure 3-7. Syntheses of $(\eta^5\text{-}C_5H_4PMePh_2)M(CO)_3$ (M = Cr, Mo, W).

3.2.2 The Characterization of the Group 6 Tricarbonyl Compounds

The IR spectra (CH_2Cl_2, Table 3-3) of the complexes exhibit two strong carbonyl stretching bands, consistent with an essentially three-fold $-M(CO)_3$ moiety and at frequencies nearly identical to those reported for the corresponding complexes of **I**.[10] The spectrum of **III** is shown in Figure 3-8 and is representative of these complexes (**III-V**).

Compound/M	$(\eta^5\text{-}C_5H_4PMePh_2)M(CO)_3$	$(\eta^5\text{-}C_6H_6)M(CO)_3$	$[(\eta^5\text{-}C_5H_5)M(CO)_3]^-$
		ν(CO) (cm^{-1})	
Cr	1915 (s), 1812 (s)	1971, 1892	1895, 1778
Mo	1918 (s), 1812 (s)	1972, 1891	1898, 1781
W	1912 (s), 1808 (s)	1971, 1887	1894, 1779

Table 3-3. Carbonyl stretching frequencies ν(CO) (cm^{-1}) for the compounds III, IV and V (in CH_2Cl_2), for the neutral arene compounds $(\eta^5\text{-}C_6H_6)M(CO)_3$ (M = Cr, Mo, W; in CH_2Cl_2)[88] and for the anionic complexes $[(\eta^5\text{-}C_5H_5)M(CO)_3]^-$ (M = Cr, Mo, W; in THF).[89]

For purposes of comparison, the ν(CO) of the analogous η^6-benzene[88] and anionic η^5-C_5H_5[89] complexes are also shown in Table 3-3, and it is clear that the donor properties of **II** lie between those of benzene and Cp^-, but possibly closer to the latter. (The data for the Cp^- complexes are believed to be for the free ions, as the spectra were run in the presence of ligands thought to coordinate to the counter cations).[89] These data provide further evidence that the neutral ylides contain significant negative charge on the C_5H_4 rings.

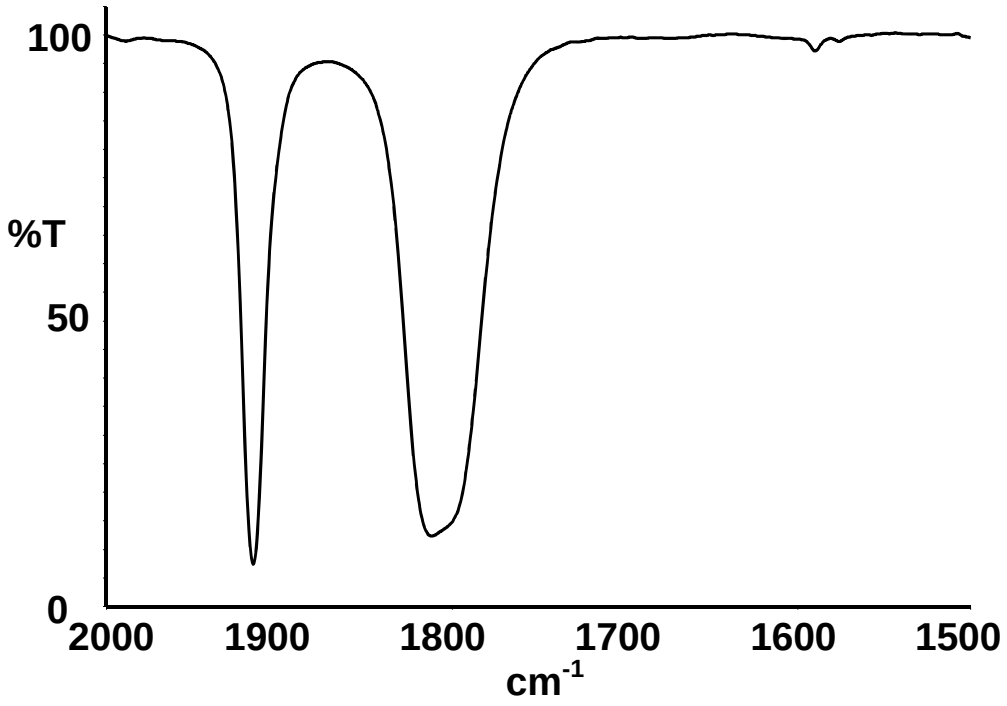

Figure 3-8. The IR spectrum of (η^5-$C_5H_4PMePh_2$)$Cr(CO)_3$ in CH_2Cl_2.

Selected ^1H NMR and ^{13}C NMR data for **III**, **IV** and **V** are listed in Table 3-1 and the ^1H NMR spectra of **III-V** are shown in Figure 3-9, where it can be seen that coordination of **II** to a metal results in the two multiplet C_5H_4 ring resonances shifting upfield relative to the free ligand, while the P-Me ^1H resonances shift downfield for the three complexes. Compound **III** shows the greatest change in the C_5H_4 ring proton resonances, which shift upfield by δ ~1.6 upon complexation of **II**. The C_5H_4 proton

resonances for **IV** and **V** exhibit very similar chemical shifts, and are downfield of complex **III** by δ ~0.6. Similar changes are observed for the group 6 complexes of **I**.[10]

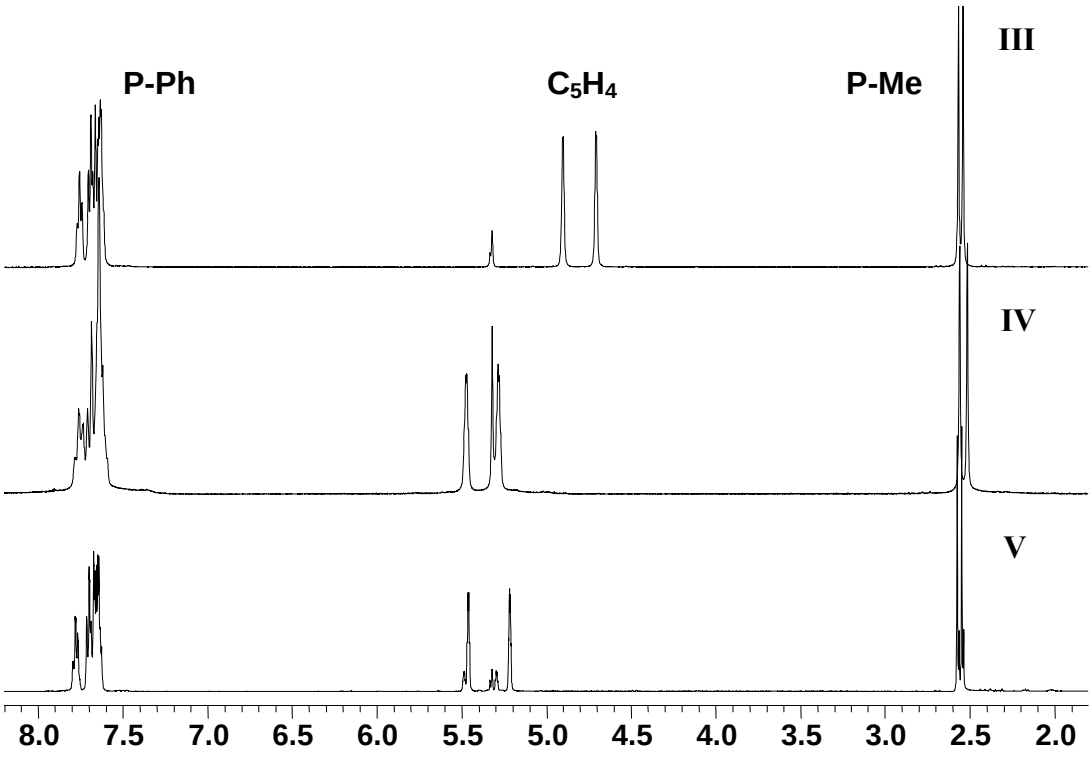

Figure 3-9. The ^{1}H NMR spectra of III-V in CD_2Cl_2.

As with **II**, the C_5H_4 ring protons of **III-V** were assigned using a NOESY experiment, which clearly indicated that the upfield resonance was that of the protons at positions 2 and 5. Using HSQC, the carbon atoms of the ligand could be assigned, except for the *ortho* and *para* carbons of the phenyl rings, which could not be assigned using HSQC due to the overlap of the proton resonances in the ^{1}H NMR spectrum, preventing accurate correlations in the HSQC spectrum. In addition, the nearly identical coupling constants ($J_{P\text{-}C}$) of these carbons prevent their unambiguous assignment.

The ^{31}P resonance of **II** shifts downfield some δ 10-12 on coordination in compounds **III-V**, but the differences between the three coordination compounds are relatively small. No spin-spin coupling to ^{183}W was observed in either the ^{13}C or ^{31}P

spectrum of **V**. On the other hand, the ^{13}C NMR spectra exhibit significant changes in the C_5H_4 ring carbon resonances on going from the free ligand to complexes **III**, **IV** and **V**. Thus the resonance of C(1) shifts from δ 79.2 in **II** to δ 65.8 in **III**, δ 71.8 in **IV** and δ 70.5 in **V**, while much more dramatic shifts are observed for the resonances of C(2) and C(3), which shift to a higher field by over δ 20.

X-ray structures of all three complexes, **III**, **IV** and **V**, were obtained; selected bond lengths and angles are listed in Table 3-4 and Table 3-5 (see appendix for full listings) and crystallographic data are provided in the Appendix. Included in Table 3-4 and Table 3-5 are the literature data for $(\eta^5\text{-}C_5H_4PPh_3)Cr(CO)_3$, in which there are two independent molecules in the unit cell (molecules 1 and 2).[15] The structure of $(\eta^5\text{-}C_5H_4PPh_3)Cr(CO)_3$ offers a good structural comparison with that of **III** and also allows for a general appraisal of structural changes in this type of ligand on coordination. The molecular structure of **III** is shown in Figure 3-10. To our knowledge, the structures of the Mo (Figure 3-11) and W (Figure 3-12) complexes are the first reported crystallographically determined structures for these metals with this class of ligand.

Compounds **III**, **IV** and **V** all assume near tetrahedral geometries around the phosphorus atoms, similar to that seen for $(\eta^5\text{-}C_5H_4PPh_3)Cr(CO)_3$.[15] The $C_5H_4PMePh_2$ is coordinated as expected in η^5-fashion in all three complexes, with little difference in the five C_5H_4-Cr distances. Ring carbon atoms C(2) and C(5) essentially eclipse two of the carbonyl ligands, C(19) and C(20), respectively, and thus the third carbonyl ligand assumes a staggered orientation relative to C(3) and C(4). The P-C_5H_4 bond is elongated on coordination to all three metals. The same degree of elongation is observed in $(\eta^5\text{-}C_5H_4PPh_3)Cr(CO)_3$,[15] and probably indicates an increase in the contribution of the

zwitterionic structure on coordination, i.e. an increase in the aromatic character in the C_5H_4 ring on coordination. The P(1)-C(1)-C_5(centroid) angle is essentially linear in **III**, **IV** and **V**, the greatest deviation from linearity being ~2.1°. This is in contrast to both free ligands **I** and **II**, for which the P-C_5H_4 bonds are bent significantly out of the C_5H_4 ring planes. The C_5H_4 ring bond lengths of **II** are slightly elongated in **III**, **IV** and **V**, as is observed in (η^5-$C_5H_4PPh_3$)$Cr(CO)_3$,[15] and the ring bond angles are all very close to those of a regular pentagon (108°).

Bond (Å)	**III**	**IV**	**V**	(η^5-$C_5H_4PPh_3$)$Cr(CO)_3$ (Molecule 1)	(Molecule 2)
P(1)-C(1)	1.759(3)	1.759(3)	1.765(4)	1.751(5)	1.755(6)
P-Me	1.789(3)	1.785(2)	1.786(4)	-	-
P-Ph avg.	1.796	1.790	1.793	1.798	1.799
M-C_5 Centroid	1.848	2.044	2.033	1.862	1.872
C(1)-C(2)	1.427(4)	1.434(3)	1.435(6)	1.431(8)	1.443(8)
C(1)-C(5)	1.429(4)	1.430(3)	1.438(6)	1.430(8)	1.441(8)
C(2)-C(3)	1.392(4)	1.403(3)	1.405(7)	1.452(9)	1.403(8)
C(4)-C(5)	1.397(4)	1.400(3)	1.393(7)	1.422(9)	1.386(9)
C(3)-C(4)	1.422(4)	1.417(3)	1.402(7)	1.394(10)	1.443(9)
C(1)-metal	2.185(2)	2.350(2)	2.342(4)	2.183(5)	2.192(6)
C(2)-metal	2.204(2)	2.352(2)	2.349(4)	2.201(6)	2.226(6)
C(3)-metal	2.226(3)	2.385(2)	2.371(4)	2.248(7)	2.257(6)
C(4)-metal	2.217(3)	2.403(3)	2.380(5)	2.249(7)	2.238(7)
C(5)-metal	2.191(3)	2.375(2)	2.367(5)	2.229(6)	2.230(6)

Table 3-4. Selected bond lengths of complexes III-V and (η^5-$C_5H_4PPh_3$)$Cr(CO)_3$.[15] Refer to Figure 3-3 for the atom labelling scheme.

Bond Angles (°)	III	IV	V	$(\eta^5\text{-}C_5H_4PPh_3)Cr(CO)_3$ (Molecule 1)	$(\eta^5\text{-}C_5H_4PPh_3)Cr(CO)_3$ (Molecule 2)
C(1)-P-Me	111.08(13)	110.91(12)	111.2(2)	-	-
C(1)-P-Ph avg.	109.78	109.48	109.19	110.3	109.4
Me-P-Ph avg.	109.38	109.36	109.35	-	-
Ph-P-Ph	107.37(12)	108.35(11)	108.4(2)	108.6	109.7
P-C(1)-C_5 Centroid	178.9	178.0	178.5	173.4	169.0
C(1)-C(2)-C(3)	108.3(3)	108.1(2)	107.4(4)	107.4(6)	107.7(6)
C(2)-C(3)-C(4)	108.3(3)	108.1(2)	108.8(4)	108.4(6)	108.3(6)
C(3)-C(4)-C(5)	108.3(3)	108.7(2)	109.1(4)	108.3(6)	108.4(6)
C(4)-C(5)-C(1)	108.0(3)	108.0(2)	107.6(4)	108.8(6)	108.4(6)
C(5)-C(1)-C(2)	107.1(2)	107.1(2)	107.1(4)	107.0(6)	107.2(6)

Table 3-5. Selected bond angles of complexes III-V and $(\eta^5\text{-}C_5H_4PPh_3)Cr(CO)_3$.[15] Refer to Figure 3-3 for the atom labelling scheme.

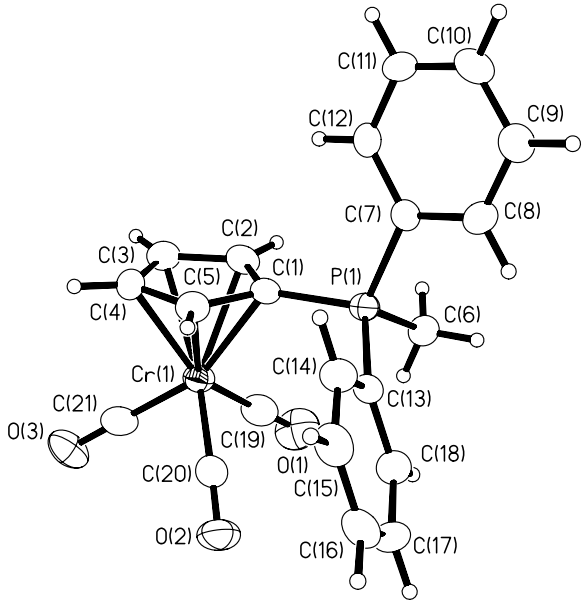

Figure 3-10. Molecular structure of $(\eta^5\text{-}C_5H_4PMePPh_2)Cr(CO)_3$ (III).

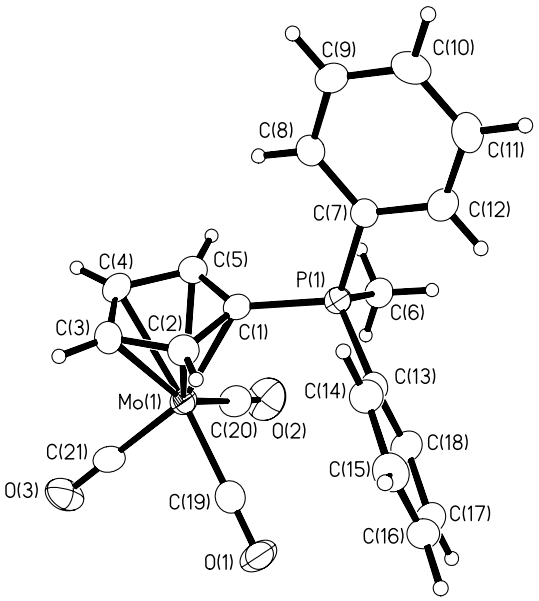

Figure 3-11. Molecular structure of (η^5-$C_5H_4PMePPh_2$)$Mo(CO)_3$ (IV).

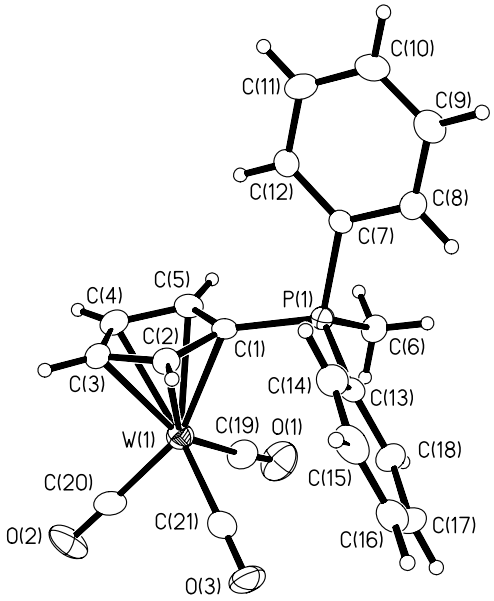

Figure 3-12. Molecular structure of (η^5-$C_5H_4PMePPh_2$)$W(CO)_3$ (V).

3.2.3 Intramolecular Interactions in II and III-V

In the crystal structures of **II-V**, the -$PMePh_2$ moieties are oriented such that one of the phenyl rings not only eclipses the C_5H_4 ring but is oriented towards it in an edge on fashion in spite of the apparently greater congestion in this conformation. Interestingly, intramolecular edge-face orientations involving interactions of aromatic hydrogen atoms with aromatic π systems have well established precedent in conformationally flexible compounds for which equilibria of the type shown generically in Figure 3-13 can be established.[90-93] In these cases, edge-face interactions are sufficiently attractive that the molecules assume Conformation 1 in the solid state, although on-off equilibria exist in solution as indicated in Figure 3-13. Conformation 1 is increasingly populated at lower temperatures as indicated by significant temperature dependence of the time averaged chemical shift of the edge hydrogen atom H_o, the observed chemical shift of H_o moving to increasingly higher field as the temperature is lowered because of ring current shielding arising in the close edge-face association of Conformation 1.

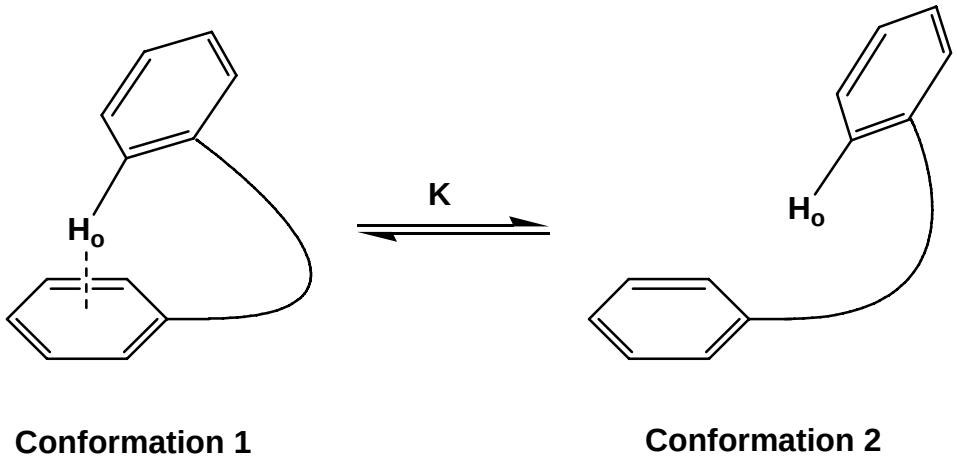

Figure 3-13. Representation of the on-off equilibrium for edge-face aromatic ring interactions.

The origin of the ring-edge attractive force is believed to be largely electrostatic in origin,[90-93] the aromatic π electrons interacting with a slightly positive H_o. In view of the apparent significance of resonance structure **IIb** and in accord with DFT calculations to be discussed below, it appears that the C_5H_4 rings of **II** and its coordination complexes are not only aromatic in character but also carry a significant partial negative charge, while the -$PMePh_2$ moieties carry a partial positive charge. In addition, for each of the compounds **II-V**, the distance between one of the phenyl *ortho* C-H groups and C(1) of the C_5H_4 ring falls well within the range of distances observed in the previously reported compounds in which attractive edge-face interactions have been established,[90-93] and one would anticipate relatively strong attractive interactions in compounds **II-V**. To seek evidence for the phenomenon in solution, we ran a series of low temperature ^{1}H NMR experiments with **II** (to 213 K) and **IV** (to 190 K). Unfortunately, no change in the ^{1}H NMR spectrum of either was observed, and thus although edge-face interactions seem to be important in the solid state, no evidence for them have been obtained in solution. However, we note that the apparent electrostatic interactions in compounds **II-V** are between phenyl *ortho* C-H groups and C(1) of the C_5H_4 rings rather with the *centroids* of the C_5H_4 rings. Thus it is possible that the *ortho* hydrogen atoms do not actually lie in the region of ring current induced enhanced shielding.

3.2.4 Reactions of the Group 6 Tricarbonyl Complexes III-V

As part of this study, and to expand on the chemistry of the Group 6 tricarbonyl ylide complexes, we have carried out an investigation of the reactivities of **III** and **IV**. Two classes of reactions were studied, ligand substitution and oxidation reactions.

3.2.5 Ligand Substitution with Phosphines

We initially began the study of ligand substitution using PPh_3, with a view to substituting CO ligands of **III** and **IV**. To this end, solutions of **III** or **IV** with one equivalent of PPh_3 were refluxed in THF for up to 22 hours while the reactions were monitored by IR spectroscopy (Figure 3-14). No changes in the IR spectra were apparent after this reaction time. We also attempted photochemical CO substitution reactions of **IV**, but after 18 hours of photolyzing a CH_2Cl_2 solution of the metal complex and one equivalent of phosphine, no change in the IR spectrum was observed. We also attempted CO substitution using PMe_3 (Figure 3-15), anticipating that the use of this smaller, better donor would promote the ligand exchange. As with the PPh_3 experiment, however, no reaction occurred with one equivalent of PMe_3 after 18 hours of photolysis.

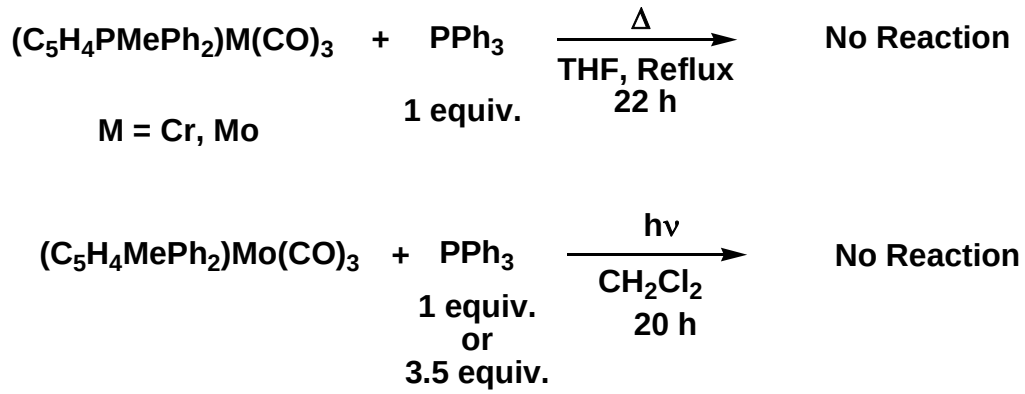

Figure 3-14. Attempted ligand exchange reaction of III and IV with PPh_3.

However, when 3.5 equivalents of PMe_3 were used in a photochemical reaction (Figure 3-15), the ν(CO) of **IV** disappeared as a new set of peaks in the carbonyl region grew in at 1830 and 1930 cm^{-1}, very similar to the literature values for *fac*-$Mo(CO)_3(PMe_3)_3$.[83]

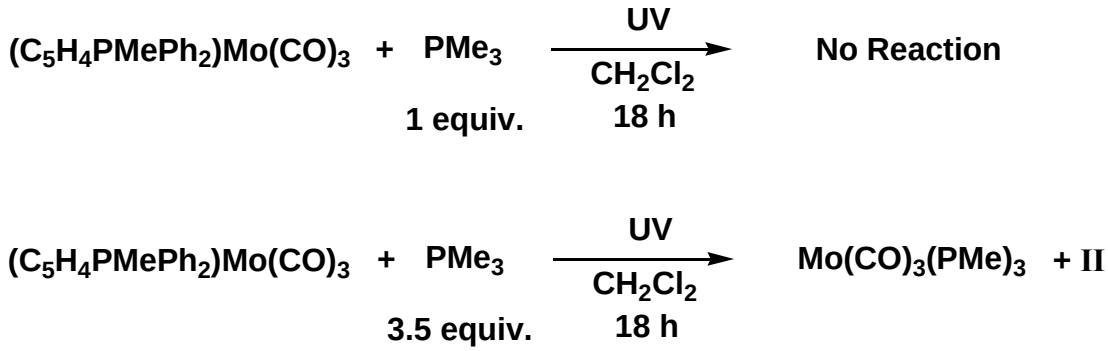

Figure 3-15. The reaction of IV with PMe_3.

Consistent with this conclusion, ^{1}H and ^{31}P NMR spectra of the crude reaction mixture clearly indicated that the ylide had been cleaved from the metal, and in addition there appeared in the ^{31}P NMR spectrum a new peak at δ –17.2, also attributable to *fac*-$Mo(CO)_3(PMe_3)_3$.[83] The displacement by phosphines of η^6-arenes of group 6 metal tricarbonyl complexes is known to give *fac*-isomers,[83] and we believe this is occurring here. When the photochemical reaction (18 h) was attempted using 3.5 equivalents of PPh_3, no reaction occurred. This may be due to the large size of PPh_3 versus PMe_3. In general, therefore, **IV** appears to be relatively inert with respect to ligand exchange.

3.2.6 Oxidation Reactions of (η^5-$C_5H_4PMePh_2$)$Mo(CO)_3$ (IV)

Reactions with electrophilic reagents, I_2, MeI and H_2, with **IV** were also investigated. The reaction of I_2 with (η^5-$C_5H_4PPh_3$)$Mo(CO)_3$ had been previously reported to give the Mo(II) complex [(η^5-$C_5H_4PPh_3$)$Mo(CO)_3I$][PF_6], but only IR and elemental analysis data were reported.[12] On the addition of one equivalent of I_2 to a solution of **IV**, the colour of the solution changed instantly to orange and, on workup, we isolated the crystalline product [(η^5-$C_5H_4PMePh_2$)$Mo(CO)_3I$]I (**VI**). NMR data are given

in Table 3-1 and the ^{1}H NMR spectrum is shown in Figure 3-16, and are consistent with this formulation. As anticipated, the P-Me and C_5H_4 ^{1}H resonances are all significantly deshielded relative to the precursor, **IV**; the C_5H_4 ring ^{13}C resonances are also significantly deshielded, but not the ^{13}C resonance of the P-Me group.

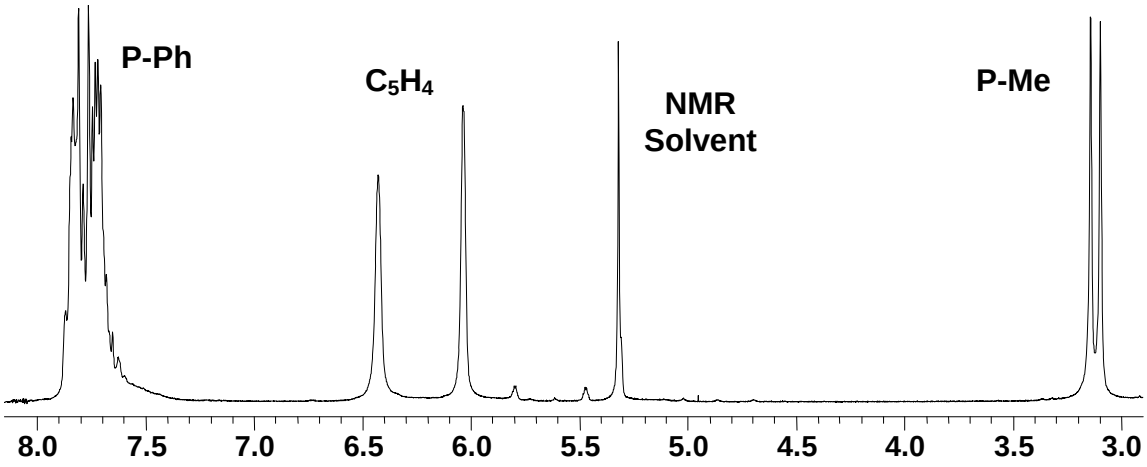

Figure 3-16. The ^{1}H NMR spectrum of $[(\eta^5\text{-}C_5H_4PMePh_2)Mo(CO)_3I]I$ (VI) in CD_2Cl_2.

The IR spectrum of **VI** (shown in Figure 3-17 as a CH_2Cl_2 solution) exhibited two strong ν(CO) at 2055 and 1979 cm^{-1}, as expected at higher frequencies than is the case for **IV**, but similar to the reported ν(CO) for $[(\eta^5\text{-}C_5H_4PPh_3)Mo(CO)_3I][PF_6]$ (2052 cm^{-1}, 1997 cm^{-1} and 1976 cm^{-1}; run as a KBr disc).[12]

Crystals suitable for X-ray crystallography were grown, and the crystal structure of **VI** is shown in Figure 3-18. Selected bond distances and angles are shown in Table 3-6 (see appendix for full listings) and crystallographic data in the Appendix. The crystal structure contains two independent molecules in the unit cell, molecules 1 and 2, and one molecule of CH_2Cl_2.

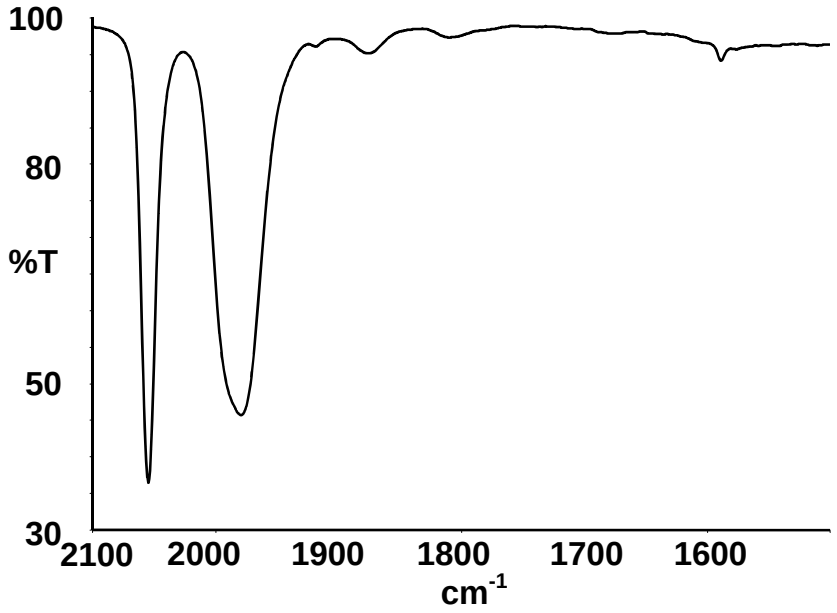

Figure 3-17. The IR spectrum of $[(\eta^5\text{-}C_5H_4PMePh_2)Mo(CO)_3I]I$ (VI) in CH_2Cl_2.

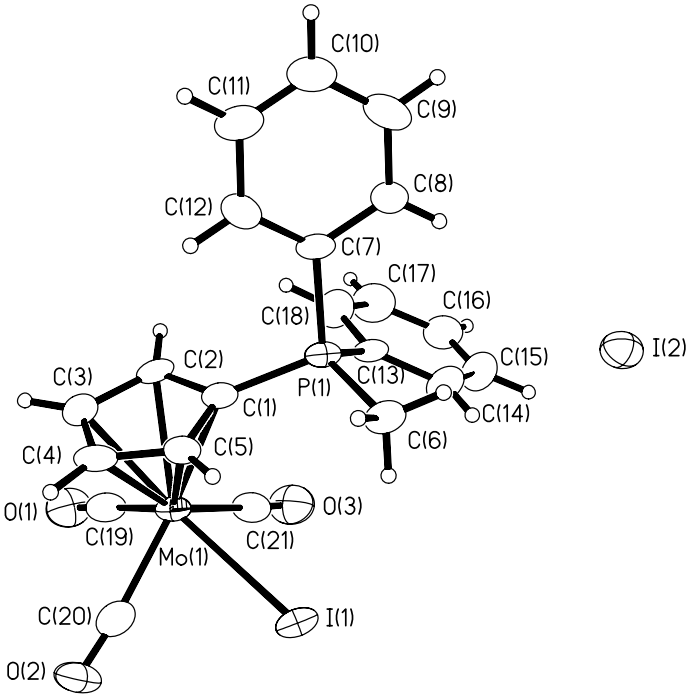

Figure 3-18. Molecular structure of $[(\eta^5\text{-}C_5H_4PMePh_2)Mo(CO)_3I]I$ (VI) showing one of the independent molecules in the unit cell.

Bond (Å)	Molecule 1	Molecule 2
P(1)-C(1)	1.780(8)	1.775(9)
P-Me	1.777(8)	1.789(8)
P-Ph avg.	1.792	1.782
M-C_5 Centroid	1.997	1.994
C(1)-C(2)	1.436(10)	1.437(11)
C(1)-C(5)	1.440(10)	1.412(11)
C(2)-C(3)	1.428(11)	1.418(12)
C(4)-C(5)	1.385(11)	1.415(11)
C(3)-C(4)	1.401(11)	1.386(12)
Mo-I(1)	2.8355(9)	2.8176(10)
C(1)-Mo	2.310(7)	2.318(8)
C(2)-Mo	2.301(8)	2.292(8)
C(3)-Mo	2.324(8)	2.312(8)
C(4)-Mo	2.360(8)	2.361(9)
C(5)-Mo	2.370(8)	2.356(8)
Bond Angles (°)		
C(1)-P-Me	108.1(4)	108.5(4)
C(1)-P-Ph avg.	110.8	109.6
Me-P-Ph avg.	110.0	111.0
Ph-P-Ph	106.9(4)	107.1(4)
P-C(1)-C_5 Centroid	170.2	172.7
C(1)-C(2)-C(3)	107.0(8)	108.1(8)
C(2)-C(3)-C(4)	108.1(7)	108.3(8)
C(3)-C(4)-C(5)	109.7(8)	108.5(8)
C(4)-C(5)-C(1)	107.9(7)	108.9(8)
C(5)-C(1)-C(2)	107.2(7)	106.2(8)

Table 3-6. Selected bond lengths and angles of the two molecules of VI; refer to Figure 3-3 for the atom labeling scheme.

As with **III**, **IV** and **V**, the molecules of **VI** assume piano stool-type structures about the metal atoms and an *ortho* hydrogen atom of a phenyl group is positioned relatively closely to C(1) of the C_5H_4 ring. Perhaps because of this, the coordinated iodine atoms are oriented relatively closely to the phosphorus atoms with the P(1)-C(1)-Mo(1)-I(1) torsional angles being 47.0(5)° and 59.7(5)° for molecules 1 and 2, respectively. Observation that the phosphorus atoms are in close proximity to the coordinated iodines seems surprising, but no covalent bonding interaction is present as the interatomic distances (4.474 Å and 4.325 Å) exceed the sum of the van der Waals radii.[94] Indeed, the P-C_5H_4 bonds are bent out of the plane of the C_5H_4 ring and away from the metals in the two molecules by ~9.8° and ~7.3°.

The P-C_5H_4 bond lengths of the two molecules of **VI** are slightly longer (1.780(8), 1.775(9) Å) than is the case with **IV** (1.759(2) Å), while the C-C distances in the C_5H_4 ring lose the alternating bond lengths found in **II** and **IV**. Both of these factors are consistent with an increase in aromatic character in the C_5H_4 ring on oxidation of the metal. The metal-C_5H_4 ring centroid distance decreases (1.997 Å and 1.994 Å) on oxidation, as is to be expected, but the individual Mo-C bond distances vary somewhat irregularly with the distances to C(4) and C(5) being somewhat longer than those to C(1), C(2) and C(3).

Reaction of **IV** with MeI was attempted as a test of nucleophilicity of **IV**. The analogous $[(\eta^5\text{-}C_5H_5)Mo(CO)_3]^-$ undergoes reaction readily with MeI to give $(\eta^5\text{-}C_5H_5)Mo(CO)_3Me$,[95] but **IV** was found to be inert to MeI. There was also no reaction of **IV** with H_2.

3.2.7 Electronic structures of $C_5H_4PMePh_2$ and $(\eta^5\text{-}C_5H_4PMePh_2)Cr(CO)_3$

All molecular calculations were performed by Hartmut Schmider of the High Performance Computing Virtual Laboratory at Queen's University. Geometry optimizations of **II** and **III** were carried out using B3LYP[72-74] in a 6-31G* basis set.[75-78] The geometries obtained in this way were kept fixed in all subsequent computations. Bond lengths and angles obtained in the DFT-optimized structures for $C_5H_4PMePh_2$ (**II**) and $(\eta^5\text{-}C_5H_4PMePh_2)Cr(CO)_3$ (**III**) are shown in Table 3-7 together with the crystallographic data for **II** and **III**. As can be seen, the calculated bond lengths and angles are generally in reasonable agreement with the experimental data for both the free and coordinated ylide ligand, and in particular the same *trends* are observed. Thus the P(1)-C(1) bonds of both compounds are calculated to be significantly shorter than the averages of the P-Ph bonds, consistent with the calculated partial double bond character in the former; the Mulliken-Mayer bond index for the P(1)-C(1) bond is about 1.2 as opposed to 0.9 for the P-Ph bonds. In addition, the experimentally observed lengthening of the P(1)-C(1) bond on coordination is also reflected in the calculations. The alternating bond lengths of the C_5H_4 rings of both free and coordinated ylide, noted above, are also reproduced in the calculated geometries, as well as in the bond indices (typically 1.2 for long and 1.5 for short bonds). This finding lends further credence to our conclusion of significant delocalization of the π system of the C_5H_4 rings.

Bond	**II** (Å, exp)	**II** (Å, calc)	**III** (Å, exp)	**III** (Å, calc)
P(1)-C(1)	1.7277(17), 1.7268(17)	1.717	1.759(3)	1.757
P-Me	1.799(2), 1.7921(19)	1.835	1.789(3)	1.825
P-Ph avg.	1.810, 1.802	1.836	1.796	1.822
C(1)-C(2)	1.429(3), 1.413(2)	1.439	1.427(4)	1.449
C(1)-C(5)	1.414(3), 1.429(2)	1.441	1.429(4)	1.443
C(2)-C(3)	1.374(3), 1.384(2)	1.387	1.392(4)	1.409
C(4)-C(5)	1.384(3), 1.383(3)	1.388	1.397(4)	1.413
C(3)-C(4)	1.405(3), 1.407(3)	1.426	1.422(4)	1.430
Bond Angle	**II** (°, exp)	**II** (°, calc)	**III** (°, exp)	**III** (°, calc)
C(1)-P(1)-Me	111.46(9), 111.96(9)	110.47	111.08(13)	110.14
C(1)-P-Ph avg.	111.44, 110.64	113.29	109.78	111.95
Me-P-Ph avg.	106.96, 108.44	106.17	109.38	107.45
Ph-P-Ph	108.37(8), 106.55(7)	106.97	107.37(12)	107.64
C(1)-C(2)-C(3)	107.42(19), 108.36(16)	107.36	108.3(3)	107.6
C(2)-C(3)-C(4)	108.85(18), 108.16(18)	108.88	108.3(3)	109.0
C(3)-C(4)-C(5)	108.74(18), 108.87(15)	108.89	108.3(3)	108.2
C(4)-C(5)-C(1)	107.47(18), 107.50(17)	107.24	108.0(3)	108.1
C(5)-C(1)-C(2)	107.51(16), 107.11(16)	107.61	107.1(2)	107.2

Table 3-7. Calculated (6-31G* B3LYP) and experimental bond lengths (Å) and angles (°) of $C_5H_4PMePh_2$ (II) and of (η^5-$C_5H_4PMePh_2$)$Cr(CO)_3$ (III); calculated bond orders for II are also given. Refer to Figure 3-3 for the atom labeling scheme.

The Mulliken charges for the free ligand **II** were computed at the B3LYP, RHF, and MP2 levels of computation, both in the Pople split-valence (6-31G*) and the Dunning double-zeta (cc-pVDZ) basis sets. While the charges calculated for individual atoms are very basis-set dependent, they become more consistent if the hydrogen atoms are combined with the heavy atoms to which they are bound, and even more so if one looks only at the overall groups (C_5H_4 ring, phenyl rings, methyl). In this case we find

that the C_5H_4 ring of the free ligand carries a charge of about –0.5 independent of the type of calculation, the phenyl rings and the methyl group are near neutral, and the charge on phosphorus is between +0.4 and +0.7 depending on level and basis set. Somewhat similar results have been reported recently for **I**.[96]

In the case of the chromium complex **III**, calculations based on all of the basis sets suggest that the C_5H_4 ring is less negative than is the case in the free ligand, as anticipated, and that the overall charge of the $Cr(CO)_3$ group is negative with the negative charge largely delocalized onto the CO ligands. Again the phosphorus atom carries a positive charge, while the methyl and phenyl groups are essentially neutral.

Schmider also calculated the ylide-$Cr(CO)_3$ bond dissociation energy and we have compared this with the analogous ring-metal bond dissociation energy of (η^6-C_6H_6)$Cr(CO)_3$.[97] The calculations were based on the B3LYP/6-31G* gas-phase geometries, i.e. without reoptimization. Values of the calculated ylide-$Cr(CO)_3$ and C_6H_6-$Cr(CO)_3$ bond dissociation energies varied considerably, being consistently greater for MP2 than for Hartree-Fock, as well as greater for the smaller basis set. Interestingly, however, the ratio of the ylide-$Cr(CO)_3$ to the C_6H_6-$Cr(CO)_3$ bond dissociation energy was consistently about 1.3, and thus the ylide-$Cr(CO)_3$ bond dissociation energy appears to be about 30% greater than the C_6H_6-$Cr(CO)_3$ bond dissociation energy.

Contour plots of the HOMO and (HOMO-1) of free $C_5H_4PMePh_2$ are shown in Figure 3-19**A** and Figure 3-19**B**. These differ by only 6 kcal/mol and, as can be seen, correspond closely to the doubly degenerate HOMO (E_1 symmetry) of the free (D_{5h}) cyclopentadienyl anion.[98, 99] That they are not degenerate reflects the lack of symmetry in the molecule. The LUMO and (LUMO+1), as well as

(HOMO-2) to (HOMO-5) of free $C_5H_4PMePh_2$ are all essentially localized on the phenyl rings and hence are not of interest here. However, Figure 3-19**C** shows the (HOMO-6) orbital which is the low energy, almost fully symmetric bonding MO of the C_5H_4 ring, corresponding to the fully symmetric bonding A_1 MO of the cyclopentadienyl anion.[98, 99] Interestingly there appears to be little π-type interactions of any of the orbitals shown in Figure 3-19**A**, Figure 3-19**B** and Figure 3-19**C** with an orbital on the phosphorus atom, consistent with a lack of significant π conjugation of the phosphorus atom with the C_5H_4 ring and suggesting that the zwitterionic resonance structure **IIb** may well be the better representation of the electronic structure of **II**.

As with cyclopentadienyl complexes,[98] the primary η^5-C_5H_4-Cr interaction involves donation from the near degenerate, filled orbitals shown as **A** and **B** of Figure 3-19 into the appropriate d orbitals of the metal. If Cartesian axes are chosen as in Figure 3-20, then the receptor orbitals are the d_{xz} and d_{yz} orbitals, as shown in the contour plots of Figure 3-20**A** and Figure 3-20**B**, respectively. Orbitals of $(\eta^5\text{-}C_5H_4PMePh_2)Cr(CO)_3$ which are largely $d_{x^2-y^2}$ (HOMO), d_{xy}, (HOMO-1) and d_{z^2} (HOMO-2) in character but which contribute to bonding with the CO ligands are shown in Figure 3-21**A**, Figure 3-21**B** and Figure 3-21**C**, respectively.

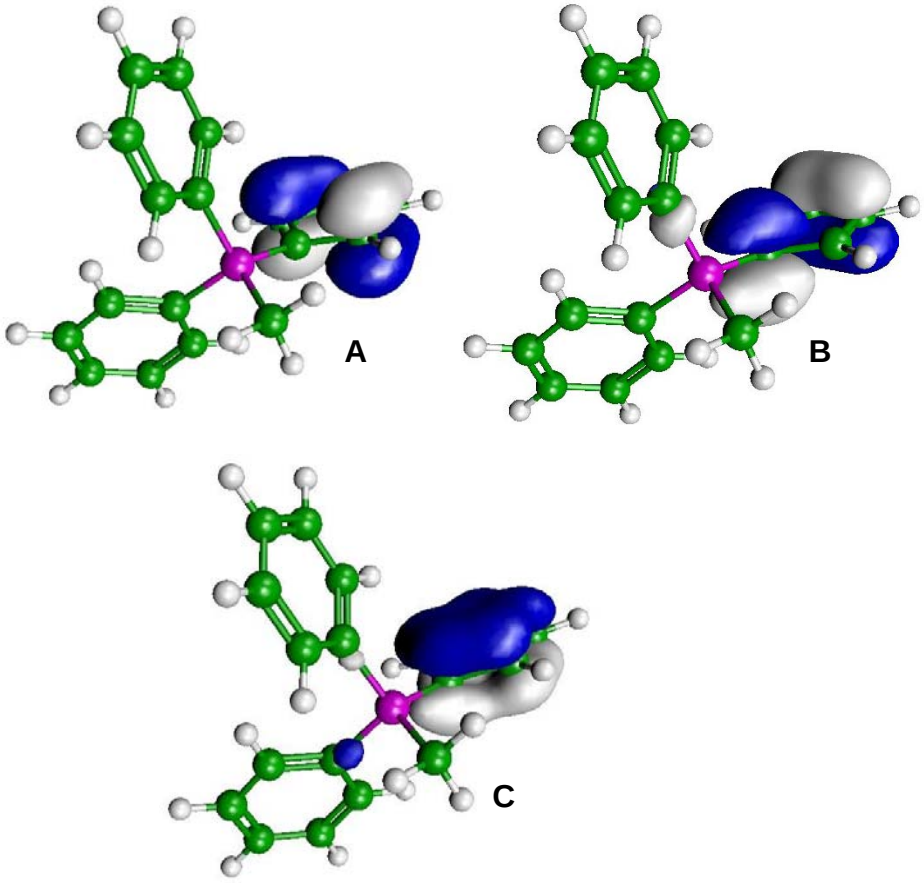

Figure 3-19. Contour plots of the HOMO (A), (HOMO-1) (B), and (HOMO-6) (C) of free $C_5H_4PMePh_2$. The contour values are ±0.05.

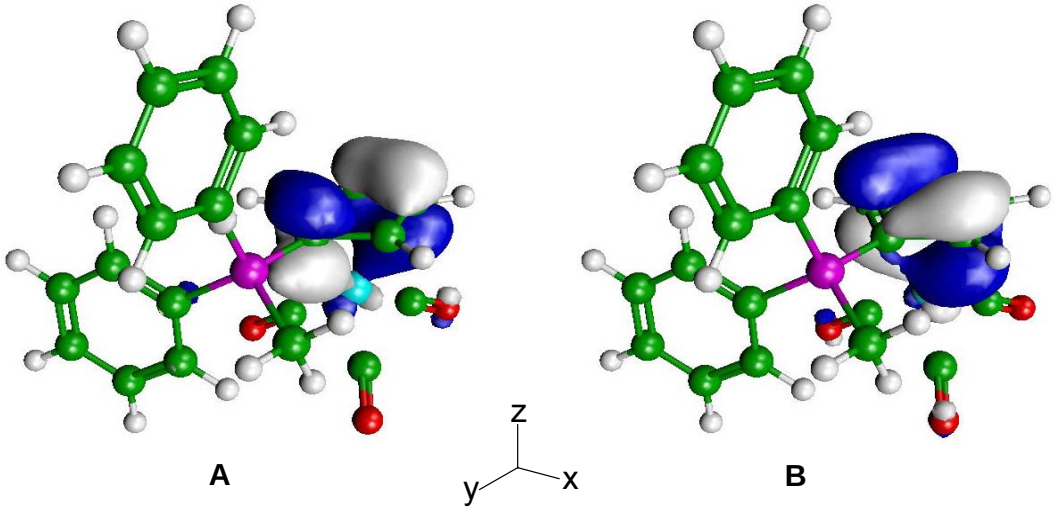

Figure 3-20. Contour plots of the primary η^5-C_5H_4-Cr interactions in (η^5-$C_5H_4PMePh_2$)$Cr(CO)_3$, involving the d_{xz} (A, HOMO-4) and d_{yz} (B, HOMO-3) orbitals on Cr. The contour values are ±0.05.

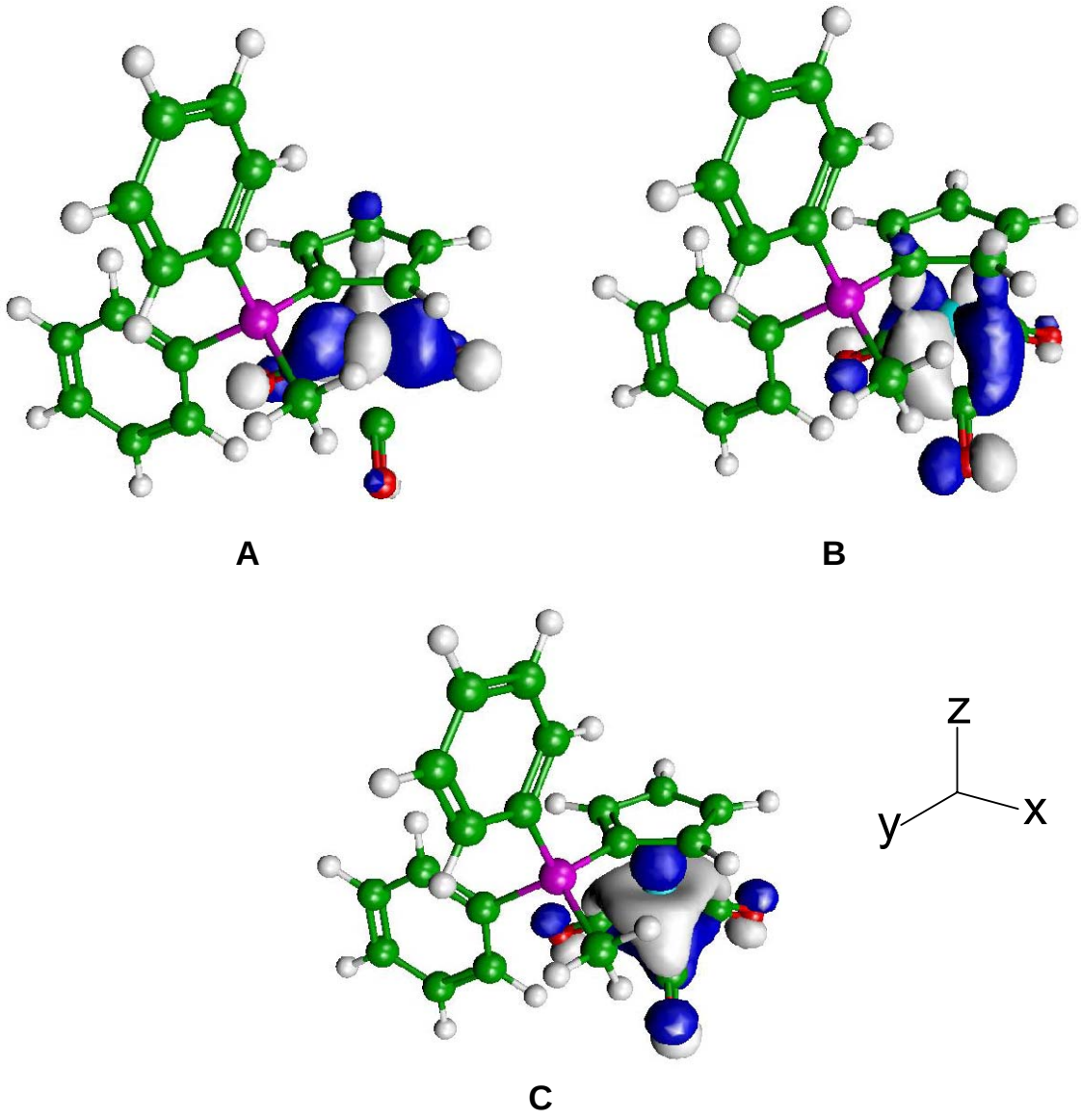

Figure 3-21. Contour plots showing the interactions between the CO ligands and the d orbitals of (η^5-$C_5H_4PMePh_2$)$Cr(CO)_3$: A the $d_{x^2-y^2}$ orbital (HOMO); B the d_{xy} orbital (HOMO-1); C the d_{z^2} orbital (HOMO-2). The contour values are ±0.05.

3.3 Single Electron Oxidations of (η^5-$C_5H_4PMePh_2$)$M(CO)_3$ (M = Cr, Mo, W)

The spectroscopic data for complexes **III-V** also demonstrated, that while the cyclopentadienylide ligand is intermediate in electron donor properties between those of

neutral η^6-arenes and the anionic η^5-C_5H_5 ligand, its properties lie rather closer to that of the latter. Therefore, in view of the equilibria which exist between the metal-metal bonded dimers $[(\eta^5\text{-}C_5H_5)Cr(CO)_3]_2$ and $[(\eta^5\text{-}C_5Me_5)Cr(CO)_3]_2$ and their corresponding 17-electron, metal-centered persistent radicals (shown in Figure 3-22),[100-111] we wondered if compounds **III-V** might undergo single electron oxidations to give the isoelectronic, persistent cationic metal-centered radicals $[(\eta^5\text{-}C_5H_4PMePh_2)M(CO)_3]^+$ (M = Cr (**III**$^+$), Mo (**IV**$^+$), W (**V**$^+$)) and, if so, to what extent would these dimerize to the dicationic, metal-metal bonded species $[(\eta^5\text{-}C_5H_4PMePh_2)M(CO)_3]_2^{2+}$ (M = Cr (**III$_2^{2+}$**), Mo (**IV$_2^{2+}$**), W (**V$_2^{2+}$**)).

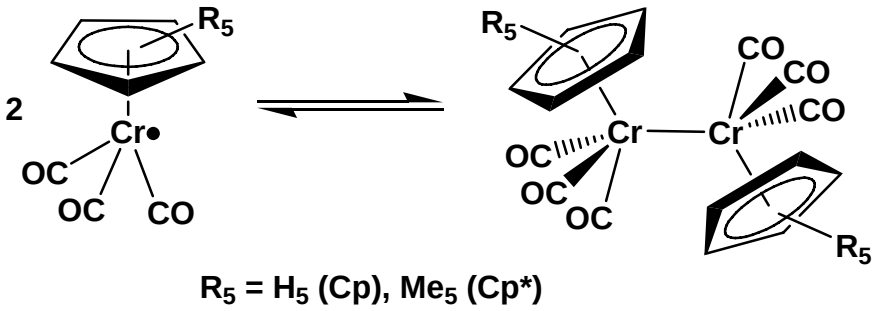

Figure 3-22. The equilibria between the metal-metal bonded dimers $[(\eta^5\text{-}C_5H_5)Cr(CO)_3]_2$ and $[(\eta^5\text{-}C_5Me_5)Cr(CO)_3]_2$ and their corresponding 17-electron, metal-centered persistent radicals.

There seems to exist only a single publication dealing with this type of redox chemistry of cyclopentadienylides. Cashman and Lalor reported in 1971 that $(\eta^5\text{-}C_5H_4PPh_3)Mo(CO)_3$ is oxidized by tris(*p*-bromophenyl)amminium hexachloroantimonate to give the metal-metal bonded, dicationic complex $[(\eta^5\text{-}C_5H_4PPh_3)Mo(CO)_3]_2^{2+}$, identified on the basis of elemental analysis and its IR spectrum.[12] However, group 6 metal compounds containing other ligands provide a rich array of cationic 17-electron complexes.[112, 113] For instance, oxidation of $M(CO)_6$ (M = Cr, Mo, W) gives the unstable

cations $[M(CO)_6]^+$ which have lifetimes on the order of seconds (Cr) or are too unstable to isolate (Mo, W).[114-116] Substituted derivatives $M(CO)_{6-n}L_n$, $M(CO)_4$L-L and $M(CO)_2$(L-L)$_2$ (n = 1-3; L, L-L = mono- and bidentate tertiary phosphines), on the other hand, yield more thermally stable oxidized complexes and these have been better characterized.[117-123] While oxidation of compounds of the type (η^6-arene)$Cr(CO)_3$ yields products that are very labile unless stabilized by weakly coordinating anions,[124-128] several phosphine-substituted complexes $[(\eta^6\text{-arene})M(CO)_2L]^+$ (M = Cr) were found to be stable enough to isolate and characterize.[124-128] However, none of these cationic, metal-centered radicals appears to form dicationic dimers.

Of relevance here, however, the anionic group 6 tricarbonyl complexes $[(\eta^5\text{-}C_5H_5)M(CO)_3]^-$ and $[(\eta^5\text{-}C_5Me_5)M(CO)_3]^-$ (M = Cr, Mo, W) can be oxidized to give the neutral radicals $(\eta^5\text{-}C_5H_5)M(CO)_3$ and $(\eta^5\text{-}C_5Me_5)M(CO)_3$, which dimerize to give the metal-metal bonded complexes $[(\eta^5\text{-}C_5H_5)M(CO)_3]_2$ and $[(\eta^5\text{-}C_5Me_5)M(CO)_3]_2$.[100-111, 129-139] Although the molybdenum and tungsten dimers do not dissociate in solution,[100-111, 129-139] the chromium dimers dissociate as mentioned above to give the corresponding persistent 17-electron radical monomers.[100-111, 129-139] We have therefore embarked on a complementary examination of the redox chemistry of compounds **III-V**, finding that they do indeed undergo oxidation to the corresponding 17-electron, metal-centered radicals $[(\eta^5\text{-}C_5H_4PMePh_2)M(CO)_3]^+$ where M = Cr (**III**$^+$), Mo (**IV**$^+$) and W (**V**$^+$), and that these in turn dimerize to the corresponding metal-bonded complexes $[(\eta^5\text{-}C_5H_4PMePh_2)M(CO)_3]_2^{2+}$ (**III**$_2^{2+}$, **IV**$_2^{2+}$ and **V**$_2^{2+}$, respectively). As with the above mentioned compounds, $[(\eta^5\text{-}C_5H_5)M(CO)_3]_2$ and $[(\eta^5\text{-}C_5Me_5)M(CO)_3]_2$, we find that the chromium dimer **III**$_2^{2+}$ dissociates extensively in solution to the persistent radical

monomer $\mathbf{III}^+$, but that the heavier metal analogues $\mathbf{IV_2}^{2+}$ and $\mathbf{V_2}^{2+}$ dissociate very little, if at all.

This study was undertaken as a collaboration with the group of Prof. William Geiger at the University of Vermont. After performing in Vermont a series of electrochemical studies, which are reported in the Appendix, the Geiger group determined that the products of oxidation were stable enough to isolate and we therefore undertook the bulk synthesis and characterization of the products of the oxidation of the complexes **III-V**.

3.3.1 Electrochemistry Summary

The following findings were made during the electrochemical study performed by the group of Prof. William Geiger at the University of Vermont.

- Oxidations of **III-V** occur through one-electron processes at potentials that are highly positive of the values previously observed for the analogous 18-electron anions $[(\eta^5\text{-}C_5H_5)M(CO)_3]^-$.
- The radical cations $\mathbf{IV}^+$ and $\mathbf{V}^+$ undergo rapid dimerization to metal-metal bonded dications $\mathbf{IV_2}^{2+}$ and $\mathbf{V_2}^{2+}$.
- CV scans of a low concentration solution of **III** in CH_2Cl_2 at temperatures from ambient to 238 K failed to show any changes that would indicate involvement of dimerization of $\mathbf{III}^+$ in detectable amounts in solution.
- In the context of other acceptor substituents, this group has a greater electronic effect than a bromine atom, an aldehyde group, or a trifluoromethyl group.

3.3.2 Bulk syntheses of $[(\eta^5\text{-}C_5H_4PMePh_2)M(CO)_3]_2[B(C_6F_5)_4]_2$ (M = Cr ($[\mathbf{III}_2][B(C_6F_5)_4]_2$), Mo ($[\mathbf{IV}_2][B(C_6F_5)_4]$), W ($[\mathbf{V}_2][B(C_6F_5)_4]_2$))

The syntheses of $[(\eta^5\text{-}C_5H_4PMePh_2)M(CO)_3]_2[B(C_6F_5)_4]_2$ (M = Cr, Mo and W) were carried out in CH_2Cl_2 (Cr) or THF (Mo, W) by combining **III, IV** or **V** with equimolar amounts of ferrocenium tetrakisperfluorophenylborate, $[FeCp_2][B(C_6F_5)_4]$ (Figure 3-23). Separations from ferrocene were readily achieved by recrystallizing the products from solutions of CH_2Cl_2 (M = Cr) or THF (M = Mo, W) by layering with hexanes. It is important to note that the three complexes do not take part in chlorine atom abstraction reactions with CH_2Cl_2, which is a common concern when handling metal-centred radicals.[112, 113]

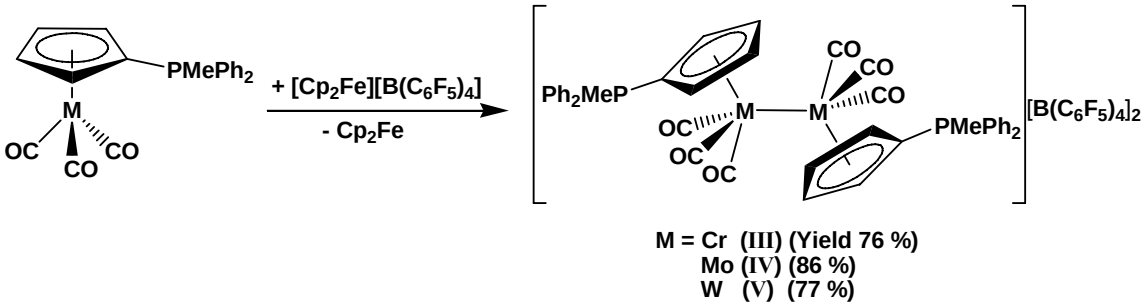

Figure 3-23. The synthetic route to the complexes $[(\eta^5\text{-}C_5H_4PMePh_2)M(CO)_3]_2[B(C_6F_5)_4]_2$ (M = Cr, Mo, W).

Oxidation of **III** could also be effected using $[Ph_3C][B(C_6F_5)_4]$ since the trityl cation (Ph_3C^+) has a reduction potential of $E_{1/2} \approx -0.12$ V versus $FeCp_2^{0/+}$.[140] The IR spectrum of the material formed was identical to that obtained using $[FeCp_2][B(C_6F_5)_4]$ and the yield was similar, and we note that the trityl cation has been used previously as an oxidant with the compound $(\eta^5\text{-}C_5H_5)Mo(CO)(dppe)H$ (dppe = $Ph_2PCH_2CH_2PPh_2$).[140] In contrast, while use of $[FeCp_2][PF_6]$ as an oxidant with **III** did result in the formation of the oxidized product $\mathbf{III}^+$ (IR), the formation of other products was evident even within

the first 5 minutes of the reaction. In addition to the υ(CO) observed for **III**$^{+}$, peaks at 1917, 1821 and 1808 cm^{-1} were also observed and were the dominant features of the spectrum after 1.5 h. While the peaks at 1917 and 1808 cm^{-1} are identical to those of **III** in THF, we cannot propose a process which would result in the reformation of **III**, and therefore these peaks must remain unassigned.

3.3.3 Crystal Structures of $[(\eta^5\text{-}C_5H_4PMePh_2)M(CO)_3]_2[B(C_6F_5)_4]_2$ (M = Cr ($[\mathbf{III}_2][B(C_6F_5)_4]_2$), Mo ($[\mathbf{IV}_2][B(C_6F_5)_4]$), W ($[\mathbf{V}_2][B(C_6F_5)_4]_2$))

X-ray quality crystals of $[(\eta^5\text{-}C_5H_4PMePh_2)Cr(CO)_3]_2[B(C_6F_5)_4]_2$ were grown from a solution of CH_2Cl_2 layered with hexanes and kept at –30°C; there are 1.5 CH_2Cl_2 molecules of solvation per mole of Cr in the unit cell, consistent with the elemental analyses. Initially, crystals of the molybdenum and tungsten analogues were grown from a 1:4 CH_2Cl_2:THF solution layered with hexanes and kept at –30 °C, but twinned crystals were obtained in both cases. While the crystals of $[(\eta^5\text{-}C_5H_4PMePh_2)Mo(CO)_3]_2[B(C_6F_5)_4]_2$ were of sufficient quality for the structure to be solved with acceptable errors on bond lengths and angles, the twinned crystals of $[(\eta^5\text{-}C_5H_4PMePh_2)W(CO)_3]_2[B(C_6F_5)_4]_2$ did not yield acceptable crystallographic data. It was however possible to obtain untwinned X-ray quality crystals of the latter from a very dilute THF solution layered with hexanes and kept at room temperature over the course of three weeks. Crystals of the molybdenum and tungsten dimeric complexes each contain 1.5 THF molecules of solvation per mole of metal in the unit cell, but in these cases the solvent molecules were removed under reduced pressure prior to obtaining elemental analyses. The structures of $[(\eta^5\text{-}C_5H_4PMePh_2)Cr(CO)_3]_2[B(C_6F_5)_4]_2$ and $[(\eta^5\text{-}$

$C_5H_4PMePh_2)W(CO)_3]_2[B(C_6F_5)_4]_2$ were solved by direct methods, but structural refinement of $[(\eta^5\text{-}C_5H_4PMePh_2)Mo(CO)_3]_2[B(C_6F_5)_4]_2$ required the use of ROTAX[64] to find the twin law and then application of SQUEEZE[65] to squeeze out the THF molecules of solvation.

The crystal structures of all three complexes show that the cations are present as dimers in the solid state. Selected bond lengths and angles are presented in Table 3-8, while crystallographic data are presented in the Appendix and the molecular structures are presented in Figure 3-24, Figure 3-25 and Figure 3-26. The Cr-Cr bond distance of the chromium complex is 3.3509(7) Å, apparently the longest Cr-Cr bond distance known for a compound not containing some type of ligand bridging the metal-metal bond. The longest Cr-Cr bond distance reported heretofore is 3.471(1) Å, observed in the bridged fulvalene (Fv) compound $[FvCr_2(CO)_6]$.[141] The metal-metal bond of $[(\eta^5\text{-}C_5H_4PMePh_2)Cr(CO)_3]_2[B(C_6F_5)_4]_2$ is significantly longer than the Cr-Cr bonds in the analogous compounds $[(\eta^5\text{-}C_5H_5)Cr(CO)_3]_2$ (3.281(1) Å) and $[(\eta^5\text{-}C_5Me_5)Cr(CO)_3]_2$ (3.3107 (7) and 3.310(1) Å for two polymorphs); comparisons are shown in Table 3-9.[100, 107, 136]

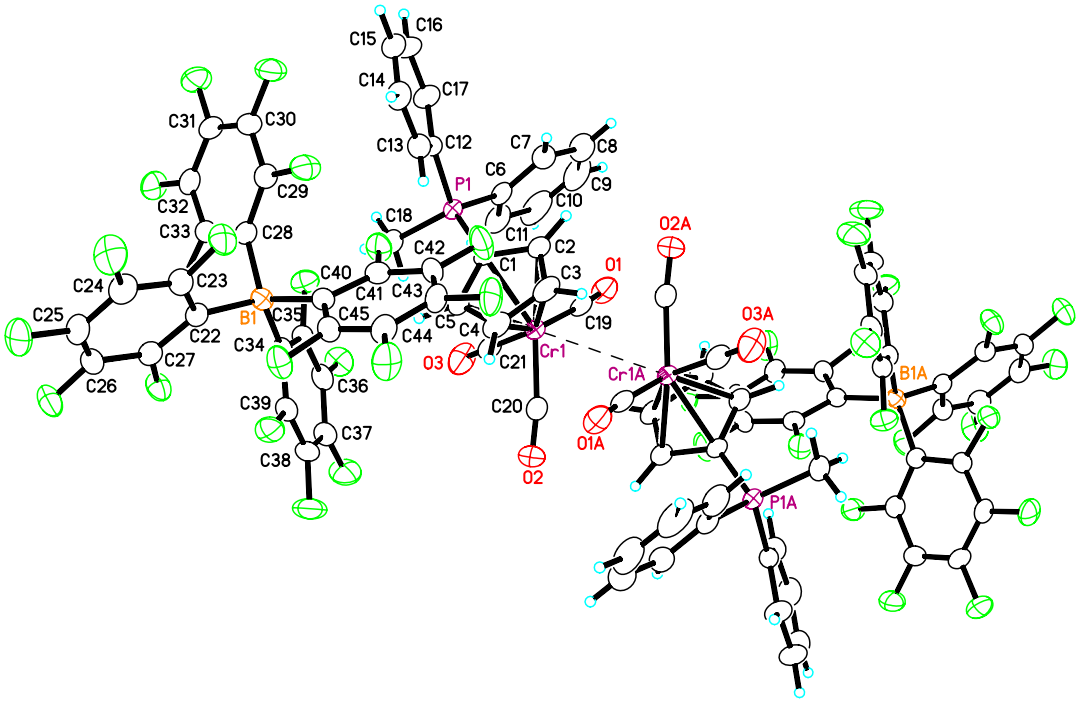

Figure 3-24. The molecular structure of $[(\eta^5\text{-}C_5H_4PMePh_2)Cr(CO)_3]_2[B(C_6F_5)_4]_2$.

The metal-metal bond distances in $[(\eta^5\text{-}C_5H_4PMePh_2)Mo(CO)_3]_2[B(C_6F_5)_4]_2$ and $[(\eta^5\text{-}C_5H_4PMePh_2)W(CO)_3]_2[B(C_6F_5)_4]_2$ are 3.2764(16) Å and 3.2507(4) Å respectively, shorter than the Cr-Cr bond of $[(\eta^5\text{-}C_5H_4PMePh_2)Cr(CO)_3]_2[B(C_6F_5)_4]_2$ as in the trend observed for the isoelectronic $\eta^5\text{-}C_5H_5$ and $\eta^5\text{-}C_5Me_5$ tricarbonyl derivatives of chromium, molybdenum and tungsten.[100-111, 129-139] The complex $[(\eta^5\text{-}C_5H_4PMePh_2)Mo(CO)_3]_2[B(C_6F_5)_4]_2$ has a Mo-Mo bond length similar to those of $[(\eta^5\text{-}C_5H_5)Mo(CO)_3]_2$ (3.235(1) Å) and $[(\eta^5\text{-}C_5Me_5)Mo(CO)_3]_2$ (3.278(14) and 3.281(1) Å, $P2_1/c$ and $P2_1/n$ polymorphs),[136, 138] while $[(\eta^5\text{-}C_5H_4PMePh_2)W(CO)_3]_2[B(C_6F_5)_4]_2$ has a shorter W-W bond length than does $[(\eta^5\text{-}C_5Me_5)W(CO)_3]_2$ (3.288(1) Å).[139]

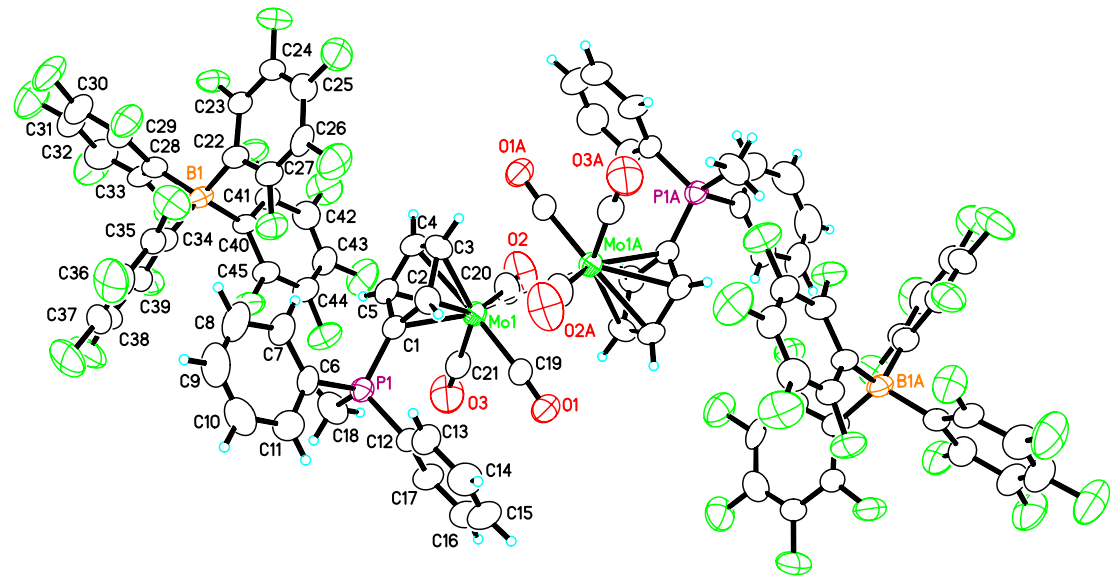

Figure 3-25. The molecular structure of $[(\eta^5\text{-}C_5H_4PMePh_2)Mo(CO)_3]_2[B(C_6F_5)_4]_2$.

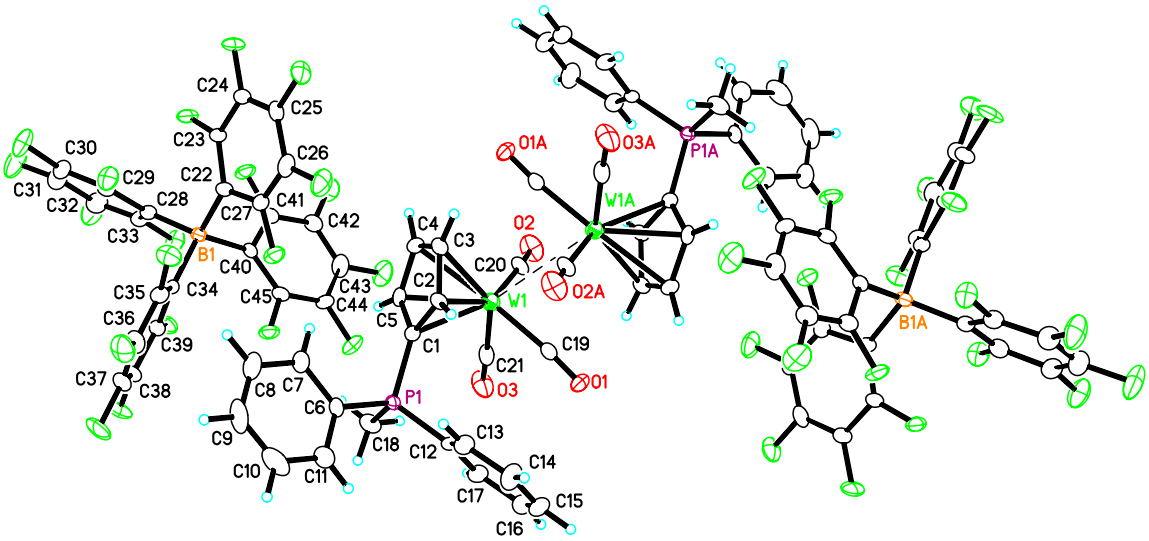

Figure 3-26. The molecular structure of $[(\eta^5\text{-}C_5H_4PMePh_2)W(CO)_3]_2[B(C_6F_5)_4]_2$.

The fact that the Cr-Cr bond of $[(\eta^5\text{-}C_5H_4PMePh_2)Cr(CO)_3]_2[B(C_6F_5)_4]_2$ is longer than that of the sterically very hindered $[(\eta^5\text{-}C_5Me_5)Cr(CO)_3]_2$ may be due in part to electrostatic repulsions generated by bringing two positively charged units together although, of course, the covalent radii of the chromium atoms in the cationic complex would also be smaller. Because of steric crowding arising from the metal-metal bonds,

the CO ligands are splayed away from the adjacent metal center; consistent with this hypothesis the M-C-O bonds are not linear but are bent away from the other monomer unit and, in all three complexes, the -$PMePh_2$ groups of the cyclopentadienylide ligands are orientated away from each other, thus minimizing steric interactions.

Bond Lengths (Å)	[**III$_2$**][$B(C_6F_5)_4]_2$	[**IV$_2$**][$B(C_6F_5)_4]_2$	[**V$_2$**][$B(C_6F_5)_4]_2$
P(1)-C(1)	1.784(2)	1.777(8)	1.777(5)
P-Me	1.792(2)	1.782(9)	1.789(5)
P-Ph avg.	1.788	1.776	1.794
M-C_5 Centroid	1.847	2.010	2.001
C(1)-C(2)	1.428(3)	1.447(12)	1.451(7)
C(1)-C(5)	1.425(3)	1.440(12)	1.445(7)
C(2)-C(3)	1.410(3)	1.399(13)	1.419(7)
C(4)-C(5)	1.411(3)	1.435(12)	1.397(7)
C(3)-C(4)	1.406(4)	1.390(15)	1.418(8)
C(1)-metal	2.164(2)	2.305(8)	2.298(5)
C(2)-metal	2.197(2)	2.319(9)	2.342(5)
C(3)-metal	2.253(2)	2.355(9)	2.388(5)
C(4)-metal	2.230(2)	2.411(8)	2.367(5)
C(5)-metal	2.178(2)	2.337(8)	2.304(5)
Bond Angles (°)			
C(1)-P-Me	108.92(11)	107.7(5)	108.3(2)
C(1)-P-Ph avg.	108.9	109.8	109.5
Me-P-Ph avg.	110.1	109.2	110
Ph-P-Ph	109.66(11)	110.8(4)	109.6(2)
P-C(1)-C_5 Centroid	173.2	172.0	172.9
C(1)-C(2)-C(3)	107.7(2)	106.6(9)	107.2(4)
C(2)-C(3)-C(4)	108.8(2)	112.1(9)	109.3(5)
C(3)-C(4)-C(5)	108.0(2)	106.1(8)	108.0(5)
C(4)-C(5)-C(1)	108.3(2)	108.7(9)	109.1(5)
C(5)-C(1)-C(2)	107.2(2)	106.6(7)	106.4(4)

Table 3-8. Selected bond lengths and angles of [III_2][$B(C_6F_5)_4]_2$, [IV_2][$B(C_6F_5)_4]_2$ and [V_2][$B(C_6F_5)_4]_2$.

Metal	$[(\eta^5\text{-}C_5H_5)M(CO)_3]_2$	$[(\eta^5\text{-}C_5Me_5)M(CO)_3]_2$	$[(\eta^5\text{-}C_5H_4PMePh_2)M(CO)_3]_2^{2+}$
Cr	3.281(1)[100]	3.311(1)[107], 3.310(1)[136]	3.3509(7)
Mo	3.235(1)[100]	3.284(1)[137], 3.281(1)[138]	3.2764(16)
W	3.222(1)[100]	3.288(1)[139]	3.2507(4)

Table 3-9. Comparison of metal-metal bond distances of $[(\eta^5\text{-}C_5H_5)M(CO)_3]_2$, $[(\eta^5\text{-}C_5Me_5)M(CO)_3]_2$ and $[(\eta^5\text{-}C_5H_4PMePh_2)M(CO)_3]_2[B(C_6F_5)_4]_2$ (M = Cr, Mo, W).

In all three cases, the P(1)-C(1)-C_5(centroid) angles are <180° such that the phosphorus atoms of the ligands are bent away from the metal centres. The out of plane bending observed for these cationic complexes is not observed for the neutral complexes **III**, **IV** and **V**, in which the P(1)-C(1)-C_5(Centroid) bond angles are nearly linear, but a similar feature is found in the crystal structure of $[(\eta^5\text{-}C_5H_4PMePh_2)Mo(CO)_3I][I]$ in which the P atom is also bent out of the C_5 ring plane. The P(1)-C(1) bonds, used as an indication of the P-C bond order, are elongated in the oxidized species relative to the neutral tricarbonyl starting materials, and again a similar lengthening of the P(1)-C(1) bond is observed in $[(\eta^5\text{-}C_5H_4PMePh_2)Mo(CO)_3I][I]$. The chromium complex has the longest P(1)-C(1) bond distance of 1.784(2) Å, but in all three complexes this bond length approaches those of the P-Ph bonds.

The C_5 ring is in all cases bound in an η^5 fashion with small variations in the M-C bond distances; carbons C(1), C(2) and C(5) are slightly closer to the metal than are C(3) and C(4). The M-C_5 bond distances are also shorter on average than those observed in the neutral complexes, consistent with the above suggestion of smaller metal covalent radii in the oxidized complexes. The C_5 ring bond lengths and angles do not differ significantly from those of the neutral precursors and the structures of the borate anions are consistent with other structures reported for this anion.[142, 143]

3.3.4 Nature of the Oxidized Complexes in Solution: IR, NMR and MS Data

Having established dimeric structures for all three oxidized species in the solid state, we carried out a series of spectroscopic studies (IR and NMR spectroscopy and ES-MS on solutions, IR spectroscopy on the crystalline solids) to determine the extent to which dissociation to monomeric species might occur in solution. The related compounds $[(\eta^5\text{-}C_5H_5)Cr(CO)_3]_2$ and $[(\eta^5\text{-}C_5Me_5)Cr(CO)_3]_2$ do dissociate significantly while the analogous molybdenum and tungsten dimers do not dissociate at all.[100-111, 129-139]

3.3.4.1 IR Spectra

IR spectra were obtained for all three compounds $[(\eta^5\text{-}C_5H_4PMePh_2)M(CO)_3]_2[B(C_6F_5)_4]_2$ (M = Cr, Mo, W) in THF solutions and in the solid state as Fluorolube mulls; all are soluble and stable in THF at room temperature. Interestingly, THF solutions of $[(\eta^5\text{-}C_5H_4PMePh_2)Cr(CO)_3]_2[B(C_6F_5)_4]_2$ are yellow rather than the green of the crystalline dimer, while those of $[(\eta^5\text{-}C_5H_4PMePh_2)Mo(CO)_3]_2[B(C_6F_5)_4]_2$ and $[(\eta^5\text{-}C_5H_4PMePh_2)W(CO)_3]_2[B(C_6F_5)_4]_2$ are red, the colour of the crystalline dimers. Data for the carbonyl stretching modes are listed in Table 3-10 and the IR spectra are shown in Figure 3-27, Figure 3-28 and Figure 3-29. As can be seen, while the average frequency of the mull spectrum of the chromium complex is similar to the averages of the solid state spectra of the molybdenum and tungsten complexes, the peak pattern of the chromium complex differs significantly from those of the other spectra. The difference is probably a result of the chromium complex assuming a different space group.

Of note, however, the mull and solution IR spectra of the chromium dimer are very different while the corresponding pairs of solid and solution phase spectra of the

molybdenum and tungsten dimers are very similar. Indeed, the pattern in the carbonyl stretching region of the solution spectrum of $[(\eta^5\text{-}C_5H_4PMePh_2)Cr(CO)_3]_2[B(C_6F_5)_4]_2$ is very similar to that of the monomeric $(\eta^5\text{-}C_5Me_5)Cr(CO)_3$, for which υ(CO) are observed at 1994 (s) and 1876 (s, br) cm^{-1} in THF, 1994 (s) and 1890 (s, br) in toluene.[107] Thus the IR data in Table 3-10 and Figure 3-27 are consistent with the presence of the **III**$^+$ ion in solution although the positive charge results in much higher frequencies than were observed for $(\eta^5\text{-}C_5Me_5)Cr(CO)_3$, and confirm the conclusion, reached on the basis of the electrochemical experiments, of extensive dissociation of $[(\eta^5\text{-}C_5H_4PMePh_2)Cr(CO)_3]_2[B(C_6F_5)_4]_2$ in solution.

Metal	THF (cm^{-1})	Fluorolube (cm^{-1})
Cr	2037 (s), 1955 (s br), 1914 (s br)	2036 (vw), 1970, 1949, 1932, 1897 (w sh)
Mo	2025 (w), 1976 (s br), 1939 (s br), ~1922 (sh)	2037 (vw), 1975, 1939, 1932
W	2023 (w), 1973 (s br), 1933 (s br), ~1922 (sh)	1972, 1925

Table 3-10. Solution (THF) and solid state (Fluorolube mulls) IR data (υ(CO)) of $[(\eta^5\text{-}C_5H_4PMePh_2)M(CO)_3]_2[B(C_6F_5)_4]_2$ (M = Cr, Mo, W).

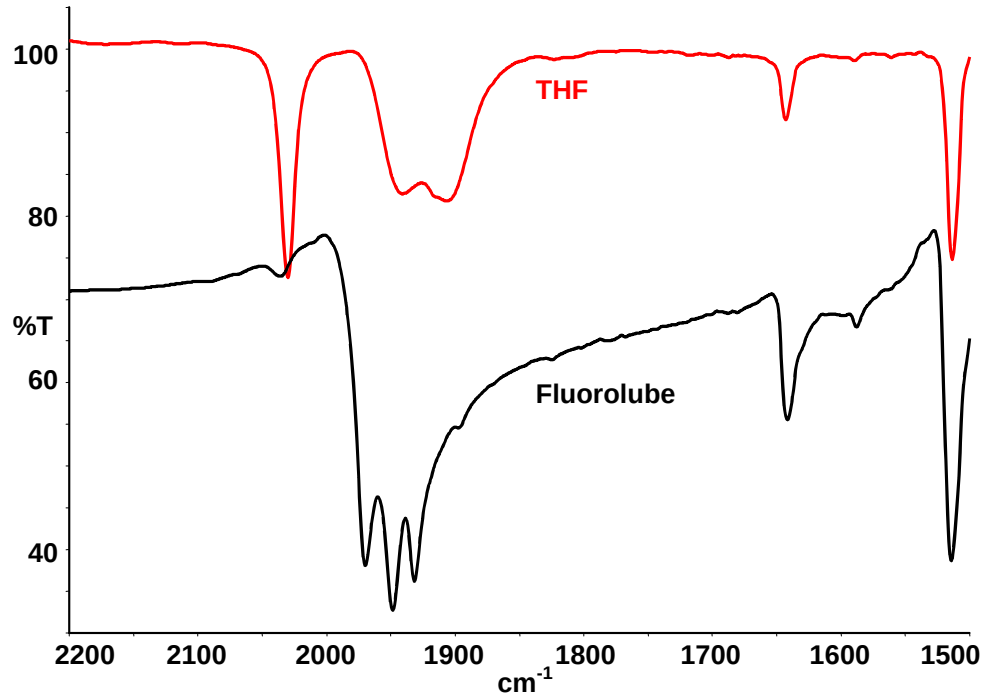

Figure 3-27. The IR spectra of $[(\eta^5\text{-}C_5H_4PMePh_2)Cr(CO)_3]_2[B(C_6F_5)_4]_2$ in solution and as a mull. The peaks at 1514 and 1643 cm^{-1} are attributed to the anion.

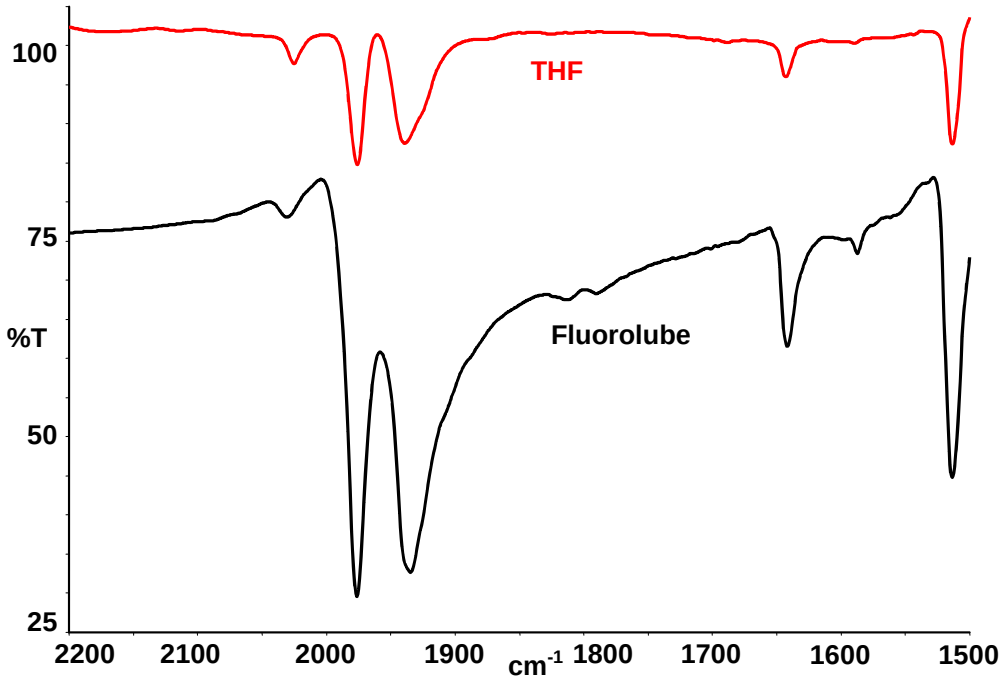

Figure 3-28. The IR spectra of $[(\eta^5\text{-}C_5H_4PMePh_2)Mo(CO)_3]_2[B(C_6F_5)_4]_2$ in solution and as a mull. The peaks at 1514 and 1643 cm^{-1} are attributed to the anion.

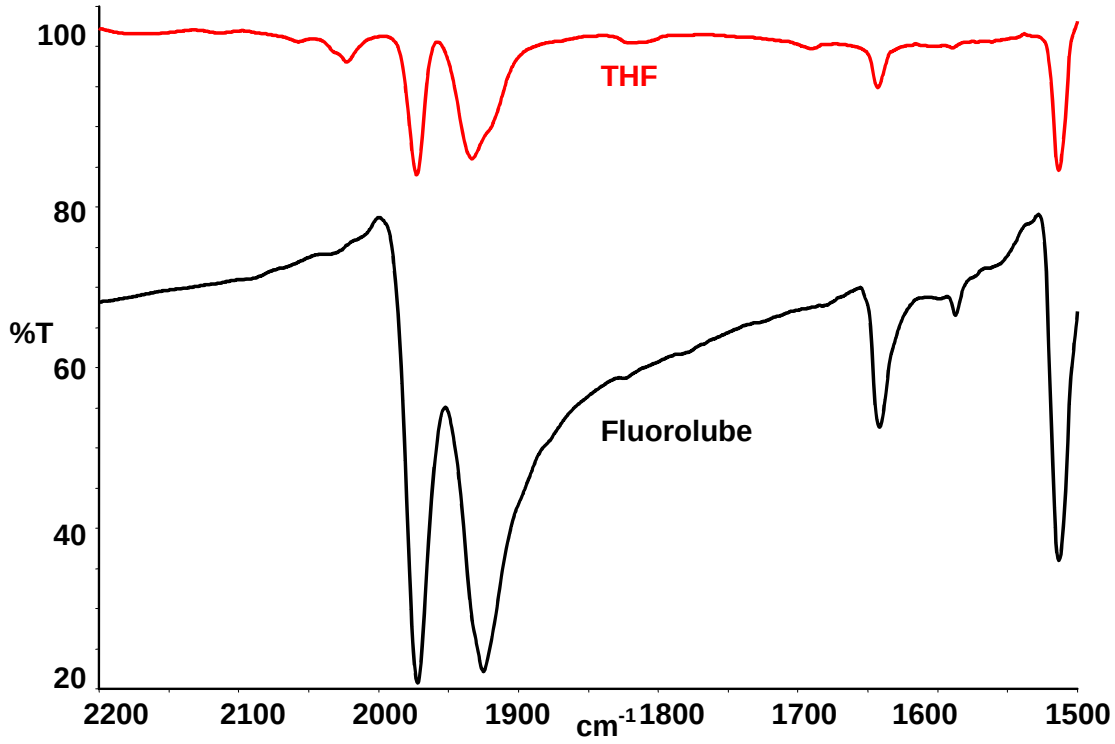

Figure 3-29. The IR spectra of $[(\eta^5\text{-}C_5H_4PMePh_2)W(CO)_3]_2[B(C_6F_5)_4]_2$ in solution and as a mull. The peaks at 1514 and 1643 cm^{-1} are attributed to the anion.

Our observations that the mull IR spectra of $[(\eta^5\text{-}C_5H_4PMePh_2)Mo(CO)_3]_2[B(C_6F_5)_4]_2$ and $[(\eta^5\text{-}C_5H_4PMePh_2)W(CO)_3]_2[B(C_6F_5)_4]_2$ are nearly identical, not only to each other but to their solution spectra seemingly also confirm the conclusions based on the electrochemical evidence that the dimeric ions $\mathbf{IV_2}^{2+}$ and $\mathbf{V_2}^{2+}$ are the dominant species in solution as well as in the solid state. Indeed, the IR spectra, which exhibit three strong peaks (one a shoulder) in the region 1900-1980 cm^{-1} in the solution spectra, are very similar in pattern to the spectra of $[(\eta^5\text{-}C_5Me_5)Cr(CO)_3]_2$ (which is formed upon dimerization of the monomeric radical $(\eta^5\text{-}C_5Me_5)Cr(CO)_3$ at lower temperatures) in THF (1919, 1902, 1876 cm^{-1}) and toluene (1920, 1900, 1875 cm^{-1}),[107] although again the frequencies of the cationic complexes are higher. Interestingly, however, the solution spectra of the molybdenum and tungsten

complexes also exhibit weak peaks at 2025 and 2023 cm^{-1}, respectively, very close in frequency to the peak observed at 2030 cm^{-1} in the solution spectrum of $[(\eta^5\text{-}C_5H_4PMePh_2)Cr(CO)_3]_2[B(C_6F_5)_4]_2$ and thus possibly evidence for the presence of very low concentrations of the monomers in equilibrium with the dimers. Although the electrochemical data discussed in the Appendix are not necessarily inconsistent with the presence of very low concentrations of $\mathbf{IV}^+$ and $\mathbf{V}^+$ in solutions of $\mathbf{IV_2}^{2+}$ and $\mathbf{V_2}^{2+}$, respectively, the evidence for these species is slight. Indeed, observation of similar high frequency peaks in the mull spectra of the chromium and molybdenum dimers would require that these compounds dissolve and dissociate slightly in Fluorolube, a problematic conclusion at best.

3.3.4.2 Electrospray Mass Spectroscopy

ES-MS data of THF solutions were used to characterize the nature of the oxidized products from the reactions of **III**, **IV** and **V** with $[Cp_2Fe][B(C_6F_5)_4]$; high-resolution spectra were also obtained. The spectra and the calculated isotopic distribution patterns are shown in Figure 3-30 ($\mathbf{III}^+$), Figure 3-31 ($\mathbf{IV}^+$) and Figure 3-32 ($\mathbf{V}^+$). For all three systems, the ES mass spectra exhibited no dimeric species, only the monomeric 17 electron radical cations, $\mathbf{III}^+$, $\mathbf{IV}^+$ or $\mathbf{V}^+$ were observed, confirmed by excellent isotopic peak distribution matches with the calculated distributions expected for each complex. The conclusions to be drawn from this information in isolation would be that the species in solution are monomeric. However, in view of the overwhelming mass of electrochemical and IR data, the molybdenum and tungsten dimers must dissociate under the conditions of the mass spectroscopy experiment.

The high-resolution data for $\mathbf{III}^+$, $\mathbf{IV}^+$ and $\mathbf{V}^+$ are in excellent agreement with the expected formulas for the 17 electron monomers, with the experimental and calculated m/z values differing by only 6.8926, 4.1748 and 3.5448 ppm, respectively. In addition, an MS-MS experiment of the molecular ion of $\mathbf{III}^+$ revealed a major fragment with a m/z of 316 m/z; this corresponds to the loss of three carbonyls.

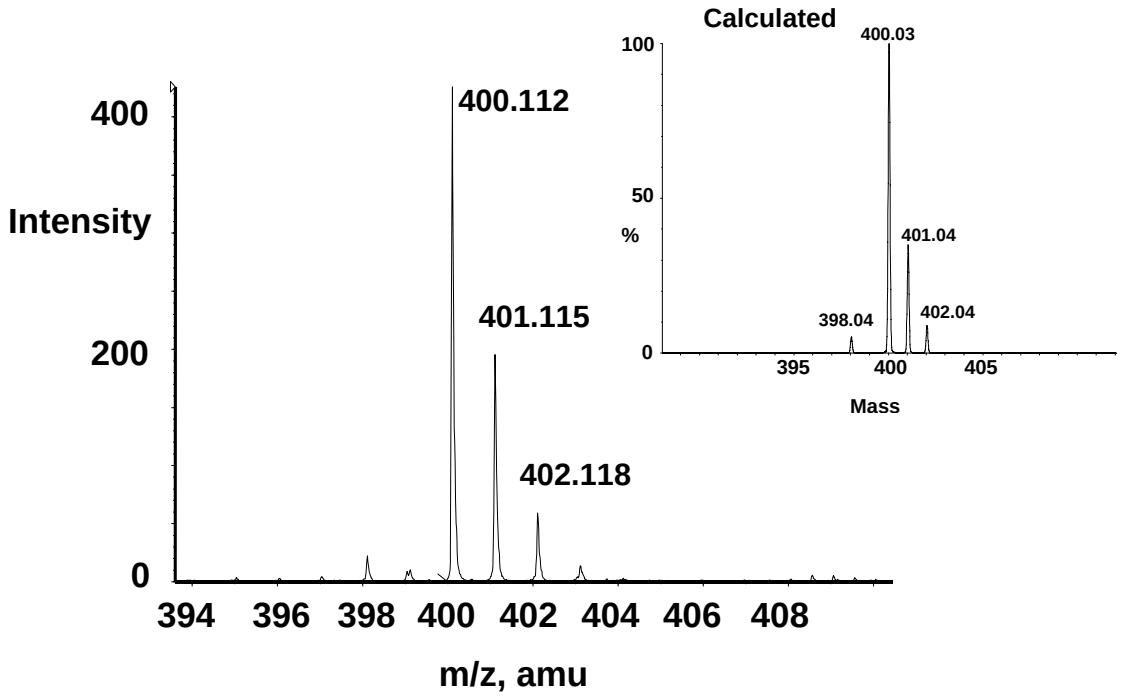

Figure 3-30. The ES-MS of $\mathbf{III}^+$ in THF. The calculated isotopic distribution for $(C_{21}H_{17}O_3P_1Cr_1)^+$ is shown in the inset figure.

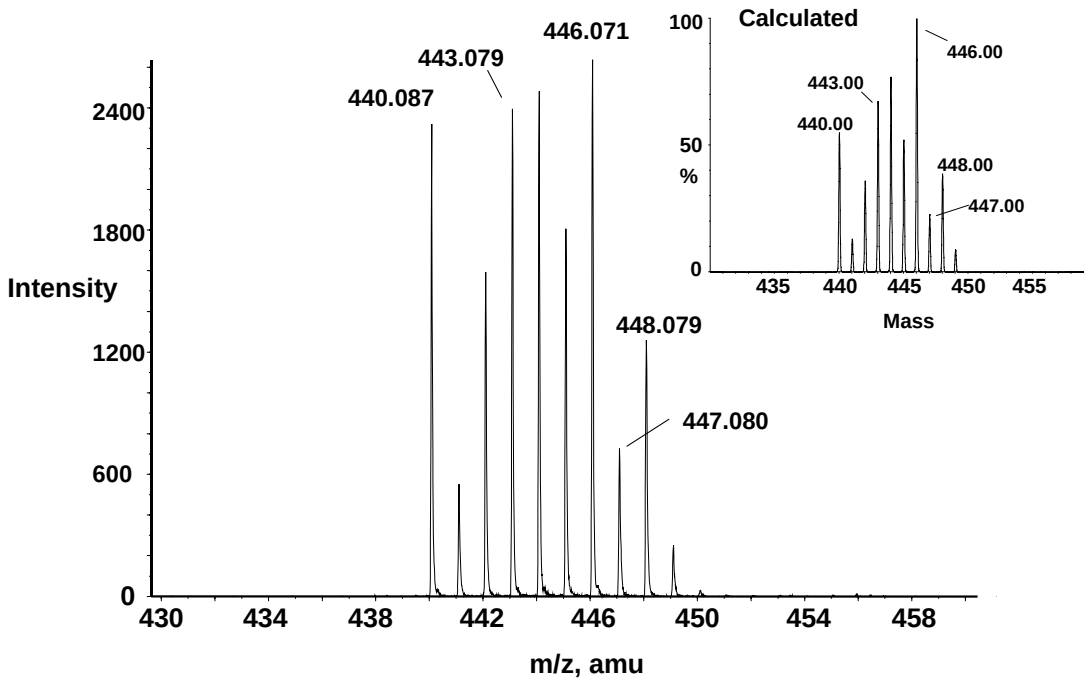

Figure 3-31. The ES-MS of IV^+ in THF. The calculated isotopic distribution for $(C_{21}H_{17}O_3P_1Mo_1)^+$ is shown in the inset figure.

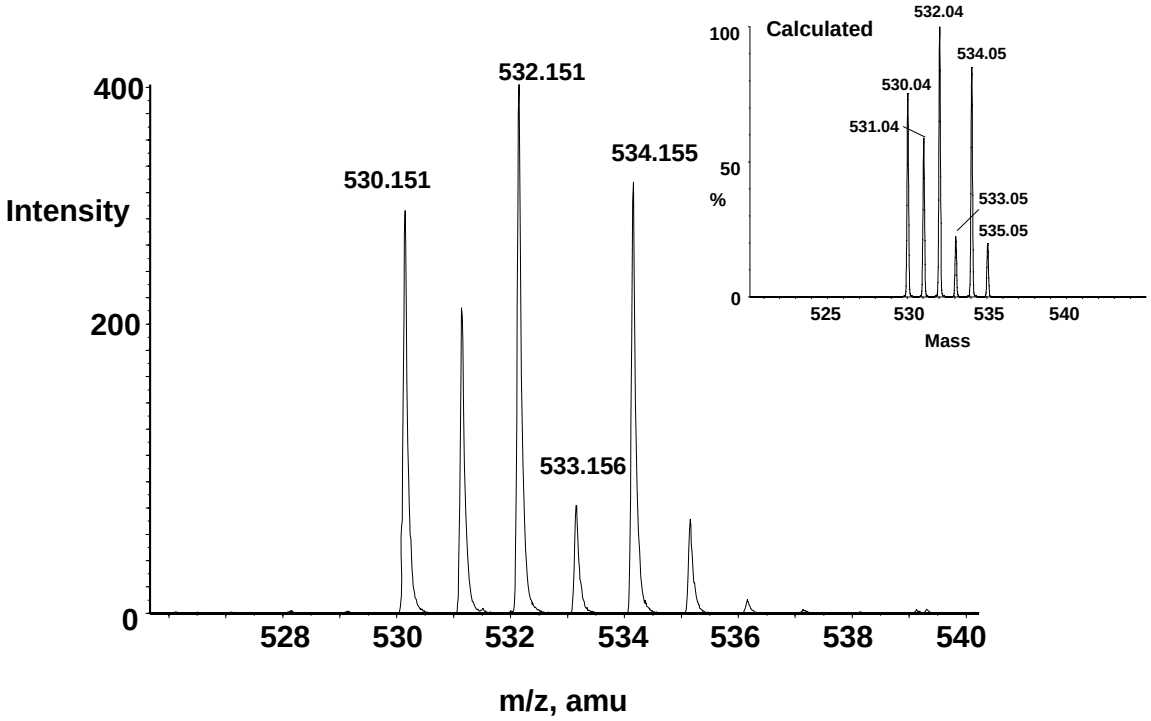

Figure 3-32. The ES-MS of V^+ in THF. The calculated isotopic distribution for $(C_{21}H_{17}O_3P_1W_1)^+$ is shown in the inset figure.

3.3.4.3 NMR of $[(\eta^5\text{-}C_5H_4PMePh_2)Cr(CO)_3]_2[B(C_6F_5)_4]_2$

NMR experiments were also carried out to characterize the solution behaviour of the oxidized species; these included ^1H, ^{13}C and ^{31}P NMR experiments and variable temperature ^1H experiments. A 600 MHz ^1H NMR spectrum (shown in Figure 3-33) of $[(\eta^5\text{-}C_5H_4PMePh_2)Cr(CO)_3]_2[B(C_6F_5)_4]_2$ in CD_2Cl_2 at 298 K exhibited two very broad C_5H_4 resonances at δ 28.90 ($\Delta\upsilon_{1/2}$ = 535 Hz) and 13.65 ($\Delta\upsilon_{1/2}$ = 470 Hz), three somewhat broadened phenyl resonances at δ 7.85, 7.65 and 7.60 and a broad methyl resonance at δ 1.18 ($\Delta\upsilon_{1/2}$ = 75 Hz); no couplings could be observed in any of the resonances.

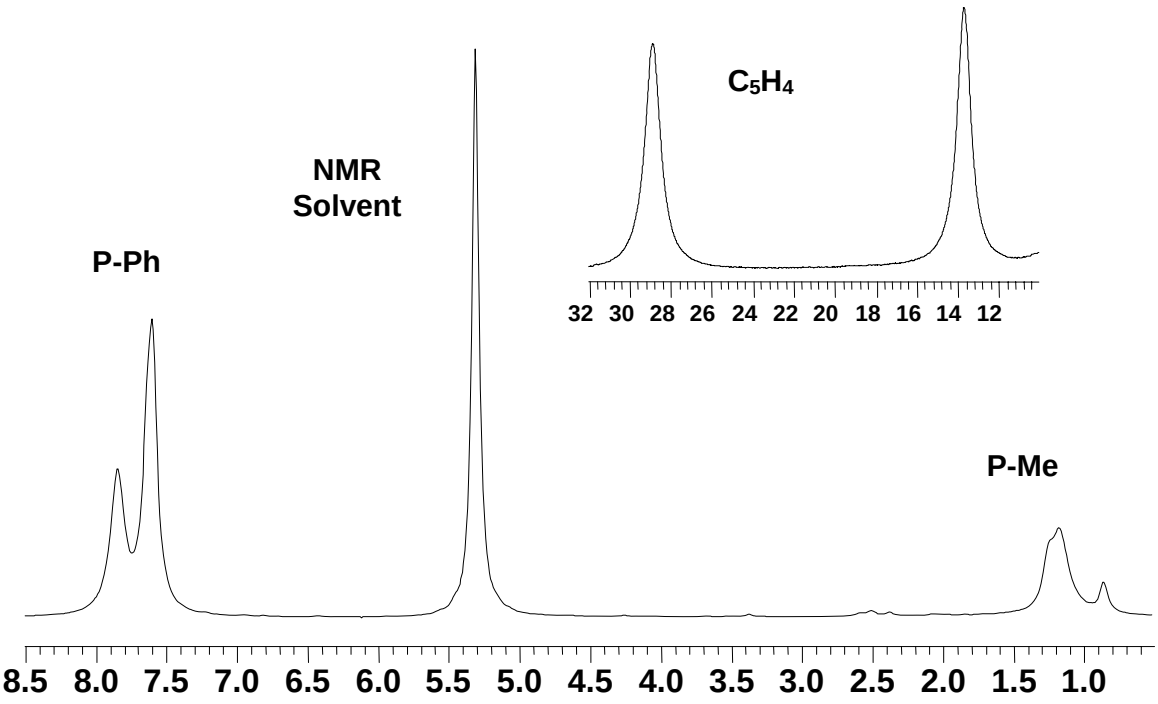

Figure 3-33. The ^1H NMR spectrum of $[III_2][B(C_6F_5)_4]_2$ in CD_2Cl_2.

The combination of significant broadening of the ^1H resonances and the very unusual chemical shifts of the C_5H_4 ring hydrogens are consistent with the species in solution being paramagnetic,[144] but an attempt to carry out a variable temperature experiment

failed because of precipitation of $[(\eta^5\text{-}C_5H_4PMePh_2)Cr(CO)_3]_2[B(C_6F_5)_4]_2$ at lower temperatures.

As shown during our IR studies, however, this complex is very soluble in THF and ^1H NMR spectra were therefore readily obtained in THF-d_8 over the temperature range 323 K to 183 K. No precipitation of either the green dimer or any other solid was noted when the sample was cooled to 183 K but the solution, which is golden yellow at room temperature, turned green reversibly on cooling. These colour changes arise, of course, from reversible dissociation of the green $\mathbf{III_2}^{2+}$ to the yellow $\mathbf{III}^+$.

The ^1H NMR spectrum of $[(\eta^5\text{-}C_5H_4PMePh_2)Cr(CO)_3]_2[B(C_6F_5)_4]_2$ in THF-d_8 at 298 K (shown in Figure 3-34 and Figure 3-35) was very similar to that observed in CD_2Cl_2, exhibiting two broad C_5H_4 resonances at δ 26.08 ($\Delta\upsilon_{1/2}$ = 565 Hz) and 13.62 ($\Delta\upsilon_{1/2}$ = 480 Hz), three broad phenyl resonances in the region δ 8.07-7.66 and a broad P-Me resonance at δ 2.34 ($\Delta\upsilon_{1/2}$ = 95 Hz). However, lowering the temperature of the sample from 323 K to 183 K resulted in major changes, the C_5H_4 resonances broadening somewhat, shifting from δ 23.72 ($\Delta\upsilon_{1/2}$ = 470 Hz) and 12.85 ($\Delta\upsilon_{1/2}$ = 385 Hz) at 323 K to δ 28.70 ($\Delta\upsilon_{1/2}$ = 820 Hz) and 14.10 ($\Delta\upsilon_{1/2}$ = 795 Hz) at 253 K, and *weakening* relative to the resonance of CH_2Cl_2 added and used as an internal reference. Concomitantly, weak new resonances began to appeared in the "normal" C_5H_4 region, at δ ~5.5-6.2.

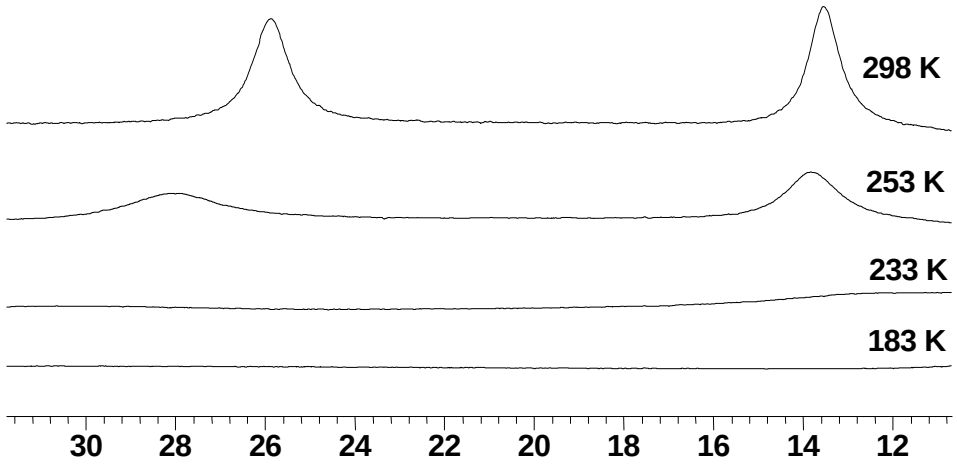

Figure 3-34. Variable temperature ^{1}H NMR spectra (THF-d_8) showing the disappearance of the C_5H_4 peaks from III^+ as the temperature is lowered.

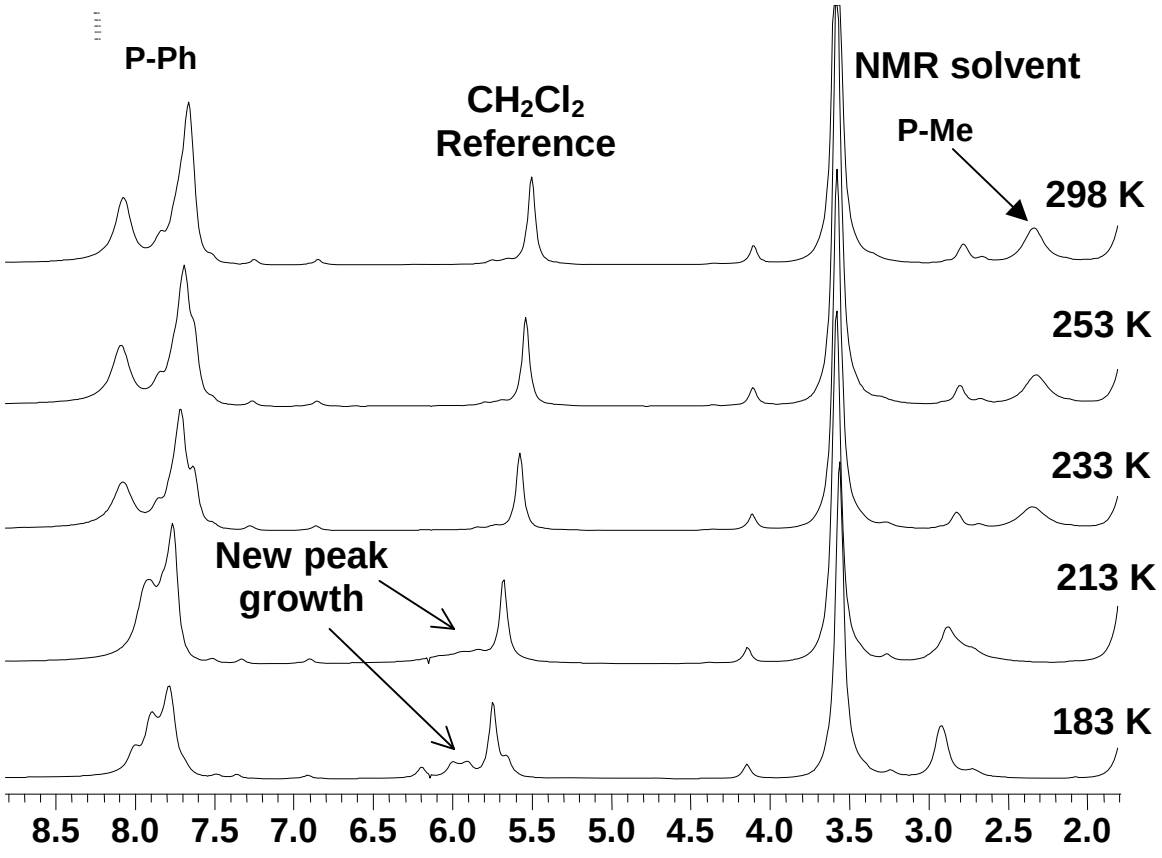

Figure 3-35. Variable temperature ^{1}H NMR spectra (normal proton region) of $[III_2][B(C_6F_5)_4]_2$ in THF-d_8.

By 233 K, the integrated intensities of the two C_5H_4 resonances, now at δ 29.97 and 12.70, had become extremely low and had been replaced by four somewhat broadened resonances of equal intensity, at δ 6.12, 5.96, 5.85 and 5.65. The chemical shifts of the latter four resonances are similar to the C_5H_4 chemical shifts of **III**, **IV**, **V**, $\mathbf{IV_2^{2+}}$ and $\mathbf{V_2^{2+}}$, supporting the assignments. That there are four separate resonances at this very low temperature rather than the two observed for the other compounds at room temperature probably arises because the cationic dimer is "frozen" in a conformation in which the four H atoms are not equivalent. Indeed, the observed lack of symmetry is consistent with the solid state structure in which the four ring protons are non-equivalent because of the fixed position of the $PMePh_2$ group; at these low temperatures, slowed rotation of the $PMePh_2$ would be expected and would give rise to magnetic nonequivalence of the C_5H_4 protons.

Simultaneously with the above changes, the P-Me resonance (δ 2.34 at 298 K) decreased in intensity as a new resonance at δ 2.79 appeared and gained in intensity. The original P-Me resonance had disappeared completely at 213 K, leaving only a broadened P-Me resonance at δ 2.89. The latter was not a singlet, but whether the splitting observed was a result of coupling to ^{31}P or of "freezing" of more than one conformation, or of a combination of both, could not be determined. Changes in the closely spaced phenyl resonances as the temperature was lowered were relatively subtle and shed no new light on the situation.

These observations extend our conclusions, discussed above and based on visual, electrochemical and IR spectroscopic evidence, that $\mathbf{III_2^{2+}}$ undergoes reversible dissociation in solution to $\mathbf{III^+}$. However, although the electrochemical investigation

(Appendix) of this equilibrium in CH_2Cl_2 at temperatures from ambient to 238 K failed to show any changes that would indicate involvement of dimerization of **III**$^+$, the NMR data suggest that significant dimerization occurs in THF, at least, at temperatures as high as 253 K and that little or no monomer is present at or below 213 K.

Similar observations have been made previously for $[(\eta^5\text{-}C_5H_5)Cr(CO)_3]_2$ and $[(\eta^5\text{-}C_5Me_5)Cr(CO)_3]_2$,[100-111, 129-139] of course, but in one sense the $[(\eta^5\text{-}C_5H_4PMePh_2)Cr(CO)_3]_2[B(C_6F_5)_4]_2$ equilibrium stands in stark contrast to the two neutral monomer-dimer systems. Exchange processes between monomer and dimer for both neutral systems are sufficiently rapid on the NMR time scale that averaged ^1H resonances are observed.[100-111, 129-139] However, for $[(\eta^5\text{-}C_5H_4PMePh_2)Cr(CO)_3]_2[B(C_6F_5)_4]_2$, separate C_5H_4 and P-Me resonances are observed over a wide temperature range and thus monomer-dimer exchange for this system must be slow on the NMR time scale. We are unaware of any other such system where this type of behaviour has been observed.

3.3.4.3.1 The Evans Method

The Evans method[66-70, 145] was used to determine the magnetic susceptibility of solution samples of $[(\eta^5\text{-}C_5H_4PMePPh_2)Cr(CO)_3]_2[B(C_6F_5)_4]_2$ in order to characterize the behaviour in solution. This method is based upon the fact that the chemical shift of a proton is influenced by the magnetic susceptibility of the sample medium. If an inert species is examined, its chemical shift will be changed by the presence of paramagnetic compounds in solution. This effect is illustrated in Figure 3-36, which shows the effect of the presence of the radical cation $(\eta^5\text{-}C_5H_4PMePPh_2)Cr(CO)_3^+$ on the shift of cyclohexane.

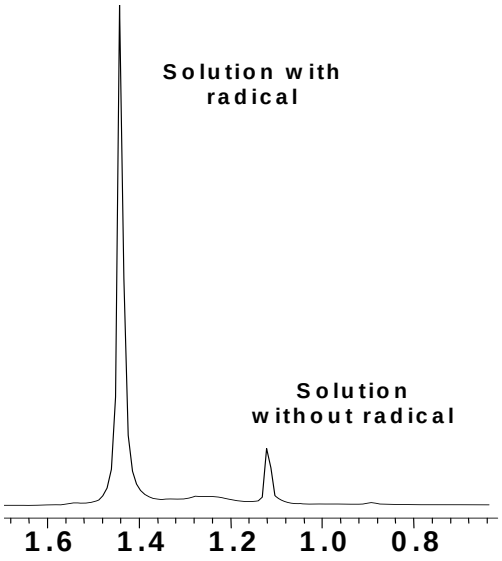

Figure 3-36. The shift of cyclohexane standard caused by a solution (CD_2Cl_2) of the radical (η^5-$C_5H_4PMePPh_2$)$Cr(CO)_3^+$. The smaller peak comes from a cyclohexane solution (CD_2Cl_2) in a capillary tube within the NMR tube.

The change in frequency of two identical protons in the inert species (Δf) is described by the equation:

$$\frac{\Delta f}{f_o} = \frac{2\pi}{3}\Delta \mathrm{K}$$

where f_0 is the spectrometer frequency (Hz) and ΔK is the change in the volume magnetic susceptibility (considered to be a dimensionless quantity). This equation can be used with high frequency FT spectrometers. The magnetic susceptibilities calculated here are done in cgs units as has been the standard in literature reports. The volume susceptibility is not as useful as the mass susceptibility (χ_g) defined as:

$$\chi_g = \frac{\mathrm{K}}{m}$$

where m is the concentration of paramagnetic substance in g/cm^3.

Using these two equations, χ_g can be calculated from the equation:

$$\chi_g = \frac{3\Delta f}{2\pi f_o m} + \chi_o$$

where χ_o is the mass susceptibility of the pure solvent. A third term which corrects for the difference in density between the pure solvent and the solution may be added to the above equation, but this correction is normally a small value which is negligible when the paramagnetism of the sample is large and this was ignored in our calculations (as is usually done). The value of χ_o can be calculated from the atomic susceptibilities of the substituent atoms or may be found in various reference sources. The resulting mass susceptibility can be converted to the molar susceptibility, χ_m, by multiplying χ_g by the molar mass (M) of the sample:

$$\chi_m = \chi_g M + corr$$

The second term in this equation must be included to correct for the diamagnetic contribution from the ligand atoms. This value is calculated by summing the diamagnetic contribution of the ligand atoms and other atoms present in the complex (anions, etc.) from tabulated values. The diamagnetism of the atoms present in solution have the effect of decreasing the paramagnetism of the solution and this must be corrected for. Finally, the magnetic moment, with units of Bohr Magnetons (B.M.), can be calculated from:

$$\mu = 2.84\sqrt{\chi_m T}$$

where T is the temperature in Kelvin.

To shed more light on the equilibrium situation implied by the ^{1}H NMR data, the Evans method[66-70, 145] was used to determine the average magnetic moment of the chromium atoms of $[(\eta^5\text{-}C_5H_4PMePh_2)Cr(CO)_3]_2[B(C_6F_5)_4]_2$ in CD_2Cl_2 at 298 K and in

THF over the temperature range 323 K to 233 K. The magnetic susceptibilities were measured using cyclohexane and the residual proton signal of CD_2Cl_2 as references, and diamagnetic corrections and magnetic susceptibilities of solvents were taken from literature sources.[66-70, 145] The resulting magnetic moments determined at each temperature are shown in Table 3-11. As can be seen, the experiments carried out at higher temperatures yielded, for both solvents, magnetic moments of ~1.8 Bohr magnetons, very close to the spin only value for one unpaired electron.[66-70, 145] However, in THF the average magnetic moment decreased to 1.46 Bohr magnetons on cooling to 233 K, a result consistent with significant dimerization of $\mathbf{III}^+$ to $\mathbf{III}_2^{2+}$.

Temperature	Solvent	μ (B.M.) (± 0.05)
323	THF-d_8	1.83
308	THF-d_8	1.78
298	THF-d_8	1.80
273	THF-d_8	1.93
253	THF-d_8	1.78
233	THF-d_8	1.46
298	CD_2Cl_2	1.71

Table 3-11. Magnetic susceptibilities of $[(\eta^5\text{-}C_5H_4PMePh_2)Cr(CO)_3]_2[B(C_6F_5)_4]_2$ at different temperatures.

3.3.4.4 NMR of $[(\eta^5\text{-}C_5H_4PMePh_2)M(CO)_3]_2[B(C_6F_5)_4]_2$ (M = Mo,W)

The ^1H, ^{31}P and ^{13}C NMR spectra of $[(\eta^5\text{-}C_5H_4PMePh_2)Mo(CO)_3]_2[B(C_6F_5)_4]_2$ and $[(\eta^5\text{-}C_5H_4PMePh_2)W(CO)_3]_2[B(C_6F_5)_4]_2$ were obtained in THF-d_8 since these compounds exhibit low solubilities in CD_2Cl_2. For both complexes**,** the proton and phosphorus resonances were somewhat broadened, possibly evidence for the presence of a small amount of monomeric radicals in the solutions.

Thus the ^{1}H NMR spectrum, shown in Figure 3-37, of $[(\eta^5\text{-}C_5H_4PMePh_2)Mo(CO)_3]_2[B(C_6F_5)_4]_2$ exhibited a poorly resolved P-Me doublet at δ 2.88, C_5H_4 resonances as broad, featureless bands in the region δ 6.10-6.04 and at δ 5.91, and phenyl resonances in the region δ 7.87-7.72. In no case could ^{1}H-^{1}H coupling be resolved but variable temperature experiments conducted in the temperature range 323-213 K showed that the phenyl resonances resolved to show three peaks at 323 K. The C_5H_4 resonances begin to overlap as the temperature was raised. The ^{31}P NMR spectrum exhibited only one resonance at δ 19.88, slightly shifted from that of **IV** (δ 18.25 in CD_2Cl_2). The ^{13}C NMR is very similar to that previously reported for $[(\eta^5\text{-}C_5H_4PMePh_2)M(CO)_3I][I]$, with nearly identical chemical shifts.

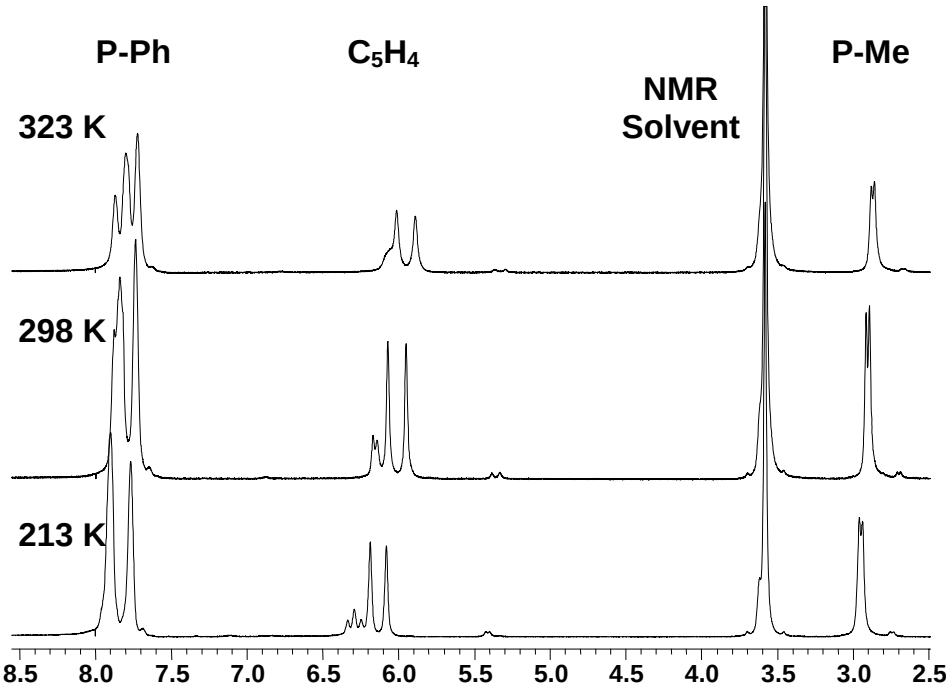

Figure 3-37. The ^{1}H NMR spectrum of $[(\eta^5\text{-}C_5H_4PMePh_2)Mo(CO)_3]_2[B(C_6F_5)_4]_2$ in THF-d_8 (213, 298, 323 K).

The ^{1}H NMR spectrum, shown in Figure 3-38, of $[(\eta^5\text{-}C_5H_4PMePh_2)W(CO)_3]_2[B(C_6F_5)_4]_2$ at 298 K exhibited two broad phenyl resonances at δ

7.80-7.71, the P-Me resonance as a broad doublet at δ 2.86 and the C_5H_4 resonances as a broad grouping of bands centred at δ 6.05. Variable temperature ^1H NMR spectra were obtained in the temperature range 198-323 K; a third phenyl resonance was observed and the C_5H_4 multiplet narrowed above 298 K.

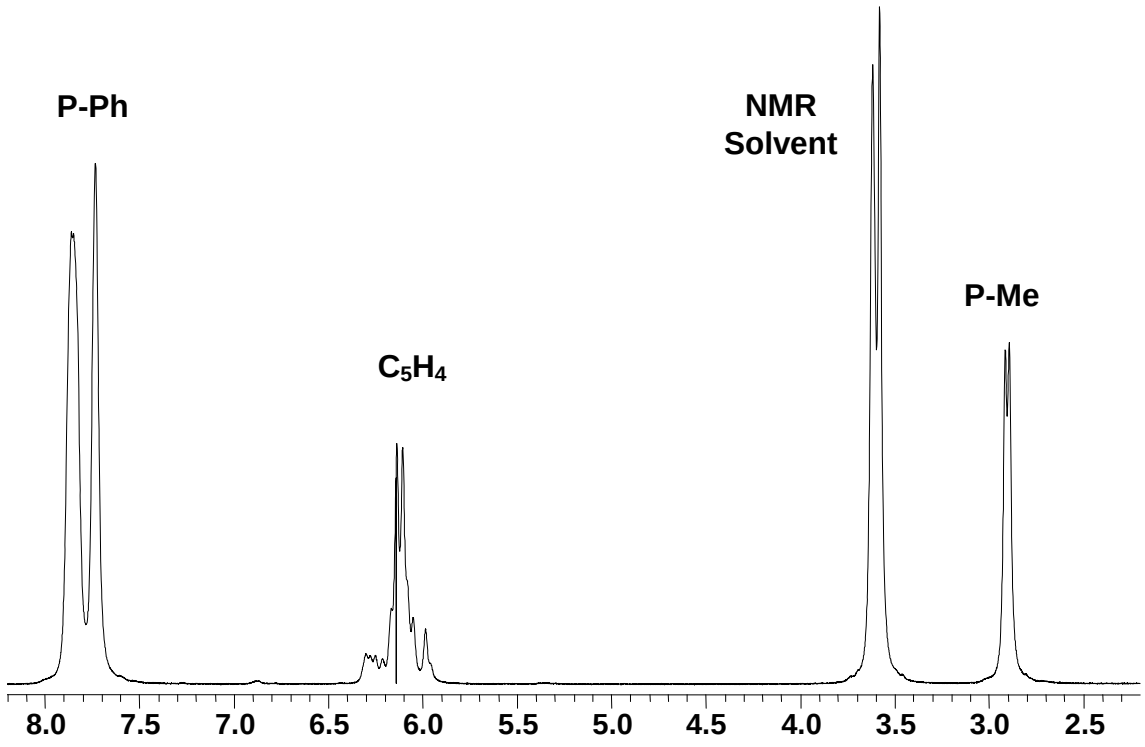

Figure 3-38. The ^1H NMR spectrum of $[(\eta^5\text{-}C_5H_4PMePh_2)W(CO)_3]_2[B(C_6F_5)_4]_2$ in THF-d_8 (298 K).

3.4 Attempts to Synthesize Titanium ylide complexes

Several titanium complexes of phosphorus ylides have been previously reported,[30] but the characterization of these complexes was incomplete and did not offer any insight into the bonding of the ylide to the metal. With the interest in group 4 metallocenes as catalysts for olefin polymerizations, examination of complexes of $C_5H_4PMePh_2$ seemed warranted. We undertook the synthesis of these complexes using two routes; the direct

addition of the ylide to the metal, and the assembly of the ylidic ligand on the metal. Herein, we report our attempts and the results obtained.

3.4.1 Direct Addition of II to $TiCl_4$

Using the same methodology used by Holy *et al.* who attempted to synthesize the complex $[(C_5H_4PPh_3)_2TiCl_2][Cl]_2$,[30] a THF solution of **II** with $TiCl_4$ was stirred, with the hope of generating a cationic complex as shown in Figure 3-39.

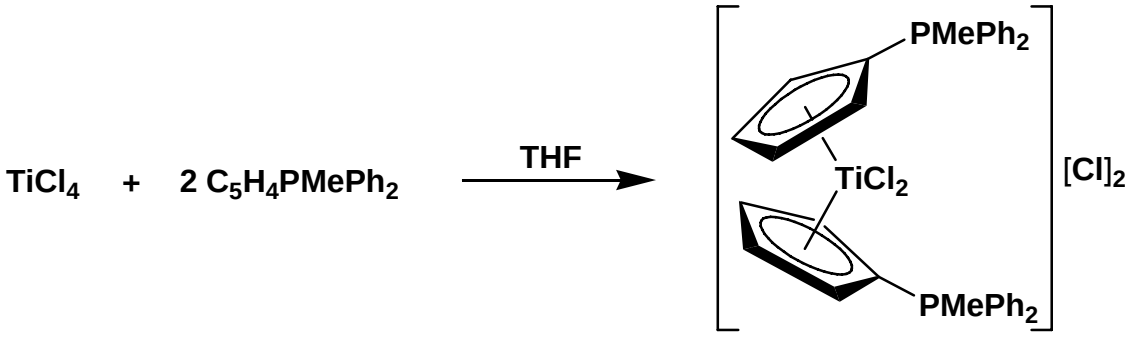

Figure 3-39. The attempted reaction of $TiCl_4$ with II.

When two equivalents of **II** were stirred with $TiCl_4$, a red solution resulted. After the addition of hexanes, a red solid precipitated from solution. ^1H and ^{31}P NMR spectra of the red solid were collected in CD_2Cl_2. The ^{31}P NMR spectrum showed four peaks at δ 24.91, 14.88, 14.42 and 10.77, with the peak at δ 24.91 being the major species. This shift at δ 24.91 is consistent with the complexation of **II** in other complexes, but it is at a lower field versus the group 6 tricarbonyl complexes of **II**. Binding to a metal in a higher oxidation state would be expected to cause this downfield shift. In the ^1H NMR spectrum (shown in Figure 3-40), at least four doublets are seen corresponding to a P-Me group. Two peaks at δ 3.22 and 2.95 are nearly equal in intensity and are the most intense

resonances in this region. Two doublets that are weaker in intensity are also present at δ 3.09 and 2.62. Several multiplets are also seen at δ 7.35-7.15 and δ 6.30-6.40 that could indicate the presence of C_5H_4 protons. A number of other peaks are also observed in the ^{1}H NMR spectrum indicating that a number of products were generated. The ^{1}H NMR resonances do not match with those reported by Holy *et al.* in DMSO-d_6.[30] Their report describes a C_5H_4 multiplet centred at δ 7.9.[30] No ^{31}P NMR data were provided. In addition, they isolated a tan solid, not a red product.[30]

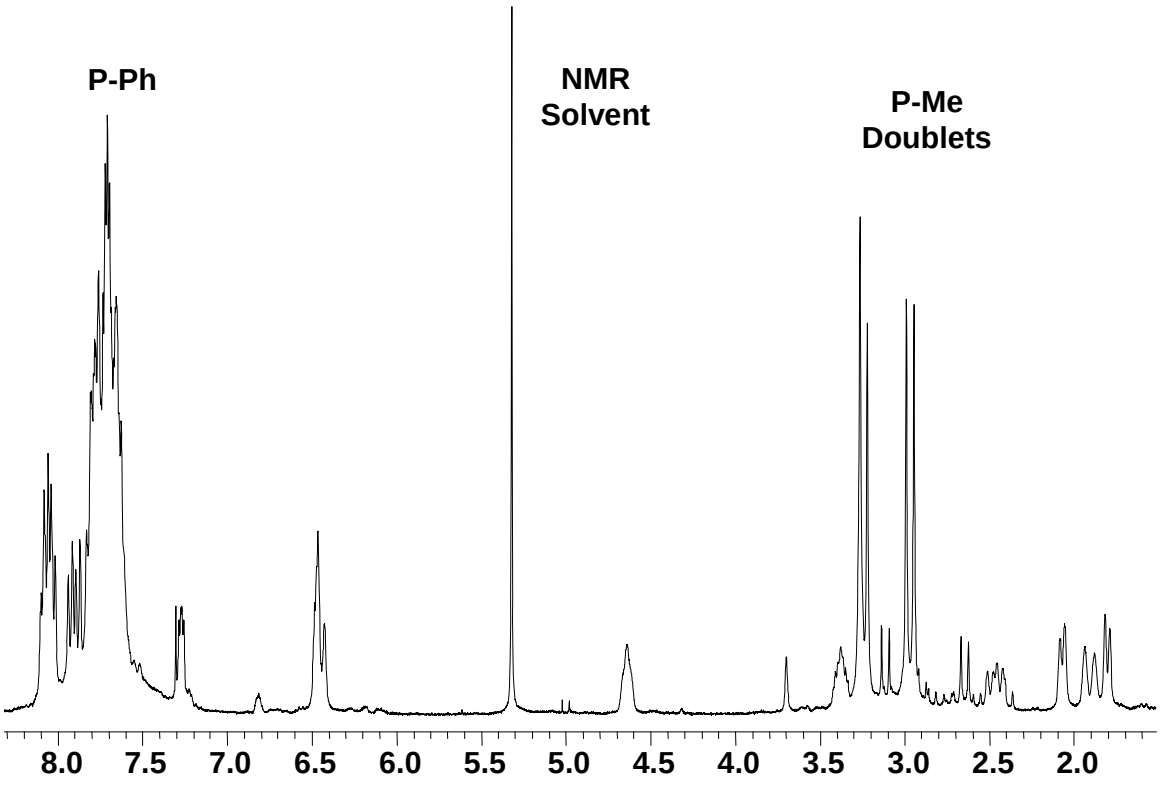

Figure 3-40. The ^{1}H NMR of the reaction of $TiCl_4$ with II.

As this product could not be purified and therefore could not be conclusively characterized, we attempted another route to synthesize titanium ylide complexes.

3.4.2 Attempts to synthesize complexes from $(\eta^5\text{-}C_5H_4PPh_2)_2TiCl_2$

We have also attempted to synthesize titanium complexes using a protocol similar to that employed in the synthesis of several iron cyclopentadienylide complexes (section 1.2.4).[51-53] This protocol of adding an alkyl halide to phosphine substituted Cp rings on iron has not been extended to other systems as a route into phosphorus ylide complexes. Using $(\eta^5\text{-}C_5H_4PPh_2)_2TiCl_2$[84] as the titanium starting material, we attempted to quaternize the phosphorus by the addition of either MeI or BzCl. It was hoped that this would result in the formation of dicationic titanium(IV) complexes with the ylidic system formed in situ. Quaternization has been used to generate ammonium salts of titanium complexes for use as anti-cancer drugs in the Baird laboratories and it was hoped that this route could also be applied to the phosphorus system.[146, 147]

Initially, we tried to generate the complex $[(\eta^5\text{-}C_5H_4PMePh_2)_2TiCl_2][I]_2$ by the addition of MeI to $(\eta^5\text{-}C_5H_4PPh_2)_2TiCl_2$ (Figure 3-41). An excess of MeI was added to the titanium starting material in THF before the solution was refluxed for 20 hours. This caused the formation of a red precipitate.

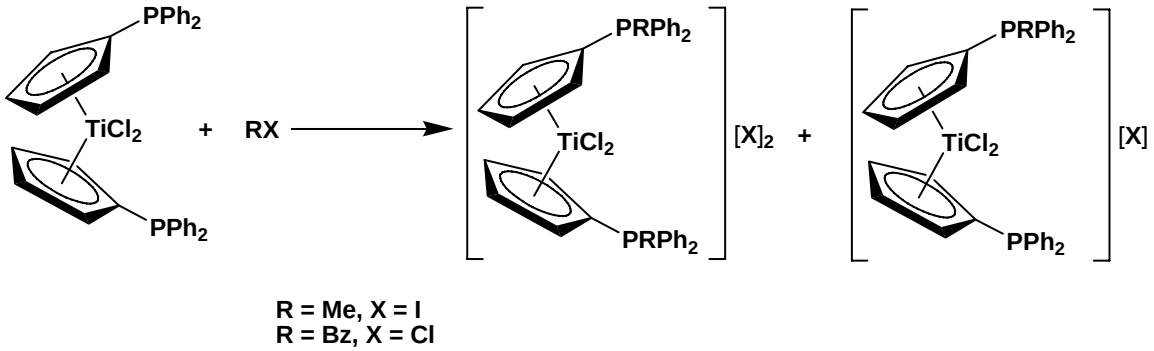

Figure 3-41. The attempted reaction of $(C_5H_4PPh_2)_2TiCl_2$ with RX (RX = MeI or BzCl).

The red solid was collected and ^{1}H and ^{31}P NMR spectra were run in CD_2Cl_2. The ^{1}H NMR spectrum, shown in Figure 3-42, revealed the presence of a number of products. The ^{31}P NMR spectrum had three peaks at δ 25.01, 14.97 and 14.12; no peak was present for the starting complex. This is similar to the spectrum recorded for the reaction of **II** with $TiCl_4$. The peaks at δ 25.01 and 14.97 are nearly equal in intensity and are more intense than the resonance at δ 14.12. These shifts could be due to the desired complex as the resonances are in the region expected for the coordinated ylide (lower field than the free ylide peak of δ 7.95). The ^{1}H NMR spectrum had two doublet resonances at δ 3.21 and 2.92 consistent with a Me group bound to phosphorus (due to ^{31}P coupling). These resonances appeared in the region expected for the coordinated ylide (~3.0 ppm). Additional peaks are present in this region of the spectrum and cannot be positively identified. Several broad resonances are observed in the region expected for the C_5H_4 protons (δ 7.35-7.15 and δ 6.60-6.35). These resonances are consistent with those obtained in the previous attempt to generate a titanium complex using **II** and $TiCl_4$.

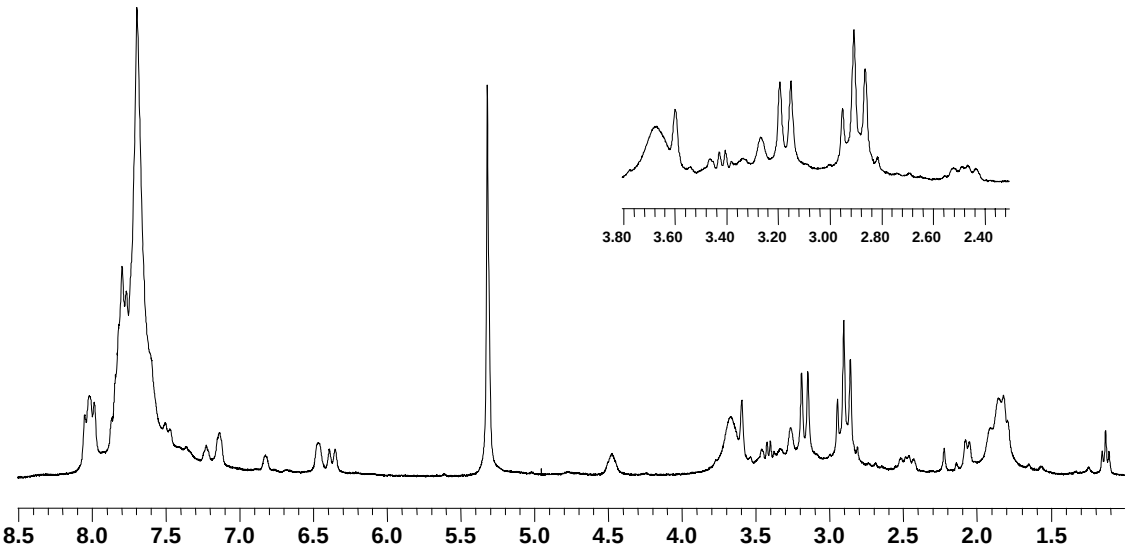

Figure 3-42. The ^{1}H NMR spectrum of the reaction of $(C_5H_4PPh_2)_2TiCl_2$ with MeI.

During this experiment it is possible that both monocationic and dicationic complexes were formed, although ^{31}P NMR resonances for the unreacted phosphine group do not appear in the spectrum. In addition, it is also possible that the iodide anion generated could exchange with the chloride ligands, generating further products in the reaction. Attempts at purification of the product failed and due to the number of products present in the NMR spectra of this reaction mixture we decided to change to another alkyl halide source.

We decided to switch the alkyl halide to benzyl chloride (BzCl) with the expectation that this would eliminate the possibility of products generated by anion exchange. In addition, BzCl also has a higher boiling point allowing for higher reaction temperatures to permit addition of the alkyl group to the phosphorus atom. In this experiment, toluene was used as a solvent, offering a higher boiling reaction medium. As the reaction proceeded, a red precipitate formed. The precipitate was collected and the ^{1}H and ^{31}P NMR spectra were recorded in CD_2Cl_2. The ^{31}P NMR spectrum revealed seven peaks between δ 30 and δ 12. Unreacted starting material was also present. The most intense resonances occurred at δ 17.13 and 12.93. Upon addition of the benzyl group to the phosphorus atom, the methylene protons would give rise to a doublet in the ^{1}H NMR spectrum due to phosphorus coupling. A number of doublets are present in the ^{1}H NMR spectrum at δ ~ 4.0. However, other peaks make the definitive assignment of methylene protons difficult. In addition to the methylene peaks, resonances which correspond to the C_5H_4 protons were observed at δ ~7.2 and 6.2.

A similar experiment, in which HCl (a solution in Et_2O) was added to (η^5-$C_5H_4PPh_2)_2TiCl_2$, was also performed, but resulted in a plethora of products being generated (^1H and ^{31}P NMR) and this method was abandoned.

In all of the previous experiments to synthesize titanium complexes, numerous products were generated which could neither be conclusively identified nor purified. With the success of the work involving the group 6 complexes, we decided not to further explore the synthesis of titanium complexes.

3.5 Indenyl-Derived Ylides

One of the notable problems that may have limited the exploration of this class of ligand is the lack of a general synthetic route, since the original Ramirez synthetic procedure[1-8, 96] has turned out not to be generally applicable to other phosphines.[148] In a further attempt to help revive the use of this class of ligand, we have begun an investigation into the use of the indenyl-derived ylide, methyldiphenylphosphonium indenylide ($C_9H_6PMePh_2$), **VII**, shown in Figure 3-43.

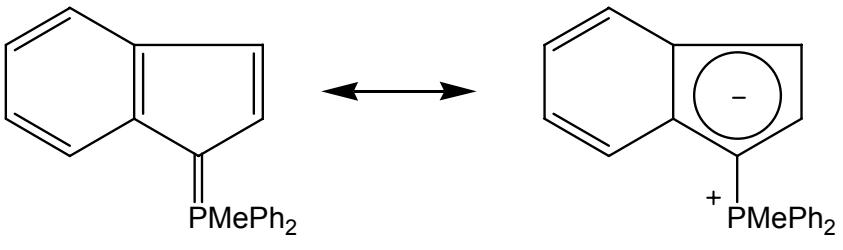

VII

Figure 3-43. The resonance structures of $C_9H_6PMePh_2$, VII.

A potentially more general route to indenyl-derived ylides involves the addition of indenyl bromide to a phosphine to give the desired phosphonium salt, which can then be deprotonated to give the ylide (see section 1.15).[43] This method was used by Crofts and Williamson to synthesize the first indenyl-derived phosphorus ylide, triphenylphosphonium indenylide ($C_9H_6PPh_3$), which they reported in 1967,[43] but few other such indenyl-derived ylides have been reported. In 2004, Rufanov *et al.* reported the synthesis of two other indenyl-derived ylides, $C_9H_6PBzPh_2$ and $C_9H_6PBz(C_6F_5)_2$, but no complex has been reported to date.[44] Rufanov *et al.* failed to realize that a body of work on phosphonium ylides preceded their report and they draw no parallels to the extensive literature reported for the Ramirez and similar ylides (including the indenyl ylide, $C_9H_6PPh_3$ of Crofts and Williamson).[44] To date, no transition metal complexes of any phosphorus indenyl-derived ylides appear to have been reported. We report herein the synthesis and characterization of the new ligand methyldiphenylphosphonium indenylidene ($C_9H_6PMePh_2$), **VII**, and its chromium complex, (η^5-$C_9H_6PMePh_2$)$Cr(CO)_3$, **VIII**.

3.5.1 Synthesis of $C_9H_6PMePh_2$ (VII)

The ylide **VII** was synthesized using a protocol very similar to that used previously by Mathey *et al.*[36] and ourselves to obtain **II**. The phosphine, $IndPPh_2$ (Ind = indenyl, C_9H_7) was synthesized from LiInd and $PClPh_2$[85] and was alkylated with MeI as shown in Figure 3-44, and the phosphonium salt was synthesized in high yield (75%) as a mixture of two isomers shown in Figure 3-44.[85] Thus the ^{1}H NMR spectrum of the phosphonium salt is very complicated in the olefinic region and also exhibits two P-Me doublets at δ 3.18 and 2.85. The ratios of the two isomers vary from experiment to

experiment. Similarly, the ^{31}P NMR spectrum exhibits two resonances at δ 26.04 and 13.52. The phosphonium salt was reasonably pure (NMR), and was used as obtained for the synthesis of **VII**.

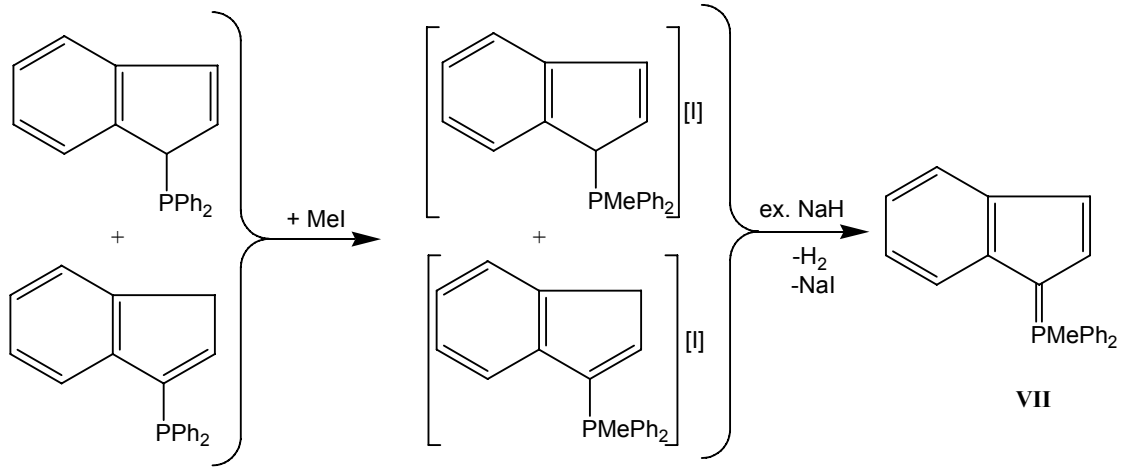

Figure 3-44. The synthesis of $C_9H_6PMePh_2$ (VII).

The ylide $C_9H_6PMePh_2$ (**VII**) was synthesized in excellent yield (87%) by deprotonation of the phosphonium salt with an excess of NaH in THF. Although this reaction is slow, the product is easily separated and purified. Analytically pure material and X-ray quality crystals of **VII** were obtained by recrystallization from a CH_2Cl_2 solution layered with hexanes and kept at –30 °C. Complete ^{1}H, ^{13}C and ^{31}P NMR data for **VII** are described below.

Using the indenyl system offers several significant advantages versus the related Cp-derived ylides **I** and **II**. In the first step of the reaction protocol, $IndPPh_2$ is used in place of $CpPPh_2$. $CpPPh_2$ is unstable and decomposes if not used immediately following its synthesis, which is not the case with $IndPPh_2$.[36, 37] In addition, the resulting ylide is generated in much higher yields than the related $C_5H_4PMePh_2$ after the deprotonation of the two phosphonium salt isomers.[36] Finally, indenyl-derived ylides have higher

solubilities in aromatic solvents than the Cp-derived ylides, as found by us and by others.[43, 44] This circumvents one of the problems previously encountered in the handling and characterization of the Cp-derived ylides, which potentially contributed to the lack of development of these compounds as ligands.

3.5.2 NMR Characterization of $C_9H_6PMePh_2$ (VII)

In addition to standard 1D ^{1}H, ^{13}C and ^{31}P NMR spectra, 2D NOESY, COSY, HSQC and HMBC spectra were collected for the title compound. A description of the determination of the NMR peaks for the indenyl ylide will follow, see Figure 3-45, for the labelling scheme (also used for the chromium complex, **VIII**) and Table 3-12 for the peak assignments.

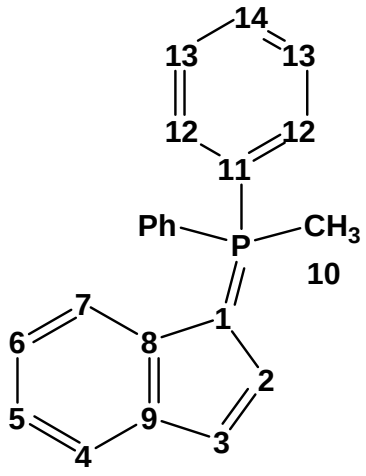

Figure 3-45. The labelling scheme used for the NMR assignments of VII and VIII.

Position	δ (^{1}H)[a]	Multiplicity	J (Hz)	δ (^{13}C)	Multiplicity	J (Hz)
1	-	-	-	66.14	d	$^{1}J_{P-C}$ = 120.8
2	6.74	t	J = 4.5	126.30	d	$^{2}J_{P-C}$ = 17.6
3	6.64	t	J = 4.2	105.00	d	$^{3}J_{P-C}$ = 15.4
4	7.68	m	-	120.82	s	-
5	6.97	t	$^{3}J_{H-H}$ = 7.2	117.28	s	-
6	6.84	t	$^{3}J_{H-H}$ = 6.8	117.91	s	-
7	7.04	d	$^{3}J_{H-H}$ = 7.9	117.36	s	-
8	-	-	-	137.79	d	$^{3}J_{P-C}$ = 15.4
9	-	-	-	135.42	d	$^{2}J_{P-C}$ = 14.3
10	2.5	d	$^{2}J_{P-H}$ = 12.6	12.97	d	$^{1}J_{P-C}$ = 62.6
11	-	-	-	127.13	d	$^{1}J_{P-C}$ = 87.8
12	7.55-7.52	m	-	129.45	d	$^{2}J_{P-C}$ = 12.1
13	7.67-7.63	m	-	132.68	d	$^{3}J_{P-C}$ = 11.0
14	7.67-7.53	m	-	132.93	d	$^{4}J_{P-C}$ = 3.3

Table 3-12. ^{1}H and ^{13}C NMR chemical shifts and coupling constants for VII. [a] The protons correspond to the proton attached to the carbon atom with the same position number in Figure 3-45.

The first step in the assignment of the ^{1}H NMR spectra of **VII** began with the assignment of the phosphorus methyl doublet; the ^{1}H NMR spectrum is shown in Figure 3-47. The NOESY spectrum (Figure 3-46) was then used to assign the protons 2 (δ 6.74) and 7 (δ 7.04), which were the only protons of the indenyl fragment that showed through-space correlations to the protons of the phosphorus methyl group. Following this, assignments of each proton were determined using the COSY spectrum (Figure 3-48).

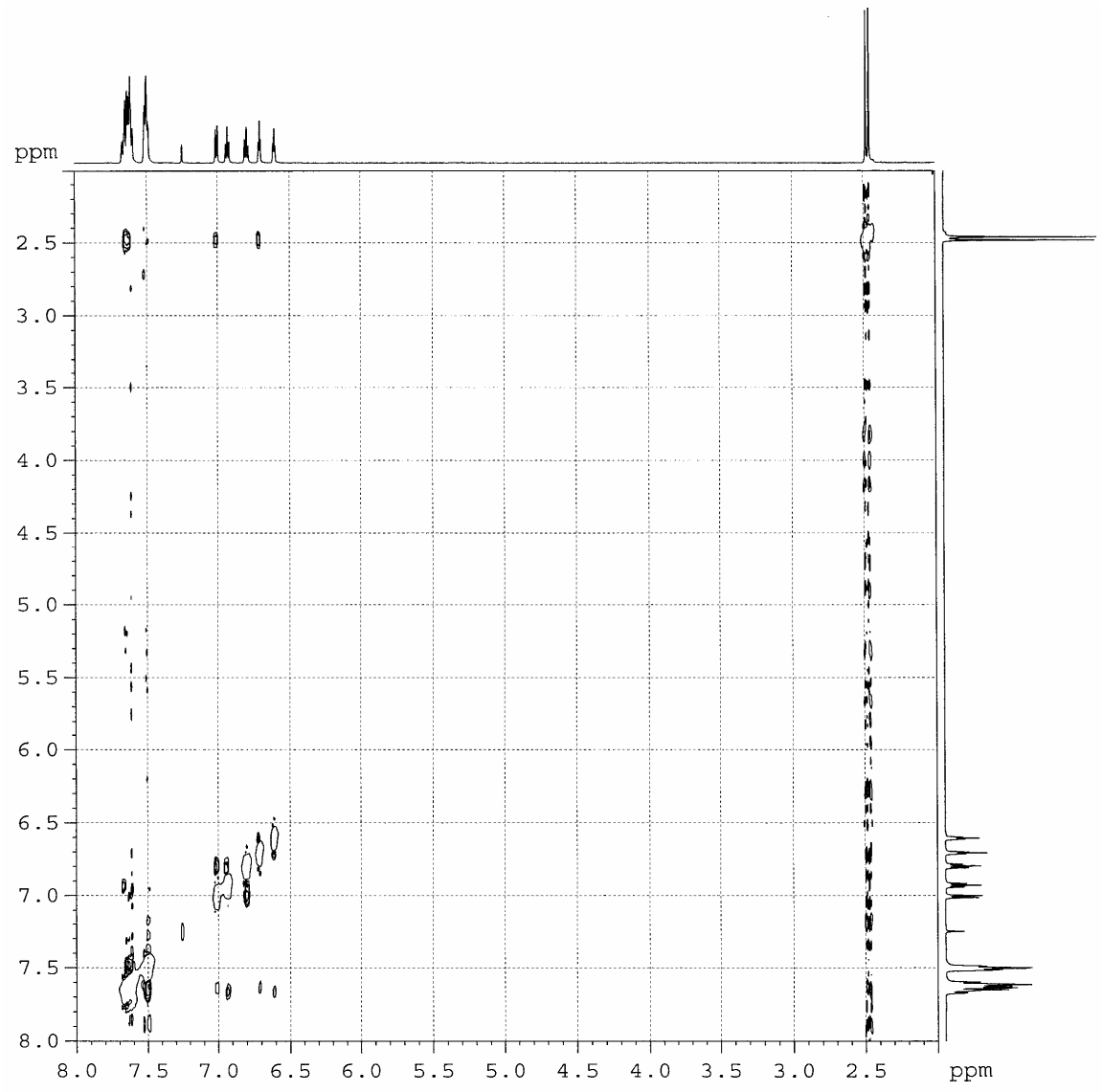

Figure 3-46. The NOESY spectrum of $C_9H_6PMePh_2$ (VII).

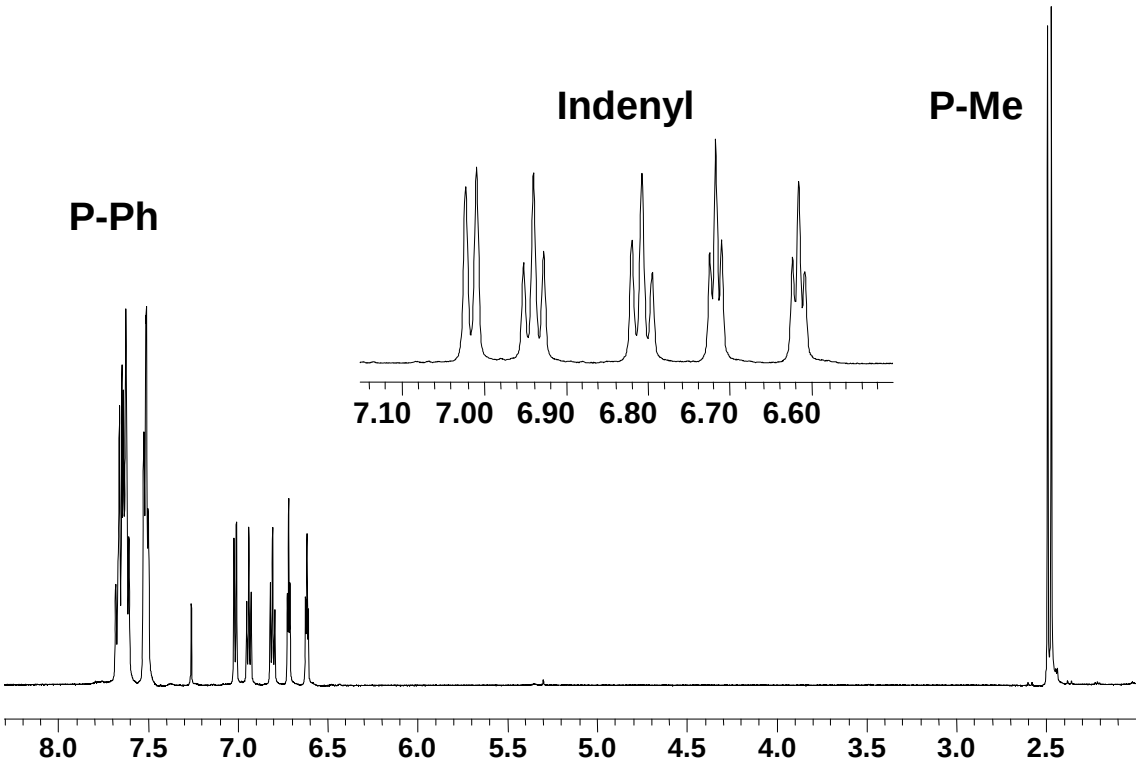

Figure 3-47. The ^{1}H NMR spectrum of $C_9H_6PMePh_2$ (VII) in $CDCl_3$.

The COSY spectrum (shown in Figure 3-48) shows correlations between the protons with chemical shifts of δ 6.64 and 6.74. The peak at δ 6.74 (proton 2) has no other correlations in the COSY spectrum. This allows the peak at δ 6.64 to be assigned to the proton at position 3. Protons 2 and 3 appear as triplets due to coupling with each other and with phosphorus. Proton 7 (δ 7.04) correlates to the peak at δ 6.84. The peak at δ 6.84 appears as a triplet, which is expected for the proton at position 6. Proton 6 is also correlated to the peak at δ 6.97. The peak at δ 6.97 was assigned to the proton at position 5. The final proton of the indenyl fragment lies in the aromatic region (δ ~7.7) and is partially obscured by the resonances of the phenyl groups attached to phosphorus. This resonance

is proton 4 and correlations can be seen between it and the peak at δ 6.97 (proton 5). The phenyl protons and the methyl doublet are easily assigned.

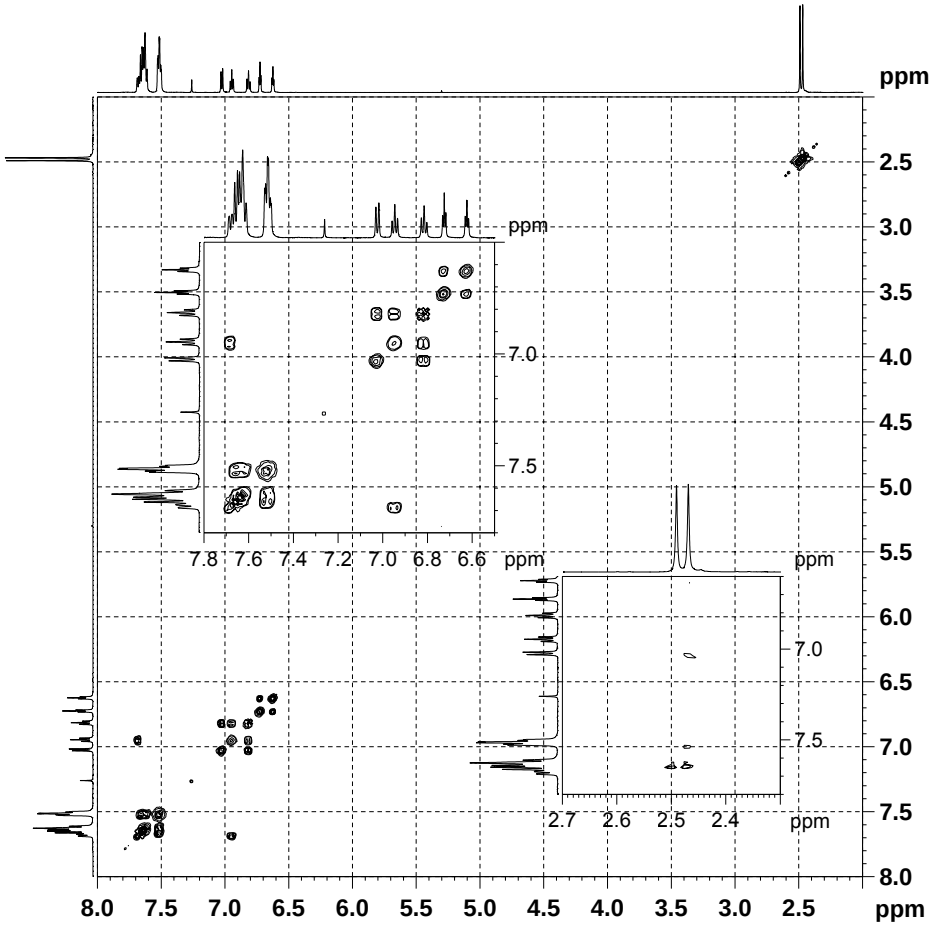

Figure 3-48. The COSY spectrum of VII in $CDCl_3$.

The HSQC (Figure 3-49) and HMBC allow the individual assignment of the carbon resonances and offer further confirmation of the proton assignments. In the HSQC spectrum, proton 2 correlates with the doublet in the ^{13}C NMR spectrum at a chemical shift of δ 126.30 and is carbon 2. The HMBC shows a correlation of proton 2 to carbon resonances occurring at δ 66.14, 105.00 and 135.42. The peak at δ 66.14 is a doublet with a coupling constant of 120.8 Hz and therefore, this must be the ylidic carbon (carbon 1). This chemical shift of carbon 1 is similar to other ylides of this class.[8] The carbon

resonance at δ 105.00 correlates to proton 3 in the HSQC spectrum. This peak is carbon 3. These correlations offer definitive proof that the assignments of protons 2 and 3 from the COSY spectrum were correct. The other indenyl fragment non-quaternary carbon shifts and the non-quaternary phenyl peaks can be assigned using the HSQC.

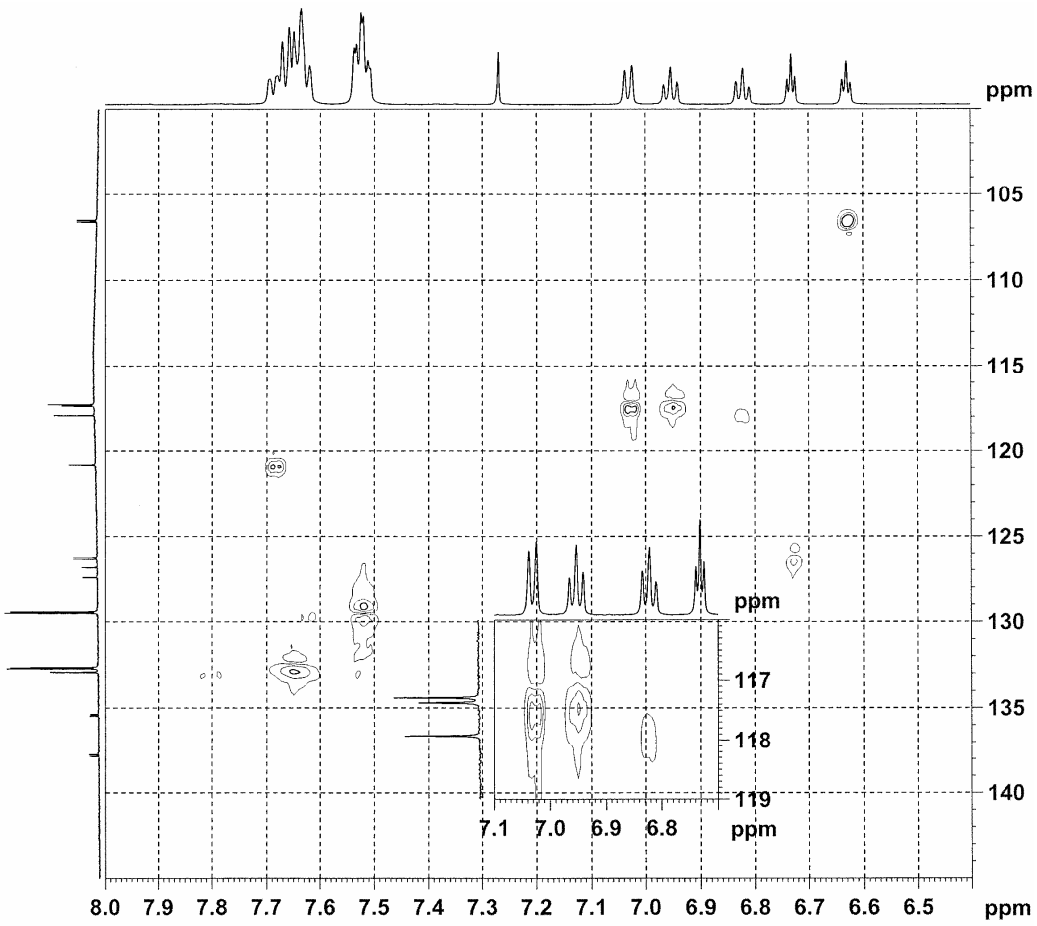

Figure 3-49. The HSQC spectrum of $C_9H_6PMePh_2$ (VII).

Assignment of the remaining quaternary carbons is accomplished using the HMBC spectrum (Figure 3-50). The carbon peak at a chemical shift of δ 135.42 has correlations to protons 2, 3 and 4. The J_{P-C} of this peak is smaller than that of the peak at δ 137.79. Based upon the HMBC and the coupling constant, the peak at δ 135.42 is

assigned to position 9. The carbon peak at δ 137.79 correlates to protons 3 and 7 and is assigned to the carbon at position 8.

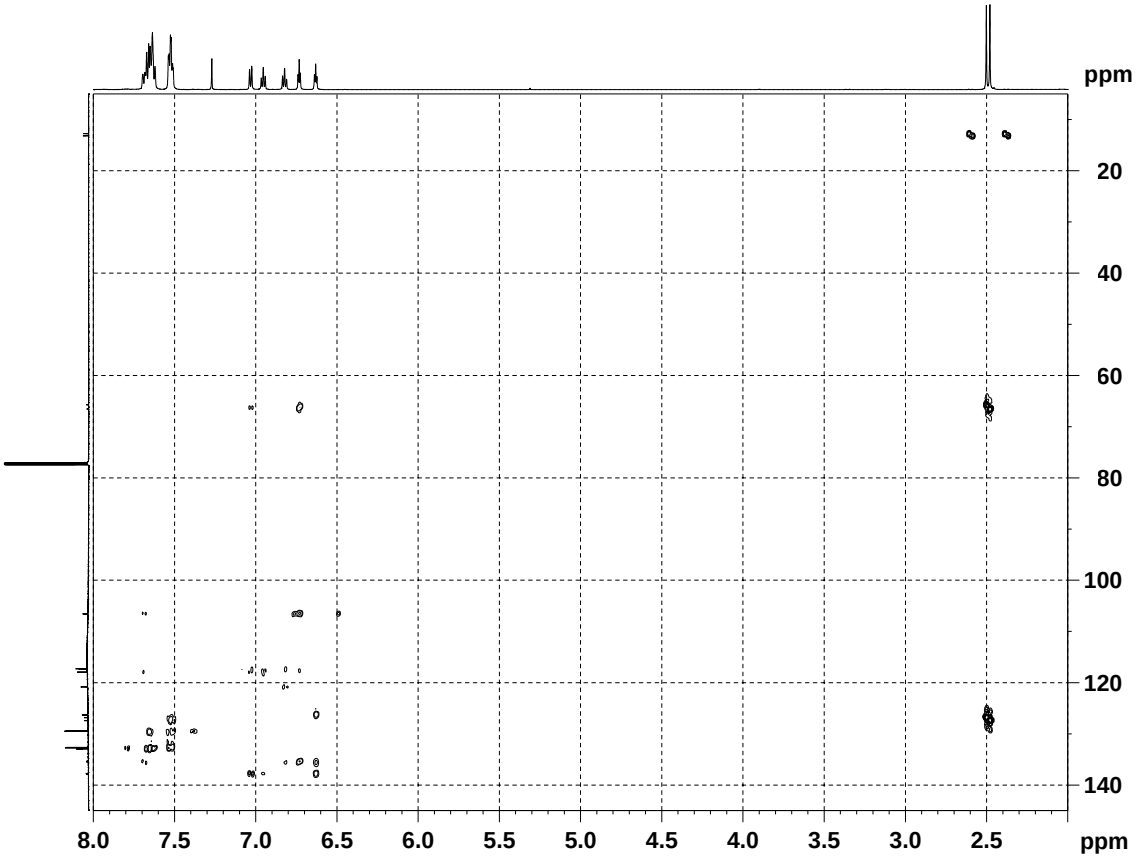

Figure 3-50. The HMBC spectrum of $C_9H_6PMePh_2$ (VII).

Peak assignments are consistent with those of the related ylides reported by Rufanov *et al.*.[44] The ^{31}P NMR resonance of **VII** (δ 5.69) is at a higher field than that of the related ylide **II** (δ 7.95). This could be an indication of a slight increase in double bond character of the ylidic P-C bond in **VII** versus **II**, consistent with a greater contribution to the bonding from resonance structure **VIIa**. The ylidic carbon (C1) ^{13}C NMR resonance appears at δ 66.1, which is δ 13 higher field than the ylidic carbon of **II**

(δ 79.2). The C1 resonance of **VII** is at a slightly lower field than seen in the indenyl-derived ylides $C_9H_6PBzPh_2$ (δ 59.9) and $C_9H_6PBz(C_6F_5)_2$ (δ 62.2).[44]

3.5.3 Synthesis of (η^5-$C_9H_6PMePh_2$)$Cr(CO)_3$ (VIII)

To synthesize (η^5-$C_9H_6PMePh_2$)$Cr(CO)_3$, **VII** was heated to reflux in diglyme with an excess (2 to 3 equiv) of $Cr(CO)_6$ (Figure 3-51). This protocol follows the procedure described by Kotz *et al.* and used by us to synthesize the Group 6 tricarbonyl complexes of $C_5H_4PMePh_2$ (**II**).[10] The product **VIII** was isolated in 40% yield. One further interesting characteristic of using indenyl-derived ylides is that upon complexation of the ylide, the complex which forms has planar chirality (Figure 3-51). Purification to yield analytically pure material and X-ray quality crystals was accomplished by recrystallization from a CH_2Cl_2 solution layered with hexanes and kept at –30°C. The elemental analysis indicated that CH_2Cl_2 was present in the crystals. The amount of CH_2Cl_2 present was the same as that observed in the crystal structure, which has 0.5 CH_2Cl_2 molecules of solvation. Full spectroscopic characterization is reported below and includes IR, ^1H, ^{13}C and ^{31}P NMR and the X-ray crystal structure.

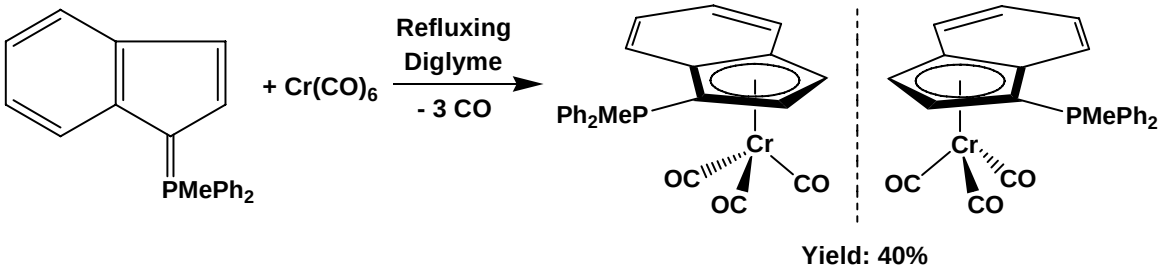

Figure 3-51. The synthesis of (η^5-$C_9H_6PMePh_2$)$Cr(CO)_3$ (VIII).

3.5.4 NMR Characterization of (η^5-$C_9H_6PMePh_2$)$Cr(CO)_3$ (VIII)

In addition to standard 1D ^1H, ^{13}C and ^{31}P NMR spectra, 2D NOESY, COSY, HSQC and HMBC spectra were collected for the title compound. A description of the determination of the NMR peaks for the indenyl ylide will follow. Please see Figure 3-45, for the labelling scheme and Table 3-13 for the NMR data.

As with the ligand **VII**, NOESY (spectrum shown in Figure 3-52) was first used to determine which protons of **VIII** correlated with the P-Me group. The methyl group resonance was easily determined from the ^1H NMR as it appears as a doublet at δ 2.88. The proton resonances at δ 4.76 and 6.90 had NOESY correlations with the methyl group indicating that peak at δ 4.76 was proton 2 and the peak at δ 6.90 was proton 7. It should be noted that in the ^1H NMR spectrum two resonances at δ 6.90 and 6.92 overlap, but the NOESY correlation clearly indicated that the higher field proton was correlated to the methyl group. In addition, the multiplicity of the peak (d) was indicative of proton 7.

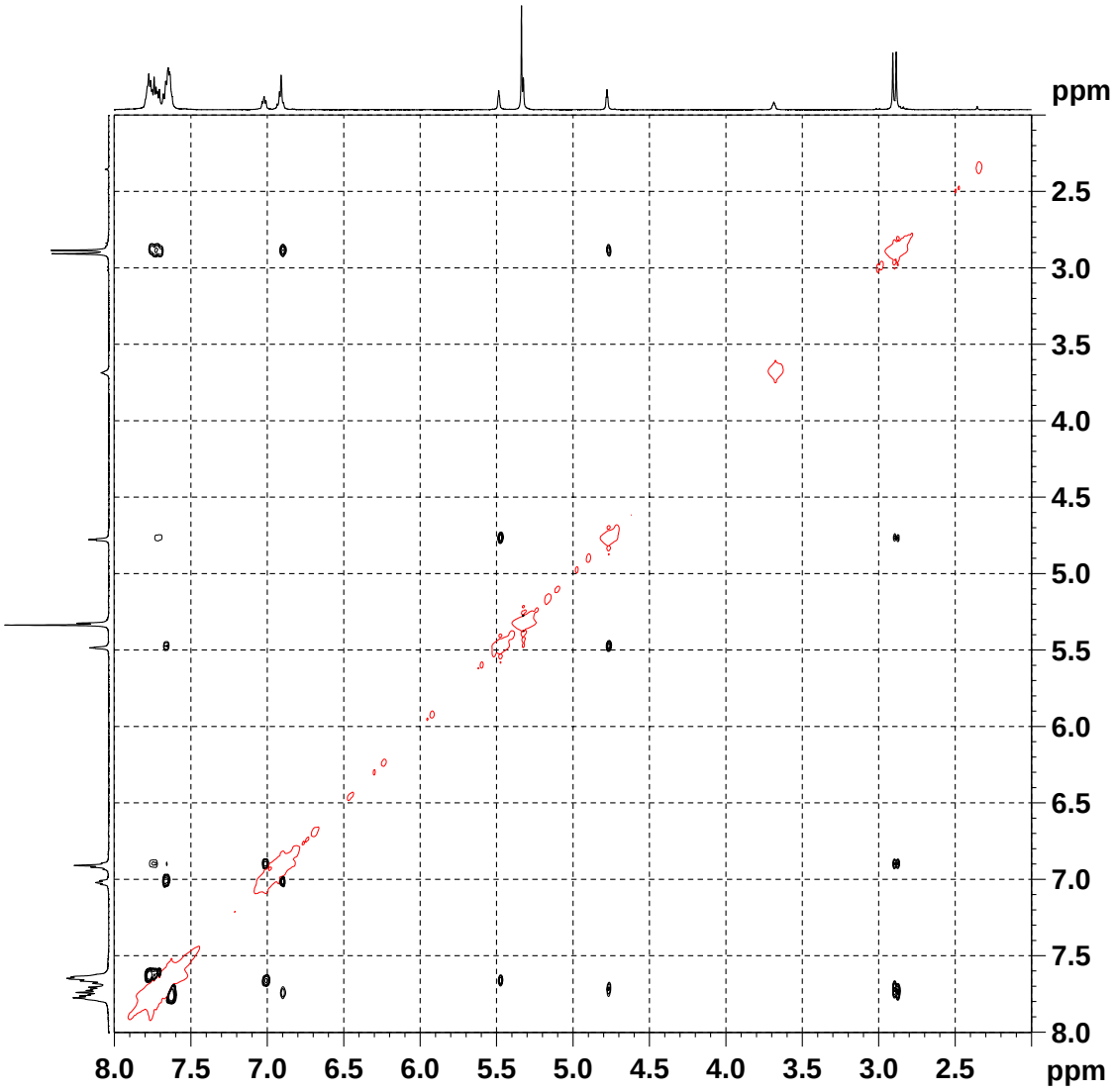

Figure 3-52. The NOESY spectrum of VIII in CD_2Cl_2.

Proton 3 was then determined to be the resonance at δ 5.47 as upon coordination in related ylides the ring protons shift upfield. Proton 3 had NOESY correlations to proton 2 and to a resonance at δ 7.66 that was overlapped by the P-Ph resonances. However, this still indicated that this resonance was proton 4.

Position	δ (^{1}H)	Multiplicity	J (Hz)	δ (^{13}C)	Multiplicity	J (Hz)
1	-	-	-	57.2	d	^{1}J(P-C) 113.8
2	4.76	m	^{3}J(H-H) 3.0	95.68	d	^{2}J(P-C) 13.9
3	5.47	m	^{3}J(H-H) 3.0	80.31	d	^{3}J(P-C) 12.5
4	7.66	m	-	127.53	s	-
5	7.00	td	^{3}J(H-H) 7.6	123.28	s	-
			^{4}J(H-H) 1.5			
6	6.92	t*	^{3}J(H-H) 8.7	122.16	s	-
7	6.90	d*	^{3}J(H-H) 7.6	124.60	s	-
8,9	-	-	-	109.80	d	J(P-C) 16.6
				109.72	d	J(P-C) 16.6
10	2.88	d	^{2}J(P-H) 13.2	14.68	d	^{1}J(P-C) 65.2
11	-	-	-	123.10	d	^{1}J(P-C) 87.4
	-	-	-	122.43	d	^{1}J(P-C) 90.2
12	7.78-7.61	m	-	130.46	d	^{2}J(P-C) 12.5
			-	130.25	d	^{2}J(P-C) 12.5
13	7.78-7.61	m	-	133.67	d	^{3}J(P-C) 9.7
			-	133.46	d	^{3}J(P-C) 9.7
14	7.78-7.61	m	-	134.97	d	^{4}J(P-C) 2.8
			-	134.93	d	^{4}J(P-C) 2.8
CO	-	-	-	241.16	s	-

Table 3-13. ^{1}H and ^{13}C NMR data for VIII. See Figure 3-45 for numbering scheme. *The peaks for protons 6 and 7 overlap and the multiplicities are described as that inferred from the observed patterns and that expected for these peaks.

The COSY spectrum (Figure 3-53) was then used to determine the remaining proton resonances. Protons 2 and 3 show correlations to each other offering further confirmation of their assignments. The proton at δ 7.00 has correlations to the resonances at δ 7.66 (proton 4) and δ 6.92. The latter was therefore assigned to proton 5. Only the peak at δ 6.92 remained unassigned and must be proton 6. Due to the overlap with the peak at δ 6.90 (proton 7) it is not possible to conclusively determine if there is a COSY correlation between these two resonances.

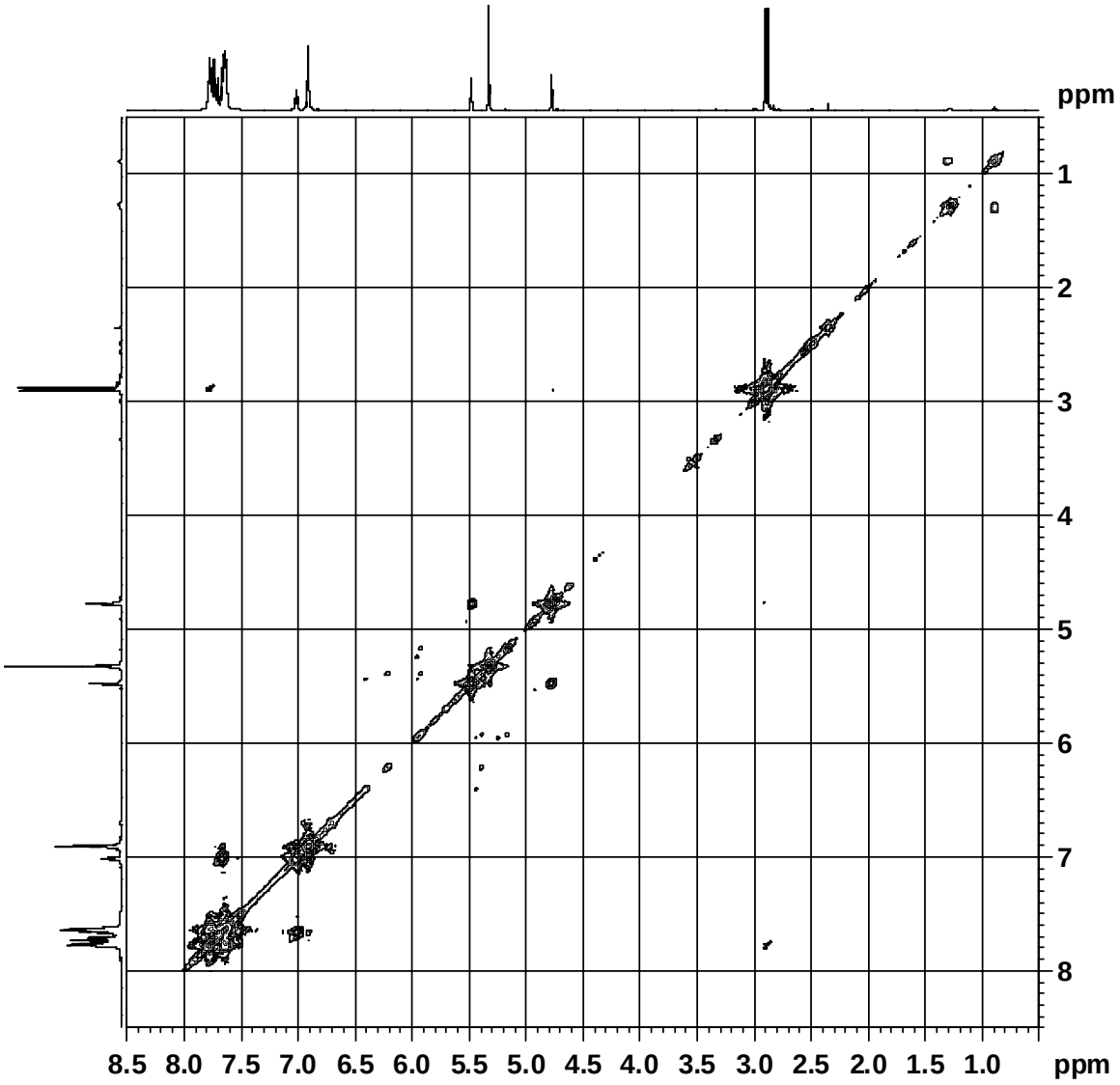

Figure 3-53. The COSY Spectrum of (η^5-$C_9H_6PMePh_2$)$Cr(CO)_3$ (VIII) in CD_2Cl_2.

The HSQC (Figure 3-54) allowed for complete determination of non-quaternary carbon resonances after the assignment of the ^{1}H NMR spectrum. The two phenyl groups have non-equivalent carbon resonances, which gives two sets of peaks in the carbon NMR with identical coupling constants. These peaks were determined from their coupling constants and by the fact that they correlate to the protons in the aromatic region

of the spectrum. All of the P-Ph resonances appear as doublets, while the indenyl fragment aromatic carbon resonances are singlets, which allowed for clear identification of each set of peaks.

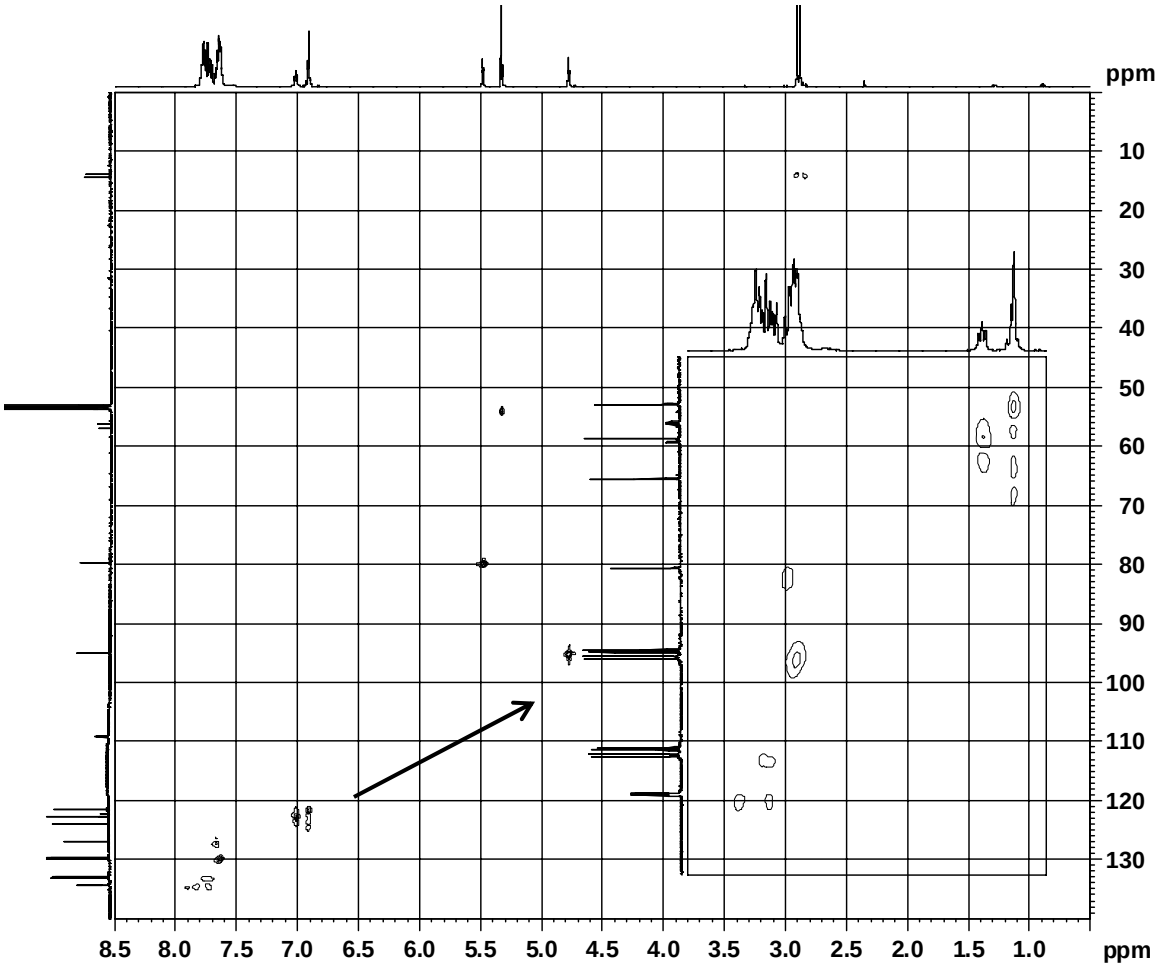

Figure 3-54. The HSQC spectrum of (η^5-$C_9H_6PMePh_2$)$Cr(CO)_3$ (VIII) in CD_2Cl_2.

The HMBC (Figure 3-55) and the ^{13}C NMR spectrum then allowed for the final assignment of the remaining carbon atoms. The ylidic carbon appears at δ 57.2 and the P-C coupling constant of 113.8 Hz is distinctive for this carbon. The *ipso*-Ph carbons were then determined from the large P-C coupling constant and the appearance of these peaks in the aromatic region of the spectrum. Only carbons 8 and 9 remained unassigned. The

HMBC spectrum showed long range coupling to protons 2, 3, 4 and 7. However, due to the proximity and overlapping of the two carbon resonances (δ 109.80 and 109.72) that have identical coupling constants, each peak could not be assigned to a single carbon atom. Finally, the CO group appears at δ 241.16.

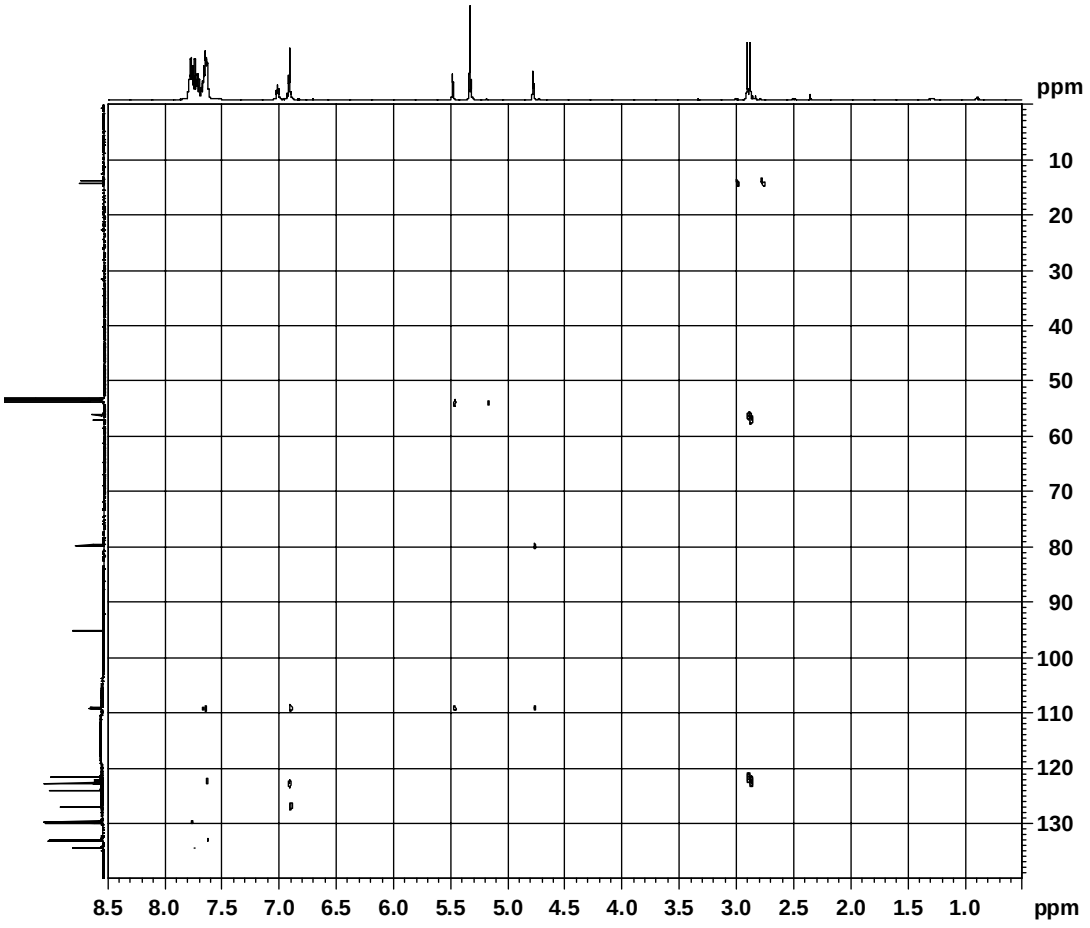

Figure 3-55. The HMBC spectrum of (η^5-$C_9H_6PMePh_2$)$Cr(CO)_3$ (VIII) in CD_2Cl_2.

Coordination of **VII** to the $Cr(CO)_3$ moiety results in a shift of the ^{31}P NMR resonance to lower field (δ 19.84). Similar shifts occur upon coordination of other related ylides such as the Group 6 complexes of **II**, in which the complex (η^5-$C_5H_4PMePh_2$)$Cr(CO)_3$ has a nearly identical ^{31}P NMR resonance of δ 19.54.

In the ^{1}H NMR spectrum of **VIII** (Figure 3-56) the C_5H_4 protons (2 and 3) shift upfield from δ 6.74 and 6.64 in the uncomplexed ligand to δ 4.76 and 5.47 upon coordination. A similar upfield shift for the ring protons is observed upon complexation of the related ylide, $C_5H_4PMePh_2$, although the shift is not nearly as large (δ ~1.5 versus δ ~2). In addition, protons 2 and 3 flip their relative positions (upfield versus downfield) upon coordination in **VIII**, this is not seen upon coordination for the related ylide, **II**. The phenyl region of the spectrum has peaks between δ 7.61-7.78. One indenyl phenyl proton peak is overlapped by the P-Ph resonances. The P-Me peak has shifted downfield to δ 2.88, indicative of a greater positive charge on phosphorus.

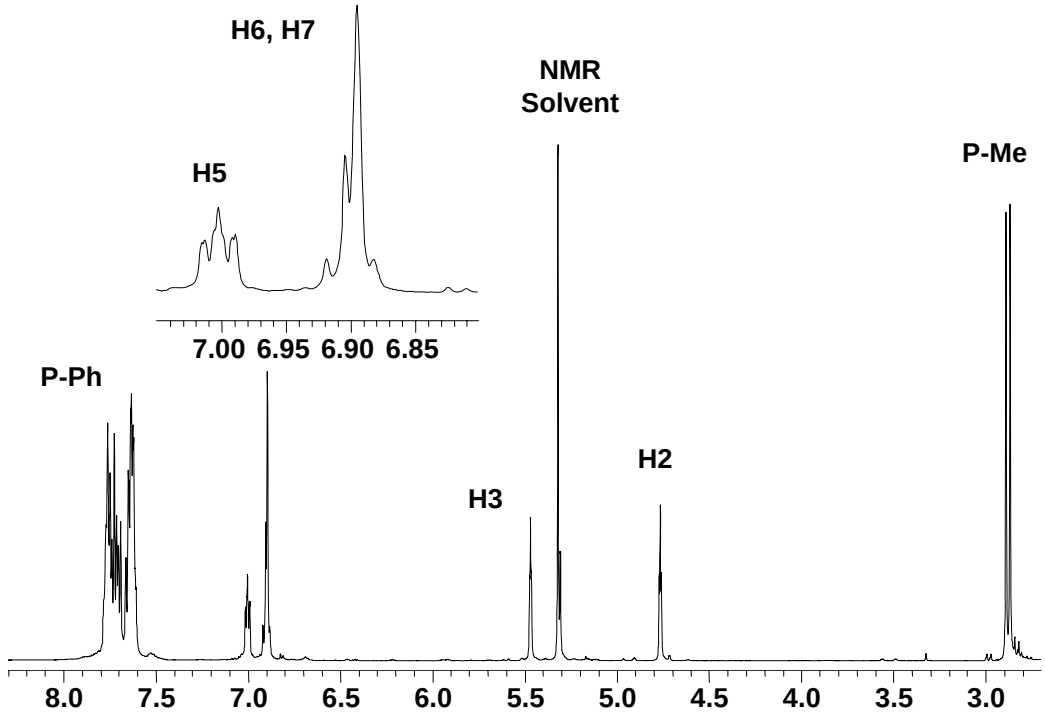

Figure 3-56. The ^{1}H NMR spectrum of (η^5-$C_9H_6PMePh_2$)$Cr(CO)_3$ (VIII) in CD_2Cl_2.

The ^{13}C NMR of **VIII** reveals some interesting changes from that of **VII**. The ylidic carbon, C1, has shifted from δ 66.14 in the free ylide to δ 57.2 in the complex. This

shift, although the smaller in magnitude, is similar to that observed for the ylidic carbon of $C_5H_4PMePh_2$ upon complexation. The C_5 ring carbons 2 and 3 have also shifted from δ 126.30 and 105.00 to δ 95.68 and 80.31, respectively. Similar changes are seen in the related Cp-derived ylide systems. The two other C_5 ring protons 8 and 9 also shift dramatically, with the uncomplexed ligand peaks shifting from δ 137.79 and 135.42 to δ 109.80 and 109.72 upon complexation. This shift in the resonances of carbons 8 and 9 resembles the shift seen in the other C_5 carbon resonances (carbons 2 and 3).

The complexity of the NMR spectra of the indenyl-derived ylide, which is not present in the cyclopentadienylides, offers one of the few drawbacks of using indenyl-derived ylides in coordination chemistry. However, this report along with that of Rufanov *et al.*[44], helps to alleviate some of the problems associated with this complexity by offering a starting point for comparison of the shifts of related systems. In addition, the use of our indenyl-derived ylide, with its P-Me group offers a simple ^{1}H NMR handle for initial characterizations.

3.5.5 Molecular Structures of VII and VIII.

Full structural data for **VII** and **VIII** are provided in the Appendix, while selected bond lengths and angles are found in Table 3-14. Also included in Table 3-14 are the bond lengths and angles for the similar ylide, methyldiphenylphosphonium cyclopentadienylide (**II**) and the structure of its -$Cr(CO)_3$ (**III**) complex, which offer good comparisons to this new ligand and its -$Cr(CO)_3$ complex. The molecular structures of **VII** and **VIII** are shown in Figure 3-57 and Figure 3-58, respectively.

Bond (Å)	**VII**	**II** (Molecule 1)	(Molecule 2)	**VIII**	**III**
P(1)-C(1)	1.711(2)	1.7277(17)	1.7268(17)	1.753(5)	1.759(3)
P-Me	1.787(2)	1.799(2)	1.7921(19)	1.781(5)	1.789(3)
P-Ph avg.	1.788	1.81	1.802	1.788	1.796
M-C_5 Centroid	-	-	-	1.854	1.848
C(1)-C(2)	1.420(3)	1.429(3)	1.413(2)	1.443(7)	1.427(4)
C(1)-C(5)	1.432(3)	1.414(3)	1.429(2)	1.461(7)	1.429(4)
C(2)-C(3)	1.364(3)	1.374(3)	1.384(2)	1.387(7)	1.392(4)
C(4)-C(5)	1.423(3)	1.384(3)	1.383(3)	1.405(7)	1.397(4)
C(3)-C(4)	1.421(3)	1.405(3)	1.407(3)	1.427(7)	1.422(4)
C(1)-metal	-	-	-	2.170(5)	2.185(2)
C(2)-metal	-	-	-	2.163(5)	2.204(2)
C(3)-metal	-	-	-	2.201(5)	2.226(3)
C(4)-metal	-	-	-	2.259(5)	2.217(3)
C(5)-metal	-	-	-	2.278(5)	2.191(3)
Bond Angles (°)					
C(1)-P-Me	111.90(10)	111.46(9)	111.96(9)	112.6(2)	111.08(13)
C(1)-P-Ph avg.	111.16	111.44	110.64	109.6	109.78
Me-P-Ph avg.	107.05	106.96	108.44	108.6	109.38
Ph-P-Ph	108.33(10)	108.37(8)	106.55(7)	107.8(2)	107.37(12)
P-C(1)-C_5 Centroid	174.9	172.4	178.1	174.7	178.9
C(1)-C(2)-C(3)	110.1(2)	107.42(19)	108.36(16)	109.3(5)	108.3(3)
C(2)-C(3)-C(4)	108.2(2)	108.85(18)	108.16(18)	107.9(5)	108.3(3)
C(3)-C(4)-C(5)	107.96(19)	108.74(18)	108.87(15)	109.6(5)	108.3(3)
C(4)-C(5)-C(1)	107.09(18)	107.47(18)	107.50(17)	106.8(4)	108.0(3)
C(5)-C(1)-C(2)	106.64(19)	107.51(16)	107.11(16)	106.4(4)	107.1(2)

Table 3-14. Selected bond lengths and angles for VII and VIII, as well as those for II and III.

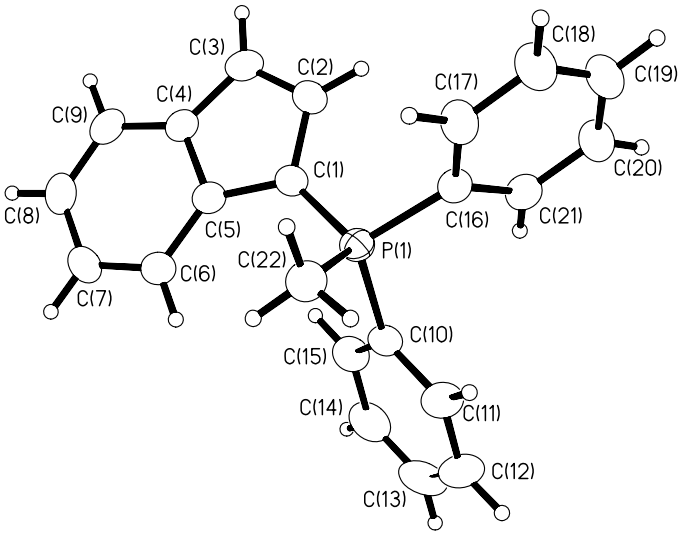

Figure 3-57. The molecular structure of $C_9H_6PMePh_2$ (VII).

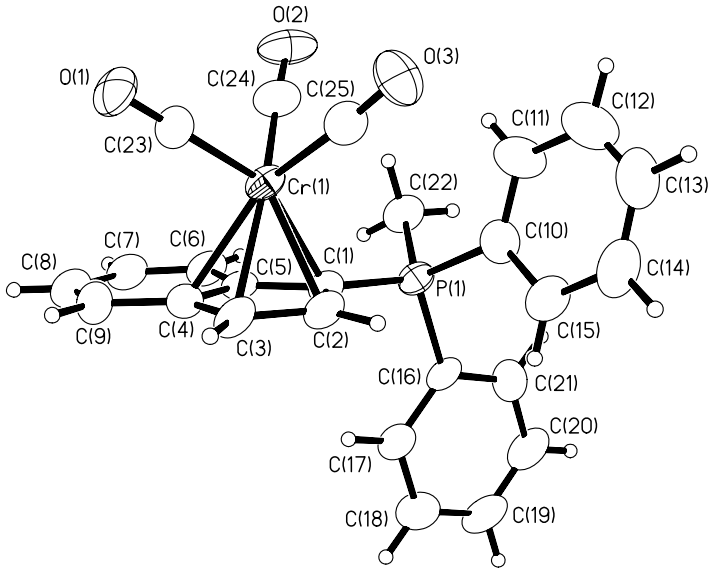

Figure 3-58. The molecular structure of (η^5-$C_9H_6PMePh_2$)$Cr(CO)_3$ (VIII).

The P(1)-C(1) bond length of cyclopentadienyl type ylides provides a good estimation of the bond character and the contribution of each resonance structure to the overall bonding situation. This bond length (1.711(2) Å) in **VII** is shorter than observed in the similar Cp derived ylide, $C_5H_4PMePh_2$ (1.727 Å average), and shorter than

observed for the same bond in the Ramirez ylide $C_5H_4PPh_3$ (1.718 (2) Å).[7] It is also shorter than the P(1)-C(1) bond of the indenyl derived ylide, $C_9H_6PBzPh_2$ (Bz = benzyl), which is 1.733(4) Å.[44] The shortening of the P(1)-C(1) bond indicates that this bond in **VII** has potentially more double bond character than that of the Cp derived ylides. The P(1)-C(1) bond is significantly shorter than the P-Ph bonds in this molecule (typical of a P-C single bond in phenyl phosphonium ylides), but longer than the $P=CH_2$ bond in $Ph_3P=CH_2$ (1.66 Å).[86] This latter bond is a typical example of a non-resonance stabilized ylide with considerable double bond character. Much like the Cp derived ylides, **VII** also has significant contributions from both ylidic and zwitterionic resonance structures.

The C_5 ring bonds of **VII** are, on average, longer than the C_5 ring bonds of **I** and **II**.[7] The C-C-C bond angles of the C_5 ring in **VII** are all close to the values expected for a regular pentagon (108°) and the similarity in the C-C lengths tend to provide evidence of some delocalisation of the π bond electron density.

Upon coordination to the -$Cr(CO)_3$ fragment, the ylidic ligand undergoes several modifications. Elongation of the P(1)-C(1) bond is observed, which is typical of this class of ligand upon coordination. The P(1)-C(1) bond length of 1.753(5) Å in **VIII** is similar in length to those observed in the complexes (η^5-$C_5H_4PMePh_2$)$Cr(CO)_3$ (1.759(3) Å) and (η^5-$C_5H_4PPh_3$)$Cr(CO)_3$ (1.751(5) Å and 1.755(6) Å).[15] The increase in bond length is indicative of a greater contribution of the zwitterionic resonance structure of the ligand upon coordination indicating a greater degree of aromatic character. The P(1)-C(1)-C_5(Centroid) bond angle (174.7°) remains similar to that observed in the free ligand, but falls between the angle observed for (η^5-$C_5H_4PMePh_2$)$Cr(CO)_3$ (178.9°) and (η^5-$C_5H_4PPh_3$)$Cr(CO)_3$ (173.4° and 169.0°).[15] The bond lengths of the C_5 ring of **VIII** are, on

average, longer than in the free ligand. Again, a similar trend is also observed for (η^5-$C_5H_4PMePh_2$)$Cr(CO)_3$.

3.5.6 IR Spectrum of VIII.

The IR spectrum of **VIII**, shown in Figure 3-59 as a CH_2Cl_2 exhibits strong stretches at 1916 cm^{-1} and 1816 cm^{-1} with a shoulder 1802 cm^{-1}. The stretching frequencies are nearly identical to those of the related Cp-derived ylide complexes (η^5-$C_5H_4PMePh_2$)$Cr(CO)_3$ and (η^5-$C_5H_4PPh_3$)$Cr(CO)_3$,[10] which exhibit peaks as shown in Table 3-15. This demonstrates that the indenyl-derived ylide, **VII**, has similar donor characteristics to the related Cp-derived ylide systems.

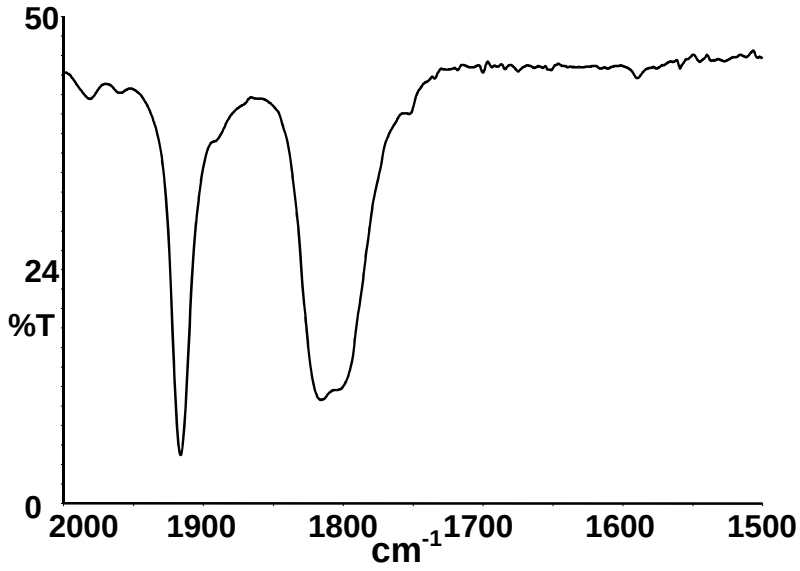

Figure 3-59. The IR spectrum of (η^5-$C_9H_6PMePh_2$)$Cr(CO)_3$ (VIII) in CH_2Cl_2.

Complex	ν(CO) (cm^{-1})
VIII	1916 (s), 1816 (s), 1802 (sh)
III	1918 (s), 1812 (s)
(η^5-$C_5H_4PPh_3$)$Cr(CO)_3$	1913 (s), 1802 (s)[10]

Table 3-15. Carbonyl Stretching Frequencies for VIII and III in CH_2Cl_2 and for (η^5-$C_5H_4PPh_3$)$Cr(CO)_3$ in $CHCl_3$.

3.6 Conclusions

Methyldiphenylphosphonium cyclopentadienylide, $C_5H_4PMePh_2$ (**II**), has been synthesized and characterized spectroscopically (^1H, $^{13}C\{^1H\}$ and $^{31}P\{^1H\}$ NMR) and crystallographically, and its electronic structure has been investigated via *ab initio* methodologies. The best representation of **II** appears to be the zwitterionic structure **IIb**, and it was found that the HOMO and (HOMO-1) orbitals of **II** are near degenerate and exhibit symmetries very similar to those of the corresponding, doubly degenerate HOMO (E_1 symmetry) of the free (D_{5h}) cyclopentadienyl anion. There is also, at a lower energy, an almost fully symmetric orbital which corresponds to the fully symmetric bonding A_1 MO of the cyclopentadienyl anion. In none of these three orbitals does there appear to be significant π interactions with an orbital on the phosphorus atom, again consistent with the zwitterionic resonance structure **IIb**. Observations that **II** forms the stable coordination compounds $(\eta^5\text{-}C_5H_4PMePh_2)M(CO)_3$ (M = Cr, Mo, W) also demonstrate that the implied aromatic cyclopentadienyl anion-like structure is of major significance.

The three group 6 metal complexes have been investigated spectroscopically (IR, ^1H, $^{13}C\{^1H\}$ and $^{31}P\{^1H\}$ NMR) and crystallographically, and via *ab initio* calculations (for **III**). In all cases the metal-carbon bond distances are very similar, consistent with a cyclopentadienyl-like structure, while comparisons of ν(CO) of the complexes $(\eta^5\text{-}C_5H_4PMePh_2)M(CO)_3$ (M = Cr, Mo, W) with those of the isoelectronic complexes $(\eta^6\text{-}C_6H_6)M(CO)_3$ and $[(\eta^5\text{-}C_5H_5)M(CO)_3]^-$ suggest that the electron donating ability of the ylide is less than that of the cyclopentadienyl anion but much greater than that of benzene. The primary bonding interaction of the ylide with the $Cr(CO)_3$ moiety involves donation of the HOMO and (HOMO-1) orbitals into the metal d_{xz} and d_{yz} orbitals, and the

calculated ylide-$Cr(CO)_3$ bond dissociation energy is about 30% higher than the analogous ring-metal bond dissociation energy of $(\eta^6\text{-}C_6H_6)Cr(CO)_3$.

Many aspects of the chemistry of the compounds $(\eta^5\text{-}C_5H_4PMePh_2)M(CO)_3$ (M = Cr, Mo) have been investigated. Thermal and photochemical substitution of the CO ligands by equimolar amounts of PMe_3 and PPh_3 were not observed, but the ylide was displaced photochemically from $(\eta^5\text{-}C_5H_4PMePh_2)Mo(CO)_3$ by excess PMe_3 to form *fac*-$Mo(CO)_3(PMe_3)_3$. The compound $(\eta^5\text{-}C_5H_4PMePh_2)Mo(CO)_3$ did not undergo reaction with MeI or H_2, but it did undergo reaction with I_2 to form $[(\eta^5\text{-}C_5H_4PMePh_2)Mo(CO)_3I]I$ which has been characterized spectroscopically (IR, ^1H, $^{13}C\{^1H\}$ and $^{31}P\{^1H\}$ NMR) and crystallographically. An interesting and unanticipated feature of the crystal structures of the free ylide and all four of its coordination complexes was that one of the ylide phenyl rings not only eclipses the C_5H_4 ring but is oriented towards it in an edge on fashion. The intramolecular edge-face orientations involve interactions of one aromatic hydrogen atom with the C_5H_4 aromatic π systems, and are rationalized in terms of electrostatic attractive forces between the slightly positive phenyl hydrogen atom and the negatively charged C_5H_4 ring.

Electrochemical studies have determined that the group 6 tricarbonyl complexes, **III**-**V**, undergo one electron oxidations that yield products that are stable enough to isolate. The oxidized products, $\mathbf{III_2}^{2+}$, $\mathbf{IV_2}^{2+}$ and $\mathbf{V_2}^{2+}$, which exist exclusively as metal-metal bonded dimers in the solid state, have been isolated and fully characterized spectroscopically (IR, ESMS, ^1H, $^{13}C\{^1H\}$ and $^{31}P\{^1H\}$ NMR) and crystallographically. The behaviour of these complexes parallels the isoelectronic Cp and Cp* group 6 tricarbonyl complexes ($[(\eta^5\text{-}C_5H_5)M(CO)_3]^-$ and $[(\eta^5\text{-}C_5Me_5)M(CO)_3]^-$), which also

undergo one electron oxidations to yield metal-metal bonded dimers in the solid state. The chromium dimer, with a metal-metal bond of 3.3509(7) Å, has the longest Cr-Cr bond in a complex without some type of bridging ligand. The heavier metal analogues have shorter metal-metal bond distances; a similar trend is observed with the related Cp and Cp* analogues. Solution behaviour of the complexes has been examined using a number of spectroscopic techniques, including the Evans method. From these studies, it has been determined that the chromium dimer, $\mathbf{III_2}^{2+}$, undergoes extensive dissociation at room temperature in solution to furnish stable 17 electron metal-centred radicals. The analogous molybdenum and tungsten complexes dissociate very little, if at all, in solution. Variable temperature ^{1}H NMR experiments have determined that at low temperatures, the chromium radicals begin to dimerize and reversibly dissociate upon warming of the solution. The behaviour of these oxidized complexes mirrors the behaviour of the related Cp and Cp* complexes ($[(\eta^5\text{-}C_5H_5)M(CO)_3]^-$ and $[(\eta^5\text{-}C_5Me_5)M(CO)_3]^-$).

The indenyl-derived ylide, $C_9H_6PMePh_2$ (**VII**), has been synthesized and characterized spectroscopically (^{1}H, ^{13}C{^{1}H} and ^{31}P{^{1}H} NMR, COSY, NOESY, HSQC and HMBC) and crystallographically. The behaviour of this compound appears to mimic the properties of the related cyclopentadienyl-derived ylides like **II**. As further evidence, beyond that collected spectroscopically and crytallographically, **VII** forms the stable coordination complex $(\eta^5\text{-}C_9H_6PMePh_2)Cr(CO)_3$ (**VIII**). This complex has been characterized spectroscopically (IR, ^{1}H, ^{13}C{^{1}H} and ^{31}P{^{1}H} NMR, COSY, NOESY, HSQC and HMBC) and crystallographically. **VIII** represents the first non-cyclopentadienyl-derived phosphorus ylide transition metal complex that has been

conclusively demonstrated to be bound to the metal in an η^5 manner. The coordination of **VII** to the metal generates two complexes with planar chirality. This investigation demonstrates that the beneficial properties of the indenyl-derived ylides (ease of synthesis and solubility in aromatic solvents) can be used to further expand upon the chemistry of this class of compound.

3.7 Future Work

Although this study has accomplished much to reinvigorate the study of phosphorus cyclopentadienylides, a great deal of chemistry remains to be explored. In some cases a reinvestigation of literature reports using modern spectroscopic techniques seems warranted and could add to the understanding of the behaviour of complexes of these ylides.

Specifically related to this project, a number of avenues for experimentation have presented themselves. Firstly, an exploration into the reactivities of the oxidized complexes, $\mathbf{III_2}^{2+}$, $\mathbf{IV_2}^{2+}$ and $\mathbf{V_2}^{2+}$, would be interesting as the related complexes ($[(\eta^5\text{-}C_5H_5)M(CO)_3]_2$ and $[(\eta^5\text{-}C_5Me_5)M(CO)_3]_2$) demonstrate interesting reactivities. Several preliminary reactions with phosphines have demonstrated that the complexes do indeed react. This should be followed up in detail. Secondly, the indenyl-derived ylide chemistry has just been touched upon, but indicates that there is much potential with these complexes. A general synthetic route for the indenyl-derived ylides must be developed as the literature methodology has only been used to synthesize one ylide. Thirdly, a general route into the cyclopentadienyl-derived ylides needs to be developed. Preliminary studies have also been started, but no success has been achieved. Fourthly, the application of

phosphorus ylide complexes to catalysis seems warranted with the similarity in behaviour to the Cp ligand that is ubiquitous in the literature. As part of the application to catalysis, other transition metal complexes in higher oxidation states must be synthesized. Finally, we have examined the reaction of the ylide **II** with a number of other metal precursors, but have not thoroughly studied this chemistry due to the success of the group 6 projects. The metal precursors that have been reacted with **II** include the following: $AlCl_3$, $[Ag][B(C_6F_5)_4]$, $HgBr_2$ (also with **VII**), $IrCl_3$, $RhCl_2{\cdot}3H_2O$, $Fe(CO)_5$, $Ni(CO)_4$ and $(PhRuCl_2)_2$.

The current work presented in this thesis and the work that still remains to be explored demonstrates the potential of this class of ligand to provide interesting chemistry; the surface of which has only been scratched…

4 References

1. Ramirez, F.; Levy, S., *J. Org. Chem.*, 1956. **21**: 488.
2. Ramirez, F.; Levy, S., *J. Org. Chem.*, 1956. **21**: 1333.
3. Ramirez, F.; Levy, S., *J. Am. Chem. Soc.*, 1957. **79**: 67.
4. Ramirez, F.; Dershowitz, S., *J. Org. Chem.*, 1957. **22**: 41.
5. Ramirez, F.; Levy, S., *J. Am. Chem. Soc.*, 1957. **79**: 6167.
6. Ramirez, F.; Levy, S., *J. Org. Chem.*, 1958. **23**: 2035.
7. Ammon, H.L.; Wheeler, G.L.; Watts Jr., P.H., *J. Am. Chem. Soc.*, 1973. **95**: 6158.
8. Gray, G.A., *J. Am. Chem. Soc.*, 1973. **95**(15): 5092.
9. Abel, E.W.; Singh, A.; Wilkinson, G., *Chem. Ind. (London)*, 1959: 1067.
10. Kotz, J.C.; Pedrotty, D.G., *J. Organomet. Chem.*, 1970. **22**: 425.
11. Cashman, D.; Lalor, F.J., *J. Organomet. Chem.*, 1970. **24**: C29.
12. Cashman, D.; Lalor, F.J., *J. Organomet. Chem.*, 1971. **32**: 351.
13. Zdanovitch, V.I.; Yurtanov, A.I.; Zhakaeva, A.Z.; Setkina, V.N.; Kursanov, D.N., *Investiya Akademii Nauk SSSR, Seriya Khimicheskaya*, 1973. **6**: 1375.
14. Setkina, V.N.; Zhakaeva, A.Z.; Panosyan, G.A.; Zdanovitch, V.I.; Petrovskii, P.V.; Kursanov, D.N., *J. Organomet. Chem.*, 1977. **129**: 361.
15. Debaerdemaeker, T., *Z. Kristallogr.*, 1980. **153**: 221.
16. Nesmeyanov, A.N.; Kolobova, N.E.; Zdanovitch, V.I.; Zhakaeva, A.Z., *J. Organomet. Chem.*, 1976. **107**: 319.
17. Zdanovitch, V.I.; Kolobova, N.E.; Vasyukova, N.I.; Nekrasov, Y.S.; Panosyan, G.A.; Petrovskii, P.V.; Zhakaeva, A.Z., *J. Organomet. Chem.*, 1978. **148**: 63.
18. Holy, N.L.; Baenziger, N.C.; Flynn, R.M., *Angew. Chem., Int. Ed. Engl.*, 1978. **17**: 686.
19. Baenziger, N.C.; Flynn, R.M.; Holy, N.L., *Acta Crystallogr., Sect. B: Struct. Sci.*, 1979. **B35**: 741.
20. Blake, A.J.; Johnson, B.F.G.; Parsons, S.; Shephard, D.S., *J. Chem. Soc., Dalton Trans.*, 1995: 495.
21. Tresoldi, G.; Recca, A.; Finocchiaro, P.; Faraone, F., *Inorg. Chem.*, 1981. **20**: 3103.
22. Tresoldi, G.; Faraone, F.; Piraino, P.; Bottino, F.A., *J. Organomet. Chem.*, 1982. **231**: 265.
23. Booth, B.L.; Smith, K.G., *J. Organomet. Chem.*, 1981. **220**: 229.
24. Pierpont, C.G.; Downs, H.H.; Itoh, K.; Nishiyama, H.; Ishii, Y., *J. Organomet. Chem.*, 1976. **124**: 93.
25. Hirai, M.-F.; Miyasaka, M.; Itoh, K.; Ishii, Y., *J. Chem. Soc., Dalton Trans.*, 1979: 1200.
26. Hirai, M.-F.; Miyasaka, M.; Itoh, K.; Ishii, Y., *J. Organomet. Chem.*, 1979. **165**: 391.
27. Bombieri, G.; Tresoldi, G.; Faraone, F.; Bruno, G.; Cavoli-Belluco, P., *Inorg. Chim. Acta*, 1982. **57**: 1.
28. Holy, N.L.; Baenziger, N.C.; Flynn, R.M.; Swenson, D.C., *J. Am. Chem. Soc.*, 1976. **98**: 7823.
29. Roberts, R.M.G., *Tetrahedron*, 1980. **36**: 3295.

30. Holy, N.L.; Nalesnik, T.E.; Warfield, L.T., *Inorg. Nucl. Chem. Letters*, 1977. **13**: 569.
31. Nalesnik, T.; Warfield, L.; Holy, N.; Layton, J.; Smith, S., *Inorg. Nucl. Chem. Letters*, 1977. **13**: 523.
32. Holy, N.L.; Nalesnik, T.; Warfield, L.; Mojesky, M., *J. Coord. Chem.*, 1983. **12**: 157.
33. Iwata, K.; Yoneda, S.; Yoshida, Z.-i., *J. Am. Chem. Soc.*, 1971. **93**: 6745.
34. Unpublished results; Lab, T.B.
35. Holy, N.; Deschler, U.; Schmidbaur, H., *Chem. Ber.*, 1982. **115**: 1379.
36. Mathey, F.; Lampin, J.-P., *Tetrahedron*, 1975. **31**: 2685.
37. Casey, C.P.; Bullock, R.M.; Fultz, W.C.; Rheingold, A.L., *Organometallics*, 1982. **1**: 1591.
38. Freeman, B.H.; Lloyd, D.; Singer, M.I.C., *Tetrahedron*, 1972. **28**: 343.
39. Lloyd, D.; Singer, M.I.C., *J. Chem. Soc. C*, 1971: 2941.
40. Ramirez, F.; Levy, S., *J. Org. Chem.*, 1958. **23**: 2036.
41. Freeman, B.H.; Lloyd, D., *Tetrahedron*, 1974. **30**: 2257.
42. Freeman, B.H.; Lloyd, D.; Singer, M.I.C., *Tetrahedron*, 1974. **30**: 211.
43. Crofts, P.C.; Williamson, M.P., *J. Chem. Soc. C*, 1967: 1093.
44. Rufanov, K.A.; Ziemer, B.; Hummert, M.; Schutte, S., *Eur. J. of Inorg. Chem.*, 2004: 4759.
45. Pinck, L.A.; Hilbert, G.E., *J. Am. Chem. Soc.*, 1947. **69**: 723.
46. Johnson, A.W.; Lee, S.Y.; Swor, R.A.; Royer, L.D., *J. Am. Chem. Soc.*, 1966. **88**: 1953.
47. Schmidbaur, H.; Deschler, U., *Chem. Ber.*, 1981. **114**: 2491.
48. Shin, J.H.; Bridgewater, B.M.; Parkin, G., *Organometallics*, 2000. **19**: 5155.
49. Kotz, J.C.; Turnipseed, C.D., *J. Chem. Soc., Chem. Commun.*, 1970: 41.
50. Alper, H.; Partis, R.A., *J. Organomet. Chem.*, 1972. **44**: 371.
51. Sollott, G.P.; Mertwoy, H.E.; Portnoy, S.; Snead, J.L., *J. Org. Chem.*, 1963. **28**: 1090.
52. McEwen, W.E.; Fountaine, J.E.; Schulz, D.N.; Shiau, W.-I., *J. Org. Chem.*, 1976. **41**: 1684.
53. McEwen, W.E.; Sullivan, C.E.; Day, R.O., *Organometallics*, 1983. **2**: 420.
54. Imrie, C.; Modro, T.A.; Van Rooyen, P.H., *Polyhedron*, 1994. **13**: 1677.
55. Kirchner, K.; Mereiter, K.; Schmid, R.; Taube, H., *Inorg. Chem.*, 1993. **32**: 5553.
56. Watanabe, M.; Sato, M.; Takayama, T., *Organometallics*, 1999. **18**: 5201.
57. Deeming, A.J.; Powell, N.I.; Whittaker, C., *J. Chem. Soc., Dalton Trans.*, 1991: 1875.
58. McKinney, R.J., *Inorg. Chem.*, 1982. **21**: 2051.
59. Rerek, M.E.; Basolo, F., *J. Am. Chem. Soc.*, 1984. **106**: 5908.
60. Abdulla, K.; Booth, B.L.; Stacey, C., *J. Organomet. Chem.*, 1985. **293**: 103.
61. Baenziger, N.C.; Flynn, R.M.; Swenson, D.C.; Holy, N.L., *Acta Crystallogr., Sect. B: Struct. Sci.*, 1978. **34**: 2300.
62. *Bruker AXS Crystal Structure Analysis Package, Version 5.10 (SMART NT (Version 5.053), SAINT-Plus (Version 6.01), SHELXTL (Version 5.1)); Bruker AXS Inc.: Madison, WI*, 1999.

63. Cromer, D.T.; Waber, J.T., *International Tables for X-ray Crystallography; Kynoch Press: Birmingham, UK, Vol. 4, Table 2.2 A.*, 1974.
64. Cooper, R.I.; Gould, R.O.; Parsons, S.; Watkin, D.J., *J. Appl. Cryst.*, 2002. **35**: 168.
65. Sluis, P.v.d.; Spek, A.L., *Acta. Cryst.*, 1990. **A46**: 194.
66. Evans, D.F., *J. Chem. Soc.*, 1959: 2003.
67. Crawford, T.H.; Swanson, J., *J. Chem. Ed.*, 1971. **48**: 382.
68. Sur, S.K., *J. Magn. Res.*, 1989. **82**: 169.
69. Earnshaw, A., *Introduction to Magnetochemistry*. 1968, New York: Academic Press.
70. Abeles, T.P.; Bos, W.G., *J. Chem. Ed.*, 1967. **44**: 438.
71. Frisch, M.J.; Trucks, G.W.; Schlegel, H.B.; Scuseria, G.E.; Robb, M.A.; Cheeseman, J.R.; Montgomery Jr., J.A.; Vreven, T.; Kudin, K.N.; Burant, J.C.; Millam, J.M.; Iyengar, S.S.; Tomasi, J.; Barone, V.; Mennucci, B.; Cossi, M.; Scalmani, G.; Rega, N.; Petersson, G.A.; Nakatsuji, H.; Hada, M.; Ehara, M.; Toyota, K.; Fukuda, R.; Hasegawa, J.; Ishida, M.; Nakajima, T.; Honda, Y.; Kitao, O.; Nakai, H.; Klene, M.; Li, X.; Knox, J.E.; Hratchian, H.P.; Cross, J.B.; Adamo, C.; Jaramillo, J.; Gomperts, R.; Stratmann, R.E.; Yazyev, O.; Austin, A.J.; Cammi, R.; Pomelli, C.; Ochterski, J.W.; Ayala, P.Y.; Morokuma, K.; Voth, G.A.; Salvador, P.; Dannenberg, J.J.; Zakrzewski, V.G.; Dapprich, S.; Daniels, A.D.; Strain, M.C.; Farkas, O.; Malick, D.K.; Rabuck, A.D.; Raghavachari, K.; Foresman, J.B.; Ortiz, J.V.; Cui, Q.; Baboul, A.G.; Clifford, S.; Cioslowski, J.; Stefanov, B.B.; Liu, G.; Liashenko, A.; Piskorz, P.; Komaromi, I.; Martin, R.L.; Fox, D.J.; Keith, T.; Al-Laham, M.A.; Peng, C.Y.; Nanayakkara, A.; Challacombe, M.; Gill, P.M.W.; Johnson, B.; Chen, W.; Wong, M.W.; Gonzalez, C.; Pople, J.A., *Gaussian '03, Revision B.04*. 2003, Gaussian Inc.: Pittsburgh PA.
72. Becke, A.D., *J. Chem. Phys.*, 1993. **98**: 5648.
73. Lee, C.; Yang, W.; ; Parr, R.G., *Phys. Rev. B*, 1988. **37**: 785.
74. Miehlich, B.; Savin, A.; Stoll, H.; Preuss, H., *Chem. Phys. Lett.*, 1989. **15**: 7200.
75. Hehre, W.J.; Ditchfield, R.; Pople, J.A., *J. Chem. Phys.*, 1972. **56**: 2257.
76. Francl, M.M.; Pietro, W.J.; Hehre, W.J.; Binkley, J.S.; Gordon, M.S.; DeFrees, D.J.; Pople, J.A., *J. Chem. Phys.*, 1982. **77**: 3654.
77. Hariharan, P.C.; Pople, J.A., *Theoret. Chimica Acta*, 1973. **28**: 213.
78. Rassolov, V.A.; Pople, J.A.; Ratner, M.A.; Windus, T.L., *J. Chem. Phys.*, 1998. **109**: 1223.
79. Woon, D.E.; Dunning Jr., T.H., *J. Chem. Phys.*, 1993. **98**: 1358.
80. Dunning Jr., T.H., *J. Chem. Phys.*, 1989. **90**: 1007.
81. Wachters, A.J.H., *J. Chem. Phys.*, 1970. **52**: 1033.
82. Hay, P.J., *J. Chem. Phys.*, 1977. **66**: 4377.
83. Mathieu, R.; Lenzi, M.; Poilblanc, R., *Inorg. Chem.*, 1970. **9**: 2030.
84. Leblanc, J.C.; Moise, C.; Maisonnat, A.; Poilblanc, R.; Charrier, C.; Mathey, F., *J. Organomet. Chem.*, 1982. **231**: C43.
85. Fallis, K.A.; Anderson, G.K.; Rath, N.P., *Organometallics*, 1992. **11**: 885.
86. Bart, J.C.J., *J. Chem. Soc. B*, 1969: 350.
87. Plíva, J.; Johns, J.W.C.; Goodman, L., *J. Mol. Spectrosc.*, 1990. **140**: 214.
88. Brown, D.A.; Hughes, F.J., *J. Chem. Soc. A*, 1968: 1519.

89. Darensbourg, M.Y.; Jimenez, P.; Sackett, J.R.; Hanckel, J.M.; Kump, R.L., *J. Am. Chem. Soc.*, 1982. **104**: 1521.
90. Desiraju, G.R., in *Crystal Engineering*. 1989, Elsevier: Amsterdam. p. 92.
91. Jennings, W.B.; Farrell, B.M.; Malone, J.F., *Acc. Chem. Res.*, 2001. **34**: 885.
92. Carver, F.J.; Hunter, C.A.; Livingstone, D.J.; McCabe, J.F.; Seward, E.M., *Chem. Eur. J.*, 2002. **8**: 2847.
93. Ercolani, G.; Mencarelli, P., *J. Org. Chem.*, 2003. **68**: 6470.
94. Emsley, J., *The Elements. 2nd Edition*. 1991, Oxford: Claredon Press.
95. Jolly, W.L., *Inorg. Synth.*, 1968. **11**: 116.
96. Laavanya, P.; Krishnamoorthy, B.S.; Panchanatheswaran, K.; Manoharan, M., *J. Mol. Struct., THEOCHEM*, 2005. **716**: 149.
97. Stoddart, M.W.; Brownie, J.H.; Schmider, H.L.; Baird, M.C., *J. Organomet. Chem.*, 2005. **690**: 3440.
98. Albright, T.A.; Burdett, J.K.; Whangbo, M.H., in *Orbital Interactions in Chemistry*. 1985, Wiley and Sons: New York, N. Y. p. 385.
99. Jorgensen, W.L.; Salem, L., in *The Organic Chemist's Book of Orbitals*. 1973, Academic Press: New York, N. Y. p. 237.
100. Adams, R.D.; Collins, D.E.; Cotton, F.A., *J. Am. Chem. Soc.*, 1974. **96**: 749.
101. Landrum, J.T.; Hoff, C.D., *J. Organomet. Chem.*, 1985. **282**: 215.
102. Cooley, N.A.; Watson, K.A.; Fortier, S.; Baird, M.C., *Organometallics*, 1986. **5**: 2563.
103. Madach, T.; Vahrenkamp, H., *Z. Naturforsch.*, 1978. **33b**: 1301.
104. McLain, S.J., *J. Am. Chem. Soc.*, 1988. **110**: 643.
105. Cooley, N.A.; MacConnachie, P.T.F.; Baird, M.C., *Polyhedron*, 1988. **7**: 1965.
106. Jaeger, T.J.; Baird, M.C., *Organometallics*, 1988. **7**: 2074.
107. Watkins, W.C.; Jaeger, T.; Kidd, C.E.; Fortier, S.; Baird, M.C.; Kiss, G.; Roper, G.C.; Hoff, C.D., *J. Am. Chem. Soc.*, 1992. **114**: 907.
108. Richards, T.C.; Geiger, W.E.; Baird, M.C., *Organometallics*, 1994. **13**: 4494.
109. Woska, D.C.; Ni, Y.; Wayland, B.B., *Inorg. Chem.*, 1999. **38**: 4135.
110. O'Callaghan, K.A.E.; Brown, S.J.; Page, J.A.; Baird, M.C.; Richards, T.C.; Geiger, W.E., *Organometallics*, 1991. **10**: 3119.
111. Yao, Q.; Bakac, A.; Espenson, J.H., *Organometallics*, 1993. **12**: 2010.
112. Baird, M.C., *Chem. Rev.*, 1988. **88**: 1217.
113. Baird, M.C., *Organometallic Radical Processes*, 1990: 49.
114. Pickett, C.J.; Pletcher, D., *J. Chem. Soc., Dalton Trans.*, 1975: 879.
115. Chum, H.L.; Koran, D.; Osteryoung, R.A., *J. Organomet. Chem.*, 1977. **140**: 349.
116. Bagchi, R.N.; Bond, A.M.; Colton, R.; Luscombe, D.L.; Moir, J.E., *J. Am. Chem. Soc.*, 1986. **108**: 3352.
117. Bond, A.M.; Colton, R.; Kevekordes, J.E.; Panagiotidou, P., *Inorg. Chem.*, 1987. **26**: 1430.
118. Bond, A.M.; Colton, R.; Kevekordes, J.E., *Inorg. Chem.*, 1986. **25**: 749.
119. Bagchi, R.N.; Bond, A.M.; Brian, G.; Colton, R.; Henderson, T.L.E.; Kevekordes, J.E., *Organometallics*, 1984. **3**: 4.
120. Bond, A.M.; Carr, S.W.; Colton, R., *Inorg. Chem.*, 1984. **23**: 2343.
121. Bond, A.M.; Carr, S.W.; Colton, R., *Organometallics*, 1984. **3**: 541.

122. Lappert, M.F.; McCabe, R.W.; MacQuitty, J.J.; Pye, P.L.; Riley, P.I., *J. Chem. Soc., Dalton Trans.*, 1980: 90.
123. Ashford, P.K.; Baker, P.K.; Connelly, N.G.; Kelly, R.L.; Woodley, V.A., *J. Chem. Soc., Dalton Trans.*, 1982: 477.
124. Connelly, N.G.; Demidowicz, Z.; Kelly, R.L., *J. Chem. Soc., Dalton Trans.*, 1975: 2335.
125. Van Order Jr., N.; Geiger, W.E.; Bitterwolf, T.E.; Rheingold, A.L., *J. Am. Chem. Soc.*, 1987. **109**: 5680.
126. Doxsee, K.M.; Grubbs, R.H.; Anson, F.C., *J. Am. Chem. Soc.*, 1984. **106**: 7819.
127. Zoski, C.G.; Sweigart, D.A.; Stone, N.J.; Rieger, P.H.; Mocellin, E.; Mann, T.F.; Mann, D.R.; Gosser, D.K.; Doeff, M.M.; Bond, A.M., *J. Am. Chem. Soc.*, 1988. **110**: 2109.
128. Camire, N.; Nafady, A.; Geiger, W.E., *J. Am. Chem. Soc.*, 2002. **124**: 7260.
129. Hackett, P.; O'Neill, P.S.; Manning, A.R., *J. Chem. Soc., Dalton Trans.*, 1974: 1625.
130. Madach, T.; Vahrenkamp, H., *Z. Naturforsch.*, 1979. **34b**: 573.
131. Goh, L.-Y.; D'Aniello Jr., M.J.; Slater, S.; Muetterties, E.L.; Tavanaiepour, I.; Chang, M.I.; Fredrich, M.F.; Day, V.W., *Inorg. Chem.*, 1979. **18**: 192.
132. Keller, H.J., *Z. Naturforsch.*, 1968. **23b**: 133.
133. Wrighton, M.S.; Ginley, D.S., *J. Am. Chem. Soc.*, 1975. **97**: 4246.
134. Hughey IV, J.L.; Bock, C.R.; Meyer, T.J., *J. Am. Chem. Soc.*, 1975. **97**: 4440.
135. Laine, R.M.; Ford, P.C., *Inorg. Chem.*, 1977. **16**: 388.
136. Goh, L.Y.; Hambley, T.W.; Darensbourg, D.J.; Reibenspies, J., *J. Organomet. Chem.*, 1990. **381**: 349.
137. Lin, G.; Wong, W.-T., *J. Organomet. Chem.*, 1996. **522**: 271.
138. Clegg, W.; Compton, N.A.; Errington, R.J.; Norman, N.C., *Acta. Cryst.*, 1988. **C44**: 568.
139. Rheingold, A.L.; Harper, J.R., *Acta. Cryst.*, 1991. **C47**: 184.
140. Cheng, T.-Y.; Szalda, D.J.; Zhang, J.; Bullock, R.M., *Inorg. Chem.*, 2006. **45**: 4712.
141. McGovern, P.A.; Vollhardt, K.P.C., *Chem. Commun.*, 1996: 1593.
142. O'Connor, A.R.; Nataro, C.; Golen, J.A.; Rheingold, A.L., *J. Organomet. Chem.*, 2004. **689**: 2411.
143. Yang, X.; Stern, C.L.; Marks, T.J., *Organometallics*, 1991. **10**: 840.
144. Bertini, I.; Luchinat, C.; Parigi, G., *Solution NMR of Paramagnetic Molecules: Applications to Metallobiomolecules and Models.* 2001, Amsterdam: Elsevier Science B.V.
145. *CRC Handbook of Chemistry and Physics*, ed. R.C. Weast and D.R. Lide. 1990, Boca Raton, Florida: CRC Press.
146. Potter, G.D.; Baird, M.C.; Chan, M.; Cole, S.P.C., *Inorg. Chem. Comm.*, 2006. **9**: 1114.
147. Causey, P.W.; Cole, S.P.C.; Baird, M.C., *Organometallics*, 2004. **23**: 4486.
148. Bavarian, N.; Baird, M.C., *Unpublished Results of The Baird Laboratories*.

5 Appendix - Electrochemical Study

In collaboration with Derek R. Laws and William E. Geiger of the Department of Chemistry, University of Vermont, Burlington, Vermont. This is their work reported to compliment the study we performed to synthesize and characterize the complexes, $\mathbf{III_2}^{2+}$, $\mathbf{IV_2}^{2+}$, $\mathbf{V_2}^{2+}$.

Experimental

All electrochemical experiments were conducted (Vermont) using Princeton Applied Research models PAR-173 and PAR-273 potentiostats interfaced to personal computers. For these experiments, CH_2Cl_2 was dried over CaH_2, distilled under nitrogen, and purified further by vacuum transfer from fresh drying agent prior to use, while $[NBu_4][B(C_6F_5)_4]$ was prepared by metathesis of $[NBu_4]Br$ with $K[B(C_6F_5)_4]\cdot n OEt_2$ (Boulder Scientific Co.) in methanol,[1] recrystallized three times from CH_2Cl_2/OEt_2, and dried at 353 K under vacuum for 12 h.

Spectroelectrochemical IR experiments were performed using Schlenk conditions under an atmosphere of argon after adding solvent and electrolyte to the electrochemical cell in a Vacuum Atmospheres drybox under nitrogen. All other experiments were conducted directly in the drybox under nitrogen. Working electrodes were glassy carbon electrodes (GCEs, 1-3 mm diameter) supplied by Bioanalytical Systems. The effective areas of the electrodes were determined through chronoamperometric measurements of ferrocene in acetonitrile/0.1 M $[NBu_4][PF_6]$. The electrodes were pretreated by polishing with successively finer diamond paste (Buehler, 3 μ to 0.25 μ) interspersed by washings with nanopure water and, finally, dried in the antechamber of the drybox. Controlled

potential coulometry was carried out using a basket-shaped Pt mesh electrode. Although the functional reference electrode was Ag/AgCl, separated from the working compartment by a fine glass frit, all potentials reported in this paper are versus the $FeCp_2^{0/+}$ redox couple, as recommended elsewhere.[2] The ferrocene potential was obtained by adding it to the solution at an appropriate point in the experiment. The supporting electrolyte in all experiments was $[NBu_4][B(C_6F_5)_4]$,[2,3] at concentrations of 0.05 M or 0.1 M, as noted in the text. Diagnostics applied to the shapes and positions of cyclic voltammetric waves were as described earlier.[4] Digital simulations of background-subtracted cyclic voltammetry experiments were performed using Digisim 3.0 (Bioanalytical Systems). More details on the electrochemical methodologies can be found in a recent paper.[5]

Results and Discussion

Electrochemical oxidation of III, IV and V

Cyclic voltammograms (CVs) of **III** in CH_2Cl_2 with 0.05 M $[NBu_4][B(C_6F_5)_4]$ exhibited an oxidation wave at $E_{1/2}$ = –0.38 V (Figure 1) having the general characteristics of a chemically reversible one-electron process as given in Equation 1. This conclusion was confirmed by bulk coulometry (*vide infra*).

$$(\eta^5\text{-}C_5H_4PMePh_2)Cr(CO)_3\ (\mathbf{III}) - e^- \rightleftharpoons [(\eta^5\text{-}C_5H_4PMePh_2)Cr(CO)_3]^+\ (\mathbf{III}^+) \qquad (1)$$

A second, chemically irreversible anodic wave of approximately one half of the height of the first wave was observed at E_{pa} = ca. 0.95 V, but the products of this second oxidation

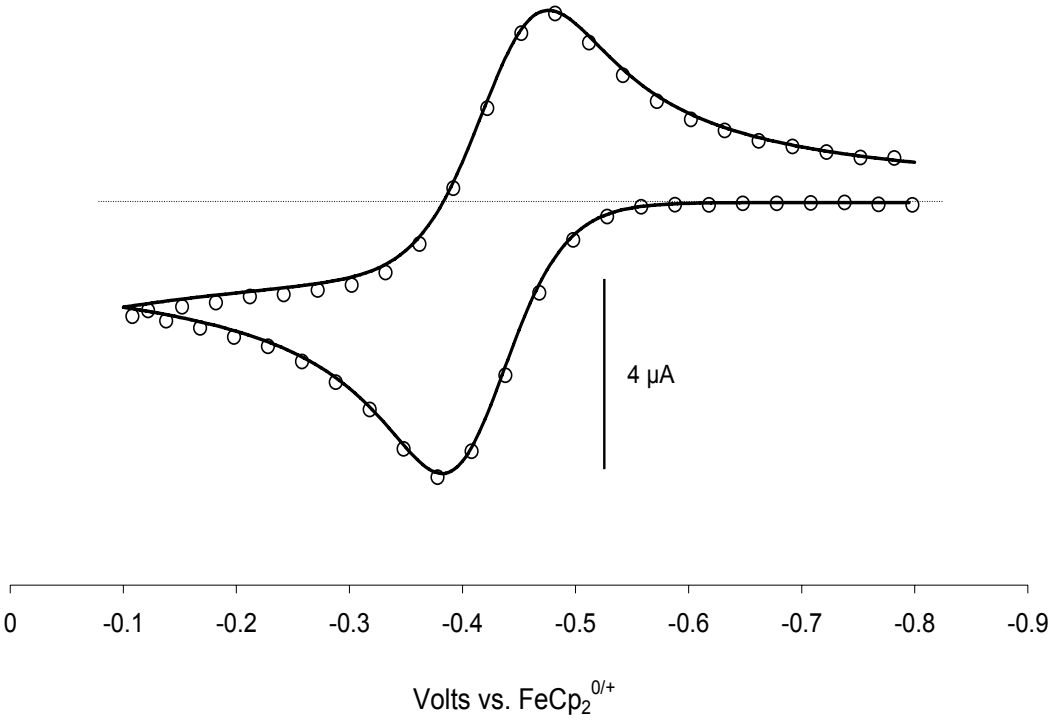

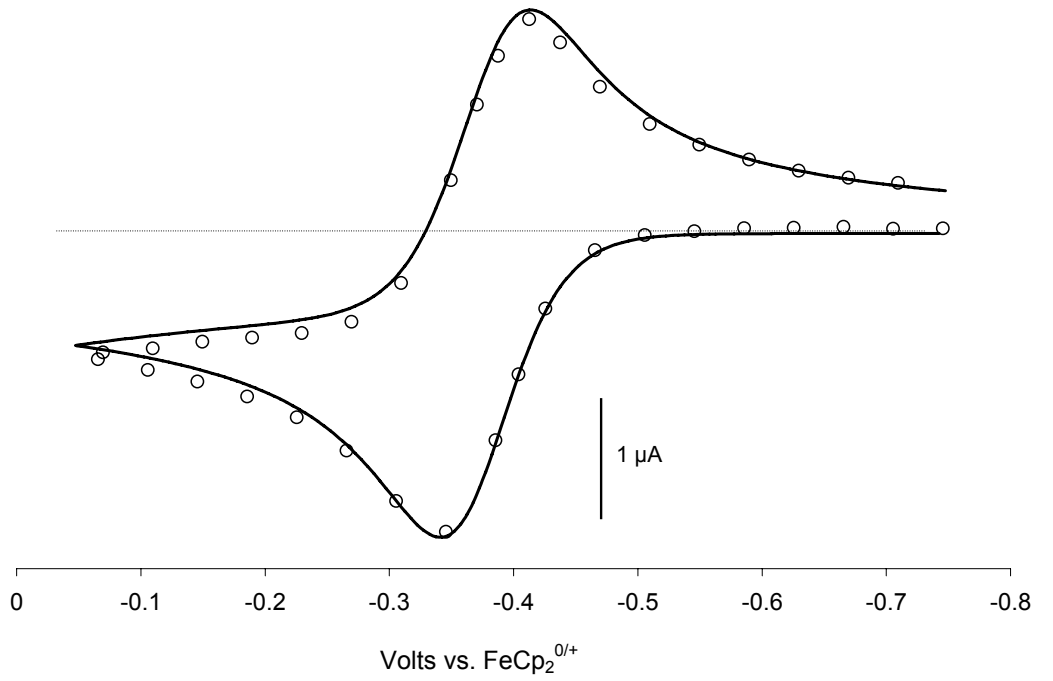

Figure 1. Experimental (circles) and simulated CVs for 0.6 mM (η^5-$C_5H_4PMePh_2$)$Cr(CO)_3$ in CH_2Cl_2/0.1 M $[NBu_4][B(C_6F_5)_4]$. Top, v = 2.0 V s^{-1}; bottom, v = 0.3 V s^{-1}. Relevant simulation parameters: k_s = 0.04 cm s^{-1}, β = 0.57.

were not studied. The free cyclopentadienylide ligand itself oxidizes (irreversibly) at E_{pa} = 0.1 V. Owing to the fact that, as will be shown, the molybdenum and tungsten analogues **IV** and **V** undergo fast dimerization reactions when oxidized, the oxidation of **III** was also investigated under conditions, specifically at lower temperatures and higher concentrations, that would be expected to favour dimerization of $\mathbf{III}^+$. CV scans of a 3.6 mM solution of **III** in CH_2Cl_2 at temperatures from ambient to 238 K failed to show any changes that would indicate involvement of dimerization of $\mathbf{III}^+$ in detectable amounts in solution. Simulations of CV scans of **III** (Figure 1) provide values of the charge-transfer coefficient, $\beta = 0.57$ (where $\beta = 1-\alpha$), and the standard heterogeneous electron-transfer rate constant, $k_s = 0.04$ cm s^{-1}, for the reversible one-electron oxidation. The diffusion coefficient of **III** was measured as $D_o = 5 \times 10^{-6}$ cm^2 s^{-1}.

Bulk electrolysis at $E_{appl} = 0.3$ V resulted in clean conversion to the radical cation $\mathbf{III}^+$ as the colour of the solution remained yellow. The coulometry was consistent with a one-electron process, with values of 0.90 and 0.95 F/eq being obtained in two separate experiments. The starting material **III** was efficiently regenerated to greater than 90% of its original concentration by back-electrolysis at $E_{appl} = -0.6$ V. When monitored by *in situ* IR spectroscopy (Figure 2), the anodic electrolysis revealed the presence of three carbonyl bands for the 17 electron species $\mathbf{III}^+$, at 2035, 1955, and 1910 cm^{-1}, comparable with the values of ν_{CO} of $[(\eta^5\text{-}C_5H_4PMePh_2)Cr(CO)_3]_2[B(C_6F_5)_4]_2$ (Table 4) and at considerably higher frequencies than ν_{CO} of the neutral $(\eta^5\text{-}C_5H_4PMePh_2)Cr(CO)_3$, 1912 and 1809 cm^{-1}. Assuming that 1809 cm^{-1} may be taken as the average of the asymmetric ν_{CO} of **III**, an average shift of +124 cm^{-1} in ν_{CO} is calculated for the one-electron oxidation, in concert with expectations.[6] Taken together, the voltammetry, electrolysis,

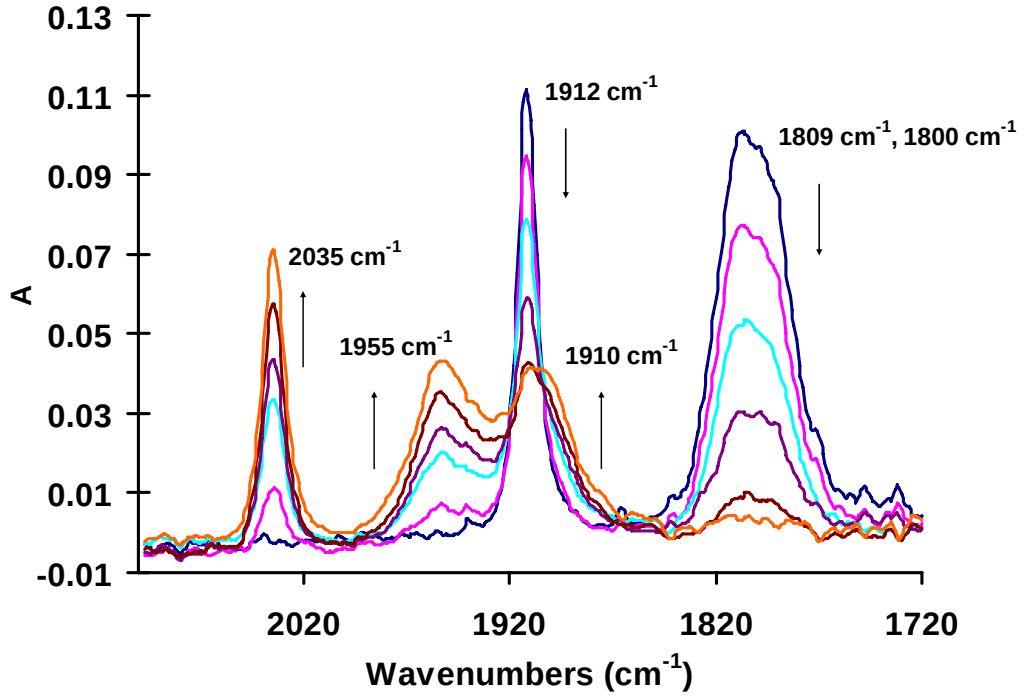

Figure 2. Infrared data for spectroelectrochemistry of 3.0 mM (η^5-$C_5H_4PMePh_2$)$Cr(CO)_3$ in CH_2Cl_2/0.05 M $[NBu_4][B(C_6F_5)_4]$ at 298 K. Arrows indicate the increase or decrease in intensity of infrared absorptions as oxidation proceeds.

and IR spectroscopy indicate that the first oxidation of **III** is a quasi-Nernstian, chemically reversible, one-electron process involving a largely metal-based orbital. There is no evidence for appreciable amounts of the chromium dimer dication, $\mathbf{III}_2^{2+}$, under these conditions of temperature and concentration.

Cyclic voltammograms of **IV** in CH_2Cl_2/0.05 M $[NBu_4][B(C_6F_5)_4]$ revealed two chemically irreversible features when the potential was scanned from –1.1 V to + 0.1 V (Figure 3). The anodic wave at $E_{pa} \approx$ –0.19 V is due to the apparent one-electron oxidation of **IV**, and the cathodic feature at more negative potentials arises from the follow-up reaction product of $\mathbf{IV}^+$. Whereas the anodic wave has the shape of an electrochemically reversible process (i.e., one having relatively fast heterogeneous charge-transfer kinetics), the cathodic wave has the characteristics of an

electrochemically irreversible process, being quite broad and exhibiting E_{pc} values that are highly scan rate dependent (e.g. –0.77 V at v = 0.1 V s^{-1} and –0.82 V at v = 1 V s^{-1}).

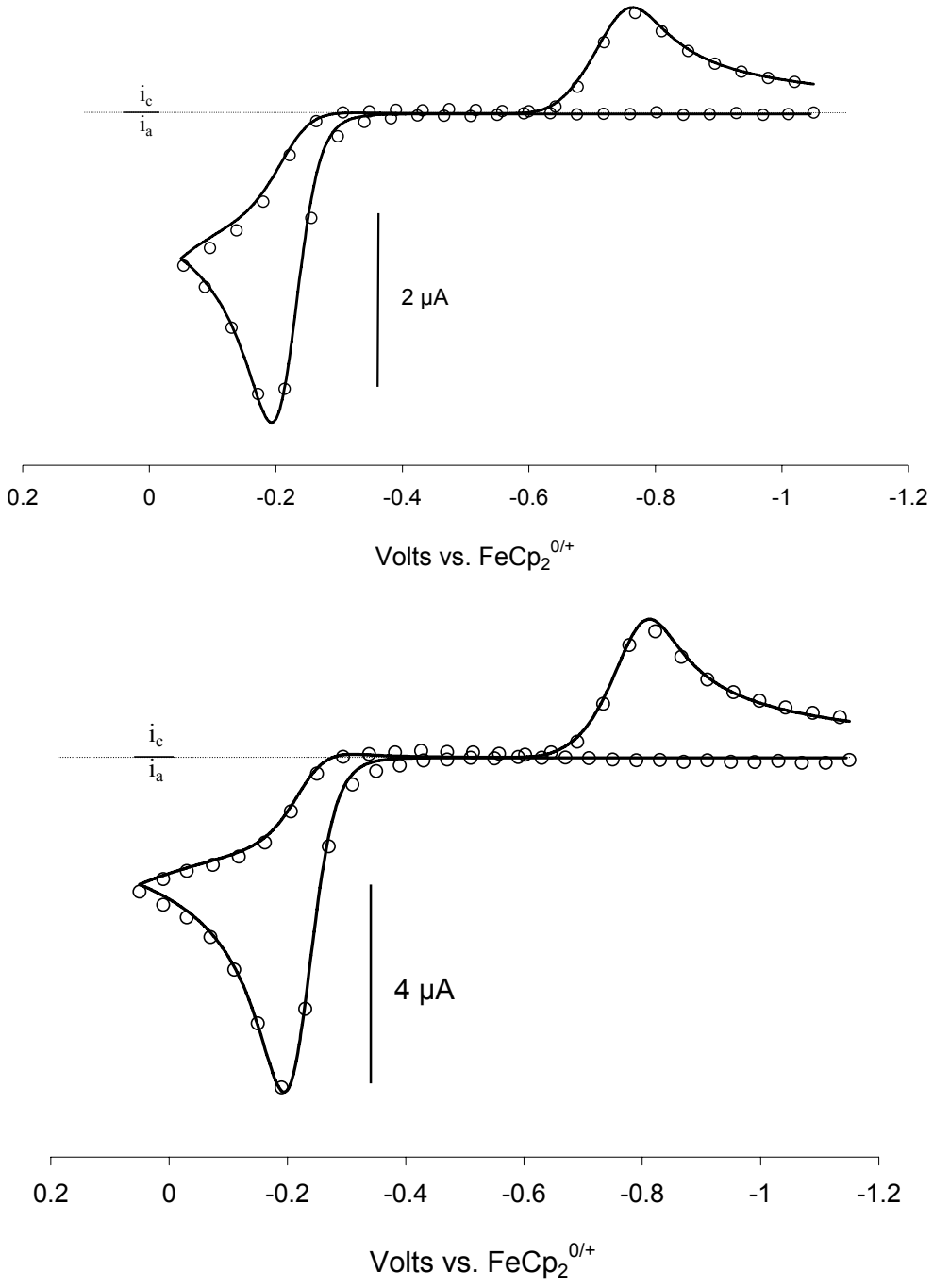

Figure 3. Experimental (circles) and simulated CVs for 0.7 mM (η^5-$C_5H_4PMePh_2$)$Mo(CO)_3$ in CH_2Cl_2/0.1 M $[NBu_4][B(C_6F_5)_4]$. Top, v = 0.5 V s^{-1}; bottom, v = 2.0 V s^{-1}. Relevant simulation parameters: k_s (oxidation) = 0.1 cm s^{-1}, k_s (reduction) = 0.0025 cm s^{-1}. K_{dim} = 1.0 x 10^6 M^{-1}, k_f = 1.0 x 10^6 M^{-1} s^{-1}.

Although there are a number of mechanisms that could account for these observations, the voltammetric behavior is most strongly reminiscent of an *anodic* EC mechanism, involving fast dimerization of $\mathbf{IV}^+$ (Equations 2 and 3), and a *cathodic* two-electron EEC process resulting in regeneration of the original 18-electron complex **IV** (Equations 4 and 5).

$$(\eta^5\text{-}C_5H_4PMePh_2)Mo(CO)_3 - e^- \rightleftharpoons [(\eta^5\text{-}C_5H_4PMePh_2)Mo(CO)_3]^+ \text{ (E)} \qquad (2)$$

$$2\,[(\eta^5\text{-}C_5H_4PMePh_2)Mo(CO)_3]^+ \rightleftharpoons [(\eta^5\text{-}C_5H_4PMePh_2)Mo(CO)_3]_2^{2+} \text{ (C)} \qquad (3)$$

$$[(\eta^5\text{-}C_5H_4PMePh_2)Mo(CO)_3]_2^{2+} + 2\,e^- \rightarrow 2\,[(\eta^5\text{-}C_5H_4PMePh_2)Mo(CO)_3]_2 \text{ (EE)} \qquad (4)$$

$$[(\eta^5\text{-}C_5H_4PMePh_2)Mo(CO)_3]_2 \rightarrow 2\,(\eta^5\text{-}C_5H_4PMePh_2)Mo(CO)_3 \text{ (C)} \qquad (5)$$

In the cathodic direction the "C" step (Equation 5) involves homolytic cleavage of the Mo-Mo bond of the dimer. Since the data are insufficient to differentiate between the proposed EEC mechanism and an ECE cathodic mechanism in which fragmentation of the metal-metal bond occurs after the acceptance of the first electron, simulations were performed only using the EEC process for the cathodic reaction. There is significant literature precedent for these types of overall mechanisms in describing the redox-based formation and cleavage of metal-metal bonded organometallic dimers.[18] In the present case, the best fit to CV scans over the scan rate range of 0.5 V s^{-1} to 2 V s^{-1} employed a dimerization equilibrium constant, K_{dim}, of 1 x 10^6 M^{-1} and a dimerization rate constant, k_{dim}, of 10^6 M^{-1} s^{-1}. It is clear from the cathodic wave shape that the charge transfer coefficient, α, is less than 0.5 for the reduction process, and a good fit was obtained with $\alpha = 0.35$. Although the simulations agreed with experiment when the effective

heterogeneous electron-transfer was 0.0025 cm s^{-1}, this value should only be taken as representative of a family of rate constants, α values, and $E_{1/2}$ values that would be consistent with the cathodic process.

When bulk anodic electrolysis of **IV** was conducted at E_{appl} = 0.15 V, the pale yellow solution turned orange/pink as the red dimer dication, $\mathbf{IV_2^{2+}}$, was formed. Voltammetry indicated essentially quantitative formation of $\mathbf{IV_2^{2+}}$ as the single product, having an irreversible cathodic wave at E_{pc} of approximately –0.77 V, and back-reduction of this solution at E_{appl} = –1.3 V regenerated **IV** in greater than 95 % yield. One nuance of these experiments is that the coulometry count was consistently somewhat lower than that expected for a one-electron process, being 0.7 to 0.8 F/eq in three separate electrolyses. *In situ* IR spectroscopy was therefore used to monitor the carbonyl region of the reactant and product. As shown in Figure 4, oxidation resulted in disappearance of the symmetric and asymmetric ν_{CO} bands of **IV** at 1915 cm^{-1} and 1810 cm^{-1}, respectively, and the appearance of at least three new terminal carbonyl bands, at 2029, 1981 and 1943 cm^{-1} and very close to the υ(CO) of $[(\eta^5\text{-}C_5H_4PMePh_2)Mo(CO)_3]_2[B(C_6F_5)_4]_2$ in THF (Table 4). The fact that there is an isosbestic point at 1920 cm^{-1} demonstrates that the new absorption bands arise from a single product, the dimer dication $\mathbf{IV_2^{2+}}$.

The cyclic voltammetric characteristics of **V** in CH_2Cl_2/0.05 M $[NBu_4][B(C_6F_5)_4]$ were very similar to those of the molybdenum analogue, with only slight shifts in potential being noted.[8] At a scan rate of 0.1 V s^{-1}, the chemically irreversible oxidation peak appeared at E_{pa} = –0.20 V and the irreversible cathodic product peak was found at E_{pc} = –0.81 V. More detailed work on this system was not pursued, owing to its apparent mechanistic similarity to $(\eta^5\text{-}C_5H_4PMePh_2)Mo(CO)_3$.

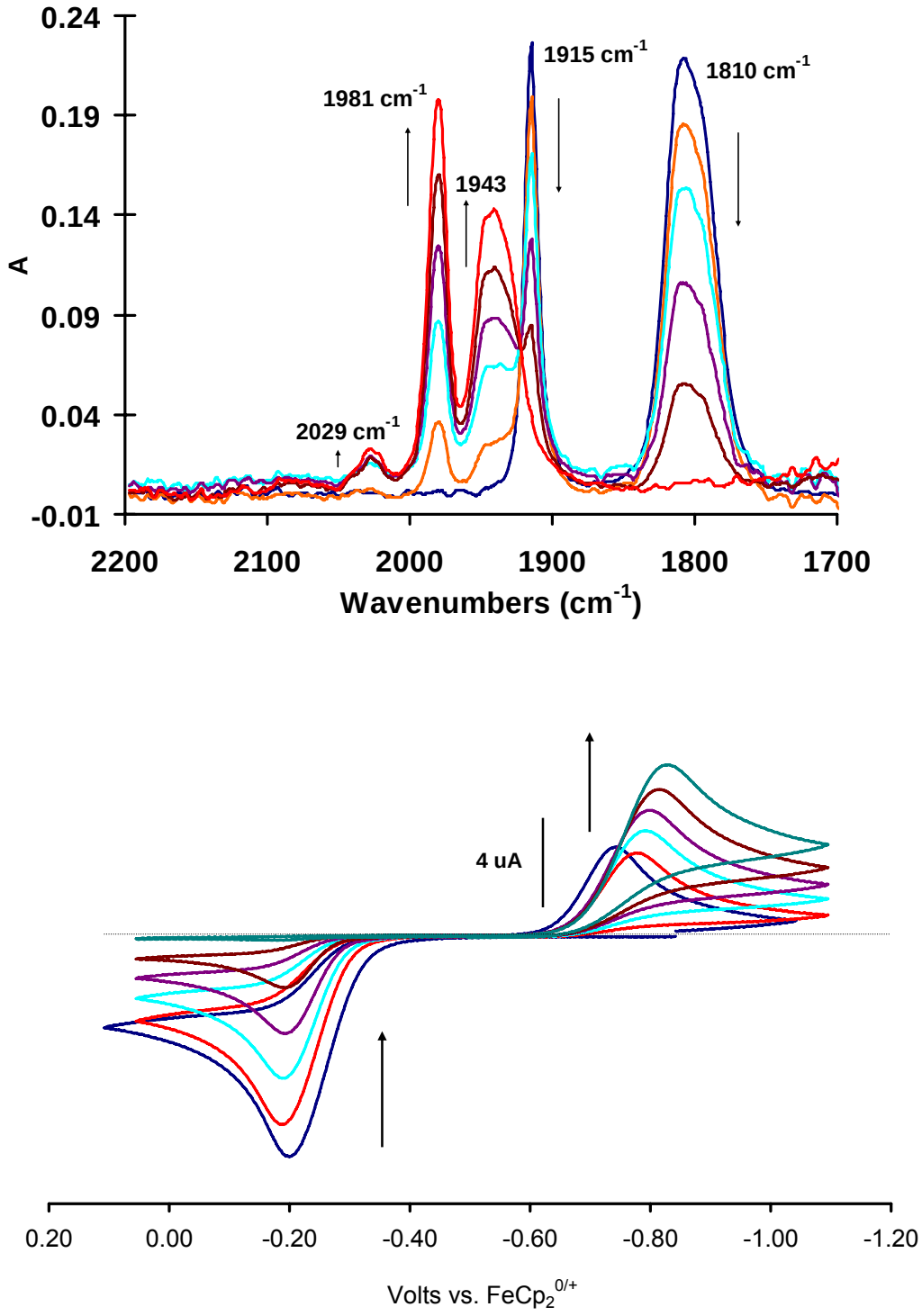

Figure 4. Spectroelectrochemical data for 3.0 mM (η^5-$C_5H_4PMePh_2$)$Mo(CO)_3$ in CH_2Cl_2/0.05 M $[NBu_4][B(C_6F_5)_4]$ at 298 K. Arrows indicate the increase or decrease in signal intensity as oxidation proceeds. CVs taken at v = 0.1 V s^{-1}.

As shown previously in this thesis, methyldiphenylphosphonium cyclopentadienylide is less electron donating than is the formally anionic η^5-cyclopentadienyl ligand. This accounts for the fact that compounds **III-V** oxidize at potentials that are considerably more positive than do their 18-electron analogues, $[(\eta^5\text{-}C_5H_5)M(CO)_3]^-$, for which $E_{1/2}$ values of –0.82 V,[9a] –0.75 V,[9b] and –0.85 V[9b] were observed for the chromium, molybdenum and tungsten complexes, respectively. The $PMePh_2$ group therefore stabilizes this family of 18-electron complexes against one-electron oxidation by 440-650 mV. The ligand electronic effect must be taken from the shift of 440 mV observed for the reversible processes of the Cr complexes. In the context of other acceptor substituents, this group has a greater electronic effect than a bromine atom, an aldehyde group, or a trifluoromethyl group (shifts of 170 mV, 280 mV and 320 mV, respectively), and about the same effect as the strongly electron-withdrawing perfluorophosphazine group, $N_3P_3F_5$.[10, 11] Put another way, the $PMePh_2$ group is at least as electron withdrawing as an amino group is electron donating, evidenced by the fact that the NH_2 substituent effect on a C_5H_4R ring is only –370 mV.[11,12]

Supplementary Material

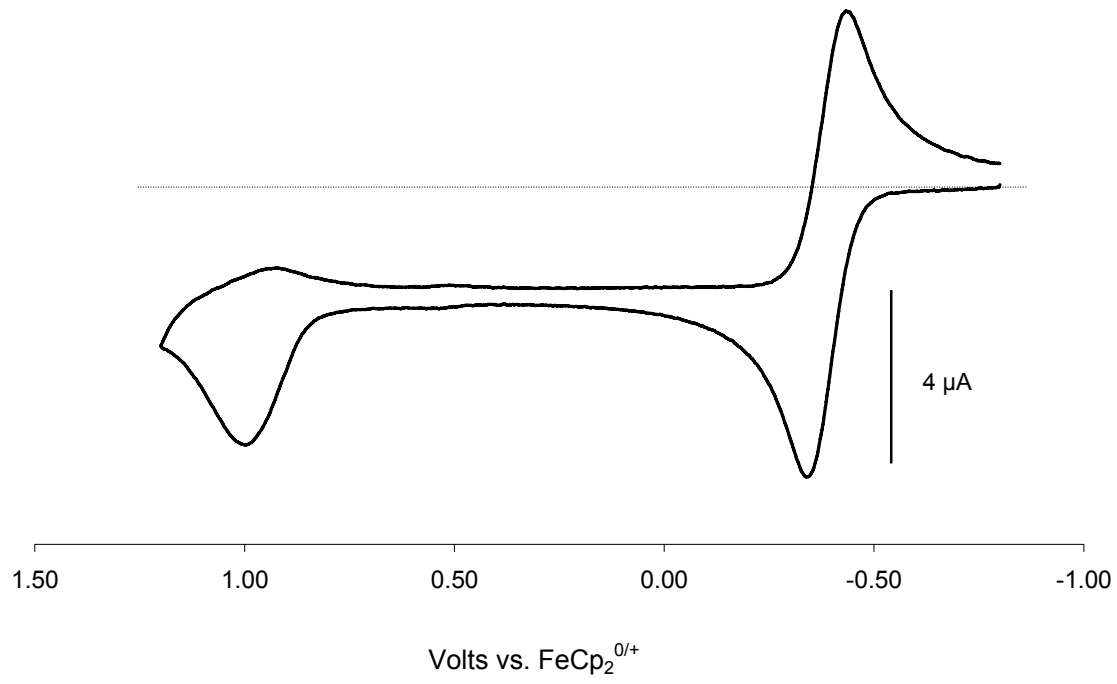

SM1. CV scan of 1.0 mM **III** at $v = 0.1$ V s^{-1} in CH_2Cl_2/0.1 M $[NBu_4][B(C_6F_5)_4]$.

References

1. LeSuer, R. J.; Buttolph, C.; Geiger, W. E. *Anal. Chem.* **2004**, *76*, 6395.
2. (a) Gritzner, G.; Kuta, J. *Pure Appl. Chem.* **1984**, *56*, 461 (b) Connelly, N. G.; Geiger, W. E. *Chem. Rev.* **1996**, *96*, 877.
3. LeSuer, R. J.; Geiger, W. E. *Angew. Chem. Int. Ed.* **2000**, *39*, 248.
4. Geiger, W. E. in *Laboratory Methods in Electroanalytical Chemistry*, 2nd ed.; Kissinger, P. T.; Heineman, W. E. (Eds); Marcel Dekker, Inc.; New York, 1996, Chapter 23.
5. Nafady, A.; Costa, P. J.; Calhorda, M. J.; Geiger, W. E. *J. Am. Chem. Soc.* **2006**, *128*, 16587.

6. Shifts of > 100 cm^{-1} are widely observed for ν_{CO} when the positive charge on a metal carbonyl complex is increased by one (Nakamoto, K. *Infrared and Raman Spectra of Inorganic and Coordination Compounds*, Wiley, New York, 1986, 4th ed., pp 292-293. For recent experimental and theoretical work showing that the origin of this effect is predominantly electrostatic, see (a) Goldman, A.S.; Krogh-Jespersen, K. *J. Am. Chem. Soc.* **1996**, *118*, 12159 (b) Willner, H.; Aubke, F. *Angew. Chem. Int. Ed.* **1997**, *36*, 2402 (c) Ehlers, A. W., Ruiz-Morales, Y.; Baerends, E. J.; Ziegler, T. *Inorg. Chem.* **1997,** *36*, 5031.

7. Chong, D.; Nafady, A.; Costa, P. J.; Calhorda, M. J.; Geiger, W. E. *J. Am. Chem. Soc.* **2005**, *127*, 15676 and references therein.

8. For both compounds **2** and **3**, a second irreversible anodic wave is observed at approximately E_{pa} = 1.40 V, apparently due to the oxidation of the respective dimer dications formed near the electrode surface.

9. (a) Richards, T.C.; Geiger, W.E.; Baird, M.C. *Organometallics* **1994**, *13*, 4494. (b) Kadish, K.M.; Lacombe, D.A.; Anderson, J.E. *Inorg. Chem.* **1986**, *25*, 2246. The potentials in this paper have been converted to the ferrocene reference potential by addition of 0.46 V.

10. Saraceno, R. A.; Riding, G. H.; Allcock, H. R.; Ewing, A. G. *J. Am. Chem. Soc.* **1988**, *110*, 980.

11. For a compilation of substituent effects on the redox potentials of cyclopentadienyl complexes see Lu, S.; Strelets, V. V.; Ryan, M. F.; Pietro, W. J.; Lever, A. B. P. *Inorg. Chem.* **1996**, *35*, 1013. Using the notation of this paper, the $PMePh_2$ group has an $E_L(L)$ value of 0.77 V [the $E_L(L)$ value of the cyclopentadienyl ligand is 0.33 V). For reference to the $C_5H_4CF_3$ ligand see Gassman, P.G.; Winter, C.H. *J. Am. Chem. Soc.* **1986**, *108*, 4228.

12. Britton, W. E.; Kashyap, R.; El-Hashash, M.; El-Kady, M.; Herberhold, M. *Organometallics* **1986**, *5*, 1029.

6 Appendix - Crystal Structure Data

Table 1. Crystal data and structure refinement for **II**.

Identification code	**II**	
Empirical formula	C18 H17 P	
Formula weight	264.29	
Temperature	180(2) K	
Wavelength	0.71073 Å	
Crystal system	Triclinic	
Space group	P-1	
Unit cell dimensions	a = 9.2856(8) Å	α= 89.602(2)°.
	b = 10.8254(9) Å	β= 83.260(2)°.
	c = 15.0721(13) Å	γ = 75.6430(10)°.
Volume	1457.2(2) $Å^3$	
Z	4	
Density (calculated)	1.205 Mg/m^3	
Absorption coefficient	0.172 mm^{-1}	
F(000)	560	
Crystal size	0.40 x 0.20 x 0.10 mm^3	
Theta range for data collection	2.28 to 25.00°.	
Index ranges	-10<=h<=11, -12<=k<=11, -17<=l<=17	
Reflections collected	8642	
Independent reflections	5090 [R(int) = 0.0171]	
Completeness to theta = 25.00°	99.5 %	
Absorption correction	Empirical (Bruker SADABS)	
Max. and min. transmission	1.0000 and 0.7520	
Refinement method	Full-matrix least-squares on F^2	
Data / restraints / parameters	5090 / 0 / 479	
Goodness-of-fit on F^2	1.001	
Final R indices [I>2sigma(I)]	R1 = 0.0362, wR2 = 0.0938	
R indices (all data)	R1 = 0.0495, wR2 = 0.0998	
Largest diff. peak and hole	0.312 and -0.298 e.$Å^{-3}$	

Table 2. Atomic coordinates (x 10^4) and equivalent isotropic displacement parameters ($Å^2$x 10^3) for **II**. U(eq) is defined as one third of the trace of the orthogonalized U^{ij} tensor.

	x	y	z	U(eq)
P(1)	-1663(1)	424(1)	-3130(1)	38(1)
P(2)	2446(1)	4919(1)	1177(1)	34(1)
C(1)	-2112(2)	1892(2)	-3623(1)	41(1)
C(2)	-3580(3)	2716(2)	-3610(2)	54(1)
C(3)	-3474(3)	3688(2)	-4185(2)	57(1)
C(4)	-1986(3)	3492(2)	-4572(1)	55(1)
C(5)	-1138(2)	2386(2)	-4241(1)	44(1)
C(6)	-2560(3)	488(2)	-2000(2)	55(1)
C(7)	329(2)	-96(1)	-3090(1)	37(1)
C(8)	999(3)	570(2)	-2536(1)	51(1)
C(9)	2523(3)	188(2)	-2492(2)	60(1)
C(10)	3398(3)	-835(2)	-3000(2)	54(1)
C(11)	2755(2)	-1490(2)	-3553(1)	47(1)
C(12)	1226(2)	-1120(2)	-3599(1)	40(1)
C(13)	-2241(2)	-792(1)	-3718(1)	35(1)
C(14)	-2062(2)	-2035(2)	-3403(1)	44(1)
C(15)	-2542(2)	-2923(2)	-3867(2)	48(1)
C(16)	-3202(2)	-2595(2)	-4634(1)	46(1)
C(17)	-3376(2)	-1377(2)	-4955(1)	46(1)
C(18)	-2892(2)	-484(2)	-4497(1)	41(1)
C(19)	2971(2)	3706(1)	376(1)	34(1)
C(20)	2973(2)	3867(2)	-555(1)	37(1)
C(21)	3516(2)	2682(2)	-977(2)	45(1)
C(22)	3857(2)	1768(2)	-316(2)	49(1)
C(23)	3523(2)	2372(2)	514(2)	42(1)
C(24)	3919(2)	4928(2)	1844(2)	48(1)
C(25)	821(2)	4820(1)	1928(1)	35(1)
C(26)	363(2)	5616(2)	2686(1)	48(1)

C(27)	-933(3)	5582(2)	3225(2)	59(1)
C(28)	-1776(3)	4756(2)	3017(2)	58(1)
C(29)	-1324(2)	3954(2)	2278(1)	46(1)
C(30)	-29(2)	3986(2)	1733(1)	38(1)
C(31)	1950(2)	6416(1)	619(1)	32(1)
C(32)	3056(2)	6916(2)	152(1)	38(1)
C(33)	2650(2)	7980(2)	-357(1)	43(1)
C(34)	1160(2)	8563(2)	-401(1)	43(1)
C(35)	67(2)	8091(2)	76(1)	42(1)
C(36)	447(2)	7019(2)	582(1)	36(1)

Table 3. Bond lengths [Å] and angles [°] for **II**.

P(1)-C(1)	1.7268(17)	C(1)-P(1)-C(6)	111.43(10)	C(30)-C(25)-C(26)	119.38(17)
P(1)-C(6)	1.800(2)	C(1)-P(1)-C(7)	110.39(8)	C(30)-C(25)-P(2)	119.97(13)
P(1)-C(7)	1.8033(18)	C(6)-P(1)-C(7)	107.40(11)	C(26)-C(25)-P(2)	120.59(13)
P(1)-C(13)	1.8125(17)	C(1)-P(1)-C(13)	112.51(8)	C(27)-C(26)-C(25)	119.86(19)
P(2)-C(19)	1.7274(17)	C(6)-P(1)-C(13)	106.50(10)	C(26)-C(27)-C(28)	120.1(2)
P(2)-C(24)	1.793(2)	C(7)-P(1)-C(13)	108.38(7)	C(29)-C(28)-C(27)	120.5(2)
P(2)-C(31)	1.8014(16)	C(19)-P(2)-C(24)	111.79(10)	C(28)-C(29)-C(30)	119.66(19)
P(2)-C(25)	1.8023(17)	C(19)-P(2)-C(31)	108.37(8)	C(29)-C(30)-C(25)	120.46(18)
C(1)-C(5)	1.416(3)	C(24)-P(2)-C(31)	109.66(9)	C(32)-C(31)-C(36)	119.44(15)
C(1)-C(2)	1.430(3)	C(19)-P(2)-C(25)	112.97(8)	C(32)-C(31)-P(2)	120.47(13)
C(2)-C(3)	1.374(3)	C(24)-P(2)-C(25)	107.36(10)	C(36)-C(31)-P(2)	119.80(12)
C(3)-C(4)	1.400(3)	C(31)-P(2)-C(25)	106.53(7)	C(33)-C(32)-C(31)	119.65(17)
C(4)-C(5)	1.384(3)	C(5)-C(1)-C(2)	107.52(17)	C(32)-C(33)-C(34)	120.62(18)
C(7)-C(12)	1.384(2)	C(5)-C(1)-P(1)	125.48(14)	C(35)-C(34)-C(33)	119.89(18)
C(7)-C(8)	1.399(3)	C(2)-C(1)-P(1)	126.14(15)	C(34)-C(35)-C(36)	120.48(17)
C(8)-C(9)	1.381(3)	C(3)-C(2)-C(1)	107.4(2)	C(35)-C(36)-C(31)	119.89(17)
C(9)-C(10)	1.375(3)	C(2)-C(3)-C(4)	108.9(2)		
C(10)-C(11)	1.375(3)	C(5)-C(4)-C(3)	109.01(19)		
C(11)-C(12)	1.386(3)	C(4)-C(5)-C(1)	107.20(19)		
C(13)-C(18)	1.384(3)	C(12)-C(7)-C(8)	118.67(17)		
C(13)-C(14)	1.400(2)	C(12)-C(7)-P(1)	122.30(13)		
C(14)-C(15)	1.381(3)	C(8)-C(7)-P(1)	119.02(14)		
C(15)-C(16)	1.376(3)	C(9)-C(8)-C(7)	120.0(2)		
C(16)-C(17)	1.379(3)	C(10)-C(9)-C(8)	120.6(2)		
C(17)-C(18)	1.382(3)	C(11)-C(10)-C(9)	119.9(2)		
C(19)-C(20)	1.413(2)	C(10)-C(11)-C(12)	120.0(2)		
C(19)-C(23)	1.430(2)	C(7)-C(12)-C(11)	120.72(18)		
C(20)-C(21)	1.384(2)	C(18)-C(13)-C(14)	118.89(16)		
C(21)-C(22)	1.406(3)	C(18)-C(13)-P(1)	119.19(12)		
C(22)-C(23)	1.382(3)	C(14)-C(13)-P(1)	121.92(14)		
C(25)-C(30)	1.392(2)	C(15)-C(14)-C(13)	119.82(19)		
C(25)-C(26)	1.395(2)	C(16)-C(15)-C(14)	120.49(17)		
C(26)-C(27)	1.378(3)	C(15)-C(16)-C(17)	120.25(19)		
C(27)-C(28)	1.385(3)	C(16)-C(17)-C(18)	119.64(19)		
C(28)-C(29)	1.377(3)	C(17)-C(18)-C(13)	120.91(17)		
C(29)-C(30)	1.382(3)	C(20)-C(19)-C(23)	107.00(16)		
C(31)-C(32)	1.394(2)	C(20)-C(19)-P(2)	125.53(12)		
C(31)-C(36)	1.395(2)	C(23)-C(19)-P(2)	127.44(15)		
C(32)-C(33)	1.378(2)	C(21)-C(20)-C(19)	108.46(16)		

C(33)-C(34)	1.380(3)	C(20)-C(21)-C(22)	108.02(18)
C(34)-C(35)	1.375(3)	C(23)-C(22)-C(21)	109.07(16)
C(35)-C(36)	1.378(2)	C(22)-C(23)-C(19)	107.44(18)
		C(30)-C(25)-C(26)	119.38(17)
		C(30)-C(25)-P(2)	119.97(13)
		C(26)-C(25)-P(2)	120.59(13)
		C(27)-C(26)-C(25)	119.86(19)
		C(26)-C(27)-C(28)	120.1(2)
		C(29)-C(28)-C(27)	120.5(2)
		C(28)-C(29)-C(30)	119.66(19)
		C(29)-C(30)-C(25)	120.46(18)
		C(32)-C(31)-C(36)	119.44(15)
		C(32)-C(31)-P(2)	120.47(13)
		C(36)-C(31)-P(2)	119.80(12)
		C(33)-C(32)-C(31)	119.65(17)
		C(32)-C(33)-C(34)	120.62(18)
		C(35)-C(34)-C(33)	119.89(18)
		C(34)-C(35)-C(36)	120.48(17)
		C(35)-C(36)-C(31)	119.89(17)

Table 4. Anisotropic displacement parameters ($Å^2 x\ 10^3$) for **II**. The anisotropic displacement factor exponent takes the form: $-2\pi^2[h^2 a^{*2} U^{11} + ... + 2 h k a^* b^* U^{12}]$

	U^{11}	U^{22}	U^{33}	U^{23}	U^{13}	U^{12}
P(1)	43(1)	32(1)	36(1)	-1(1)	3(1)	-8(1)
P(2)	33(1)	35(1)	34(1)	1(1)	-1(1)	-12(1)
C(1)	50(1)	30(1)	42(1)	-2(1)	-2(1)	-9(1)
C(2)	56(1)	39(1)	62(2)	-4(1)	-3(1)	-6(1)
C(3)	75(2)	36(1)	56(1)	-1(1)	-20(1)	-2(1)
C(4)	92(2)	38(1)	39(1)	2(1)	-11(1)	-22(1)
C(5)	62(1)	35(1)	38(1)	-5(1)	-4(1)	-15(1)
C(6)	61(2)	52(1)	45(1)	-1(1)	11(1)	-12(1)
C(7)	47(1)	34(1)	31(1)	3(1)	-3(1)	-14(1)
C(8)	65(1)	43(1)	47(1)	-7(1)	-9(1)	-15(1)
C(9)	68(2)	65(1)	61(2)	2(1)	-24(1)	-34(1)
C(10)	47(1)	59(1)	60(2)	13(1)	-11(1)	-21(1)
C(11)	43(1)	47(1)	52(1)	2(1)	2(1)	-15(1)
C(12)	44(1)	41(1)	38(1)	-2(1)	-2(1)	-16(1)
C(13)	32(1)	34(1)	38(1)	1(1)	1(1)	-7(1)
C(14)	44(1)	37(1)	50(1)	8(1)	-9(1)	-10(1)
C(15)	50(1)	34(1)	61(1)	6(1)	-5(1)	-14(1)
C(16)	40(1)	45(1)	54(1)	-8(1)	1(1)	-16(1)
C(17)	42(1)	51(1)	43(1)	0(1)	-6(1)	-8(1)
C(18)	41(1)	34(1)	44(1)	5(1)	0(1)	-7(1)
C(19)	28(1)	34(1)	40(1)	1(1)	2(1)	-9(1)
C(20)	29(1)	38(1)	43(1)	-1(1)	-2(1)	-9(1)
C(21)	38(1)	50(1)	47(1)	-13(1)	3(1)	-13(1)
C(22)	36(1)	35(1)	75(2)	-10(1)	6(1)	-10(1)
C(23)	33(1)	37(1)	55(1)	6(1)	2(1)	-9(1)
C(24)	45(1)	55(1)	48(1)	3(1)	-10(1)	-19(1)
C(25)	37(1)	37(1)	31(1)	5(1)	-1(1)	-11(1)
C(26)	59(1)	49(1)	38(1)	-5(1)	5(1)	-22(1)
C(27)	68(2)	65(1)	41(1)	-9(1)	16(1)	-21(1)
C(28)	49(1)	78(1)	45(1)	11(1)	11(1)	-20(1)
C(29)	45(1)	58(1)	41(1)	12(1)	-5(1)	-23(1)
C(30)	40(1)	42(1)	33(1)	5(1)	-4(1)	-13(1)
C(31)	34(1)	31(1)	31(1)	-3(1)	0(1)	-10(1)
C(32)	31(1)	37(1)	45(1)	0(1)	0(1)	-9(1)
C(33)	41(1)	40(1)	48(1)	5(1)	3(1)	-15(1)
C(34)	46(1)	33(1)	49(1)	2(1)	-6(1)	-9(1)

C(35)	34(1)	38(1)	52(1)	-5(1)	-7(1)	-5(1)
C(36)	32(1)	37(1)	40(1)	-5(1)	-1(1)	-12(1)

Table 5. Hydrogen coordinates (x 10^4) and isotropic displacement parameters ($Å^2$x 10^3) for **II**.

	x	y	z	U(eq)
H(2)	-4480(20)	2594(17)	-3272(14)	56(6)
H(3)	-4290(20)	4381(18)	-4307(13)	54(6)
H(4)	-1560(20)	3984(18)	-4979(14)	55(6)
H(5)	-70(20)	2028(16)	-4367(13)	46(5)
H(6A)	-2340(20)	-320(20)	-1756(14)	61(6)
H(6B)	-2200(20)	1100(20)	-1634(15)	74(7)
H(6C)	-3560(30)	770(20)	-2038(15)	69(7)
H(8)	380(20)	1254(18)	-2192(13)	55(6)
H(9)	2970(20)	607(18)	-2121(15)	68(7)
H(10)	4410(20)	-1101(17)	-2937(13)	55(6)
H(11)	3350(20)	-2175(17)	-3913(13)	49(5)
H(12)	806(19)	-1591(15)	-3982(13)	44(5)
H(14)	-1620(20)	-2242(16)	-2857(13)	47(5)
H(15)	-2420(20)	-3727(18)	-3675(13)	54(5)
H(16)	-3540(20)	-3204(18)	-4948(14)	61(6)
H(17)	-3820(20)	-1157(17)	-5495(14)	54(6)
H(18)	-2992(19)	316(16)	-4695(12)	46(5)
H(20)	2638(18)	4637(15)	-822(11)	36(5)
H(21)	3650(20)	2547(16)	-1638(14)	49(5)
H(22)	4270(20)	871(17)	-425(13)	57(6)
H(23)	3641(19)	2023(16)	1111(13)	44(5)
H(24A)	3540(20)	5571(18)	2323(14)	53(6)
H(24B)	4250(20)	4080(20)	2086(14)	68(6)
H(24C)	4720(30)	5156(19)	1458(16)	76(7)
H(26)	930(20)	6212(16)	2839(12)	48(5)
H(27)	-1180(20)	6134(18)	3759(15)	64(6)
H(28)	-2610(20)	4723(17)	3383(14)	55(6)
H(29)	-1910(20)	3369(18)	2127(14)	61(6)
H(30)	290(19)	3451(15)	1218(12)	39(5)
H(32)	4050(20)	6520(15)	183(12)	40(5)
H(33)	3380(20)	8255(16)	-685(13)	51(6)
H(34)	910(20)	9307(17)	-757(13)	50(5)
H(35)	-910(20)	8437(17)	54(13)	50(5)
H(36)	-317(19)	6699(15)	894(12)	40(5)

Table 6. Torsion angles [°] for **II**.

C(6)-P(1)-C(1)-C(5)	144.79(17)	C(24)-P(2)-C(19)-C(20)	-122.40(16)
C(7)-P(1)-C(1)-C(5)	25.54(19)	C(31)-P(2)-C(19)-C(20)	-1.42(17)
C(13)-P(1)-C(1)-C(5)	-95.68(17)	C(25)-P(2)-C(19)-C(20)	116.38(15)
C(6)-P(1)-C(1)-C(2)	-47.2(2)	C(24)-P(2)-C(19)-C(23)	55.51(18)
C(7)-P(1)-C(1)-C(2)	-166.41(16)	C(31)-P(2)-C(19)-C(23)	176.48(14)
C(13)-P(1)-C(1)-C(2)	72.37(19)	C(25)-P(2)-C(19)-C(23)	-65.72(17)
C(5)-C(1)-C(2)-C(3)	-1.4(2)	C(23)-C(19)-C(20)-C(21)	-0.47(19)
P(1)-C(1)-C(2)-C(3)	-171.24(15)	P(2)-C(19)-C(20)-C(21)	177.79(12)
C(1)-C(2)-C(3)-C(4)	0.8(2)	C(19)-C(20)-C(21)-C(22)	0.1(2)
C(2)-C(3)-C(4)-C(5)	0.1(2)	C(20)-C(21)-C(22)-C(23)	0.3(2)
C(3)-C(4)-C(5)-C(1)	-1.0(2)	C(21)-C(22)-C(23)-C(19)	-0.6(2)
C(2)-C(1)-C(5)-C(4)	1.5(2)	C(20)-C(19)-C(23)-C(22)	0.66(19)
P(1)-C(1)-C(5)-C(4)	171.38(14)	P(2)-C(19)-C(23)-C(22)	-177.55(13)
C(1)-P(1)-C(7)-C(12)	-111.37(15)	C(19)-P(2)-C(25)-C(30)	-11.70(16)
C(6)-P(1)-C(7)-C(12)	126.96(16)	C(24)-P(2)-C(25)-C(30)	-135.41(15)
C(13)-P(1)-C(7)-C(12)	12.26(17)	C(31)-P(2)-C(25)-C(30)	107.17(14)
C(1)-P(1)-C(7)-C(8)	67.57(17)	C(19)-P(2)-C(25)-C(26)	171.30(14)
C(6)-P(1)-C(7)-C(8)	-54.10(17)	C(24)-P(2)-C(25)-C(26)	47.59(17)

C(13)-P(1)-C(7)-C(8)	-168.80(14)	C(31)-P(2)-C(25)-C(26)	-69.83(16)
C(12)-C(7)-C(8)-C(9)	-1.2(3)	C(30)-C(25)-C(26)-C(27)	-0.9(3)
P(1)-C(7)-C(8)-C(9)	179.85(16)	P(2)-C(25)-C(26)-C(27)	176.11(16)
C(7)-C(8)-C(9)-C(10)	1.0(3)	C(25)-C(26)-C(27)-C(28)	0.3(3)
C(8)-C(9)-C(10)-C(11)	-0.4(3)	C(26)-C(27)-C(28)-C(29)	0.6(3)
C(9)-C(10)-C(11)-C(12)	0.0(3)	C(27)-C(28)-C(29)-C(30)	-0.8(3)
C(8)-C(7)-C(12)-C(11)	0.8(3)	C(28)-C(29)-C(30)-C(25)	0.2(3)
P(1)-C(7)-C(12)-C(11)	179.75(14)	C(26)-C(25)-C(30)-C(29)	0.7(3)
C(10)-C(11)-C(12)-C(7)	-0.2(3)	P(2)-C(25)-C(30)-C(29)	-176.35(14)
C(1)-P(1)-C(13)-C(18)	3.09(17)	C(19)-P(2)-C(31)-C(32)	-73.10(16)
C(6)-P(1)-C(13)-C(18)	125.45(16)	C(24)-P(2)-C(31)-C(32)	49.18(17)
C(7)-P(1)-C(13)-C(18)	-119.26(14)	C(25)-P(2)-C(31)-C(32)	165.06(14)
C(1)-P(1)-C(13)-C(14)	-176.34(14)	C(19)-P(2)-C(31)-C(36)	100.74(14)
C(6)-P(1)-C(13)-C(14)	-53.98(18)	C(24)-P(2)-C(31)-C(36)	-136.97(15)
C(7)-P(1)-C(13)-C(14)	61.31(16)	C(25)-P(2)-C(31)-C(36)	-21.10(15)
C(18)-C(13)-C(14)-C(15)	-0.5(3)	C(36)-C(31)-C(32)-C(33)	-1.5(3)
P(1)-C(13)-C(14)-C(15)	178.96(15)	P(2)-C(31)-C(32)-C(33)	172.33(13)
C(13)-C(14)-C(15)-C(16)	-0.3(3)	C(31)-C(32)-C(33)-C(34)	0.7(3)
C(14)-C(15)-C(16)-C(17)	0.8(3)	C(32)-C(33)-C(34)-C(35)	0.8(3)
C(15)-C(16)-C(17)-C(18)	-0.5(3)	C(33)-C(34)-C(35)-C(36)	-1.5(3)
C(16)-C(17)-C(18)-C(13)	-0.3(3)	C(34)-C(35)-C(36)-C(31)	0.7(3)
C(14)-C(13)-C(18)-C(17)	0.8(3)	C(32)-C(31)-C(36)-C(35)	0.8(2)
P(1)-C(13)-C(18)-C(17)	-178.66(14)	P(2)-C(31)-C(36)-C(35)	-173.08(13)

Figure 1. Molecular structure of **II**.

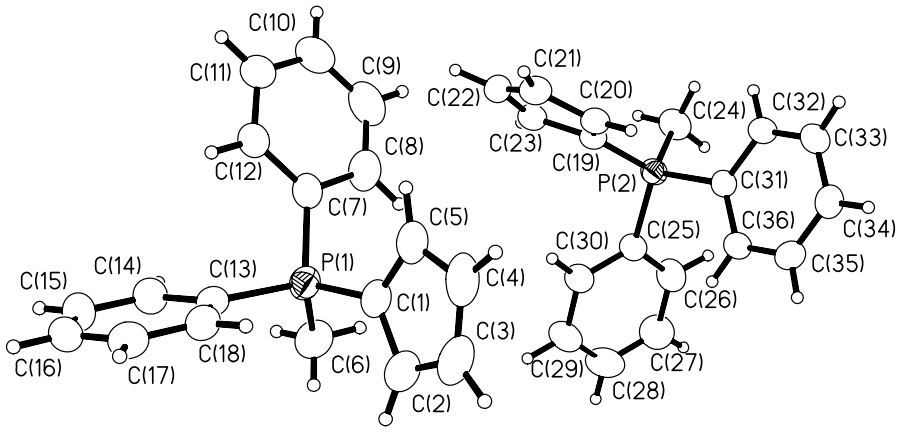

Table 7. Crystal data and structure refinement for **III**.

Identification code	**III**	
Empirical formula	C21 H17 Cr O3 P	
Formula weight	400.32	
Temperature	180(2) K	
Wavelength	0.71073 Å	
Crystal system	Monoclinic	
Space group	P2(1)/c	
Unit cell dimensions	a = 9.738(2) Å	α= 90°.
	b = 14.410(3) Å	β= 108.742(4)°.
	c = 13.927(3) Å	γ = 90°.
Volume	1850.8(6) $Å^3$	
Z	4	

Density (calculated)	1.437 Mg/m^3
Absorption coefficient	0.722 mm^{-1}
F(000)	824
Crystal size	0.30 x 0.15 x 0.05 mm^3
Theta range for data collection	2.09 to 25.00°.
Index ranges	-11<=h<=10, -17<=k<=15, -16<=l<=16
Reflections collected	10657
Independent reflections	3263 [R(int) = 0.0373]
Completeness to theta = 25.00°	100.0 %
Absorption correction	Empirical (Bruker SADABS)
Max. and min. transmission	1.0000 and 0.8567
Refinement method	Full-matrix least-squares on F^2
Data / restraints / parameters	3263 / 0 / 303
Goodness-of-fit on F^2	1.001
Final R indices [I>2sigma(I)]	R1 = 0.0370, wR2 = 0.0614
R indices (all data)	R1 = 0.0611, wR2 = 0.0651
Largest diff. peak and hole	0.470 and -0.330 e.$Å^{-3}$

Table 8. Atomic coordinates (x 10^4) and equivalent isotropic displacement parameters ($Å^2$x 10^3) for **III**. U(eq) is defined as one third of the trace of the orthogonalized U^{ij} tensor.

	x	y	z	U(eq)
P(1)	-1335(1)	1740(1)	1962(1)	26(1)
Cr(1)	1970(1)	1851(1)	3902(1)	29(1)
O(1)	1586(2)	3888(2)	4069(2)	58(1)
O(2)	356(2)	1503(1)	5359(1)	49(1)
O(3)	4641(2)	1888(1)	5710(1)	46(1)
C(1)	1748(3)	3088(2)	4011(2)	39(1)
C(2)	973(3)	1641(2)	4776(2)	32(1)
C(3)	3596(3)	1889(2)	4988(2)	34(1)
C(4)	506(3)	1428(2)	2419(2)	27(1)
C(5)	1692(3)	1917(2)	2271(2)	35(1)
C(6)	2956(3)	1426(2)	2733(2)	38(1)
C(7)	2591(3)	624(2)	3179(2)	36(1)
C(8)	1102(3)	618(2)	2991(2)	31(1)
C(9)	-2263(3)	1233(2)	2752(2)	25(1)
C(10)	-2519(3)	286(2)	2697(2)	33(1)
C(11)	-3134(3)	-138(2)	3342(2)	38(1)
C(12)	-3504(3)	391(3)	4054(2)	42(1)
C(13)	-3273(3)	1330(2)	4112(2)	38(1)
C(14)	-2644(3)	1758(2)	3462(2)	33(1)
C(15)	-2160(3)	1292(2)	702(2)	26(1)
C(16)	-3659(3)	1254(2)	292(2)	34(1)
C(17)	-4303(4)	925(2)	-679(2)	42(1)
C(18)	-3450(4)	615(2)	-1236(2)	40(1)
C(19)	-1970(3)	654(2)	-838(2)	34(1)
C(20)	-1319(3)	998(2)	123(2)	30(1)
C(21)	-1548(4)	2972(2)	1917(2)	31(1)

Table 9. Bond lengths [Å] and angles [°] for **III**.

P(1)-C(4)	1.758(3)	C(4)-P(1)-C(21)	111.12(14)	O(3)-C(3)-Cr(1)	177.8(2)
P(1)-C(21)	1.786(3)	C(4)-P(1)-C(9)	109.35(12)	C(5)-C(4)-C(8)	106.4(3)
P(1)-C(9)	1.789(2)	C(21)-P(1)-C(9)	110.57(14)	C(5)-C(4)-P(1)	127.0(2)
P(1)-C(15)	1.799(2)	C(4)-P(1)-C(15)	110.19(12)	C(8)-C(4)-P(1)	126.5(2)
Cr(1)-C(3)	1.805(3)	C(21)-P(1)-C(15)	108.18(13)	C(5)-C(4)-Cr(1)	71.69(15)
Cr(1)-C(1)	1.808(3)	C(9)-P(1)-C(15)	107.35(12)	C(8)-C(4)-Cr(1)	71.08(15)
Cr(1)-C(2)	1.809(3)	C(3)-Cr(1)-C(1)	89.79(13)	P(1)-C(4)-Cr(1)	123.38(13)
Cr(1)-C(4)	2.186(2)	C(3)-Cr(1)-C(2)	87.56(11)	C(6)-C(5)-C(4)	108.8(3)
Cr(1)-C(8)	2.189(3)	C(1)-Cr(1)-C(2)	90.25(12)	C(6)-C(5)-Cr(1)	72.70(16)
Cr(1)-C(5)	2.202(3)	C(3)-Cr(1)-C(4)	158.47(11)	C(4)-C(5)-Cr(1)	70.48(14)
Cr(1)-C(7)	2.212(3)	C(1)-Cr(1)-C(4)	107.13(11)	C(5)-C(6)-C(7)	108.1(3)
Cr(1)-C(6)	2.226(3)	C(2)-Cr(1)-C(4)	105.17(11)	C(5)-C(6)-Cr(1)	70.83(16)

O(1)-C(1)	1.170(3)	C(3)-Cr(1)-C(8)	125.58(12)	C(7)-C(6)-Cr(1)	70.95(17)
O(2)-C(2)	1.172(3)	C(1)-Cr(1)-C(8)	144.52(12)	C(8)-C(7)-C(6)	108.6(3)
O(3)-C(3)	1.179(3)	C(2)-Cr(1)-C(8)	93.67(12)	C(8)-C(7)-Cr(1)	70.72(17)
C(4)-C(5)	1.423(4)	C(4)-Cr(1)-C(8)	38.07(9)	C(6)-C(7)-Cr(1)	72.00(18)
C(4)-C(8)	1.427(4)	C(3)-Cr(1)-C(5)	130.30(11)	C(7)-C(8)-C(4)	108.2(3)
C(5)-C(6)	1.386(4)	C(1)-Cr(1)-C(5)	93.74(12)	C(7)-C(8)-Cr(1)	72.52(18)
C(6)-C(7)	1.410(4)	C(2)-Cr(1)-C(5)	141.87(11)	C(4)-C(8)-Cr(1)	70.85(16)
C(7)-C(8)	1.388(4)	C(4)-Cr(1)-C(5)	37.83(10)	C(10)-C(9)-C(14)	119.6(3)
C(9)-C(10)	1.385(4)	C(8)-Cr(1)-C(5)	62.62(12)	C(10)-C(9)-P(1)	119.0(2)
C(9)-C(14)	1.386(3)	C(3)-Cr(1)-C(7)	96.38(12)	C(14)-C(9)-P(1)	121.2(2)
C(10)-C(11)	1.374(4)	C(1)-Cr(1)-C(7)	152.02(12)	C(11)-C(10)-C(9)	120.6(3)
C(11)-C(12)	1.386(4)	C(2)-Cr(1)-C(7)	117.20(12)	C(10)-C(11)-C(12)	119.5(3)
C(12)-C(13)	1.371(4)	C(4)-Cr(1)-C(7)	62.46(10)	C(13)-C(12)-C(11)	120.6(3)
C(13)-C(14)	1.389(4)	C(8)-Cr(1)-C(7)	36.76(10)	C(12)-C(13)-C(14)	119.9(3)
C(15)-C(16)	1.387(4)	C(5)-Cr(1)-C(7)	61.68(12)	C(9)-C(14)-C(13)	119.8(3)
C(15)-C(20)	1.387(3)	C(3)-Cr(1)-C(6)	98.77(11)	C(16)-C(15)-C(20)	119.3(3)
C(16)-C(17)	1.380(4)	C(1)-Cr(1)-C(6)	115.05(12)	C(16)-C(15)-P(1)	119.8(2)
C(17)-C(18)	1.380(4)	C(2)-Cr(1)-C(6)	153.77(13)	C(20)-C(15)-P(1)	121.0(2)
C(18)-C(19)	1.369(4)	C(4)-Cr(1)-C(6)	62.31(10)	C(17)-C(16)-C(15)	120.2(3)
C(19)-C(20)	1.377(4)	C(8)-Cr(1)-C(6)	61.94(12)	C(16)-C(17)-C(18)	119.8(3)
		C(5)-Cr(1)-C(6)	36.48(10)	C(19)-C(18)-C(17)	120.3(3)
		C(7)-Cr(1)-C(6)	37.05(11)	C(18)-C(19)-C(20)	120.3(3)
		O(1)-C(1)-Cr(1)	179.0(3)	C(19)-C(20)-C(15)	120.1(3)
		O(2)-C(2)-Cr(1)	178.5(2)		

Table 10. Anisotropic displacement parameters ($Å^2 x\ 10^3$) for **III**. The anisotropic displacement factor exponent takes the form: $-2\pi^2[\ h^2\ a^{*2}U^{11} + ...\ + 2\ h\ k\ a^*\ b^*\ U^{12}\ ]$

	U^{11}	U^{22}	U^{33}	U^{23}	U^{13}	U^{12}
P(1)	27(1)	29(1)	23(1)	-1(1)	9(1)	0(1)
Cr(1)	29(1)	34(1)	25(1)	-3(1)	9(1)	-2(1)
O(1)	76(2)	33(1)	70(2)	-5(1)	30(1)	-3(1)
O(2)	39(1)	78(2)	35(1)	-4(1)	19(1)	-4(1)
O(3)	37(1)	62(2)	34(1)	4(1)	2(1)	-19(1)
C(1)	42(2)	43(2)	33(2)	-3(2)	13(1)	-6(2)
C(2)	28(2)	39(2)	26(1)	-7(1)	2(1)	-2(2)
C(3)	38(2)	36(2)	31(2)	-1(1)	17(1)	-10(2)
C(4)	26(2)	34(2)	19(1)	-4(1)	6(1)	0(1)
C(5)	36(2)	44(2)	25(2)	3(2)	11(1)	0(2)
C(6)	24(2)	63(2)	29(2)	-4(2)	10(2)	2(2)
C(7)	34(2)	42(2)	27(2)	-5(2)	4(2)	14(2)
C(8)	34(2)	31(2)	28(2)	-7(1)	8(1)	-1(2)
C(9)	22(2)	31(2)	21(1)	0(1)	6(1)	-2(1)
C(10)	34(2)	36(2)	29(2)	-2(2)	11(1)	-1(2)
C(11)	36(2)	36(2)	40(2)	9(2)	10(2)	-4(2)
C(12)	28(2)	68(3)	31(2)	15(2)	8(2)	-5(2)
C(13)	30(2)	58(2)	30(2)	-6(2)	14(2)	1(2)
C(14)	29(2)	38(2)	31(2)	-6(2)	8(1)	-3(2)
C(15)	28(2)	23(2)	25(1)	3(1)	7(1)	2(1)
C(16)	32(2)	39(2)	34(2)	-5(1)	13(2)	4(2)
C(17)	25(2)	58(2)	37(2)	-12(2)	3(2)	-4(2)
C(18)	46(2)	41(2)	27(2)	-8(2)	2(2)	-1(2)
C(19)	43(2)	34(2)	28(2)	1(1)	16(2)	11(2)
C(20)	26(2)	32(2)	30(2)	5(1)	7(2)	6(2)
C(21)	31(2)	32(2)	32(2)	-1(2)	12(2)	2(2)

Table 11. Hydrogen coordinates (x 10^4) and isotropic displacement parameters ($Å^2$x 10^3) for **III**.

	x	y	z	U(eq)
H(5)	1590(30)	2439(16)	1970(17)	24(8)
H(6)	3830(30)	1624(17)	2721(16)	30(8)
H(7)	3180(20)	195(15)	3525(15)	16(7)
H(8)	560(20)	209(16)	3185(15)	20(7)
H(10)	-2280(30)	-54(16)	2249(16)	27(7)
H(11)	-3300(30)	-768(17)	3321(17)	31(8)
H(12)	-3890(30)	108(18)	4480(19)	52(9)
H(13)	-3560(20)	1685(16)	4571(16)	29(7)
H(14)	-2480(30)	2380(16)	3504(16)	26(8)
H(16)	-4210(20)	1452(16)	645(16)	28(8)
H(17)	-5250(30)	881(17)	-903(17)	32(8)
H(18)	-3880(30)	373(17)	-1859(17)	36(8)
H(19)	-1400(20)	449(16)	-1165(15)	24(7)
H(20)	-370(20)	1036(14)	374(15)	9(6)
H(21A)	-2530(30)	3106(17)	1703(16)	29(7)
H(21B)	-1100(30)	3220(17)	2554(18)	32(7)
H(21C)	-1140(30)	3187(18)	1457(18)	41(8)

Table 12. Torsion angles [°] for **III**.

C(3)-Cr(1)-C(1)-O(1)	-179(100)	C(4)-Cr(1)-C(6)-C(5)	37.75(18)
C(2)-Cr(1)-C(1)-O(1)	-92(16)	C(8)-Cr(1)-C(6)-C(5)	81.1(2)
C(4)-Cr(1)-C(1)-O(1)	14(16)	C(7)-Cr(1)-C(6)-C(5)	117.9(3)
C(8)-Cr(1)-C(1)-O(1)	5(16)	C(3)-Cr(1)-C(6)-C(7)	88.98(19)
C(5)-Cr(1)-C(1)-O(1)	50(16)	C(1)-Cr(1)-C(6)-C(7)	-177.12(18)
C(7)-Cr(1)-C(1)-O(1)	77(16)	C(2)-Cr(1)-C(6)-C(7)	-13.5(3)
C(6)-Cr(1)-C(1)-O(1)	81(16)	C(4)-Cr(1)-C(6)-C(7)	-80.12(19)
C(3)-Cr(1)-C(2)-O(2)	-10(10)	C(8)-Cr(1)-C(6)-C(7)	-36.81(17)
C(1)-Cr(1)-C(2)-O(2)	-100(10)	C(5)-Cr(1)-C(6)-C(7)	-117.9(3)
C(4)-Cr(1)-C(2)-O(2)	152(10)	C(5)-C(6)-C(7)-C(8)	0.2(3)
C(8)-Cr(1)-C(2)-O(2)	115(10)	Cr(1)-C(6)-C(7)-C(8)	61.6(2)
C(5)-Cr(1)-C(2)-O(2)	164(10)	C(5)-C(6)-C(7)-Cr(1)	-61.4(2)
C(7)-Cr(1)-C(2)-O(2)	86(10)	C(3)-Cr(1)-C(7)-C(8)	145.94(18)
C(6)-Cr(1)-C(2)-O(2)	95(10)	C(1)-Cr(1)-C(7)-C(8)	-112.4(3)
C(1)-Cr(1)-C(3)-O(3)	133(7)	C(2)-Cr(1)-C(7)-C(8)	55.4(2)
C(2)-Cr(1)-C(3)-O(3)	43(7)	C(4)-Cr(1)-C(7)-C(8)	-38.24(17)
C(4)-Cr(1)-C(3)-O(3)	-85(7)	C(5)-Cr(1)-C(7)-C(8)	-81.29(19)
C(8)-Cr(1)-C(3)-O(3)	-50(7)	C(6)-Cr(1)-C(7)-C(8)	-117.9(3)
C(5)-Cr(1)-C(3)-O(3)	-132(7)	C(3)-Cr(1)-C(7)-C(6)	-96.12(19)
C(7)-Cr(1)-C(3)-O(3)	-74(7)	C(1)-Cr(1)-C(7)-C(6)	5.6(4)
C(6)-Cr(1)-C(3)-O(3)	-112(7)	C(2)-Cr(1)-C(7)-C(6)	173.36(17)
C(21)-P(1)-C(4)-C(5)	-33.2(3)	C(4)-Cr(1)-C(7)-C(6)	79.70(19)
C(9)-P(1)-C(4)-C(5)	-155.5(2)	C(8)-Cr(1)-C(7)-C(6)	117.9(3)
C(15)-P(1)-C(4)-C(5)	86.7(2)	C(5)-Cr(1)-C(7)-C(6)	36.65(17)
C(21)-P(1)-C(4)-C(8)	148.6(2)	C(6)-C(7)-C(8)-C(4)	-0.2(3)
C(9)-P(1)-C(4)-C(8)	26.3(3)	Cr(1)-C(7)-C(8)-C(4)	62.25(18)
C(15)-P(1)-C(4)-C(8)	-91.5(2)	C(6)-C(7)-C(8)-Cr(1)	-62.4(2)
C(21)-P(1)-C(4)-Cr(1)	58.3(2)	C(5)-C(4)-C(8)-C(7)	0.1(3)
C(9)-P(1)-C(4)-Cr(1)	-64.02(19)	P(1)-C(4)-C(8)-C(7)	178.65(19)
C(15)-P(1)-C(4)-Cr(1)	178.22(14)	Cr(1)-C(4)-C(8)-C(7)	-63.33(19)
C(3)-Cr(1)-C(4)-C(5)	-67.0(4)	C(5)-C(4)-C(8)-Cr(1)	63.43(18)
C(1)-Cr(1)-C(4)-C(5)	73.4(2)	P(1)-C(4)-C(8)-Cr(1)	-118.0(2)

C(2)-Cr(1)-C(4)-C(5)	168.46(19)	C(3)-Cr(1)-C(8)-C(7)	-43.2(2)
C(8)-Cr(1)-C(4)-C(5)	-115.3(2)	C(1)-Cr(1)-C(8)-C(7)	131.6(2)
C(7)-Cr(1)-C(4)-C(5)	-78.42(19)	C(2)-Cr(1)-C(8)-C(7)	-132.80(19)
C(6)-Cr(1)-C(4)-C(5)	-36.40(18)	C(4)-Cr(1)-C(8)-C(7)	117.1(3)
C(3)-Cr(1)-C(4)-C(8)	48.3(4)	C(5)-Cr(1)-C(8)-C(7)	78.50(19)
C(1)-Cr(1)-C(4)-C(8)	-171.26(17)	C(6)-Cr(1)-C(8)-C(7)	37.10(17)
C(2)-Cr(1)-C(4)-C(8)	-76.20(18)	C(3)-Cr(1)-C(8)-C(4)	-160.30(15)
C(5)-Cr(1)-C(4)-C(8)	115.3(2)	C(1)-Cr(1)-C(8)-C(4)	14.5(3)
C(7)-Cr(1)-C(4)-C(8)	36.93(17)	C(2)-Cr(1)-C(8)-C(4)	110.08(17)
C(6)-Cr(1)-C(4)-C(8)	78.95(18)	C(5)-Cr(1)-C(8)-C(4)	-38.62(16)
C(3)-Cr(1)-C(4)-P(1)	170.2(2)	C(7)-Cr(1)-C(8)-C(4)	-117.1(3)
C(1)-Cr(1)-C(4)-P(1)	-49.40(19)	C(6)-Cr(1)-C(8)-C(4)	-80.02(17)
C(2)-Cr(1)-C(4)-P(1)	45.66(19)	C(4)-P(1)-C(9)-C(10)	-72.5(2)
C(8)-Cr(1)-C(4)-P(1)	121.9(2)	C(21)-P(1)-C(9)-C(10)	164.8(2)
C(5)-Cr(1)-C(4)-P(1)	-122.8(3)	C(15)-P(1)-C(9)-C(10)	47.0(2)
C(7)-Cr(1)-C(4)-P(1)	158.8(2)	C(4)-P(1)-C(9)-C(14)	103.3(2)
C(6)-Cr(1)-C(4)-P(1)	-159.2(2)	C(21)-P(1)-C(9)-C(14)	-19.4(3)
C(8)-C(4)-C(5)-C(6)	0.0(3)	C(15)-P(1)-C(9)-C(14)	-137.2(2)
P(1)-C(4)-C(5)-C(6)	-178.53(19)	C(14)-C(9)-C(10)-C(11)	-0.5(4)
Cr(1)-C(4)-C(5)-C(6)	63.0(2)	P(1)-C(9)-C(10)-C(11)	175.3(2)
C(8)-C(4)-C(5)-Cr(1)	-63.03(17)	C(9)-C(10)-C(11)-C(12)	0.1(4)
P(1)-C(4)-C(5)-Cr(1)	118.4(2)	C(10)-C(11)-C(12)-C(13)	0.6(5)
C(3)-Cr(1)-C(5)-C(6)	35.8(3)	C(11)-C(12)-C(13)-C(14)	-0.9(5)
C(1)-Cr(1)-C(5)-C(6)	128.7(2)	C(10)-C(9)-C(14)-C(13)	0.2(4)
C(2)-Cr(1)-C(5)-C(6)	-136.1(2)	P(1)-C(9)-C(14)-C(13)	-175.5(2)
C(4)-Cr(1)-C(5)-C(6)	-117.9(3)	C(12)-C(13)-C(14)-C(9)	0.5(4)
C(8)-Cr(1)-C(5)-C(6)	-79.0(2)	C(4)-P(1)-C(15)-C(16)	164.2(2)
C(7)-Cr(1)-C(5)-C(6)	-37.23(19)	C(21)-P(1)-C(15)-C(16)	-74.1(3)
C(3)-Cr(1)-C(5)-C(4)	153.70(18)	C(9)-P(1)-C(15)-C(16)	45.2(3)
C(1)-Cr(1)-C(5)-C(4)	-113.40(19)	C(4)-P(1)-C(15)-C(20)	-17.0(3)
C(2)-Cr(1)-C(5)-C(4)	-18.2(3)	C(21)-P(1)-C(15)-C(20)	104.7(2)
C(8)-Cr(1)-C(5)-C(4)	38.87(16)	C(9)-P(1)-C(15)-C(20)	-136.0(2)
C(7)-Cr(1)-C(5)-C(4)	80.65(19)	C(20)-C(15)-C(16)-C(17)	0.1(4)
C(6)-Cr(1)-C(5)-C(4)	117.9(3)	P(1)-C(15)-C(16)-C(17)	179.0(2)
C(4)-C(5)-C(6)-C(7)	-0.1(3)	C(15)-C(16)-C(17)-C(18)	1.4(5)
Cr(1)-C(5)-C(6)-C(7)	61.5(2)	C(16)-C(17)-C(18)-C(19)	-1.7(5)
C(4)-C(5)-C(6)-Cr(1)	-61.62(18)	C(17)-C(18)-C(19)-C(20)	0.4(5)
C(3)-Cr(1)-C(6)-C(5)	-153.2(2)	C(18)-C(19)-C(20)-C(15)	1.2(4)
C(1)-Cr(1)-C(6)-C(5)	-59.3(2)	C(16)-C(15)-C(20)-C(19)	-1.4(4)
C(2)-Cr(1)-C(6)-C(5)	104.4(3)	P(1)-C(15)-C(20)-C(19)	179.7(2)

Figure 2. The molecular structure of **III**.

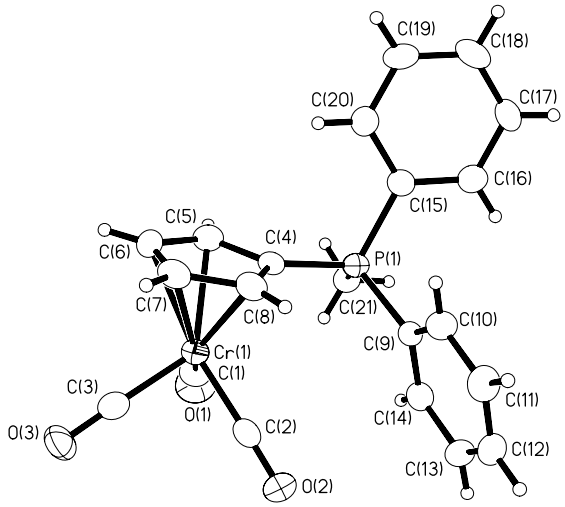

Table 13. Crystal data and structure refinement for **IV**.

Identification code	**IV**	
Empirical formula	C21 H17 Mo O3 P	
Formula weight	444.26	
Temperature	180(2) K	
Wavelength	0.71073 Å	
Crystal system	Monoclinic	
Space group	P2(1)/c	
Unit cell dimensions	a = 9.6728(7) Å	α= 90°.
	b = 14.5246(10) Å	β= 108.3930(10)°.
	c = 14.1801(10) Å	γ = 90°.
Volume	1890.4(2) $Å^3$	
Z	4	
Density (calculated)	1.561 Mg/m^3	
Absorption coefficient	0.795 mm^{-1}	
F(000)	896	
Crystal size	0.30 x 0.15 x 0.08 mm^3	
Theta range for data collection	2.06 to 25.00°.	
Index ranges	-11<=h<=11, -17<=k<=17, -15<=l<=16	
Reflections collected	10967	
Independent reflections	3334 [R(int) = 0.0283]	
Completeness to theta = 25.00°	100.0 %	
Absorption correction	Empirical (Bruker SADABS)	
Max. and min. transmission	1.0000 and 0.8555	
Refinement method	Full-matrix least-squares on F^2	
Data / restraints / parameters	3334 / 0 / 303	
Goodness-of-fit on F^2	1.000	
Final R indices [I>2sigma(I)]	R1 = 0.0248, wR2 = 0.0436	
R indices (all data)	R1 = 0.0379, wR2 = 0.0456	
Largest diff. peak and hole	0.360 and -0.259 e.$Å^{-3}$	

Table 14. Atomic coordinates (x 10^4) and equivalent isotropic displacement parameters ($Å^2$x 10^3) for **IV**. U(eq) is defined as one third of the trace of the orthogonalized U^{ij} tensor.

	x	y	z	U(eq)
P(1)	-1271(1)	1708(1)	1982(1)	24(1)
Mo(1)	2109(1)	1822(1)	3986(1)	26(1)
O(1)	433(2)	1490(1)	5493(1)	49(1)
O(2)	1736(2)	3928(1)	4188(2)	57(1)
O(3)	4881(2)	1844(1)	5839(1)	46(1)
C(1)	1061(3)	1624(2)	4927(2)	33(1)
C(2)	1901(3)	3131(2)	4135(2)	37(1)
C(3)	3836(3)	1855(2)	5133(2)	30(1)

C(4)	567(3)	1367(2)	2416(2)	25(1)
C(5)	1123(3)	550(2)	2969(2)	29(1)
C(6)	2626(3)	513(2)	3136(2)	33(1)
C(7)	3026(3)	1296(2)	2690(2)	35(1)
C(8)	1778(3)	1822(2)	2254(2)	31(1)
C(9)	-1424(3)	2933(2)	1976(2)	30(1)
C(10)	-2212(3)	1213(2)	2755(2)	25(1)
C(11)	-2571(3)	280(2)	2658(2)	32(1)
C(12)	-3196(3)	-129(2)	3305(2)	37(1)
C(13)	-3472(3)	390(2)	4039(2)	39(1)
C(14)	-3144(3)	1309(2)	4131(2)	37(1)
C(15)	-2517(3)	1725(2)	3490(2)	31(1)
C(16)	-2099(3)	1298(2)	737(2)	23(1)
C(17)	-1254(3)	1027(2)	158(2)	28(1)
C(18)	-1904(3)	716(2)	-800(2)	32(1)
C(19)	-3403(3)	686(2)	-1189(2)	39(1)
C(20)	-4256(3)	967(2)	-623(2)	41(1)
C(21)	-3612(3)	1264(2)	337(2)	34(1)

Table 15. Bond lengths [Å] and angles [°] for **IV**.

P(1)-C(4)	1.759(2)	C(4)-P(1)-C(10)	109.06(11)	O(3)-C(3)-Mo(1)	177.6(2)
P(1)-C(10)	1.783(2)	C(4)-P(1)-C(9)	110.83(13)	C(8)-C(4)-C(5)	106.7(2)
P(1)-C(9)	1.785(3)	C(10)-P(1)-C(9)	110.32(13)	C(8)-C(4)-P(1)	127.12(19)
P(1)-C(16)	1.794(2)	C(4)-P(1)-C(16)	109.85(11)	C(5)-C(4)-P(1)	126.1(2)
Mo(1)-C(3)	1.930(3)	C(10)-P(1)-C(16)	108.34(11)	C(8)-C(4)-Mo(1)	73.39(14)
Mo(1)-C(2)	1.932(3)	C(9)-P(1)-C(16)	108.40(13)	C(5)-C(4)-Mo(1)	72.40(14)
Mo(1)-C(1)	1.935(3)	C(3)-Mo(1)-C(2)	88.60(11)	P(1)-C(4)-Mo(1)	121.46(12)
Mo(1)-C(4)	2.350(2)	C(3)-Mo(1)-C(1)	85.69(10)	C(6)-C(5)-C(4)	108.4(2)
Mo(1)-C(5)	2.353(2)	C(2)-Mo(1)-C(1)	88.59(10)	C(6)-C(5)-Mo(1)	74.18(15)
Mo(1)-C(8)	2.375(2)	C(3)-Mo(1)-C(4)	158.04(9)	C(4)-C(5)-Mo(1)	72.18(14)
Mo(1)-C(6)	2.387(2)	C(2)-Mo(1)-C(4)	108.88(9)	C(5)-C(6)-C(7)	108.1(2)
Mo(1)-C(7)	2.403(3)	C(1)-Mo(1)-C(4)	107.33(9)	C(5)-C(6)-Mo(1)	71.50(14)
O(1)-C(1)	1.165(3)	C(3)-Mo(1)-C(5)	127.74(9)	C(7)-C(6)-Mo(1)	73.47(15)
O(2)-C(2)	1.174(3)	C(2)-Mo(1)-C(5)	143.55(10)	C(8)-C(7)-C(6)	108.6(3)
O(3)-C(3)	1.177(3)	C(1)-Mo(1)-C(5)	96.17(10)	C(8)-C(7)-Mo(1)	71.89(15)
C(4)-C(8)	1.426(3)	C(4)-Mo(1)-C(5)	35.42(8)	C(6)-C(7)-Mo(1)	72.22(15)
C(4)-C(5)	1.430(3)	C(3)-Mo(1)-C(8)	132.07(10)	C(7)-C(8)-C(4)	108.3(2)
C(5)-C(6)	1.399(4)	C(2)-Mo(1)-C(8)	97.34(10)	C(7)-C(8)-Mo(1)	74.11(15)
C(6)-C(7)	1.413(4)	C(1)-Mo(1)-C(8)	141.68(10)	C(4)-C(8)-Mo(1)	71.48(14)
C(7)-C(8)	1.397(4)	C(4)-Mo(1)-C(8)	35.13(8)	C(15)-C(10)-C(11)	119.3(2)
C(10)-C(15)	1.387(3)	C(5)-Mo(1)-C(8)	57.99(9)	C(15)-C(10)-P(1)	121.17(18)
C(10)-C(11)	1.395(3)	C(3)-Mo(1)-C(6)	100.48(10)	C(11)-C(10)-P(1)	119.43(19)
C(11)-C(12)	1.381(4)	C(2)-Mo(1)-C(6)	152.24(10)	C(12)-C(11)-C(10)	120.0(3)
C(12)-C(13)	1.377(4)	C(1)-Mo(1)-C(6)	118.01(10)	C(13)-C(12)-C(11)	119.8(3)
C(13)-C(14)	1.368(4)	C(4)-Mo(1)-C(6)	57.93(9)	C(14)-C(13)-C(12)	120.8(3)
C(14)-C(15)	1.380(4)	C(5)-Mo(1)-C(6)	34.32(9)	C(13)-C(14)-C(15)	120.0(3)
C(16)-C(17)	1.386(3)	C(8)-Mo(1)-C(6)	57.26(9)	C(14)-C(15)-C(10)	120.2(2)
C(16)-C(21)	1.394(3)	C(3)-Mo(1)-C(7)	102.84(10)	C(17)-C(16)-C(21)	119.3(2)
C(17)-C(18)	1.381(3)	C(2)-Mo(1)-C(7)	118.19(10)	C(17)-C(16)-P(1)	120.9(2)
C(18)-C(19)	1.380(4)	C(1)-Mo(1)-C(7)	151.70(10)	C(21)-C(16)-P(1)	119.8(2)
C(19)-C(20)	1.383(4)	C(4)-Mo(1)-C(7)	57.54(9)	C(18)-C(17)-C(16)	120.3(3)
C(20)-C(21)	1.375(4)	C(5)-Mo(1)-C(7)	57.16(10)	C(19)-C(18)-C(17)	119.9(3)
		C(8)-Mo(1)-C(7)	34.00(8)	C(18)-C(19)-C(20)	120.2(3)

C(6)-Mo(1)-C(7)	34.31(9)	C(21)-C(20)-C(19)	120.0(3)
O(1)-C(1)-Mo(1)	178.9(2)	C(20)-C(21)-C(16)	120.2(3)
O(2)-C(2)-Mo(1)	177.4(2)		

Table 16. Anisotropic displacement parameters ($Å^2 x\ 10^3$) for **IV**. The anisotropic displacement factor exponent takes the form: $-2\pi^2[\ h^2\ a^{*2}U^{11} + ...\ + 2\ h\ k\ a^*\ b^*\ U^{12}\ ]$

	U^{11}	U^{22}	U^{33}	U^{23}	U^{13}	U^{12}
P(1)	23(1)	28(1)	22(1)	-1(1)	8(1)	0(1)
Mo(1)	23(1)	30(1)	24(1)	-2(1)	8(1)	-1(1)
O(1)	38(1)	78(1)	36(1)	-4(1)	21(1)	-2(1)
O(2)	67(2)	34(1)	76(2)	-5(1)	31(1)	-1(1)
O(3)	33(1)	64(1)	35(1)	8(1)	1(1)	-15(1)
C(1)	27(2)	40(2)	28(2)	-7(1)	3(1)	-1(1)
C(2)	35(2)	40(2)	37(2)	-2(1)	13(1)	-5(2)
C(3)	32(2)	34(1)	28(2)	2(1)	14(1)	-6(1)
C(4)	22(2)	31(1)	21(1)	-1(1)	8(1)	0(1)
C(5)	31(2)	29(1)	27(2)	-4(1)	8(1)	1(1)
C(6)	31(2)	38(2)	27(2)	-7(1)	5(1)	11(1)
C(7)	23(2)	55(2)	28(2)	-6(1)	10(1)	2(2)
C(8)	28(2)	42(2)	26(2)	4(1)	10(1)	2(2)
C(9)	28(2)	33(2)	32(2)	0(1)	11(2)	1(1)
C(10)	20(2)	31(1)	23(2)	1(1)	4(1)	0(1)
C(11)	30(2)	37(2)	30(2)	-2(1)	10(1)	0(1)
C(12)	33(2)	36(2)	42(2)	10(1)	9(2)	-4(1)
C(13)	24(2)	63(2)	30(2)	13(2)	9(1)	-3(2)
C(14)	27(2)	57(2)	28(2)	-3(1)	10(1)	1(2)
C(15)	27(2)	36(2)	32(2)	-3(1)	12(1)	-5(1)
C(16)	24(2)	22(1)	24(2)	0(1)	8(1)	2(1)
C(17)	25(2)	31(1)	26(2)	3(1)	6(1)	2(1)
C(18)	37(2)	35(2)	27(2)	1(1)	14(2)	8(1)
C(19)	45(2)	43(2)	25(2)	-7(1)	4(2)	4(1)
C(20)	26(2)	53(2)	38(2)	-11(1)	2(2)	1(2)
C(21)	31(2)	42(2)	30(2)	-7(1)	11(2)	6(1)

Table 17. Hydrogen coordinates ($x\ 10^4$) and isotropic displacement parameters ($Å^2 x\ 10^3$) for **IV**.

	x	y	z	U(eq)
H(5)	570(20)	120(14)	3182(16)	30(7)
H(6)	3270(20)	46(14)	3483(16)	31(7)
H(7)	3920(30)	1455(16)	2668(18)	41(8)
H(8)	1780(20)	2355(13)	1965(16)	23(7)
H(9A)	-990(20)	3172(14)	2620(18)	30(7)
H(9B)	-2420(30)	3073(14)	1732(17)	32(7)
H(9C)	-1000(30)	3143(16)	1504(19)	52(9)
H(11)	-2410(20)	-40(14)	2153(16)	26(7)
H(12)	-3370(20)	-721(15)	3265(16)	30(7)
H(13)	-3860(30)	105(15)	4475(17)	38(8)
H(14)	-3370(20)	1699(14)	4608(16)	28(7)
H(15)	-2290(20)	2332(14)	3559(15)	25(7)
H(17)	-270(20)	1046(13)	408(16)	19(6)
H(18)	-1310(30)	519(14)	-1207(16)	32(7)
H(19)	-3840(20)	522(14)	-1862(16)	30(7)
H(20)	-5210(30)	921(15)	-878(18)	38(8)
H(21)	-4140(30)	1436(15)	687(17)	30(8)

Table 18. Torsion angles [°] for **IV**.

C(3)-Mo(1)-C(1)-O(1)	-92(12)	C(8)-C(4)-C(5)-C(6)	0.0(3)	Mo(1)-C(7)-C(8)-C(4)	-63.78(18)
C(2)-Mo(1)-C(1)-O(1)	180(100)	P(1)-C(4)-C(5)-C(6)	177.60(18)	C(6)-C(7)-C(8)-Mo(1)	63.34(19)
C(4)-Mo(1)-C(1)-O(1)	70(12)	Mo(1)-C(4)-C(5)-C(6)	-65.90(18)	C(5)-C(4)-C(8)-C(7)	0.3(3)
C(5)-Mo(1)-C(1)-O(1)	36(12)	C(8)-C(4)-C(5)-Mo(1)	65.90(17)	P(1)-C(4)-C(8)-C(7)	-177.29(18)
C(8)-Mo(1)-C(1)-O(1)	80(12)	P(1)-C(4)-C(5)-Mo(1)	-116.51(19)	Mo(1)-C(4)-C(8)-C(7)	65.50(19)
C(6)-Mo(1)-C(1)-O(1)	8(12)	C(3)-Mo(1)-C(5)-C(6)	-43.5(2)	C(5)-C(4)-C(8)-Mo(1)	-65.23(17)
C(7)-Mo(1)-C(1)-O(1)	18(12)	C(2)-Mo(1)-C(5)-C(6)	131.19(19)	P(1)-C(4)-C(8)-Mo(1)	117.21(19)

C(3)-Mo(1)-C(2)-O(2)	165(5)	C(1)-Mo(1)-C(5)-C(6)	-132.80(17)	C(3)-Mo(1)-C(8)-C(7)	36.6(2)
C(1)-Mo(1)-C(2)-O(2)	-109(5)	C(4)-Mo(1)-C(5)-C(6)	115.8(2)	C(2)-Mo(1)-C(8)-C(7)	131.37(18)
C(4)-Mo(1)-C(2)-O(2)	-1(5)	C(8)-Mo(1)-C(5)-C(6)	77.55(18)	C(1)-Mo(1)-C(8)-C(7)	-131.57(19)
C(5)-Mo(1)-C(2)-O(2)	-11(5)	C(7)-Mo(1)-C(5)-C(6)	37.03(16)	C(4)-Mo(1)-C(8)-C(7)	-116.1(2)
C(8)-Mo(1)-C(2)-O(2)	33(5)	C(3)-Mo(1)-C(5)-C(4)	-159.27(15)	C(5)-Mo(1)-C(8)-C(7)	-77.48(18)
C(6)-Mo(1)-C(2)-O(2)	55(5)	C(2)-Mo(1)-C(5)-C(4)	15.4(3)	C(6)-Mo(1)-C(8)-C(7)	-36.59(16)
C(7)-Mo(1)-C(2)-O(2)	61(5)	C(1)-Mo(1)-C(5)-C(4)	111.41(16)	C(3)-Mo(1)-C(8)-C(4)	152.66(15)
C(2)-Mo(1)-C(3)-O(3)	153(5)	C(8)-Mo(1)-C(5)-C(4)	-38.25(15)	C(2)-Mo(1)-C(8)-C(4)	-112.58(16)
C(1)-Mo(1)-C(3)-O(3)	64(5)	C(6)-Mo(1)-C(5)-C(4)	-115.8(2)	C(1)-Mo(1)-C(8)-C(4)	-15.5(2)
C(4)-Mo(1)-C(3)-O(3)	-63(5)	C(7)-Mo(1)-C(5)-C(4)	-78.77(17)	C(5)-Mo(1)-C(8)-C(4)	38.57(14)
C(5)-Mo(1)-C(3)-O(3)	-30(5)	C(4)-C(5)-C(6)-C(7)	-0.3(3)	C(6)-Mo(1)-C(8)-C(4)	79.46(16)
C(8)-Mo(1)-C(3)-O(3)	-108(5)	Mo(1)-C(5)-C(6)-C(7)	-64.87(18)	C(7)-Mo(1)-C(8)-C(4)	116.1(2)
C(6)-Mo(1)-C(3)-O(3)	-53(5)	C(4)-C(5)-C(6)-Mo(1)	64.59(17)	C(4)-P(1)-C(10)-C(15)	100.7(2)
C(7)-Mo(1)-C(3)-O(3)	-88(5)	C(3)-Mo(1)-C(6)-C(5)	146.40(16)	C(9)-P(1)-C(10)-C(15)	-21.3(3)
C(10)-P(1)-C(4)-C(8)	-157.1(2)	C(2)-Mo(1)-C(6)-C(5)	-106.3(2)	C(16)-P(1)-C(10)-C(15)	-139.8(2)
C(9)-P(1)-C(4)-C(8)	-35.5(3)	C(1)-Mo(1)-C(6)-C(5)	55.72(19)	C(4)-P(1)-C(10)-C(11)	-75.4(2)
C(16)-P(1)-C(4)-C(8)	84.3(2)	C(4)-Mo(1)-C(6)-C(5)	-38.00(15)	C(9)-P(1)-C(10)-C(11)	162.6(2)
C(10)-P(1)-C(4)-C(5)	25.8(2)	C(8)-Mo(1)-C(6)-C(5)	-79.88(17)	C(16)-P(1)-C(10)-C(11)	44.1(2)
C(9)-P(1)-C(4)-C(5)	147.4(2)	C(7)-Mo(1)-C(6)-C(5)	-116.1(2)	C(15)-C(10)-C(11)-C(12)	-1.3(4)
C(16)-P(1)-C(4)-C(5)	-92.8(2)	C(3)-Mo(1)-C(6)-C(7)	-97.46(17)	P(1)-C(10)-C(11)-C(12)	174.8(2)
C(10)-P(1)-C(4)-Mo(1)	-64.66(15)	C(2)-Mo(1)-C(6)-C(7)	9.9(3)	C(10)-C(11)-C(12)-C(13)	0.5(4)
C(9)-P(1)-C(4)-Mo(1)	56.97(18)	C(1)-Mo(1)-C(6)-C(7)	171.86(16)	C(11)-C(12)-C(13)-C(14)	0.5(4)
C(16)-P(1)-C(4)-Mo(1)	176.73(11)	C(4)-Mo(1)-C(6)-C(7)	78.13(17)	C(12)-C(13)-C(14)-C(15)	-0.6(4)
C(3)-Mo(1)-C(4)-C(8)	-65.7(3)	C(5)-Mo(1)-C(6)-C(7)	116.1(2)	C(13)-C(14)-C(15)-C(10)	-0.2(4)
C(2)-Mo(1)-C(4)-C(8)	75.43(17)	C(8)-Mo(1)-C(6)-C(7)	36.26(16)	C(11)-C(10)-C(15)-C(14)	1.2(4)
C(1)-Mo(1)-C(4)-C(8)	169.99(16)	C(5)-C(6)-C(7)-C(8)	0.5(3)	P(1)-C(10)-C(15)-C(14)	-174.9(2)
C(5)-Mo(1)-C(4)-C(8)	-114.2(2)	Mo(1)-C(6)-C(7)-C(8)	-63.12(19)	C(4)-P(1)-C(16)-C(17)	-18.4(2)
C(6)-Mo(1)-C(4)-C(8)	-77.36(17)	C(5)-C(6)-C(7)-Mo(1)	63.58(18)	C(10)-P(1)-C(16)-C(17)	-137.4(2)
C(7)-Mo(1)-C(4)-C(8)	-36.54(15)	C(3)-Mo(1)-C(7)-C(8)	-153.00(17)	C(9)-P(1)-C(16)-C(17)	102.9(2)
C(3)-Mo(1)-C(4)-C(5)	48.4(3)	C(2)-Mo(1)-C(7)-C(8)	-57.6(2)	C(4)-P(1)-C(16)-C(21)	162.8(2)
C(2)-Mo(1)-C(4)-C(5)	-170.40(16)	C(1)-Mo(1)-C(7)-C(8)	101.9(2)	C(10)-P(1)-C(16)-C(21)	43.7(2)
C(1)-Mo(1)-C(4)-C(5)	-75.84(17)	C(4)-Mo(1)-C(7)-C(8)	37.78(16)	C(9)-P(1)-C(16)-C(21)	-76.0(2)
C(8)-Mo(1)-C(4)-C(5)	114.2(2)	C(5)-Mo(1)-C(7)-C(8)	80.13(18)	C(21)-C(16)-C(17)-C(18)	-0.9(4)
C(6)-Mo(1)-C(4)-C(5)	36.80(15)	C(6)-Mo(1)-C(7)-C(8)	117.2(3)	P(1)-C(16)-C(17)-C(18)	-179.79(18)
C(7)-Mo(1)-C(4)-C(5)	77.62(17)	C(3)-Mo(1)-C(7)-C(6)	89.83(17)	C(16)-C(17)-C(18)-C(19)	1.0(4)
C(3)-Mo(1)-C(4)-P(1)	170.52(19)	C(2)-Mo(1)-C(7)-C(6)	-174.80(16)	C(17)-C(18)-C(19)-C(20)	-0.1(4)
C(2)-Mo(1)-C(4)-P(1)	-48.33(16)	C(1)-Mo(1)-C(7)-C(6)	-15.3(3)	C(18)-C(19)-C(20)-C(21)	-1.0(4)
C(1)-Mo(1)-C(4)-P(1)	46.23(16)	C(4)-Mo(1)-C(7)-C(6)	-79.39(17)	C(19)-C(20)-C(21)-C(16)	1.0(4)
C(5)-Mo(1)-C(4)-P(1)	122.1(2)	C(5)-Mo(1)-C(7)-C(6)	-37.04(15)	C(17)-C(16)-C(21)-C(20)	-0.1(4)
C(8)-Mo(1)-C(4)-P(1)	-123.8(2)	C(8)-Mo(1)-C(7)-C(6)	-117.2(3)	P(1)-C(16)-C(21)-C(20)	178.8(2)
C(6)-Mo(1)-C(4)-P(1)	158.87(18)	C(6)-C(7)-C(8)-C(4)	-0.4(3)		
C(7)-Mo(1)-C(4)-P(1)	-160.30(18)				

Figure 3. The molecular structure of **IV**.

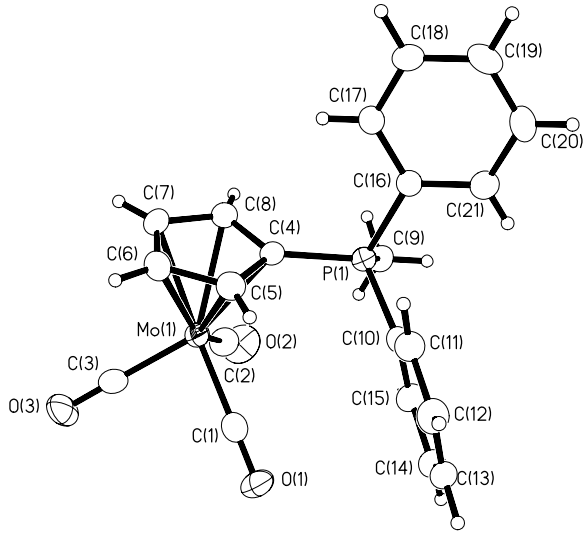

Table 19. Crystal data and structure refinement for **V**

Identification code	**V**	
Empirical formula	C21 H17 O3 P W	
Formula weight	532.17	
Temperature	180(2) K	
Wavelength	0.71073 Å	
Crystal system	Monoclinic	
Space group	P2(1)/c	
Unit cell dimensions	a = 9.6818(12) Å	α= 90°.
	b = 14.5322(17) Å	β= 108.514(2)°.
	c = 14.1153(17) Å	γ = 90°.
Volume	1883.2(4) $Å^3$	
Z	4	
Density (calculated)	1.877 Mg/m^3	
Absorption coefficient	6.236 mm^{-1}	
F(000)	1024	
Crystal size	0.35 x 0.25 x 0.05 mm^3	
Theta range for data collection	2.22 to 25.00°.	
Index ranges	-11<=h<=11, -17<=k<=16, -16<=l<=16	
Reflections collected	10698	
Independent reflections	3319 [R(int) = 0.0540]	
Completeness to theta = 25.00°	99.9 %	
Absorption correction	Empirical	
Max. and min. transmission	0.5984 and 0.2118	
Refinement method	Full-matrix least-squares on F^2	
Data / restraints / parameters	3319 / 0 / 235	
Goodness-of-fit on F^2	1.001	
Final R indices [I>2sigma(I)]	R1 = 0.0270, wR2 = 0.0849	
R indices (all data)	R1 = 0.0295, wR2 = 0.0864	
Largest diff. peak and hole	0.923 and -0.796 e.$Å^{-3}$	

Table 20. Atomic coordinates (x 10^4) and equivalent isotropic displacement parameters ($Å^2$x 10^3) for **V**. U(eq) is defined as one third of the trace of the orthogonalized U^{ij} tensor.

	x	y	z	U(eq)
P(1)	-1285(1)	1715(1)	6981(1)	19(1)
W(1)	2096(1)	1826(1)	8991(1)	26(1)
C(1)	1879(6)	3147(3)	9135(4)	31(1)
C(2)	3839(6)	1857(3)	10152(4)	26(1)
C(3)	1044(5)	1621(3)	9935(3)	28(1)
C(4)	558(5)	1369(3)	7419(3)	21(1)
C(5)	1114(5)	551(3)	7979(3)	25(1)

C(6)	2622(5)	530(3)	8144(3)	30(1)
C(7)	3015(5)	1311(4)	7706(3)	32(1)
C(8)	1774(5)	1834(3)	7257(3)	26(1)
C(9)	-2219(5)	1215(3)	7758(3)	21(1)
C(10)	-2530(6)	1741(3)	8492(4)	28(1)
C(11)	-3177(5)	1301(4)	9137(3)	34(1)
C(12)	-3502(5)	394(4)	9041(3)	34(1)
C(13)	-3192(5)	-123(3)	8310(3)	34(1)
C(14)	-2570(5)	281(3)	7661(3)	28(1)
C(15)	-2114(4)	1301(3)	5724(3)	20(1)
C(16)	-3636(5)	1267(3)	5333(3)	28(1)
C(17)	-4274(6)	966(4)	4360(4)	38(1)
C(18)	-3410(6)	682(4)	3800(3)	35(1)
C(19)	-1911(6)	712(3)	4186(3)	29(1)
C(20)	-1256(5)	1030(3)	5149(3)	24(1)
C(21)	-1446(5)	2939(3)	6972(3)	25(1)
O(1)	1700(5)	3930(3)	9165(3)	51(1)
O(2)	4868(4)	1839(2)	10837(3)	43(1)
O(3)	413(4)	1471(3)	10494(3)	43(1)

Table 21. Bond lengths [Å] and angles [°] for **V**.

P(1)-C(4)	1.765(4)	C(4)-P(1)-C(9)	108.8(2)	O(3)-C(3)-W(1)	178.0(4)
P(1)-C(9)	1.783(4)	C(4)-P(1)-C(21)	111.2(2)	C(5)-C(4)-C(8)	107.1(4)
P(1)-C(21)	1.786(4)	C(9)-P(1)-C(21)	110.4(2)	C(5)-C(4)-P(1)	126.1(3)
P(1)-C(15)	1.803(4)	C(4)-P(1)-C(15)	109.58(19)	C(8)-C(4)-P(1)	126.7(3)
W(1)-C(3)	1.940(5)	C(9)-P(1)-C(15)	108.4(2)	C(5)-C(4)-W(1)	72.5(2)
W(1)-C(2)	1.944(5)	C(21)-P(1)-C(15)	108.3(2)	C(8)-C(4)-W(1)	73.2(2)
W(1)-C(1)	1.948(4)	C(3)-W(1)-C(2)	85.97(19)	P(1)-C(4)-W(1)	121.3(2)
W(1)-C(4)	2.342(4)	C(3)-W(1)-C(1)	89.0(2)	C(6)-C(5)-C(4)	107.4(4)
W(1)-C(5)	2.349(4)	C(2)-W(1)-C(1)	89.0(2)	C(6)-C(5)-W(1)	73.6(2)
W(1)-C(8)	2.367(5)	C(3)-W(1)-C(4)	106.99(17)	C(4)-C(5)-W(1)	71.9(2)
W(1)-C(6)	2.371(4)	C(2)-W(1)-C(4)	157.84(17)	C(7)-C(6)-C(5)	108.8(4)
W(1)-C(7)	2.380(5)	C(1)-W(1)-C(4)	108.69(18)	C(7)-C(6)-W(1)	73.2(3)
C(1)-O(1)	1.155(6)	C(3)-W(1)-C(5)	95.56(18)	C(5)-C(6)-W(1)	71.8(2)
C(2)-O(2)	1.148(6)	C(2)-W(1)-C(5)	127.36(16)	C(8)-C(7)-C(6)	109.1(4)
C(3)-O(3)	1.162(6)	C(1)-W(1)-C(5)	143.53(19)	C(8)-C(7)-W(1)	72.4(3)
C(4)-C(5)	1.435(6)	C(4)-W(1)-C(5)	35.62(15)	C(6)-C(7)-W(1)	72.5(3)
C(4)-C(8)	1.438(6)	C(3)-W(1)-C(8)	141.75(18)	C(7)-C(8)-C(4)	107.6(4)
C(5)-C(6)	1.405(7)	C(2)-W(1)-C(8)	131.72(19)	C(7)-C(8)-W(1)	73.5(3)
C(6)-C(7)	1.402(7)	C(1)-W(1)-C(8)	96.87(19)	C(4)-C(8)-W(1)	71.3(2)
C(7)-C(8)	1.393(7)	C(4)-W(1)-C(8)	35.55(15)	C(10)-C(9)-C(14)	120.2(4)
C(9)-C(10)	1.395(6)	C(5)-W(1)-C(8)	58.68(15)	C(10)-C(9)-P(1)	120.4(3)
C(9)-C(14)	1.395(6)	C(3)-W(1)-C(6)	117.89(19)	C(14)-C(9)-P(1)	119.4(3)
C(10)-C(11)	1.412(7)	C(2)-W(1)-C(6)	100.12(17)	C(9)-C(10)-C(11)	118.4(4)
C(11)-C(12)	1.350(8)	C(1)-W(1)-C(6)	152.0(2)	C(12)-C(11)-C(10)	120.9(5)
C(12)-C(13)	1.385(7)	C(4)-W(1)-C(6)	58.07(15)	C(11)-C(12)-C(13)	120.4(5)
C(13)-C(14)	1.377(6)	C(5)-W(1)-C(6)	34.62(16)	C(14)-C(13)-C(12)	120.6(5)
C(15)-C(20)	1.389(6)	C(8)-W(1)-C(6)	57.43(15)	C(13)-C(14)-C(9)	119.6(4)
C(15)-C(16)	1.401(6)	C(3)-W(1)-C(7)	151.6(2)	C(20)-C(15)-C(16)	120.6(4)
C(16)-C(17)	1.386(6)	C(2)-W(1)-C(7)	102.42(19)	C(20)-C(15)-P(1)	120.5(3)
C(17)-C(18)	1.383(7)	C(1)-W(1)-C(7)	117.9(2)	C(16)-C(15)-P(1)	118.9(3)
C(18)-C(19)	1.380(8)	C(4)-W(1)-C(7)	57.87(15)	C(17)-C(16)-C(15)	118.9(4)
C(19)-C(20)	1.384(6)	C(5)-W(1)-C(7)	57.70(17)	C(18)-C(17)-C(16)	120.0(5)

C(8)-W(1)-C(7)	34.12(17)	C(19)-C(18)-C(17)	121.1(4)
C(6)-W(1)-C(7)	34.32(18)	C(18)-C(19)-C(20)	119.7(5)
O(1)-C(1)-W(1)	176.2(5)	C(19)-C(20)-C(15)	119.7(4)
O(2)-C(2)-W(1)	177.3(4)		

Table 22. Anisotropic displacement parameters ($Å^2 x\ 10^3$) for **V**. The anisotropic displacement factor exponent takes the form: $-2\pi^2[\ h^2\ a^{*2}U^{11} + ...\ + 2\ h\ k\ a^*\ b^*\ U^{12}\ ]$

	U^{11}	U^{22}	U^{33}	U^{23}	U^{13}	U^{12}
P(1)	17(1)	22(1)	17(1)	-2(1)	5(1)	0(1)
W(1)	23(1)	31(1)	23(1)	-2(1)	6(1)	-1(1)
C(1)	36(3)	25(3)	33(3)	-4(2)	13(2)	-3(2)
C(2)	29(3)	30(3)	23(2)	-1(2)	13(2)	-11(2)
C(3)	20(2)	38(2)	21(2)	-6(2)	0(2)	-4(2)
C(4)	21(2)	27(2)	14(2)	-4(2)	4(2)	0(2)
C(5)	26(2)	25(2)	21(2)	-8(2)	3(2)	2(2)
C(6)	30(3)	36(3)	21(2)	-9(2)	5(2)	11(2)
C(7)	22(2)	52(3)	24(2)	-8(2)	9(2)	2(2)
C(8)	23(3)	37(3)	20(2)	0(2)	8(2)	-4(2)
C(9)	17(2)	28(2)	16(2)	1(2)	3(2)	0(2)
C(10)	24(3)	36(3)	25(2)	-4(2)	11(2)	-2(2)
C(11)	25(3)	59(4)	21(2)	-2(2)	11(2)	0(2)
C(12)	20(2)	54(3)	28(2)	14(2)	8(2)	-1(2)
C(13)	26(3)	36(3)	36(2)	11(2)	4(2)	-5(2)
C(14)	25(2)	31(2)	27(2)	1(2)	8(2)	-2(2)
C(15)	21(2)	21(2)	16(2)	1(2)	4(2)	5(2)
C(16)	23(2)	36(2)	25(2)	-4(2)	7(2)	4(2)
C(17)	24(3)	51(3)	32(2)	-14(2)	-1(2)	-2(2)
C(18)	38(3)	40(3)	22(2)	-9(2)	2(2)	3(2)
C(19)	44(3)	27(2)	21(2)	4(2)	15(2)	8(2)
C(20)	22(2)	26(2)	22(2)	2(2)	5(2)	4(2)
C(21)	25(3)	24(2)	27(2)	-1(2)	10(2)	1(2)
O(1)	60(3)	32(2)	66(3)	-5(2)	29(2)	-1(2)
O(2)	23(2)	66(3)	31(2)	12(2)	-6(2)	-18(2)
O(3)	30(2)	76(3)	28(2)	-4(2)	17(2)	-3(2)

Table 23. Hydrogen coordinates ($x\ 10^4$) and isotropic displacement parameters ($Å^2 x\ 10^3$) for **V**.

	x	y	z	U(eq)
H(5A)	520	48	8141	30
H(6A)	3290	13	8464	36
H(7A)	4011	1442	7670	39
H(8A)	1722	2393	6833	31
H(10A)	-2311	2380	8557	33
H(11A)	-3388	1646	9646	41
H(12A)	-3945	110	9477	41
H(13A)	-3410	-762	8255	41
H(14A)	-2380	-74	7150	34
H(16A)	-4222	1447	5729	34
H(17A)	-5305	956	4077	46
H(18A)	-3857	463	3139	42
H(19A)	-1331	516	3793	35
H(20A)	-225	1062	5417	28
H(21A)	-1002	3177	7651	37
H(21B)	-2478	3111	6730	37
H(21C)	-947	3202	6530	37

Table 24. Torsion angles [°] for **V**.

C(3)-W(1)-C(1)-O(1)	-114(8)	C(8)-C(4)-C(5)-C(6)	-0.1(4)	C(6)-C(7)-C(8)-W(1)	63.7(3)
C(2)-W(1)-C(1)-O(1)	160(8)	P(1)-C(4)-C(5)-C(6)	178.1(3)	C(5)-C(4)-C(8)-C(7)	0.0(5)
C(4)-W(1)-C(1)-O(1)	-6(8)	W(1)-C(4)-C(5)-C(6)	-65.6(3)	P(1)-C(4)-C(8)-C(7)	-178.2(3)
C(5)-W(1)-C(1)-O(1)	-16(8)	C(8)-C(4)-C(5)-W(1)	65.5(3)	W(1)-C(4)-C(8)-C(7)	65.0(3)
C(8)-W(1)-C(1)-O(1)	28(8)	P(1)-C(4)-C(5)-W(1)	-116.4(3)	C(5)-C(4)-C(8)-W(1)	-65.0(3)

C(6)-W(1)-C(1)-O(1)	50(8)	C(3)-W(1)-C(5)-C(6)	-133.3(3)	P(1)-C(4)-C(8)-W(1)	116.9(3)
C(7)-W(1)-C(1)-O(1)	57(8)	C(2)-W(1)-C(5)-C(6)	-44.2(4)	C(3)-W(1)-C(8)-C(7)	-131.4(4)
C(3)-W(1)-C(2)-O(2)	80(9)	C(1)-W(1)-C(5)-C(6)	130.9(4)	C(2)-W(1)-C(8)-C(7)	36.7(4)
C(1)-W(1)-C(2)-O(2)	169(9)	C(4)-W(1)-C(5)-C(6)	115.0(4)	C(1)-W(1)-C(8)-C(7)	131.5(3)
C(4)-W(1)-C(2)-O(2)	-47(10)	C(8)-W(1)-C(5)-C(6)	76.8(3)	C(4)-W(1)-C(8)-C(7)	-115.7(4)
C(5)-W(1)-C(2)-O(2)	-13(9)	C(7)-W(1)-C(5)-C(6)	36.5(3)	C(5)-W(1)-C(8)-C(7)	-77.5(3)
C(8)-W(1)-C(2)-O(2)	-92(9)	C(3)-W(1)-C(5)-C(4)	111.6(3)	C(6)-W(1)-C(8)-C(7)	-36.4(3)
C(6)-W(1)-C(2)-O(2)	-37(9)	C(2)-W(1)-C(5)-C(4)	-159.2(3)	C(3)-W(1)-C(8)-C(4)	-15.7(4)
C(7)-W(1)-C(2)-O(2)	-72(9)	C(1)-W(1)-C(5)-C(4)	15.8(5)	C(2)-W(1)-C(8)-C(4)	152.4(3)
C(2)-W(1)-C(3)-O(3)	-98(12)	C(8)-W(1)-C(5)-C(4)	-38.2(3)	C(1)-W(1)-C(8)-C(4)	-112.7(3)
C(1)-W(1)-C(3)-O(3)	172(12)	C(6)-W(1)-C(5)-C(4)	-115.0(4)	C(5)-W(1)-C(8)-C(4)	38.3(2)
C(4)-W(1)-C(3)-O(3)	63(12)	C(7)-W(1)-C(5)-C(4)	-78.6(3)	C(6)-W(1)-C(8)-C(4)	79.3(3)
C(5)-W(1)-C(3)-O(3)	29(12)	C(4)-C(5)-C(6)-C(7)	0.2(5)	C(7)-W(1)-C(8)-C(4)	115.7(4)
C(8)-W(1)-C(3)-O(3)	73(12)	W(1)-C(5)-C(6)-C(7)	-64.3(3)	C(4)-P(1)-C(9)-C(10)	101.6(4)
C(6)-W(1)-C(3)-O(3)	1(12)	C(4)-C(5)-C(6)-W(1)	64.5(3)	C(21)-P(1)-C(9)-C(10)	-20.7(4)
C(7)-W(1)-C(3)-O(3)	10(12)	C(3)-W(1)-C(6)-C(7)	172.0(3)	C(15)-P(1)-C(9)-C(10)	-139.3(4)
C(9)-P(1)-C(4)-C(5)	25.3(4)	C(2)-W(1)-C(6)-C(7)	-97.2(3)	C(4)-P(1)-C(9)-C(14)	-75.1(4)
C(21)-P(1)-C(4)-C(5)	147.2(4)	C(1)-W(1)-C(6)-C(7)	10.1(5)	C(21)-P(1)-C(9)-C(14)	162.6(3)
C(15)-P(1)-C(4)-C(5)	-93.0(4)	C(4)-W(1)-C(6)-C(7)	78.5(3)	C(15)-P(1)-C(9)-C(14)	44.0(4)
C(9)-P(1)-C(4)-C(8)	-156.9(4)	C(5)-W(1)-C(6)-C(7)	117.0(4)	C(14)-C(9)-C(10)-C(11)	1.1(7)
C(21)-P(1)-C(4)-C(8)	-35.0(4)	C(8)-W(1)-C(6)-C(7)	36.2(3)	P(1)-C(9)-C(10)-C(11)	-175.5(4)
C(15)-P(1)-C(4)-C(8)	84.8(4)	C(3)-W(1)-C(6)-C(5)	55.0(3)	C(9)-C(10)-C(11)-C(12)	-0.6(7)
C(9)-P(1)-C(4)-W(1)	-65.1(3)	C(2)-W(1)-C(6)-C(5)	145.8(3)	C(10)-C(11)-C(12)-C(13)	0.6(7)
C(21)-P(1)-C(4)-W(1)	56.8(3)	C(1)-W(1)-C(6)-C(5)	-106.9(5)	C(11)-C(12)-C(13)-C(14)	-1.0(7)
C(15)-P(1)-C(4)-W(1)	176.6(2)	C(4)-W(1)-C(6)-C(5)	-38.4(3)	C(12)-C(13)-C(14)-C(9)	1.5(7)
C(3)-W(1)-C(4)-C(5)	-75.4(3)	C(8)-W(1)-C(6)-C(5)	-80.8(3)	C(10)-C(9)-C(14)-C(13)	-1.6(7)
C(2)-W(1)-C(4)-C(5)	48.4(5)	C(7)-W(1)-C(6)-C(5)	-117.0(4)	P(1)-C(9)-C(14)-C(13)	175.1(3)
C(1)-W(1)-C(4)-C(5)	-170.2(3)	C(5)-C(6)-C(7)-C(8)	-0.2(5)	C(4)-P(1)-C(15)-C(20)	-18.4(4)
C(8)-W(1)-C(4)-C(5)	114.7(4)	W(1)-C(6)-C(7)-C(8)	-63.6(3)	C(9)-P(1)-C(15)-C(20)	-137.0(3)
C(6)-W(1)-C(4)-C(5)	37.3(3)	C(5)-C(6)-C(7)-W(1)	63.4(3)	C(21)-P(1)-C(15)-C(20)	103.2(4)
C(7)-W(1)-C(4)-C(5)	78.1(3)	C(3)-W(1)-C(7)-C(8)	102.3(4)	C(4)-P(1)-C(15)-C(16)	162.3(3)
C(3)-W(1)-C(4)-C(8)	169.9(3)	C(2)-W(1)-C(7)-C(8)	-152.8(3)	C(9)-P(1)-C(15)-C(16)	43.7(4)
C(2)-W(1)-C(4)-C(8)	-66.3(5)	C(1)-W(1)-C(7)-C(8)	-57.3(4)	C(21)-P(1)-C(15)-C(16)	-76.2(4)
C(1)-W(1)-C(4)-C(8)	75.1(3)	C(4)-W(1)-C(7)-C(8)	38.2(3)	C(20)-C(15)-C(16)-C(17)	-0.6(7)
C(5)-W(1)-C(4)-C(8)	-114.7(4)	C(5)-W(1)-C(7)-C(8)	80.6(3)	P(1)-C(15)-C(16)-C(17)	178.7(4)
C(6)-W(1)-C(4)-C(8)	-77.4(3)	C(6)-W(1)-C(7)-C(8)	117.4(4)	C(15)-C(16)-C(17)-C(18)	1.8(8)
C(7)-W(1)-C(4)-C(8)	-36.6(3)	C(3)-W(1)-C(7)-C(6)	-15.1(5)	C(16)-C(17)-C(18)-C(19)	-1.6(8)
C(3)-W(1)-C(4)-P(1)	46.7(3)	C(2)-W(1)-C(7)-C(6)	89.8(3)	C(17)-C(18)-C(19)-C(20)	0.1(7)
C(2)-W(1)-C(4)-P(1)	170.5(3)	C(1)-W(1)-C(7)-C(6)	-174.7(3)	C(18)-C(19)-C(20)-C(15)	1.0(6)
C(1)-W(1)-C(4)-P(1)	-48.1(3)	C(4)-W(1)-C(7)-C(6)	-79.2(3)	C(16)-C(15)-C(20)-C(19)	-0.8(6)
C(5)-W(1)-C(4)-P(1)	122.1(4)	C(5)-W(1)-C(7)-C(6)	-36.8(3)	P(1)-C(15)-C(20)-C(19)	179.9(3)
C(8)-W(1)-C(4)-P(1)	-123.2(4)	C(8)-W(1)-C(7)-C(6)	-117.4(4)		
C(6)-W(1)-C(4)-P(1)	159.4(3)	C(6)-C(7)-C(8)-C(4)	0.2(5)		
C(7)-W(1)-C(4)-P(1)	-159.8(3)	W(1)-C(7)-C(8)-C(4)	-63.5(3)		

Figure 4. The molecular structure of **V**.

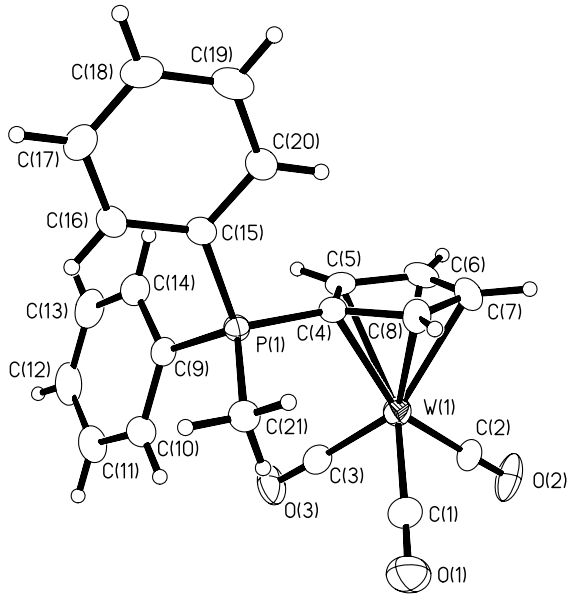

Table 25. Crystal data and structure refinement for **VI**.

Identification code	**VI**	
Empirical formula	C21.50 H18 Cl I2 Mo O3 P	
Formula weight	740.52	
Temperature	180(2) K	
Wavelength	0.71073 Å	
Crystal system	Triclinic	
Space group	P-1	
Unit cell dimensions	a = 9.3488(10) Å	α= 94.800(2)°.
	b = 16.5390(18) Å	β= 103.058(2)°.
	c = 16.6312(18) Å	γ = 90.427(2)°.
Volume	2495.3(5) $Å^3$	
Z	4	
Density (calculated)	1.971 Mg/m^3	
Absorption coefficient	3.191 mm^{-1}	
F(000)	1404	
Crystal size	0.35 x 0.10 x 0.06 mm^3	
Theta range for data collection	1.69 to 25.00°.	
Index ranges	-10<=h<=11, -18<=k<=19, -19<=l<=19	
Reflections collected	14730	
Independent reflections	8747 [R(int) = 0.0384]	
Completeness to theta = 25.00°	99.4 %	
Absorption correction	Empirical (Bruker SADABS)	
Max. and min. transmission	1.0000 and 0.6904	
Refinement method	Full-matrix least-squares on F^2	
Data / restraints / parameters	8747 / 0 / 532	
Goodness-of-fit on F^2	1.000	
Final R indices [I>2sigma(I)]	R1 = 0.0489, wR2 = 0.0996	
R indices (all data)	R1 = 0.0832, wR2 = 0.1063	
Largest diff. peak and hole	1.642 and -1.349 e.$Å^{-3}$	

Table 26. Atomic coordinates (x 10^4) and equivalent isotropic displacement parameters ($Å^2$x 10^3) for **VI**. U(eq) is defined as one third of the trace of the orthogonalized U^{ij} tensor.

	x	y	z	U(eq)
Mo(1)	10876(1)	7313(1)	2381(1)	28(1)
Mo(2)	2989(1)	5859(1)	-3701(1)	33(1)
I(1)	8703(1)	6698(1)	3132(1)	45(1)
I(2)	3551(1)	6168(1)	-5243(1)	52(1)
I(3)	3929(1)	9797(1)	2770(1)	42(1)
I(4)	4773(1)	7056(1)	-136(1)	43(1)

P(1)	8103(2)	8884(1)	1829(1)	28(1)
P(2)	5856(2)	7410(1)	-2757(1)	32(1)
O(1)	14291(7)	7374(4)	2926(4)	52(2)
O(2)	11706(7)	5485(4)	2556(4)	50(2)
O(3)	11431(7)	8351(4)	4101(4)	56(2)
O(4)	1400(8)	4425(4)	-4957(4)	59(2)
O(5)	90(8)	5718(4)	-3085(5)	68(2)
O(6)	1311(7)	7451(4)	-4080(5)	69(2)
C(1)	9379(8)	8175(5)	1564(5)	28(2)
C(2)	10868(9)	8323(5)	1510(5)	34(2)
C(3)	11331(9)	7602(5)	1117(5)	35(2)
C(4)	10155(9)	7036(5)	930(5)	35(2)
C(5)	8957(9)	7368(5)	1183(5)	28(2)
C(6)	7673(8)	9545(5)	1007(5)	28(2)
C(7)	8086(10)	9393(6)	269(6)	46(3)
C(8)	7685(11)	9918(6)	-355(6)	55(3)
C(9)	6859(10)	10557(6)	-250(6)	46(2)
C(10)	6433(9)	10717(5)	495(6)	44(2)
C(11)	6824(9)	10217(5)	1129(5)	35(2)
C(12)	8777(8)	9514(5)	2766(5)	29(2)
C(13)	10041(9)	10010(6)	2857(6)	42(2)
C(14)	10485(11)	10541(6)	3559(6)	51(3)
C(15)	9664(10)	10607(6)	4137(5)	41(2)
C(16)	8450(10)	10141(6)	4059(5)	43(2)
C(17)	7985(9)	9578(6)	3379(5)	41(2)
C(18)	6491(8)	8335(5)	1884(5)	35(2)
C(19)	13047(11)	7364(6)	2733(6)	41(2)
C(20)	11397(9)	6141(6)	2536(5)	38(2)
C(21)	11235(10)	7971(6)	3498(6)	38(2)
C(22)	5157(9)	6397(5)	-2850(5)	32(2)
C(23)	4247(9)	6092(6)	-2347(5)	40(2)
C(24)	4086(10)	5238(6)	-2530(5)	42(2)
C(25)	4892(9)	5010(6)	-3112(6)	42(2)
C(26)	5553(9)	5715(5)	-3314(5)	34(2)
C(27)	7639(9)	7466(5)	-2090(5)	35(2)
C(28)	8316(11)	6804(6)	-1748(6)	51(3)
C(29)	9738(11)	6877(6)	-1272(6)	53(3)
C(30)	10484(10)	7615(7)	-1128(6)	50(3)
C(31)	9798(10)	8283(6)	-1455(6)	57(3)
C(32)	8383(10)	8205(6)	-1939(6)	52(3)
C(33)	6051(9)	7696(5)	-3739(5)	33(2)
C(34)	5079(11)	8234(5)	-4175(6)	47(3)
C(35)	5278(13)	8431(6)	-4934(6)	58(3)
C(36)	6408(13)	8117(7)	-5248(7)	62(3)
C(37)	7346(11)	7592(7)	-4829(6)	52(3)
C(38)	7166(10)	7387(6)	-4065(6)	44(2)
C(39)	4659(9)	8060(5)	-2316(5)	40(2)
C(40)	1936(10)	4943(6)	-4511(6)	45(2)
C(41)	1143(11)	5750(6)	-3300(6)	47(3)
C(42)	1895(10)	6887(7)	-3992(7)	52(3)
C(43)	13044(10)	4942(6)	-81(7)	62(3)
Cl(1)	11800(4)	4841(2)	-1042(2)	85(1)
Cl(2)	12158(4)	5069(2)	730(2)	103(1)

Table 27. Bond lengths [Å] and angles [°] for **VI**.

Mo(1)-C(19)	1.981(10)	C(19)-Mo(1)-C(20)	76.8(4)	C(24)-Mo(2)-I(2)	139.1(2)	C(22)-C(26)-C(25)	108.9(8)
Mo(1)-C(20)	2.024(10)	C(19)-Mo(1)-C(21)	77.3(4)	C(22)-Mo(2)-I(2)	98.7(2)	C(22)-C(26)-Mo(2)	70.9(5)
Mo(1)-C(21)	2.030(10)	C(20)-Mo(1)-C(21)	110.1(3)	C(26)-Mo(2)-I(2)	83.8(2)	C(25)-C(26)-Mo(2)	72.7(5)
Mo(1)-C(2)	2.301(8)	C(19)-Mo(1)-C(2)	91.9(3)	C(25)-Mo(2)-I(2)	105.0(2)	C(28)-C(27)-C(32)	119.1(8)
Mo(1)-C(1)	2.310(7)	C(20)-Mo(1)-C(2)	143.2(3)	C(18)-P(1)-C(1)	108.1(4)	C(28)-C(27)-P(2)	122.9(7)
Mo(1)-C(3)	2.324(8)	C(21)-Mo(1)-C(2)	101.1(3)	C(18)-P(1)-C(12)	110.5(4)	C(32)-C(27)-P(2)	117.9(7)
Mo(1)-C(4)	2.360(8)	C(19)-Mo(1)-C(1)	127.5(3)	C(1)-P(1)-C(12)	114.7(4)	C(27)-C(28)-C(29)	120.1(9)
Mo(1)-C(5)	2.370(8)	C(20)-Mo(1)-C(1)	145.2(3)	C(18)-P(1)-C(6)	109.6(4)	C(30)-C(29)-C(28)	120.7(9)
Mo(1)-I(1)	2.8355(9)	C(21)-Mo(1)-C(1)	100.4(3)	C(1)-P(1)-C(6)	107.0(4)	C(31)-C(30)-C(29)	119.3(9)
Mo(2)-C(41)	1.997(10)	C(2)-Mo(1)-C(1)	36.3(3)	C(12)-P(1)-C(6)	106.9(4)	C(30)-C(31)-C(32)	119.8(10)

Mo(2)-C(40)	2.028(11)	C(19)-Mo(1)-C(3)	82.9(3)	C(22)-P(2)-C(27)	108.7(4)	C(27)-C(32)-C(31)	120.9(9)
Mo(2)-C(42)	2.029(11)	C(20)-Mo(1)-C(3)	107.3(3)	C(22)-P(2)-C(33)	110.6(4)	C(38)-C(33)-C(34)	119.8(9)
Mo(2)-C(23)	2.292(8)	C(21)-Mo(1)-C(3)	131.9(3)	C(27)-P(2)-C(33)	107.1(4)	C(38)-C(33)-P(2)	119.3(7)
Mo(2)-C(24)	2.312(9)	C(2)-Mo(1)-C(3)	36.0(3)	C(22)-P(2)-C(39)	108.5(4)	C(34)-C(33)-P(2)	121.0(7)
Mo(2)-C(22)	2.318(8)	C(1)-Mo(1)-C(3)	59.6(3)	C(27)-P(2)-C(39)	109.6(4)	C(35)-C(34)-C(33)	118.4(10)
Mo(2)-C(26)	2.357(8)	C(19)-Mo(1)-C(4)	109.7(3)	C(33)-P(2)-C(39)	112.4(4)	C(36)-C(35)-C(34)	120.8(10)
Mo(2)-C(25)	2.361(9)	C(20)-Mo(1)-C(4)	91.7(3)	C(2)-C(1)-C(5)	107.2(7)	C(37)-C(36)-C(35)	120.8(10)
Mo(2)-I(2)	2.8176(10)	C(21)-Mo(1)-C(4)	158.1(3)	C(2)-C(1)-P(1)	128.4(6)	C(36)-C(37)-C(38)	119.3(10)
P(1)-C(18)	1.777(8)	C(2)-Mo(1)-C(4)	58.9(3)	C(5)-C(1)-P(1)	123.1(6)	C(33)-C(38)-C(37)	120.8(9)
P(1)-C(1)	1.780(8)	C(1)-Mo(1)-C(4)	58.6(3)	C(2)-C(1)-Mo(1)	71.5(4)	O(4)-C(40)-Mo(2)	177.5(9)
P(1)-C(12)	1.785(9)	C(3)-Mo(1)-C(4)	34.8(3)	C(5)-C(1)-Mo(1)	74.4(4)	O(5)-C(41)-Mo(2)	177.2(9)
P(1)-C(6)	1.799(8)	C(19)-Mo(1)-C(5)	140.9(3)	P(1)-C(1)-Mo(1)	129.6(4)	O(6)-C(42)-Mo(2)	174.0(10)
P(2)-C(22)	1.775(9)	C(20)-Mo(1)-C(5)	109.4(3)	C(3)-C(2)-C(1)	107.0(8)	Cl(2)-C(43)-Cl(1)	111.8(5)
P(2)-C(27)	1.780(9)	C(21)-Mo(1)-C(5)	130.4(3)	C(3)-C(2)-Mo(1)	72.9(5)		
P(2)-C(33)	1.784(9)	C(2)-Mo(1)-C(5)	59.4(3)	C(1)-C(2)-Mo(1)	72.2(4)		
P(2)-C(39)	1.789(8)	C(1)-Mo(1)-C(5)	35.8(3)	C(4)-C(3)-C(2)	108.1(7)		
O(1)-C(19)	1.134(10)	C(3)-Mo(1)-C(5)	58.1(3)	C(4)-C(3)-Mo(1)	74.0(5)		
O(2)-C(20)	1.126(10)	C(4)-Mo(1)-C(5)	34.1(3)	C(2)-C(3)-Mo(1)	71.1(5)		
O(3)-C(21)	1.115(9)	C(19)-Mo(1)-I(1)	131.5(3)	C(5)-C(4)-C(3)	109.7(8)		
O(4)-C(40)	1.120(10)	C(20)-Mo(1)-I(1)	75.1(2)	C(5)-C(4)-Mo(1)	73.4(5)		
O(5)-C(41)	1.124(10)	C(21)-Mo(1)-I(1)	76.4(3)	C(3)-C(4)-Mo(1)	71.2(5)		
O(6)-C(42)	1.088(11)	C(2)-Mo(1)-I(1)	132.7(2)	C(4)-C(5)-C(1)	107.9(7)		
C(1)-C(2)	1.436(10)	C(1)-Mo(1)-I(1)	96.9(2)	C(4)-C(5)-Mo(1)	72.6(5)		
C(1)-C(5)	1.440(10)	C(3)-Mo(1)-I(1)	143.2(2)	C(1)-C(5)-Mo(1)	69.8(4)		
C(2)-C(3)	1.428(11)	C(4)-Mo(1)-I(1)	109.8(2)	C(7)-C(6)-C(11)	120.0(8)		
C(3)-C(4)	1.401(11)	C(5)-Mo(1)-I(1)	86.0(2)	C(7)-C(6)-P(1)	122.8(7)		
C(4)-C(5)	1.385(11)	C(41)-Mo(2)-C(40)	79.5(4)	C(11)-C(6)-P(1)	117.2(6)		
C(6)-C(7)	1.373(11)	C(41)-Mo(2)-C(42)	75.4(4)	C(6)-C(7)-C(8)	120.1(8)		
C(6)-C(11)	1.399(11)	C(40)-Mo(2)-C(42)	107.0(4)	C(9)-C(8)-C(7)	120.5(9)		
C(7)-C(8)	1.398(12)	C(41)-Mo(2)-C(23)	88.5(4)	C(8)-C(9)-C(10)	119.9(9)		
C(8)-C(9)	1.336(12)	C(40)-Mo(2)-C(23)	140.2(3)	C(11)-C(10)-C(9)	121.2(9)		
C(9)-C(10)	1.390(12)	C(42)-Mo(2)-C(23)	106.3(4)	C(10)-C(11)-C(6)	118.3(8)		
C(10)-C(11)	1.381(12)	C(41)-Mo(2)-C(24)	85.1(4)	C(17)-C(12)-C(13)	119.1(8)		
C(12)-C(17)	1.387(11)	C(40)-Mo(2)-C(24)	104.8(3)	C(17)-C(12)-P(1)	120.4(6)		
C(12)-C(13)	1.407(11)	C(42)-Mo(2)-C(24)	138.5(4)	C(13)-C(12)-P(1)	120.3(6)		
C(13)-C(14)	1.381(12)	C(23)-Mo(2)-C(24)	35.9(3)	C(14)-C(13)-C(12)	119.6(9)		
C(14)-C(15)	1.357(12)	C(41)-Mo(2)-C(22)	122.4(3)	C(15)-C(14)-C(13)	120.0(9)		
C(15)-C(16)	1.343(12)	C(40)-Mo(2)-C(22)	148.6(3)	C(16)-C(15)-C(14)	121.2(9)		
C(16)-C(17)	1.389(12)	C(42)-Mo(2)-C(22)	100.8(3)	C(15)-C(16)-C(17)	121.1(9)		
C(22)-C(26)	1.412(11)	C(23)-Mo(2)-C(22)	36.3(3)	C(12)-C(17)-C(16)	119.0(9)		
C(22)-C(23)	1.437(11)	C(24)-Mo(2)-C(22)	59.9(3)	O(1)-C(19)-Mo(1)	178.3(9)		
C(23)-C(24)	1.418(12)	C(41)-Mo(2)-C(26)	142.8(4)	O(2)-C(20)-Mo(1)	174.2(8)		
C(24)-C(25)	1.386(12)	C(40)-Mo(2)-C(26)	113.6(3)	O(3)-C(21)-Mo(1)	178.1(8)		
C(25)-C(26)	1.415(11)	C(42)-Mo(2)-C(26)	127.2(3)	C(26)-C(22)-C(23)	106.2(8)		
C(27)-C(28)	1.368(12)	C(23)-Mo(2)-C(26)	58.7(3)	C(26)-C(22)-P(2)	127.9(7)		
C(27)-C(32)	1.378(12)	C(24)-Mo(2)-C(26)	58.3(3)	C(23)-C(22)-P(2)	125.1(7)		
C(28)-C(29)	1.384(12)	C(22)-Mo(2)-C(26)	35.2(3)	C(26)-C(22)-Mo(2)	73.9(5)		
C(29)-C(30)	1.377(13)	C(41)-Mo(2)-C(25)	114.7(4)	C(23)-C(22)-Mo(2)	70.8(5)		

C(30)-C(31)	1.371(13)	C(40)-Mo(2)-C(25)	92.5(3)	P(2)-C(22)-Mo(2)	127.7(4)
C(31)-C(32)	1.384(12)	C(42)-Mo(2)-C(25)	159.6(3)	C(24)-C(23)-C(22)	108.1(8)
C(33)-C(38)	1.364(11)	C(23)-Mo(2)-C(25)	58.4(3)	C(24)-C(23)-Mo(2)	72.8(5)
C(33)-C(34)	1.402(12)	C(24)-Mo(2)-C(25)	34.5(3)	C(22)-C(23)-Mo(2)	72.8(5)
C(34)-C(35)	1.382(13)	C(22)-Mo(2)-C(25)	58.9(3)	C(25)-C(24)-C(23)	108.3(8)
C(35)-C(36)	1.367(14)	C(26)-Mo(2)-C(25)	34.9(3)	C(25)-C(24)-Mo(2)	74.7(5)
C(36)-C(37)	1.358(14)	C(41)-Mo(2)-I(2)	133.1(3)	C(23)-C(24)-Mo(2)	71.3(5)
C(37)-C(38)	1.387(13)	C(40)-Mo(2)-I(2)	74.8(3)	C(24)-C(25)-C(26)	108.5(8)
C(43)-Cl(2)	1.734(10)	C(42)-Mo(2)-I(2)	75.6(3)	C(24)-C(25)-Mo(2)	70.8(5)
C(43)-Cl(1)	1.746(11)	C(23)-Mo(2)-I(2)	135.0(2)	C(26)-C(25)-Mo(2)	72.4(5)

Table 28. Anisotropic displacement parameters ($Å^2 x\ 10^3$) for **VI**. The anisotropic displacement factor exponent takes the form: $-2\pi^2[\ h^2\ a^{*2}U^{11} + ... + 2\ h\ k\ a^*\ b^*\ U^{12}\ ]$

	U^{11}	U^{22}	U^{33}	U^{23}	U^{13}	U^{12}
Mo(1)	35(1)	24(1)	26(1)	10(1)	5(1)	-1(1)
Mo(2)	43(1)	26(1)	30(1)	8(1)	5(1)	-5(1)
I(1)	55(1)	40(1)	47(1)	19(1)	22(1)	-3(1)
I(2)	80(1)	46(1)	31(1)	13(1)	9(1)	-10(1)
I(3)	41(1)	34(1)	49(1)	7(1)	7(1)	-3(1)
I(4)	55(1)	29(1)	39(1)	7(1)	-3(1)	2(1)
P(1)	31(1)	24(1)	29(1)	10(1)	5(1)	-2(1)
P(2)	40(1)	27(1)	29(1)	8(1)	6(1)	-6(1)
O(1)	39(4)	60(5)	55(5)	15(4)	0(3)	-2(4)
O(2)	61(4)	31(4)	61(5)	18(4)	12(4)	5(3)
O(3)	78(5)	50(5)	38(4)	1(4)	8(4)	-4(4)
O(4)	87(5)	31(4)	48(5)	1(4)	-6(4)	-14(4)
O(5)	72(5)	62(5)	76(6)	12(4)	31(5)	-13(4)
O(6)	59(5)	42(5)	97(6)	-1(5)	3(4)	22(4)
C(1)	33(5)	31(5)	20(5)	13(4)	2(4)	4(4)
C(2)	47(5)	29(5)	32(5)	13(4)	16(4)	-4(4)
C(3)	35(5)	43(6)	29(5)	15(4)	9(4)	7(4)
C(4)	57(6)	25(5)	21(5)	9(4)	2(4)	-2(5)
C(5)	40(5)	22(5)	22(5)	4(4)	5(4)	-1(4)
C(6)	32(4)	28(5)	23(5)	12(4)	1(4)	-2(4)
C(7)	59(6)	39(6)	43(6)	14(5)	14(5)	20(5)
C(8)	78(7)	56(7)	35(6)	21(5)	16(6)	12(6)
C(9)	50(6)	44(7)	42(6)	16(5)	2(5)	1(5)
C(10)	48(6)	28(5)	50(7)	7(5)	-2(5)	4(4)
C(11)	44(5)	35(6)	27(5)	9(4)	8(4)	8(4)
C(12)	32(5)	26(5)	32(5)	15(4)	7(4)	0(4)
C(13)	44(5)	44(6)	37(6)	-1(5)	10(5)	-4(5)
C(14)	62(6)	37(6)	51(7)	-6(5)	9(6)	-14(5)
C(15)	50(6)	46(6)	23(5)	6(5)	-1(5)	3(5)
C(16)	43(6)	64(7)	24(5)	9(5)	7(5)	5(5)
C(17)	38(5)	57(7)	32(6)	17(5)	9(5)	3(5)
C(18)	30(5)	34(5)	42(6)	10(4)	6(4)	-8(4)
C(19)	56(6)	35(6)	33(6)	13(5)	8(5)	2(5)
C(20)	44(5)	43(6)	27(5)	3(5)	8(4)	-8(5)
C(21)	50(6)	31(6)	31(6)	7(5)	5(5)	1(5)
C(22)	47(5)	28(5)	19(5)	9(4)	5(4)	0(4)
C(23)	49(5)	38(6)	28(5)	7(4)	-3(5)	-4(5)
C(24)	61(6)	34(6)	27(5)	14(4)	-1(5)	-5(5)
C(25)	49(6)	28(5)	42(6)	7(5)	-3(5)	-2(5)
C(26)	44(5)	28(5)	29(5)	12(4)	0(4)	5(4)
C(27)	47(5)	25(5)	30(5)	5(4)	4(4)	-2(4)
C(28)	75(7)	30(6)	43(6)	9(5)	1(6)	-4(5)
C(29)	75(7)	32(6)	44(6)	17(5)	-10(6)	8(6)
C(30)	47(6)	63(8)	37(6)	11(6)	-3(5)	5(6)
C(31)	49(6)	51(7)	65(8)	13(6)	-4(6)	-13(5)
C(32)	50(6)	41(6)	56(7)	15(5)	-8(5)	1(5)
C(33)	37(5)	29(5)	30(5)	7(4)	3(4)	-11(4)
C(34)	63(6)	35(6)	39(6)	10(5)	2(5)	-14(5)
C(35)	87(8)	43(7)	35(6)	18(5)	-11(6)	-21(6)
C(36)	91(9)	58(8)	41(7)	12(6)	19(7)	-39(7)

C(37)	56(6)	56(7)	44(7)	-7(6)	15(5)	-12(6)
C(38)	56(6)	38(6)	35(6)	9(5)	5(5)	-16(5)
C(39)	52(6)	35(6)	36(6)	7(4)	18(5)	-4(5)
C(40)	59(6)	34(6)	44(6)	18(5)	14(5)	-5(5)
C(41)	51(6)	39(6)	53(7)	4(5)	16(6)	-3(5)
C(42)	45(6)	53(7)	59(7)	12(6)	7(5)	-5(5)
C(43)	44(6)	36(6)	107(10)	1(6)	20(6)	10(5)
Cl(1)	113(2)	62(2)	77(2)	8(2)	16(2)	-24(2)
Cl(2)	167(3)	76(2)	88(3)	38(2)	64(3)	36(2)

Table 29. Hydrogen coordinates (x 10^4) and isotropic displacement parameters ($Å^2$x 10^3) for **VI**.

	x	y	z	U(eq)
H(2A)	11427	8853	1650	41
H(3A)	12288	7535	949	41
H(4A)	10158	6489	624	42
H(5A)	7957	7107	1088	34
H(7A)	8646	8930	182	55
H(8A)	8002	9821	-858	65
H(9A)	6562	10902	-684	55
H(10A)	5863	11179	569	52
H(11A)	6523	10327	1635	42
H(13A)	10588	9981	2439	50
H(14A)	11363	10859	3636	61
H(15A)	9954	10991	4606	49
H(16A)	7901	10197	4475	52
H(17A)	7137	9243	3335	50
H(18A)	6725	7977	2334	53
H(18B)	6113	8009	1358	53
H(18C)	5744	8717	1990	53
H(23A)	3892	6414	-1899	48
H(24A)	3584	4860	-2237	50
H(25A)	5036	4440	-3325	50
H(26A)	6242	5725	-3694	41
H(28A)	7809	6293	-1839	62
H(29A)	10204	6414	-1042	64
H(30A)	11463	7661	-806	61
H(31A)	10293	8798	-1348	68
H(32A)	7918	8668	-2172	62
H(34A)	4301	8458	-3954	56
H(35A)	4623	8789	-5242	70
H(36A)	6539	8268	-5766	75
H(37A)	8116	7368	-5056	62
H(38A)	7829	7027	-3766	52
H(39A)	3677	8029	-2685	59
H(39B)	5044	8621	-2247	59
H(39C)	4601	7887	-1775	59
H(43A)	13649	4453	-18	75
H(43B)	13710	5416	-57	75

Table 30. Torsion angles [°] for **VI**.

C(18)-P(1)-C(1)-C(2)	-174.8(7)	C(18)-P(1)-C(6)-C(7)	-106.2(8)	C(41)-Mo(2)-C(24)-C(25)	150.0(6)
C(12)-P(1)-C(1)-C(2)	-51.1(8)	C(1)-P(1)-C(6)-C(7)	10.7(8)	C(40)-Mo(2)-C(24)-C(25)	72.3(6)
C(6)-P(1)-C(1)-C(2)	67.2(8)	C(12)-P(1)-C(6)-C(7)	134.0(7)	C(42)-Mo(2)-C(24)-C(25)	-148.5(6)
C(18)-P(1)-C(1)-C(5)	19.7(8)	C(18)-P(1)-C(6)-C(11)	70.8(7)	C(23)-Mo(2)-C(24)-C(25)	-115.8(8)
C(12)-P(1)-C(1)-C(5)	143.4(6)	C(1)-P(1)-C(6)-C(11)	-172.3(6)	C(22)-Mo(2)-C(24)-C(25)	-77.8(6)
C(6)-P(1)-C(1)-C(5)	-98.2(7)	C(12)-P(1)-C(6)-C(11)	-49.0(7)	C(26)-Mo(2)-C(24)-C(25)	-36.6(5)
C(18)-P(1)-C(1)-Mo(1)	-77.3(6)	C(11)-C(6)-C(7)-C(8)	1.3(14)	I(2)-Mo(2)-C(24)-C(25)	-11.6(7)
C(12)-P(1)-C(1)-Mo(1)	46.4(7)	P(1)-C(6)-C(7)-C(8)	178.3(7)	C(41)-Mo(2)-C(24)-C(23)	-94.1(6)
C(6)-P(1)-C(1)-Mo(1)	164.8(5)	C(6)-C(7)-C(8)-C(9)	-2.2(15)	C(40)-Mo(2)-C(24)-C(23)	-171.9(6)
C(19)-Mo(1)-C(1)-C(2)	12.7(6)	C(7)-C(8)-C(9)-C(10)	2.1(15)	C(42)-Mo(2)-C(24)-C(23)	-32.7(8)
C(20)-Mo(1)-C(1)-C(2)	-114.3(6)	C(8)-C(9)-C(10)-C(11)	-1.3(14)	C(22)-Mo(2)-C(24)-C(23)	38.0(5)
C(21)-Mo(1)-C(1)-C(2)	94.6(5)	C(9)-C(10)-C(11)-C(6)	0.5(13)	C(26)-Mo(2)-C(24)-C(23)	79.2(6)

C(3)-Mo(1)-C(1)-C(2)	-38.2(5)	C(7)-C(6)-C(11)-C(10)	-0.5(12)	C(25)-Mo(2)-C(24)-C(23)	115.8(8)
C(4)-Mo(1)-C(1)-C(2)	-79.0(5)	P(1)-C(6)-C(11)-C(10)	-177.6(7)	I(2)-Mo(2)-C(24)-C(23)	104.3(5)
C(5)-Mo(1)-C(1)-C(2)	-114.7(7)	C(18)-P(1)-C(12)-C(17)	-5.5(8)	C(23)-C(24)-C(25)-C(26)	-0.8(10)
I(1)-Mo(1)-C(1)-C(2)	172.0(4)	C(1)-P(1)-C(12)-C(17)	-128.0(7)	Mo(2)-C(24)-C(25)-C(26)	63.0(6)
C(19)-Mo(1)-C(1)-C(5)	127.3(5)	C(6)-P(1)-C(12)-C(17)	113.6(7)	C(23)-C(24)-C(25)-Mo(2)	-63.8(6)
C(20)-Mo(1)-C(1)-C(5)	0.4(8)	C(18)-P(1)-C(12)-C(13)	-179.4(7)	C(41)-Mo(2)-C(25)-C(24)	-33.3(6)
C(21)-Mo(1)-C(1)-C(5)	-150.7(5)	C(1)-P(1)-C(12)-C(13)	58.2(8)	C(40)-Mo(2)-C(25)-C(24)	-112.8(6)
C(2)-Mo(1)-C(1)-C(5)	114.7(7)	C(6)-P(1)-C(12)-C(13)	-60.2(7)	C(42)-Mo(2)-C(25)-C(24)	83.2(12)
C(3)-Mo(1)-C(1)-C(5)	76.5(5)	C(17)-C(12)-C(13)-C(14)	1.1(13)	C(23)-Mo(2)-C(25)-C(24)	38.2(5)
C(4)-Mo(1)-C(1)-C(5)	35.7(4)	P(1)-C(12)-C(13)-C(14)	175.0(7)	C(22)-Mo(2)-C(25)-C(24)	81.0(6)
I(1)-Mo(1)-C(1)-C(5)	-73.3(4)	C(12)-C(13)-C(14)-C(15)	-3.0(14)	C(26)-Mo(2)-C(25)-C(24)	117.5(8)
C(19)-Mo(1)-C(1)-P(1)	-112.3(6)	C(13)-C(14)-C(15)-C(16)	2.7(15)	I(2)-Mo(2)-C(25)-C(24)	172.2(5)
C(20)-Mo(1)-C(1)-P(1)	120.7(6)	C(14)-C(15)-C(16)-C(17)	-0.5(14)	C(41)-Mo(2)-C(25)-C(26)	-150.8(5)
C(21)-Mo(1)-C(1)-P(1)	-30.4(6)	C(13)-C(12)-C(17)-C(16)	1.1(12)	C(40)-Mo(2)-C(25)-C(26)	129.6(6)
C(2)-Mo(1)-C(1)-P(1)	-125.0(8)	P(1)-C(12)-C(17)-C(16)	-172.9(7)	C(42)-Mo(2)-C(25)-C(26)	-34.4(14)
C(3)-Mo(1)-C(1)-P(1)	-163.2(7)	C(15)-C(16)-C(17)-C(12)	-1.4(13)	C(23)-Mo(2)-C(25)-C(26)	-79.3(6)
C(4)-Mo(1)-C(1)-P(1)	156.0(7)	C(20)-Mo(1)-C(19)-O(1)	30(30)	C(24)-Mo(2)-C(25)-C(26)	-117.5(8)
C(5)-Mo(1)-C(1)-P(1)	120.3(8)	C(21)-Mo(1)-C(19)-O(1)	145(30)	C(22)-Mo(2)-C(25)-C(26)	-36.5(5)
I(1)-Mo(1)-C(1)-P(1)	47.0(5)	C(2)-Mo(1)-C(19)-O(1)	-114(30)	I(2)-Mo(2)-C(25)-C(26)	54.6(5)
C(5)-C(1)-C(2)-C(3)	-1.3(9)	C(1)-Mo(1)-C(19)-O(1)	-122(30)	C(23)-C(22)-C(26)-C(25)	0.7(9)
P(1)-C(1)-C(2)-C(3)	-168.6(6)	C(3)-Mo(1)-C(19)-O(1)	-79(30)	P(2)-C(22)-C(26)-C(25)	171.2(6)
Mo(1)-C(1)-C(2)-C(3)	65.1(6)	C(4)-Mo(1)-C(19)-O(1)	-57(30)	Mo(2)-C(22)-C(26)-C(25)	-63.2(6)
C(5)-C(1)-C(2)-Mo(1)	-66.4(5)	C(5)-Mo(1)-C(19)-O(1)	-74(30)	C(23)-C(22)-C(26)-Mo(2)	63.9(5)
P(1)-C(1)-C(2)-Mo(1)	126.3(7)	I(1)-Mo(1)-C(19)-O(1)	86(30)	P(2)-C(22)-C(26)-Mo(2)	-125.6(7)
C(19)-Mo(1)-C(2)-C(3)	75.2(5)	C(19)-Mo(1)-C(20)-O(2)	-84(8)	C(24)-C(25)-C(26)-C(22)	0.1(10)
C(20)-Mo(1)-C(2)-C(3)	4.9(8)	C(21)-Mo(1)-C(20)-O(2)	-155(8)	Mo(2)-C(25)-C(26)-C(22)	62.1(6)
C(21)-Mo(1)-C(2)-C(3)	152.7(5)	C(2)-Mo(1)-C(20)-O(2)	-9(8)	C(24)-C(25)-C(26)-Mo(2)	-62.0(6)
C(1)-Mo(1)-C(2)-C(3)	-114.8(7)	C(1)-Mo(1)-C(20)-O(2)	55(8)	C(41)-Mo(2)-C(26)-C(22)	-70.6(7)
C(4)-Mo(1)-C(2)-C(3)	-36.8(5)	C(3)-Mo(1)-C(20)-O(2)	-6(8)	C(40)-Mo(2)-C(26)-C(22)	-174.9(5)
C(5)-Mo(1)-C(2)-C(3)	-76.7(5)	C(4)-Mo(1)-C(20)-O(2)	26(8)	C(42)-Mo(2)-C(26)-C(22)	47.9(7)
I(1)-Mo(1)-C(2)-C(3)	-125.7(4)	C(5)-Mo(1)-C(20)-O(2)	56(8)	C(23)-Mo(2)-C(26)-C(22)	-39.2(5)
C(19)-Mo(1)-C(2)-C(1)	-170.0(5)	I(1)-Mo(1)-C(20)-O(2)	136(8)	C(24)-Mo(2)-C(26)-C(22)	-81.6(5)
C(20)-Mo(1)-C(2)-C(1)	119.7(6)	C(19)-Mo(1)-C(21)-O(3)	92(25)	C(25)-Mo(2)-C(26)-C(22)	-117.8(8)
C(21)-Mo(1)-C(2)-C(1)	-92.5(5)	C(20)-Mo(1)-C(21)-O(3)	163(25)	I(2)-Mo(2)-C(26)-C(22)	114.6(5)
C(3)-Mo(1)-C(2)-C(1)	114.8(7)	C(2)-Mo(1)-C(21)-O(3)	3(25)	C(41)-Mo(2)-C(26)-C(25)	47.2(8)
C(4)-Mo(1)-C(2)-C(1)	78.1(5)	C(1)-Mo(1)-C(21)-O(3)	-34(25)	C(40)-Mo(2)-C(26)-C(25)	-57.1(6)
C(5)-Mo(1)-C(2)-C(1)	38.2(4)	C(3)-Mo(1)-C(21)-O(3)	24(25)	C(42)-Mo(2)-C(26)-C(25)	165.7(6)
I(1)-Mo(1)-C(2)-C(1)	-10.8(6)	C(4)-Mo(1)-C(21)-O(3)	-19(26)	C(23)-Mo(2)-C(26)-C(25)	78.5(6)
C(1)-C(2)-C(3)-C(4)	0.7(9)	C(5)-Mo(1)-C(21)-O(3)	-56(25)	C(24)-Mo(2)-C(26)-C(25)	36.2(5)
Mo(1)-C(2)-C(3)-C(4)	65.3(6)	I(1)-Mo(1)-C(21)-O(3)	-129(25)	C(22)-Mo(2)-C(26)-C(25)	117.8(8)
C(1)-C(2)-C(3)-Mo(1)	-64.6(5)	C(27)-P(2)-C(22)-C(26)	-75.4(8)	I(2)-Mo(2)-C(26)-C(25)	-127.6(5)
C(19)-Mo(1)-C(3)-C(4)	140.7(5)	C(33)-P(2)-C(22)-C(26)	41.9(9)	C(22)-P(2)-C(27)-C(28)	2.1(9)
C(20)-Mo(1)-C(3)-C(4)	66.9(5)	C(39)-P(2)-C(22)-C(26)	165.6(7)	C(33)-P(2)-C(27)-C(28)	-117.4(8)
C(21)-Mo(1)-C(3)-C(4)	-153.4(5)	C(27)-P(2)-C(22)-C(23)	93.5(8)	C(39)-P(2)-C(27)-C(28)	120.5(8)
C(2)-Mo(1)-C(3)-C(4)	-116.1(7)	C(33)-P(2)-C(22)-C(23)	-149.2(7)	C(22)-P(2)-C(27)-C(32)	179.6(7)
C(1)-Mo(1)-C(3)-C(4)	-77.6(5)	C(39)-P(2)-C(22)-C(23)	-25.6(8)	C(33)-P(2)-C(27)-C(32)	60.1(8)
C(5)-Mo(1)-C(3)-C(4)	-35.5(5)	C(27)-P(2)-C(22)-Mo(2)	-174.5(5)	C(39)-P(2)-C(27)-C(32)	-62.1(9)
I(1)-Mo(1)-C(3)-C(4)	-21.2(7)	C(33)-P(2)-C(22)-Mo(2)	-57.2(6)	C(32)-C(27)-C(28)-C(29)	-1.2(14)

C(19)-Mo(1)-C(3)-C(2)	-103.2(5)	C(39)-P(2)-C(22)-Mo(2)	66.5(6)	P(2)-C(27)-C(28)-C(29)	176.3(7)
C(20)-Mo(1)-C(3)-C(2)	-177.0(5)	C(41)-Mo(2)-C(22)-C(26)	137.5(5)	C(27)-C(28)-C(29)-C(30)	0.7(15)
C(21)-Mo(1)-C(3)-C(2)	-37.2(7)	C(40)-Mo(2)-C(22)-C(26)	8.9(9)	C(28)-C(29)-C(30)-C(31)	0.7(16)
C(1)-Mo(1)-C(3)-C(2)	38.5(5)	C(42)-Mo(2)-C(22)-C(26)	-143.0(5)	C(29)-C(30)-C(31)-C(32)	-1.5(16)
C(4)-Mo(1)-C(3)-C(2)	116.1(7)	C(23)-Mo(2)-C(22)-C(26)	114.1(7)	C(28)-C(27)-C(32)-C(31)	0.3(15)
C(5)-Mo(1)-C(3)-C(2)	80.6(5)	C(24)-Mo(2)-C(22)-C(26)	76.5(5)	P(2)-C(27)-C(32)-C(31)	-177.2(8)
I(1)-Mo(1)-C(3)-C(2)	95.0(6)	C(25)-Mo(2)-C(22)-C(26)	36.3(5)	C(30)-C(31)-C(32)-C(27)	1.0(16)
C(2)-C(3)-C(4)-C(5)	0.3(9)	I(2)-Mo(2)-C(22)-C(26)	-66.1(5)	C(22)-P(2)-C(33)-C(38)	-73.6(7)
Mo(1)-C(3)-C(4)-C(5)	63.7(6)	C(41)-Mo(2)-C(22)-C(23)	23.5(7)	C(27)-P(2)-C(33)-C(38)	44.7(8)
C(2)-C(3)-C(4)-Mo(1)	-63.4(6)	C(40)-Mo(2)-C(22)-C(23)	-105.1(7)	C(39)-P(2)-C(33)-C(38)	165.1(7)
C(19)-Mo(1)-C(4)-C(5)	-160.2(5)	C(42)-Mo(2)-C(22)-C(23)	102.9(6)	C(22)-P(2)-C(33)-C(34)	106.6(7)
C(20)-Mo(1)-C(4)-C(5)	123.2(5)	C(24)-Mo(2)-C(22)-C(23)	-37.6(5)	C(27)-P(2)-C(33)-C(34)	-135.1(7)
C(21)-Mo(1)-C(4)-C(5)	-54.7(11)	C(26)-Mo(2)-C(22)-C(23)	-114.1(7)	C(39)-P(2)-C(33)-C(34)	-14.7(8)
C(2)-Mo(1)-C(4)-C(5)	-80.3(5)	C(25)-Mo(2)-C(22)-C(23)	-77.8(5)	C(38)-C(33)-C(34)-C(35)	0.5(13)
C(1)-Mo(1)-C(4)-C(5)	-37.5(5)	I(2)-Mo(2)-C(22)-C(23)	179.8(5)	P(2)-C(33)-C(34)-C(35)	-179.7(7)
C(3)-Mo(1)-C(4)-C(5)	-118.3(7)	C(41)-Mo(2)-C(22)-P(2)	-96.6(6)	C(33)-C(34)-C(35)-C(36)	-0.8(14)
I(1)-Mo(1)-C(4)-C(5)	48.4(5)	C(40)-Mo(2)-C(22)-P(2)	134.8(6)	C(34)-C(35)-C(36)-C(37)	1.2(15)
C(19)-Mo(1)-C(4)-C(3)	-41.9(6)	C(42)-Mo(2)-C(22)-P(2)	-17.1(6)	C(35)-C(36)-C(37)-C(38)	-1.3(15)
C(20)-Mo(1)-C(4)-C(3)	-118.5(5)	C(23)-Mo(2)-C(22)-P(2)	-120.1(8)	C(34)-C(33)-C(38)-C(37)	-0.6(13)
C(21)-Mo(1)-C(4)-C(3)	63.6(11)	C(24)-Mo(2)-C(22)-P(2)	-157.6(7)	P(2)-C(33)-C(38)-C(37)	179.6(7)
C(2)-Mo(1)-C(4)-C(3)	38.0(5)	C(26)-Mo(2)-C(22)-P(2)	125.9(8)	C(36)-C(37)-C(38)-C(33)	1.0(14)
C(1)-Mo(1)-C(4)-C(3)	80.8(5)	C(25)-Mo(2)-C(22)-P(2)	162.1(7)	C(41)-Mo(2)-C(40)-O(4)	-141(19)
C(5)-Mo(1)-C(4)-C(3)	118.3(7)	I(2)-Mo(2)-C(22)-P(2)	59.7(5)	C(42)-Mo(2)-C(40)-O(4)	148(19)
I(1)-Mo(1)-C(4)-C(3)	166.7(4)	C(26)-C(22)-C(23)-C(24)	-1.2(9)	C(23)-Mo(2)-C(40)-O(4)	-67(20)
C(3)-C(4)-C(5)-C(1)	-1.1(9)	P(2)-C(22)-C(23)-C(24)	-172.1(6)	C(24)-Mo(2)-C(40)-O(4)	-59(19)
Mo(1)-C(4)-C(5)-C(1)	61.2(5)	Mo(2)-C(22)-C(23)-C(24)	64.8(6)	C(22)-Mo(2)-C(40)-O(4)	-3(20)
C(3)-C(4)-C(5)-Mo(1)	-62.3(6)	C(26)-C(22)-C(23)-Mo(2)	-66.0(6)	C(26)-Mo(2)-C(40)-O(4)	2(19)
C(2)-C(1)-C(5)-C(4)	1.5(9)	P(2)-C(22)-C(23)-Mo(2)	123.1(6)	C(25)-Mo(2)-C(40)-O(4)	-26(19)
P(1)-C(1)-C(5)-C(4)	169.6(6)	C(41)-Mo(2)-C(23)-C(24)	83.8(6)	I(2)-Mo(2)-C(40)-O(4)	78(19)
Mo(1)-C(1)-C(5)-C(4)	-63.0(6)	C(40)-Mo(2)-C(23)-C(24)	12.3(8)	C(40)-Mo(2)-C(41)-O(5)	-112(20)
C(2)-C(1)-C(5)-Mo(1)	64.5(5)	C(42)-Mo(2)-C(23)-C(24)	158.1(6)	C(42)-Mo(2)-C(41)-O(5)	-2(20)
P(1)-C(1)-C(5)-Mo(1)	-127.4(6)	C(22)-Mo(2)-C(23)-C(24)	-115.9(8)	C(23)-Mo(2)-C(41)-O(5)	106(20)
C(19)-Mo(1)-C(5)-C(4)	30.3(8)	C(26)-Mo(2)-C(23)-C(24)	-77.9(6)	C(24)-Mo(2)-C(41)-O(5)	142(20)
C(20)-Mo(1)-C(5)-C(4)	-62.5(6)	C(25)-Mo(2)-C(23)-C(24)	-36.7(5)	C(22)-Mo(2)-C(41)-O(5)	92(20)
C(21)-Mo(1)-C(5)-C(4)	156.4(5)	I(2)-Mo(2)-C(23)-C(24)	-116.2(5)	C(26)-Mo(2)-C(41)-O(5)	132(20)
C(2)-Mo(1)-C(5)-C(4)	78.6(5)	C(41)-Mo(2)-C(23)-C(22)	-160.4(5)	C(25)-Mo(2)-C(41)-O(5)	160(20)
C(1)-Mo(1)-C(5)-C(4)	117.3(7)	C(40)-Mo(2)-C(23)-C(22)	128.2(6)	I(2)-Mo(2)-C(41)-O(5)	-55(20)
C(3)-Mo(1)-C(5)-C(4)	36.3(5)	C(42)-Mo(2)-C(23)-C(22)	-86.0(6)	C(41)-Mo(2)-C(42)-O(6)	58(9)
I(1)-Mo(1)-C(5)-C(4)	-135.1(5)	C(24)-Mo(2)-C(23)-C(22)	115.9(8)	C(40)-Mo(2)-C(42)-O(6)	132(9)
C(19)-Mo(1)-C(5)-C(1)	-87.0(6)	C(26)-Mo(2)-C(23)-C(22)	38.0(5)	C(23)-Mo(2)-C(42)-O(6)	-26(9)
C(20)-Mo(1)-C(5)-C(1)	-179.8(5)	C(25)-Mo(2)-C(23)-C(22)	79.2(5)	C(24)-Mo(2)-C(42)-O(6)	-7(9)
C(21)-Mo(1)-C(5)-C(1)	39.1(6)	I(2)-Mo(2)-C(23)-C(22)	-0.3(7)	C(22)-Mo(2)-C(42)-O(6)	-63(9)
C(2)-Mo(1)-C(5)-C(1)	-38.7(4)	C(22)-C(23)-C(24)-C(25)	1.3(10)	C(26)-Mo(2)-C(42)-O(6)	-89(9)
C(3)-Mo(1)-C(5)-C(1)	-81.0(5)	Mo(2)-C(23)-C(24)-C(25)	66.1(6)	C(25)-Mo(2)-C(42)-O(6)	-65(9)
C(4)-Mo(1)-C(5)-C(1)	-117.3(7)	C(22)-C(23)-C(24)-Mo(2)	-64.8(6)	I(2)-Mo(2)-C(42)-O(6)	-159(9)

Figure 5. The molecular structure of **VI**.

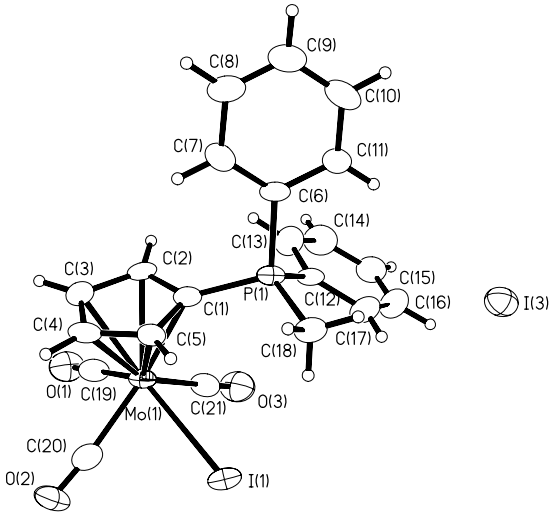

Table 31. Crystal data and structure refinement for **$[III_2][B(C_6F_5)_4]_2$**.

Identification code	**$[III_2][B(C_6F_5)_4]_2$**	
Empirical formula	C93 H40 B2 Cl6 Cr2 F40 O6 P2	
Formula weight	2413.51	
Temperature	180(2) K	
Wavelength	0.71073 Å	
Crystal system	Triclinic	
Space group	P-1	
Unit cell dimensions	a = 9.8319(4) Å	α= 70.9350(10)°.
	b = 12.8275(6) Å	β= 83.1200(10)°.
	c = 19.6330(9) Å	γ = 88.6700(10)°.
Volume	2323.09(18) $Å^3$	
Z	1	
Density (calculated)	1.725 Mg/m^3	
Absorption coefficient	0.577 mm^{-1}	
F(000)	1196	
Crystal size	0.15 x 0.15 x 0.10 mm^3	
Theta range for data collection	2.09 to 25.00°.	
Index ranges	-11<=h<=11, -15<=k<=15, -23<=l<=23	
Reflections collected	16270	
Independent reflections	8129 [R(int) = 0.0191]	
Completeness to theta = 25.00°	99.3 %	
Absorption correction	Multiscan	
Max. and min. transmission	0.9445 and 0.9184	
Refinement method	Full-matrix least-squares on F^2	
Data / restraints / parameters	8129 / 2 / 738	
Goodness-of-fit on F^2	1.000	
Final R indices [I>2sigma(I)]	R1 = 0.0351, wR2 = 0.0940	
R indices (all data)	R1 = 0.0467, wR2 = 0.1023	
Largest diff. peak and hole	0.352 and -0.449 e.$Å^{-3}$	

Table 32. Atomic coordinates (x 10^4) and equivalent isotropic displacement parameters ($Å^2$x 10^3) for **$[III_2][B(C_6F_5)_4]_2$**. U(eq) is defined as one third of the trace of the orthogonalized U^{ij} tensor.

	x	y	z	U(eq)
P(1)	1506(1)	1611(1)	2335(1)	23(1)
B(1)	-2079(3)	6433(2)	2033(1)	24(1)
Cr(1)	-223(1)	618(1)	4127(1)	24(1)
O(1)	1316(2)	-1483(2)	4227(1)	40(1)
O(2)	-3032(2)	65(2)	4976(1)	49(1)
O(3)	-1819(2)	-248(2)	3214(1)	53(1)
C(1)	862(2)	1800(2)	3174(1)	23(1)

C(2)	1642(2)	1657(2)	3766(1)	29(1)
C(3)	853(3)	2043(2)	4281(1)	34(1)
C(4)	-417(3)	2395(2)	4032(1)	37(1)
C(5)	-417(2)	2256(2)	3348(1)	30(1)
C(6)	2362(2)	322(2)	2498(1)	28(1)
C(7)	3656(3)	224(2)	2731(1)	35(1)
C(8)	4299(3)	-785(2)	2903(2)	49(1)
C(9)	3666(4)	-1678(2)	2836(2)	56(1)
C(10)	2400(4)	-1590(2)	2597(2)	55(1)
C(11)	1726(3)	-585(2)	2427(1)	40(1)
C(12)	2691(2)	2716(2)	1856(1)	25(1)
C(13)	2554(3)	3718(2)	1980(1)	32(1)
C(14)	3415(3)	4597(2)	1578(2)	40(1)
C(15)	4419(3)	4469(2)	1062(2)	47(1)
C(16)	4564(3)	3478(3)	935(2)	49(1)
C(17)	3703(3)	2592(2)	1327(1)	38(1)
C(18)	111(3)	1679(2)	1813(1)	34(1)
C(19)	738(2)	-698(2)	4226(1)	29(1)
C(20)	-1928(3)	255(2)	4701(1)	33(1)
C(21)	-1199(3)	70(2)	3563(1)	35(1)
C(22)	-2945(2)	7579(2)	1714(1)	25(1)
C(23)	-2336(2)	8594(2)	1613(1)	29(1)
C(24)	-2930(3)	9603(2)	1317(1)	35(1)
C(25)	-4183(3)	9640(2)	1075(1)	34(1)
C(26)	-4829(2)	8670(2)	1142(1)	30(1)
C(27)	-4211(2)	7673(2)	1460(1)	27(1)
C(28)	-941(2)	6489(2)	1323(1)	24(1)
C(29)	439(2)	6759(2)	1220(1)	28(1)
C(30)	1315(2)	6807(2)	602(1)	31(1)
C(31)	816(2)	6585(2)	40(1)	30(1)
C(32)	-550(2)	6331(2)	101(1)	28(1)
C(33)	-1386(2)	6307(2)	722(1)	26(1)
C(34)	-3011(2)	5274(2)	2318(1)	24(1)
C(35)	-2669(2)	4299(2)	2184(1)	26(1)
C(36)	-3423(2)	3325(2)	2484(1)	30(1)
C(37)	-4568(2)	3280(2)	2966(1)	33(1)
C(38)	-4954(2)	4209(2)	3133(1)	33(1)
C(39)	-4176(2)	5163(2)	2813(1)	28(1)
C(40)	-1405(2)	6381(2)	2777(1)	25(1)
C(41)	-375(2)	5649(2)	3025(1)	27(1)
C(42)	243(2)	5541(2)	3641(1)	31(1)
C(43)	-201(3)	6183(2)	4063(1)	31(1)
C(44)	-1263(3)	6880(2)	3868(1)	31(1)
C(45)	-1844(2)	6965(2)	3245(1)	27(1)
C(46A)	-3958(16)	3418(8)	5343(4)	74(3)
C(46B)	-4911(17)	3362(8)	5215(5)	82(3)
C(47)	-1169(7)	10337(6)	-342(3)	57(2)
Cl(1A)	-3231(6)	4380(4)	4569(2)	63(1)
Cl(1B)	-3433(9)	4266(8)	4732(6)	133(3)
Cl(2A)	-4726(9)	2359(8)	5129(5)	148(3)
Cl(2B)	-4752(8)	2147(5)	5047(4)	97(2)
Cl(3)	-1794(2)	9087(1)	-274(1)	70(1)
Cl(4)	256(2)	10297(2)	134(1)	89(1)
F(23)	-1074(2)	8628(1)	1820(1)	39(1)
F(24)	-2278(2)	10547(1)	1261(1)	53(1)
F(25)	-4776(2)	10617(1)	774(1)	48(1)
F(26)	-6073(2)	8694(1)	919(1)	43(1)
F(27)	-4949(1)	6763(1)	1514(1)	35(1)
F(29)	1039(1)	7008(1)	1736(1)	40(1)
F(30)	2648(1)	7069(1)	543(1)	45(1)
F(31)	1656(2)	6607(1)	-556(1)	46(1)
F(32)	-1060(2)	6102(1)	-442(1)	39(1)
F(33)	-2720(1)	6066(1)	737(1)	34(1)
F(35)	-1522(1)	4226(1)	1745(1)	33(1)
F(36)	-3038(2)	2413(1)	2315(1)	41(1)
F(37)	-5292(2)	2328(1)	3273(1)	51(1)
F(38)	-6071(2)	4186(1)	3604(1)	52(1)
F(39)	-4599(1)	6041(1)	3019(1)	38(1)
F(41)	88(1)	4970(1)	2647(1)	36(1)
F(42)	1263(2)	4830(1)	3826(1)	47(1)

F(43)	383(2)	6113(1)	4662(1)	44(1)
F(44)	-1758(2)	7476(1)	4295(1)	44(1)
F(45)	-2896(1)	7671(1)	3116(1)	37(1)

Table 33. Bond lengths [Å] and angles [°] for **[III$_2$][B(C$_6$F$_5$)$_4$]$_2$**.

P(1)-C(1)	1.784(2)	C(36)-C(37)	1.371(3)	C(19)-Cr(1)-C(3)	118.48(10)	C(33)-C(28)-B(1)	119.01(19)
P(1)-C(12)	1.788(2)	C(37)-F(37)	1.349(3)	C(20)-Cr(1)-C(3)	113.07(10)	F(29)-C(29)-C(28)	121.0(2)
P(1)-C(6)	1.788(2)	C(37)-C(38)	1.369(4)	C(1)-Cr(1)-C(3)	62.48(8)	F(29)-C(29)-C(30)	114.6(2)
P(1)-C(18)	1.792(2)	C(38)-F(38)	1.344(3)	C(5)-Cr(1)-C(3)	61.87(9)	C(28)-C(29)-C(30)	124.5(2)
B(1)-C(40)	1.657(3)	C(38)-C(39)	1.379(3)	C(2)-Cr(1)-C(3)	36.92(9)	F(30)-C(30)-C(31)	119.3(2)
B(1)-C(22)	1.658(3)	C(39)-F(39)	1.357(3)	C(4)-Cr(1)-C(3)	36.55(10)	F(30)-C(30)-C(29)	121.1(2)
B(1)-C(34)	1.662(3)	C(40)-C(41)	1.385(3)	C(5)-C(1)-C(2)	107.2(2)	C(31)-C(30)-C(29)	119.6(2)
B(1)-C(28)	1.662(3)	C(40)-C(45)	1.389(3)	C(5)-C(1)-P(1)	127.62(18)	F(31)-C(31)-C(32)	120.7(2)
Cr(1)-C(21)	1.853(3)	C(41)-F(41)	1.358(3)	C(2)-C(1)-P(1)	124.65(18)	F(31)-C(31)-C(30)	120.4(2)
Cr(1)-C(19)	1.880(3)	C(41)-C(42)	1.383(3)	C(5)-C(1)-Cr(1)	71.38(13)	C(32)-C(31)-C(30)	118.9(2)
Cr(1)-C(20)	1.880(3)	C(42)-F(42)	1.342(3)	C(2)-C(1)-Cr(1)	72.13(13)	F(32)-C(32)-C(31)	119.9(2)
Cr(1)-C(1)	2.164(2)	C(42)-C(43)	1.377(3)	P(1)-C(1)-Cr(1)	128.20(11)	F(32)-C(32)-C(33)	120.7(2)
Cr(1)-C(5)	2.178(2)	C(43)-F(43)	1.346(3)	C(3)-C(2)-C(1)	107.7(2)	C(31)-C(32)-C(33)	119.4(2)
Cr(1)-C(2)	2.197(2)	C(43)-C(44)	1.366(3)	C(3)-C(2)-Cr(1)	73.72(13)	F(33)-C(33)-C(32)	115.83(19)
Cr(1)-C(4)	2.230(2)	C(44)-F(44)	1.352(3)	C(1)-C(2)-Cr(1)	69.64(12)	F(33)-C(33)-C(28)	119.4(2)
Cr(1)-C(3)	2.253(2)	C(44)-C(45)	1.382(3)	C(4)-C(3)-C(2)	108.8(2)	C(32)-C(33)-C(28)	124.8(2)
O(1)-C(19)	1.145(3)	C(45)-F(45)	1.351(3)	C(4)-C(3)-Cr(1)	70.83(14)	C(35)-C(34)-C(39)	112.7(2)
O(2)-C(20)	1.146(3)	C(46A)-Cl(1A)	1.703(8)	C(2)-C(3)-Cr(1)	69.36(13)	C(35)-C(34)-B(1)	126.5(2)
O(3)-C(21)	1.142(3)	C(46A)-Cl(2A)	1.757(13)	C(3)-C(4)-C(5)	108.0(2)	C(39)-C(34)-B(1)	120.39(19)
C(1)-C(5)	1.425(3)	C(46B)-Cl(2B)	1.695(10)	C(3)-C(4)-Cr(1)	72.62(14)	F(35)-C(35)-C(36)	114.2(2)
C(1)-C(2)	1.428(3)	C(46B)-Cl(1B)	1.840(13)	C(5)-C(4)-Cr(1)	69.33(13)	F(35)-C(35)-C(34)	121.4(2)
C(2)-C(3)	1.410(3)	C(47)-Cl(4)#1	1.212(7)	C(4)-C(5)-C(1)	108.3(2)	C(36)-C(35)-C(34)	124.4(2)
C(3)-C(4)	1.406(4)	C(47)-Cl(3)	1.689(8)	C(4)-C(5)-Cr(1)	73.36(14)	F(36)-C(36)-C(37)	119.5(2)
C(4)-C(5)	1.411(3)	C(47)-Cl(4)	1.766(8)	C(1)-C(5)-Cr(1)	70.31(13)	F(36)-C(36)-C(35)	120.9(2)
C(6)-C(11)	1.387(3)	Cl(3)-Cl(4)#1	1.812(3)	C(11)-C(6)-C(7)	120.1(2)	C(37)-C(36)-C(35)	119.6(2)
C(6)-C(7)	1.392(3)	Cl(4)-Cl(4)#1	1.206(5)	C(11)-C(6)-P(1)	120.8(2)	F(37)-C(37)-C(38)	120.9(2)
C(7)-C(8)	1.384(4)	Cl(4)-C(47)#1	1.212(7)	C(7)-C(6)-P(1)	119.07(18)	F(37)-C(37)-C(36)	120.0(2)
C(8)-C(9)	1.367(5)	Cl(4)-Cl(3)#1	1.812(3)	C(8)-C(7)-C(6)	119.9(3)	C(38)-C(37)-C(36)	119.1(2)
C(9)-C(10)	1.371(5)			C(9)-C(8)-C(7)	119.8(3)	F(38)-C(38)-C(37)	120.2(2)
C(10)-C(11)	1.395(4)	C(1)-P(1)-C(12)	107.62(10)	C(8)-C(9)-C(10)	120.9(3)	F(38)-C(38)-C(39)	120.7(2)
C(12)-C(13)	1.384(3)	C(1)-P(1)-C(6)	110.18(10)	C(9)-C(10)-C(11)	120.3(3)	C(37)-C(38)-C(39)	119.1(2)
C(12)-C(17)	1.395(3)	C(12)-P(1)-C(6)	109.66(11)	C(6)-C(11)-C(10)	119.0(3)	F(39)-C(39)-C(38)	115.8(2)
C(13)-C(14)	1.383(4)	C(1)-P(1)-C(18)	108.92(11)	C(13)-C(12)-C(17)	119.9(2)	F(39)-C(39)-C(34)	119.1(2)
C(14)-C(15)	1.375(4)	C(12)-P(1)-C(18)	109.05(11)	C(13)-C(12)-P(1)	119.94(18)	C(38)-C(39)-C(34)	125.1(2)
C(15)-C(16)	1.374(4)	C(6)-P(1)-C(18)	111.33(12)	C(17)-C(12)-P(1)	120.03(18)	C(41)-C(40)-C(45)	112.6(2)
C(16)-C(17)	1.384(4)	C(40)-B(1)-C(22)	112.11(18)	C(14)-C(13)-C(12)	120.1(2)	C(41)-C(40)-B(1)	121.09(19)
C(22)-C(27)	1.384(3)	C(40)-B(1)-C(34)	101.54(17)	C(15)-C(14)-C(13)	119.8(3)	C(45)-C(40)-B(1)	126.1(2)
C(22)-C(23)	1.389(3)	C(22)-B(1)-C(34)	115.22(18)	C(16)-C(15)-C(14)	120.5(2)	F(41)-C(41)-C(42)	115.7(2)
C(23)-F(23)	1.357(3)	C(40)-B(1)-C(28)	114.70(18)	C(15)-C(16)-C(17)	120.5(3)	F(41)-C(41)-C(40)	119.0(2)
C(23)-C(24)	1.382(3)	C(22)-B(1)-C(28)	101.81(18)	C(16)-C(17)-C(12)	119.2(3)	C(42)-C(41)-C(40)	125.3(2)
C(24)-F(24)	1.350(3)	C(34)-B(1)-C(28)	112.01(18)	O(1)-C(19)-Cr(1)	174.4(2)	F(42)-C(42)-C(43)	120.2(2)
C(24)-C(25)	1.366(4)	C(21)-Cr(1)-C(19)	81.64(11)	O(2)-C(20)-Cr(1)	172.0(2)	F(42)-C(42)-C(41)	120.9(2)
C(25)-F(25)	1.351(3)	C(21)-Cr(1)-C(20)	77.90(11)	O(3)-C(21)-Cr(1)	178.5(2)	C(43)-C(42)-C(41)	118.9(2)

C(25)-C(26)	1.371(3)	C(19)-Cr(1)-C(20)	107.90(10)	C(27)-C(22)-C(23)	113.0(2)	F(43)-C(43)-C(44)	120.6(2)
C(26)-F(26)	1.343(3)	C(21)-Cr(1)-C(1)	91.64(9)	C(27)-C(22)-B(1)	127.1(2)	F(43)-C(43)-C(42)	120.8(2)
C(26)-C(27)	1.388(3)	C(19)-Cr(1)-C(1)	103.96(9)	C(23)-C(22)-B(1)	119.60(19)	C(44)-C(43)-C(42)	118.6(2)
C(27)-F(27)	1.356(3)	C(20)-Cr(1)-C(1)	144.43(10)	F(23)-C(23)-C(24)	115.9(2)	F(44)-C(44)-C(43)	119.5(2)
C(28)-C(29)	1.383(3)	C(21)-Cr(1)-C(5)	87.89(10)	F(23)-C(23)-C(22)	119.4(2)	F(44)-C(44)-C(45)	120.1(2)
C(28)-C(33)	1.394(3)	C(19)-Cr(1)-C(5)	140.70(9)	C(24)-C(23)-C(22)	124.7(2)	C(43)-C(44)-C(45)	120.4(2)
C(29)-F(29)	1.357(3)	C(20)-Cr(1)-C(5)	106.68(10)	F(24)-C(24)-C(25)	120.1(2)	F(45)-C(45)-C(44)	114.8(2)
C(29)-C(30)	1.385(3)	C(1)-Cr(1)-C(5)	38.32(9)	F(24)-C(24)-C(23)	120.5(2)	F(45)-C(45)-C(40)	121.2(2)
C(30)-F(30)	1.342(3)	C(21)-Cr(1)-C(2)	127.03(10)	C(25)-C(24)-C(23)	119.4(2)	C(44)-C(45)-C(40)	124.0(2)
C(30)-C(31)	1.372(3)	C(19)-Cr(1)-C(2)	93.59(10)	F(25)-C(25)-C(24)	120.5(2)	Cl(1A)-C(46A)-Cl(2A)	109.8(6)
C(31)-F(31)	1.342(3)	C(20)-Cr(1)-C(2)	149.99(10)	F(25)-C(25)-C(26)	120.4(2)	Cl(2B)-C(46B)-Cl(1B)	109.3(7)
C(31)-C(32)	1.371(3)	C(1)-Cr(1)-C(2)	38.23(8)	C(24)-C(25)-C(26)	119.0(2)	Cl(4)#1-C(47)-Cl(3)	75.3(4)
C(32)-F(32)	1.347(3)	C(5)-Cr(1)-C(2)	63.34(9)	F(26)-C(26)-C(25)	119.6(2)	Cl(4)#1-C(47)-Cl(4)	42.9(3)
C(32)-C(33)	1.378(3)	C(21)-Cr(1)-C(4)	118.84(11)	F(26)-C(26)-C(27)	120.7(2)	Cl(3)-C(47)-Cl(4)	114.6(4)
C(33)-F(33)	1.349(3)	C(19)-Cr(1)-C(4)	154.44(10)	C(25)-C(26)-C(27)	119.7(2)	C(47)-Cl(3)-Cl(4)#1	40.3(2)
C(34)-C(35)	1.386(3)	C(20)-Cr(1)-C(4)	92.22(10)	F(27)-C(27)-C(22)	120.9(2)	Cl(4)#1-Cl(4)-C(47)#1	93.9(5)
C(34)-C(39)	1.388(3)	C(1)-Cr(1)-C(4)	63.04(9)	F(27)-C(27)-C(26)	115.0(2)	Cl(4)#1-Cl(4)-C(47)	43.2(3)
C(35)-F(35)	1.355(3)	C(5)-Cr(1)-C(4)	37.31(9)	C(22)-C(27)-C(26)	124.1(2)	C(47)#1-Cl(4)-C(47)	137.1(3)
C(35)-C(36)	1.384(3)	C(2)-Cr(1)-C(4)	62.29(10)	C(29)-C(28)-C(33)	112.8(2)	Cl(4)#1-Cl(4)-Cl(3)#1	148.4(3)
C(36)-F(36)	1.350(3)	C(21)-Cr(1)-C(3)	149.47(10)	C(29)-C(28)-B(1)	128.13(19)	C(47)#1-Cl(4)-Cl(3)#1	64.4(4)
						C(47)-Cl(4)-Cl(3)#1	151.4(3)

Symmetry transformations used to generate equivalent atoms: #1 -x,-y+2,-z

Table 34. Anisotropic displacement parameters ($Å^2 x\ 10^3$)for **[III$_2$][B(C$_6$F$_5$)$_4$]$_2$**. The anisotropic displacement factor exponent takes the form: $-2\pi^2[\ h^2a^{*2}U^{11} + ... + 2\ h\ k\ a^*\ b^*\ U^{12}\ ]$

	U^{11}	U^{22}	U^{33}	U^{23}	U^{13}	U^{12}
P(1)	26(1)	22(1)	20(1)	-6(1)	-2(1)	-1(1)
B(1)	23(1)	26(1)	26(1)	-12(1)	-5(1)	1(1)
Cr(1)	25(1)	23(1)	21(1)	-6(1)	0(1)	-1(1)
O(1)	54(1)	30(1)	33(1)	-10(1)	4(1)	9(1)
O(2)	27(1)	69(1)	41(1)	-7(1)	2(1)	-2(1)
O(3)	68(1)	50(1)	40(1)	-9(1)	-16(1)	-26(1)
C(1)	27(1)	21(1)	20(1)	-5(1)	2(1)	-3(1)
C(2)	30(1)	29(1)	24(1)	-5(1)	-2(1)	-9(1)
C(3)	50(2)	28(1)	25(1)	-9(1)	1(1)	-13(1)
C(4)	51(2)	25(1)	31(1)	-9(1)	7(1)	3(1)
C(5)	34(1)	24(1)	26(1)	-3(1)	0(1)	5(1)
C(6)	39(1)	24(1)	20(1)	-6(1)	0(1)	2(1)
C(7)	39(2)	31(1)	33(1)	-8(1)	-1(1)	6(1)
C(8)	54(2)	45(2)	40(2)	-9(1)	1(1)	22(1)
C(9)	94(3)	35(2)	35(2)	-10(1)	2(2)	27(2)
C(10)	108(3)	23(1)	35(2)	-15(1)	6(2)	-5(2)
C(11)	63(2)	30(2)	28(1)	-11(1)	-4(1)	-6(1)
C(12)	23(1)	24(1)	24(1)	-3(1)	-3(1)	0(1)
C(13)	33(1)	27(1)	34(1)	-8(1)	-6(1)	0(1)
C(14)	45(2)	28(1)	43(2)	-3(1)	-13(1)	-7(1)
C(15)	38(2)	45(2)	41(2)	10(1)	-10(1)	-16(1)
C(16)	36(2)	60(2)	36(2)	-1(1)	10(1)	-3(1)
C(17)	40(2)	36(2)	33(1)	-7(1)	8(1)	2(1)
C(18)	35(1)	40(2)	25(1)	-7(1)	-8(1)	-3(1)
C(19)	36(1)	30(1)	19(1)	-5(1)	3(1)	-6(1)
C(20)	34(2)	35(1)	26(1)	-6(1)	-5(1)	1(1)
C(21)	40(2)	30(1)	28(1)	-3(1)	-1(1)	-11(1)
C(22)	29(1)	24(1)	22(1)	-9(1)	-3(1)	0(1)
C(23)	32(1)	28(1)	30(1)	-11(1)	-7(1)	-1(1)
C(24)	45(2)	23(1)	38(1)	-12(1)	-5(1)	-5(1)
C(25)	44(2)	24(1)	32(1)	-8(1)	-5(1)	11(1)
C(26)	28(1)	33(1)	30(1)	-10(1)	-6(1)	6(1)
C(27)	30(1)	24(1)	27(1)	-9(1)	-2(1)	-2(1)

C(28)	28(1)	19(1)	24(1)	-7(1)	-3(1)	-1(1)
C(29)	31(1)	29(1)	26(1)	-10(1)	-6(1)	-2(1)
C(30)	26(1)	32(1)	32(1)	-7(1)	-1(1)	-5(1)
C(31)	34(1)	31(1)	24(1)	-7(1)	4(1)	2(1)
C(32)	38(1)	25(1)	23(1)	-7(1)	-7(1)	1(1)
C(33)	25(1)	24(1)	27(1)	-6(1)	-5(1)	-1(1)
C(34)	25(1)	26(1)	23(1)	-8(1)	-7(1)	2(1)
C(35)	26(1)	29(1)	25(1)	-10(1)	-5(1)	2(1)
C(36)	30(1)	23(1)	39(1)	-11(1)	-13(1)	3(1)
C(37)	25(1)	27(1)	41(2)	-3(1)	-8(1)	-6(1)
C(38)	21(1)	37(1)	35(1)	-5(1)	1(1)	1(1)
C(39)	27(1)	26(1)	31(1)	-10(1)	-5(1)	7(1)
C(40)	23(1)	23(1)	27(1)	-8(1)	-3(1)	-1(1)
C(41)	27(1)	26(1)	28(1)	-12(1)	1(1)	1(1)
C(42)	26(1)	28(1)	34(1)	-4(1)	-9(1)	5(1)
C(43)	39(1)	32(1)	24(1)	-7(1)	-11(1)	-3(1)
C(44)	41(1)	27(1)	27(1)	-13(1)	-5(1)	1(1)
C(45)	29(1)	25(1)	29(1)	-10(1)	-5(1)	7(1)
C(46A)	80(8)	84(6)	36(4)	3(4)	14(5)	39(5)
C(46B)	102(10)	76(6)	73(6)	-33(5)	-11(6)	37(6)
C(47)	56(4)	59(4)	33(3)	11(3)	8(3)	9(3)
Cl(1A)	53(2)	78(2)	44(2)	2(1)	-14(1)	6(1)
Cl(1B)	71(3)	187(6)	157(6)	-82(5)	-10(4)	20(3)
Cl(2A)	125(5)	127(5)	135(5)	40(4)	-33(4)	-18(4)
Cl(2B)	133(4)	70(2)	88(2)	-33(2)	-7(2)	46(2)
Cl(3)	109(2)	45(1)	47(1)	-14(1)	19(1)	10(1)
Cl(4)	76(2)	124(2)	60(1)	-29(1)	11(1)	7(1)
F(23)	38(1)	32(1)	49(1)	-10(1)	-16(1)	-7(1)
F(24)	64(1)	24(1)	71(1)	-13(1)	-21(1)	-7(1)
F(25)	60(1)	28(1)	56(1)	-10(1)	-14(1)	16(1)
F(26)	35(1)	43(1)	52(1)	-13(1)	-18(1)	9(1)
F(27)	31(1)	27(1)	50(1)	-11(1)	-14(1)	-2(1)
F(29)	33(1)	61(1)	32(1)	-21(1)	-4(1)	-13(1)
F(30)	28(1)	64(1)	41(1)	-16(1)	1(1)	-11(1)
F(31)	42(1)	65(1)	30(1)	-18(1)	6(1)	-1(1)
F(32)	47(1)	49(1)	26(1)	-18(1)	-8(1)	-3(1)
F(33)	29(1)	45(1)	32(1)	-15(1)	-6(1)	-6(1)
F(35)	36(1)	28(1)	37(1)	-14(1)	6(1)	1(1)
F(36)	46(1)	24(1)	55(1)	-17(1)	-8(1)	0(1)
F(37)	38(1)	35(1)	69(1)	-6(1)	1(1)	-15(1)
F(38)	31(1)	51(1)	63(1)	-9(1)	16(1)	0(1)
F(39)	39(1)	33(1)	41(1)	-14(1)	5(1)	8(1)
F(41)	40(1)	38(1)	35(1)	-18(1)	-6(1)	15(1)
F(42)	42(1)	50(1)	50(1)	-14(1)	-20(1)	20(1)
F(43)	60(1)	42(1)	35(1)	-10(1)	-26(1)	1(1)
F(44)	64(1)	44(1)	35(1)	-26(1)	-15(1)	12(1)
F(45)	42(1)	40(1)	37(1)	-23(1)	-14(1)	18(1)

Table 35. Hydrogen coordinates (x 10^4) and isotropic displacement parameters ($Å^2$x 10^3) for **[III$_2$][B(C$_6$F$_5$)$_4$]$_2$**.

	x	y	z	U(eq)
H(2A)	2605	1391	3791	35
H(3A)	1147	2061	4747	41
H(4A)	-1169	2721	4283	44
H(5A)	-1156	2493	3023	35
H(7A)	4097	848	2771	42
H(8A)	5178	-856	3067	59
H(9A)	4109	-2370	2956	67
H(10A)	1979	-2217	2547	66
H(11)	880(30)	-510(20)	2289(15)	38(8)
H(13A)	1868	3802	2341	38
H(14)	3310(30)	5260(20)	1700(14)	37(7)
H(15A)	5018	5070	791	56
H(16A)	5260	3400	576	58
H(17A)	3800	1909	1237	46
H(18A)	456	1571	1351	51
H(18B)	-316	2403	1717	51
H(18C)	-568	1100	2084	51
H(46A)	-4657	3768	5601	89
H(46B)	-3249	3105	5668	89

H(46C)	-4953	3229	5743	98
H(46D)	-5770	3722	5050	98
H(47A)	-830(80)	10760(60)	-842(19)	110(30)
H(47B)	-1870(50)	10710(50)	-110(30)	61(19)

Table 36. Torsion angles [°] for **[III$_2$][B(C$_6$F$_5$)$_4$]$_2$**.

C(12)-P(1)-C(1)-C(5)	100.3(2)	C(19)-Cr(1)-C(5)-C(1)	-21.3(2)	C(33)-C(28)-C(29)-F(29)	177.3(2)
C(6)-P(1)-C(1)-C(5)	-140.2(2)	C(20)-Cr(1)-C(5)-C(1)	-172.03(14)	B(1)-C(28)-C(29)-F(29)	1.0(4)
C(18)-P(1)-C(1)-C(5)	-17.8(2)	C(2)-Cr(1)-C(5)-C(1)	38.53(13)	C(33)-C(28)-C(29)-C(30)	-2.3(3)
C(12)-P(1)-C(1)-C(2)	-70.4(2)	C(4)-Cr(1)-C(5)-C(1)	117.0(2)	B(1)-C(28)-C(29)-C(30)	-178.6(2)
C(6)-P(1)-C(1)-C(2)	49.2(2)	C(3)-Cr(1)-C(5)-C(1)	80.29(14)	F(29)-C(29)-C(30)-F(30)	0.8(3)
C(18)-P(1)-C(1)-C(2)	171.54(19)	C(1)-P(1)-C(6)-C(11)	102.1(2)	C(28)-C(29)-C(30)-F(30)	-179.5(2)
C(12)-P(1)-C(1)-Cr(1)	-164.34(13)	C(12)-P(1)-C(6)-C(11)	-139.7(2)	F(29)-C(29)-C(30)-C(31)	-179.2(2)
C(6)-P(1)-C(1)-Cr(1)	-44.81(18)	C(18)-P(1)-C(6)-C(11)	-18.9(2)	C(28)-C(29)-C(30)-C(31)	0.5(4)
C(18)-P(1)-C(1)-Cr(1)	77.57(17)	C(1)-P(1)-C(6)-C(7)	-75.0(2)	F(30)-C(30)-C(31)-F(31)	1.3(4)
C(21)-Cr(1)-C(1)-C(5)	84.51(15)	C(12)-P(1)-C(6)-C(7)	43.3(2)	C(29)-C(30)-C(31)-F(31)	-178.7(2)
C(19)-Cr(1)-C(1)-C(5)	166.31(14)	C(18)-P(1)-C(6)-C(7)	164.03(19)	F(30)-C(30)-C(31)-C(32)	-179.3(2)
C(20)-Cr(1)-C(1)-C(5)	13.2(2)	C(11)-C(6)-C(7)-C(8)	-1.1(4)	C(29)-C(30)-C(31)-C(32)	0.8(4)
C(2)-Cr(1)-C(1)-C(5)	-115.89(19)	P(1)-C(6)-C(7)-C(8)	176.0(2)	F(31)-C(31)-C(32)-F(32)	-0.1(3)
C(4)-Cr(1)-C(1)-C(5)	-37.28(14)	C(6)-C(7)-C(8)-C(9)	0.7(4)	C(30)-C(31)-C(32)-F(32)	-179.6(2)
C(3)-Cr(1)-C(1)-C(5)	-78.57(15)	C(7)-C(8)-C(9)-C(10)	0.3(4)	F(31)-C(31)-C(32)-C(33)	179.5(2)
C(21)-Cr(1)-C(1)-C(2)	-159.60(15)	C(8)-C(9)-C(10)-C(11)	-0.8(4)	C(30)-C(31)-C(32)-C(33)	0.1(4)
C(19)-Cr(1)-C(1)-C(2)	-77.80(15)	C(7)-C(6)-C(11)-C(10)	0.5(4)	F(32)-C(32)-C(33)-F(33)	-1.3(3)
C(20)-Cr(1)-C(1)-C(2)	129.10(18)	P(1)-C(6)-C(11)-C(10)	-176.6(2)	C(31)-C(32)-C(33)-F(33)	179.1(2)
C(5)-Cr(1)-C(1)-C(2)	115.89(19)	C(9)-C(10)-C(11)-C(6)	0.5(4)	F(32)-C(32)-C(33)-C(28)	177.4(2)
C(4)-Cr(1)-C(1)-C(2)	78.62(15)	C(1)-P(1)-C(12)-C(13)	-27.0(2)	C(31)-C(32)-C(33)-C(28)	-2.3(4)
C(3)-Cr(1)-C(1)-C(2)	37.32(14)	C(6)-P(1)-C(12)-C(13)	-146.86(19)	C(29)-C(28)-C(33)-F(33)	-178.17(19)
C(21)-Cr(1)-C(1)-P(1)	-39.17(16)	C(18)-P(1)-C(12)-C(13)	91.0(2)	B(1)-C(28)-C(33)-F(33)	-1.5(3)
C(19)-Cr(1)-C(1)-P(1)	42.63(17)	C(1)-P(1)-C(12)-C(17)	156.90(19)	C(29)-C(28)-C(33)-C(32)	3.2(3)
C(20)-Cr(1)-C(1)-P(1)	-110.48(19)	C(6)-P(1)-C(12)-C(17)	37.0(2)	B(1)-C(28)-C(33)-C(32)	179.9(2)
C(5)-Cr(1)-C(1)-P(1)	-123.7(2)	C(18)-P(1)-C(12)-C(17)	-85.1(2)	C(40)-B(1)-C(34)-C(35)	-102.1(2)
C(2)-Cr(1)-C(1)-P(1)	120.4(2)	C(17)-C(12)-C(13)-C(14)	0.2(4)	C(22)-B(1)-C(34)-C(35)	136.5(2)
C(4)-Cr(1)-C(1)-P(1)	-160.96(19)	P(1)-C(12)-C(13)-C(14)	-175.91(19)	C(28)-B(1)-C(34)-C(35)	20.8(3)
C(3)-Cr(1)-C(1)-P(1)	157.75(19)	C(12)-C(13)-C(14)-C(15)	-0.8(4)	C(40)-B(1)-C(34)-C(39)	69.2(2)
C(5)-C(1)-C(2)-C(3)	-1.2(3)	C(13)-C(14)-C(15)-C(16)	0.8(4)	C(22)-B(1)-C(34)-C(39)	-52.2(3)
P(1)-C(1)-C(2)-C(3)	171.07(16)	C(14)-C(15)-C(16)-C(17)	-0.2(4)	C(28)-B(1)-C(34)-C(39)	-168.0(2)
Cr(1)-C(1)-C(2)-C(3)	-64.39(16)	C(15)-C(16)-C(17)-C(12)	-0.4(4)	C(39)-C(34)-C(35)-F(35)	-176.45(19)
C(5)-C(1)-C(2)-Cr(1)	63.18(15)	C(13)-C(12)-C(17)-C(16)	0.4(4)	B(1)-C(34)-C(35)-F(35)	-4.6(3)
P(1)-C(1)-C(2)-Cr(1)	-124.54(17)	P(1)-C(12)-C(17)-C(16)	176.5(2)	C(39)-C(34)-C(35)-C(36)	2.4(3)
C(21)-Cr(1)-C(2)-C(3)	142.38(16)	C(21)-Cr(1)-C(19)-O(1)	41(2)	B(1)-C(34)-C(35)-C(36)	174.2(2)
C(19)-Cr(1)-C(2)-C(3)	-135.39(15)	C(20)-Cr(1)-C(19)-O(1)	115(2)	F(35)-C(35)-C(36)-F(36)	-2.5(3)
C(20)-Cr(1)-C(2)-C(3)	1.0(3)	C(1)-Cr(1)-C(19)-O(1)	-49(2)	C(34)-C(35)-C(36)-F(36)	178.6(2)
C(1)-Cr(1)-C(2)-C(3)	116.5(2)	C(5)-Cr(1)-C(19)-O(1)	-36(2)	F(35)-C(35)-C(36)-C(37)	176.7(2)
C(5)-Cr(1)-C(2)-C(3)	77.87(15)	C(2)-Cr(1)-C(19)-O(1)	-86(2)	C(34)-C(35)-C(36)-C(37)	-2.2(4)
C(4)-Cr(1)-C(2)-C(3)	35.74(15)	C(4)-Cr(1)-C(19)-O(1)	-105(2)	F(36)-C(36)-C(37)-F(37)	0.6(3)
C(21)-Cr(1)-C(2)-C(1)	25.89(19)	C(3)-Cr(1)-C(19)-O(1)	-115(2)	C(35)-C(36)-C(37)-F(37)	-178.6(2)
C(19)-Cr(1)-C(2)-C(1)	108.12(14)	C(21)-Cr(1)-C(20)-O(2)	-32.3(17)	F(36)-C(36)-C(37)-C(38)	-179.8(2)
C(20)-Cr(1)-C(2)-C(1)	-115.5(2)	C(19)-Cr(1)-C(20)-O(2)	-109.2(17)	C(35)-C(36)-C(37)-C(38)	1.0(3)
C(5)-Cr(1)-C(2)-C(1)	-38.62(13)	C(1)-Cr(1)-C(20)-O(2)	43.3(18)	F(37)-C(37)-C(38)-F(38)	-0.4(4)

C(4)-Cr(1)-C(2)-C(1)	-80.75(15)	C(5)-Cr(1)-C(20)-O(2)	51.8(17)	C(36)-C(37)-C(38)-F(38)	-180.0(2)
C(3)-Cr(1)-C(2)-C(1)	-116.5(2)	C(2)-Cr(1)-C(20)-O(2)	117.1(16)	F(37)-C(37)-C(38)-C(39)	179.3(2)
C(1)-C(2)-C(3)-C(4)	1.7(3)	C(4)-Cr(1)-C(20)-O(2)	86.8(17)	C(36)-C(37)-C(38)-C(39)	-0.3(4)
Cr(1)-C(2)-C(3)-C(4)	-60.07(17)	C(3)-Cr(1)-C(20)-O(2)	117.8(17)	F(38)-C(38)-C(39)-F(39)	1.4(3)
C(1)-C(2)-C(3)-Cr(1)	61.73(15)	C(19)-Cr(1)-C(21)-O(3)	178(100)	C(37)-C(38)-C(39)-F(39)	-178.2(2)
C(21)-Cr(1)-C(3)-C(4)	46.1(3)	C(20)-Cr(1)-C(21)-O(3)	68(9)	F(38)-C(38)-C(39)-C(34)	-179.7(2)
C(19)-Cr(1)-C(3)-C(4)	172.60(14)	C(1)-Cr(1)-C(21)-O(3)	-78(9)	C(37)-C(38)-C(39)-C(34)	0.7(4)
C(20)-Cr(1)-C(3)-C(4)	-59.74(17)	C(5)-Cr(1)-C(21)-O(3)	-40(9)	C(35)-C(34)-C(39)-F(39)	177.28(19)
C(1)-Cr(1)-C(3)-C(4)	81.06(15)	C(2)-Cr(1)-C(21)-O(3)	-94(9)	B(1)-C(34)-C(39)-F(39)	4.9(3)
C(5)-Cr(1)-C(3)-C(4)	37.50(14)	C(4)-Cr(1)-C(21)-O(3)	-18(9)	C(35)-C(34)-C(39)-C(38)	-1.6(3)
C(2)-Cr(1)-C(3)-C(4)	119.7(2)	C(3)-Cr(1)-C(21)-O(3)	-48(9)	B(1)-C(34)-C(39)-C(38)	-174.0(2)
C(21)-Cr(1)-C(3)-C(2)	-73.6(3)	C(40)-B(1)-C(22)-C(27)	-136.4(2)	C(22)-B(1)-C(40)-C(41)	-163.6(2)
C(19)-Cr(1)-C(3)-C(2)	52.88(17)	C(34)-B(1)-C(22)-C(27)	-20.9(3)	C(34)-B(1)-C(40)-C(41)	72.9(2)
C(20)-Cr(1)-C(3)-C(2)	-179.45(14)	C(28)-B(1)-C(22)-C(27)	100.5(2)	C(28)-B(1)-C(40)-C(41)	-48.1(3)
C(1)-Cr(1)-C(3)-C(2)	-38.65(14)	C(40)-B(1)-C(22)-C(23)	50.4(3)	C(22)-B(1)-C(40)-C(45)	21.9(3)
C(5)-Cr(1)-C(3)-C(2)	-82.21(15)	C(34)-B(1)-C(22)-C(23)	165.8(2)	C(34)-B(1)-C(40)-C(45)	-101.7(2)
C(4)-Cr(1)-C(3)-C(2)	-119.7(2)	C(28)-B(1)-C(22)-C(23)	-72.7(2)	C(28)-B(1)-C(40)-C(45)	137.3(2)
C(2)-C(3)-C(4)-C(5)	-1.5(3)	C(27)-C(22)-C(23)-F(23)	-178.3(2)	C(45)-C(40)-C(41)-F(41)	175.6(2)
Cr(1)-C(3)-C(4)-C(5)	-60.62(17)	B(1)-C(22)-C(23)-F(23)	-4.2(3)	B(1)-C(40)-C(41)-F(41)	0.3(3)
C(2)-C(3)-C(4)-Cr(1)	59.16(16)	C(27)-C(22)-C(23)-C(24)	2.4(3)	C(45)-C(40)-C(41)-C(42)	-4.3(3)
C(21)-Cr(1)-C(4)-C(3)	-155.28(15)	B(1)-C(22)-C(23)-C(24)	176.5(2)	B(1)-C(40)-C(41)-C(42)	-179.6(2)
C(19)-Cr(1)-C(4)-C(3)	-15.2(3)	F(23)-C(23)-C(24)-F(24)	-1.5(3)	F(41)-C(41)-C(42)-F(42)	2.1(3)
C(20)-Cr(1)-C(4)-C(3)	127.32(15)	C(22)-C(23)-C(24)-F(24)	177.8(2)	C(40)-C(41)-C(42)-F(42)	-178.0(2)
C(1)-Cr(1)-C(4)-C(3)	-79.36(15)	F(23)-C(23)-C(24)-C(25)	178.0(2)	F(41)-C(41)-C(42)-C(43)	-178.3(2)
C(5)-Cr(1)-C(4)-C(3)	-117.7(2)	C(22)-C(23)-C(24)-C(25)	-2.6(4)	C(40)-C(41)-C(42)-C(43)	1.6(4)
C(2)-Cr(1)-C(4)-C(3)	-36.11(14)	F(24)-C(24)-C(25)-F(25)	0.5(4)	F(42)-C(42)-C(43)-F(43)	0.4(4)
C(21)-Cr(1)-C(4)-C(5)	-37.63(19)	C(23)-C(24)-C(25)-F(25)	-179.1(2)	C(41)-C(42)-C(43)-F(43)	-179.2(2)
C(19)-Cr(1)-C(4)-C(5)	102.4(2)	F(24)-C(24)-C(25)-C(26)	-179.6(2)	F(42)-C(42)-C(43)-C(44)	-178.5(2)
C(20)-Cr(1)-C(4)-C(5)	-115.03(16)	C(23)-C(24)-C(25)-C(26)	0.9(4)	C(41)-C(42)-C(43)-C(44)	1.9(4)
C(1)-Cr(1)-C(4)-C(5)	38.29(14)	F(25)-C(25)-C(26)-F(26)	-1.4(4)	F(43)-C(43)-C(44)-F(44)	-2.2(4)
C(2)-Cr(1)-C(4)-C(5)	81.54(16)	C(24)-C(25)-C(26)-F(26)	178.7(2)	C(42)-C(43)-C(44)-F(44)	176.7(2)
C(3)-Cr(1)-C(4)-C(5)	117.7(2)	F(25)-C(25)-C(26)-C(27)	-179.3(2)	F(43)-C(43)-C(44)-C(45)	178.8(2)
C(3)-C(4)-C(5)-C(1)	0.7(3)	C(24)-C(25)-C(26)-C(27)	0.8(4)	C(42)-C(43)-C(44)-C(45)	-2.3(4)
Cr(1)-C(4)-C(5)-C(1)	-62.03(16)	C(23)-C(22)-C(27)-F(27)	180.0(2)	F(44)-C(44)-C(45)-F(45)	0.2(3)
C(3)-C(4)-C(5)-Cr(1)	62.73(17)	B(1)-C(22)-C(27)-F(27)	6.4(3)	C(43)-C(44)-C(45)-F(45)	179.2(2)
C(2)-C(1)-C(5)-C(4)	0.3(3)	C(23)-C(22)-C(27)-C(26)	-0.6(3)	F(44)-C(44)-C(45)-C(40)	-179.8(2)
P(1)-C(1)-C(5)-C(4)	-171.66(17)	B(1)-C(22)-C(27)-C(26)	-174.2(2)	C(43)-C(44)-C(45)-C(40)	-0.8(4)
Cr(1)-C(1)-C(5)-C(4)	64.00(17)	F(26)-C(26)-C(27)-F(27)	0.7(3)	C(41)-C(40)-C(45)-F(45)	-176.1(2)
C(2)-C(1)-C(5)-Cr(1)	-63.68(15)	C(25)-C(26)-C(27)-F(27)	178.6(2)	B(1)-C(40)-C(45)-F(45)	-1.2(4)
P(1)-C(1)-C(5)-Cr(1)	124.35(18)	F(26)-C(26)-C(27)-C(22)	-178.8(2)	C(41)-C(40)-C(45)-C(44)	3.9(3)
C(21)-Cr(1)-C(5)-C(4)	147.64(17)	C(25)-C(26)-C(27)-C(22)	-0.9(4)	B(1)-C(40)-C(45)-C(44)	178.8(2)
C(19)-Cr(1)-C(5)-C(4)	-138.30(18)	C(40)-B(1)-C(28)-C(29)	-16.9(3)	Cl(4)-C(47)-Cl(3)-Cl(4)#1	-17.7(2)
C(20)-Cr(1)-C(5)-C(4)	70.94(17)	C(22)-B(1)-C(28)-C(29)	104.4(2)	Cl(3)-C(47)-Cl(4)-Cl(4)#1	25.6(3)
C(1)-Cr(1)-C(5)-C(4)	-117.0(2)	C(34)-B(1)-C(28)-C(29)	-132.0(2)	Cl(4)#1-C(47)-Cl(4)-C(47)#1	0
C(2)-Cr(1)-C(5)-C(4)	-78.50(16)	C(40)-B(1)-C(28)-C(33)	167.0(2)	Cl(3)-C(47)-Cl(4)-C(47)#1	25.6(3)
C(3)-Cr(1)-C(5)-C(4)	-36.74(15)	C(22)-B(1)-C(28)-C(33)	-71.7(2)	Cl(4)#1-C(47)-Cl(4)-Cl(3)#1	130.2(6)
C(21)-Cr(1)-C(5)-C(1)	-95.33(15)	C(34)-B(1)-C(28)-C(33)	51.9(3)	Cl(3)-C(47)-Cl(4)-Cl(3)#1	155.7(3)

Symmetry transformations used to generate equivalent atoms: #1 -x,-y+2,-z

Figure 6. The molecular structure of **[III$_2$][B(C$_6$F$_5$)$_4$]$_2$**.

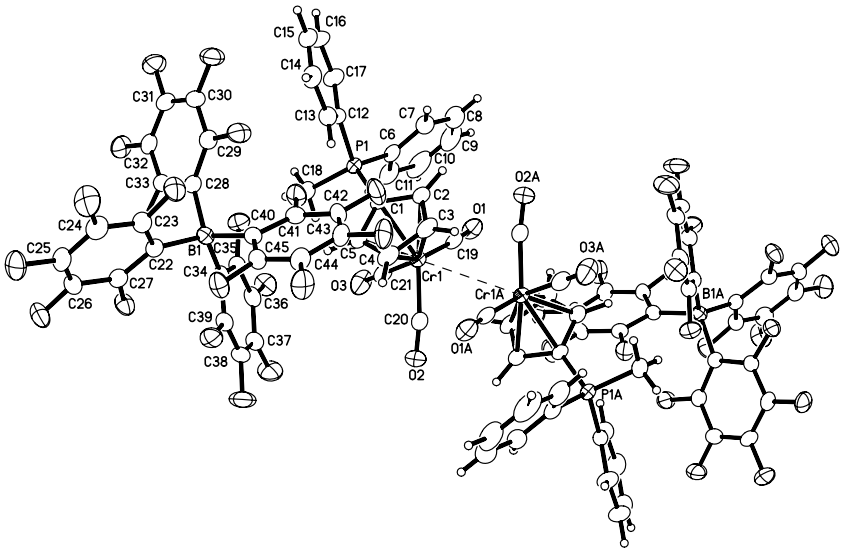

Table 37. Crystal data and structure refinement for **[IV$_2$][B(C$_6$F$_5$)$_4$]$_2$**.

Identification code	**[IV$_2$][B(C$_6$F$_5$)$_4$]$_2$**	
Empirical formula	C102 H58 B2 F40 Mo2 O9 P2	
Formula weight	2462.92	
Temperature	298(2) K	
Wavelength	0.71073 Å	
Crystal system	Monoclinic	
Space group	P2/n	
Unit cell dimensions	a = 13.0003(18) Å	α= 90°.
	b = 10.0517(14) Å	β= 92.466(2)°.
	c = 38.132(5) Å	γ = 90°.
Volume	4978.3(12) Å^3	
Z	2	
Density (calculated)	1.643 Mg/m^3	
Absorption coefficient	0.418 mm^{-1}	
F(000)	2452	
Crystal size	0.25 x 0.20 x 0.06 mm^3	
Theta range for data collection	2.03 to 25.19°.	
Index ranges	-15<=h<=15, -12<=k<=12, -45<=l<=45	
Reflections collected	44366	
Independent reflections	8919 [R(int) = 0.0840]	
Completeness to theta = 25.19°	99.5 %	
Absorption correction	Numerical	
Max. and min. transmission	0.9754 and 0.9028	
Refinement method	Full-matrix least-squares on F^2	
Data / restraints / parameters	8919 / 0 / 641	
Goodness-of-fit on F^2	1.054	
Final R indices [I>2sigma(I)]	R1 = 0.0881, wR2 = 0.2110	
R indices (all data)	R1 = 0.1209, wR2 = 0.2248	
Largest diff. peak and hole	1.192 and -0.928 e.Å^{-3}	

Table 38. Atomic coordinates (x 10^4) and equivalent isotropic displacement parameters (Å^{2}x 10^3) for **[IV$_2$][B(C$_6$F$_5$)$_4$]$_2$**. U(eq) is defined as one third of the trace of the orthogonalized U^{ij} tensor.

	x	y	z	U(eq)
Mo(1)	4841(1)	4581(1)	10409(1)	39(1)
P(1)	4759(2)	5871(2)	11306(1)	38(1)
B(1)	145(7)	2212(10)	11476(3)	40(2)
C(1)	4116(6)	5461(9)	10899(2)	42(2)
C(2)	3917(6)	6391(9)	10617(2)	47(2)

C(3)	3236(7)	5779(11)	10359(2)	55(3)
C(4)	3052(6)	4501(13)	10480(2)	63(3)
C(5)	3559(6)	4258(10)	10805(2)	50(2)
C(6)	3930(6)	6900(8)	11544(2)	41(2)
C(7)	2856(7)	6805(10)	11491(3)	54(2)
C(8)	2211(9)	7550(12)	11689(3)	73(3)
C(9)	2610(10)	8412(13)	11933(3)	80(4)
C(10)	3647(10)	8498(14)	11994(3)	90(4)
C(11)	4353(8)	7774(11)	11797(3)	64(3)
C(12)	5954(6)	6682(10)	11243(2)	46(2)
C(13)	5943(8)	8024(11)	11136(3)	59(3)
C(14)	6875(10)	8647(15)	11078(3)	89(4)
C(15)	7774(9)	7938(19)	11114(4)	94(5)
C(16)	7786(9)	6670(20)	11217(3)	94(5)
C(17)	6876(7)	6009(13)	11281(3)	68(3)
C(18)	4938(8)	4369(9)	11549(2)	60(3)
C(19)	6194(7)	5459(10)	10383(2)	48(2)
C(20)	4953(8)	2994(11)	10115(3)	59(3)
C(21)	5682(7)	3382(11)	10694(3)	56(3)
C(22)	-195(6)	3020(9)	11118(2)	42(2)
C(23)	-1038(6)	2731(9)	10885(2)	41(2)
C(24)	-1272(6)	3433(10)	10577(2)	48(2)
C(25)	-680(7)	4431(11)	10480(2)	61(3)
C(26)	155(7)	4767(11)	10689(3)	59(3)
C(27)	394(7)	4062(10)	10995(2)	50(2)
C(28)	-825(6)	1332(9)	11625(2)	42(2)
C(29)	-1766(7)	1909(9)	11675(2)	50(2)
C(30)	-2618(7)	1296(11)	11818(3)	61(3)
C(31)	-2492(8)	23(12)	11926(3)	71(3)
C(32)	-1589(8)	-638(9)	11906(3)	64(3)
C(33)	-788(6)	35(9)	11754(2)	49(2)
C(34)	440(6)	3161(9)	11825(2)	45(2)
C(35)	278(6)	4495(10)	11872(2)	47(2)
C(36)	564(8)	5198(11)	12171(3)	60(3)
C(37)	994(8)	4524(13)	12458(3)	68(3)
C(38)	1138(7)	3178(12)	12429(2)	61(3)
C(39)	874(7)	2562(11)	12124(2)	51(2)
C(40)	1123(6)	1332(8)	11344(2)	39(2)
C(41)	974(6)	260(9)	11116(2)	43(2)
C(42)	1753(7)	-400(9)	10965(2)	53(2)
C(43)	2748(7)	-74(9)	11045(2)	50(2)
C(44)	2958(6)	961(9)	11266(2)	48(2)
C(45)	2169(6)	1636(8)	11415(2)	41(2)
O(1)	6990(5)	6012(8)	10389(2)	71(2)
O(2)	4966(8)	1959(8)	9968(2)	89(3)
O(3)	6170(6)	2624(9)	10872(2)	90(3)
F(23)	-1674(4)	1702(5)	10952(1)	57(1)
F(24)	-2081(4)	3025(7)	10370(2)	77(2)
F(25)	-904(4)	5106(7)	10182(2)	77(2)
F(26)	769(5)	5810(6)	10598(2)	77(2)
F(27)	1262(4)	4394(5)	11179(1)	59(1)
F(29)	-1925(4)	3185(6)	11571(2)	65(2)
F(30)	-3517(4)	1929(7)	11829(2)	87(2)
F(31)	-3307(5)	-626(8)	12073(2)	107(3)
F(32)	-1473(5)	-1853(7)	12021(2)	100(2)
F(33)	79(4)	-713(5)	11731(2)	65(2)
F(35)	-190(5)	5214(5)	11614(2)	68(2)
F(36)	388(6)	6500(6)	12198(2)	88(2)
F(37)	1265(6)	5167(8)	12754(2)	100(2)
F(38)	1547(6)	2498(8)	12710(2)	97(2)
F(39)	1075(4)	1228(6)	12121(1)	61(2)
F(41)	12(4)	-79(5)	11014(1)	58(1)
F(42)	1544(5)	-1441(6)	10749(2)	85(2)
F(43)	3520(5)	-716(6)	10892(2)	83(2)
F(44)	3949(4)	1333(6)	11342(2)	69(2)
F(45)	2446(4)	2676(5)	11623(1)	57(1)

Table 39. Bond lengths [Å] and angles [°] for **$[IV_2][B(C_6F_5)_4]_2$**.

Mo(1)-C(21)	1.928(10)	C(34)-C(35)	1.371(13)	C(22)-B(1)-C(28)	111.6(7)	F(27)-C(27)-C(22)	118.2(8)
Mo(1)-C(20)	1.959(11)	C(34)-C(39)	1.388(12)	C(40)-B(1)-C(28)	115.2(7)	C(26)-C(27)-C(22)	124.2(8)
Mo(1)-C(19)	1.974(10)	C(35)-F(35)	1.342(10)	C(22)-B(1)-C(34)	115.3(7)	C(29)-C(28)-C(33)	111.3(8)
Mo(1)-C(1)	2.306(8)	C(35)-C(36)	1.379(13)	C(40)-B(1)-C(34)	113.4(6)	C(29)-C(28)-B(1)	121.1(8)
Mo(1)-C(5)	2.319(8)	C(36)-F(36)	1.333(12)	C(28)-B(1)-C(34)	100.6(7)	C(33)-C(28)-B(1)	127.1(7)
Mo(1)-C(2)	2.337(8)	C(36)-C(37)	1.384(15)	C(2)-C(1)-C(5)	106.6(7)	F(29)-C(29)-C(28)	119.0(8)
Mo(1)-C(4)	2.355(9)	C(37)-F(37)	1.336(11)	C(2)-C(1)-P(1)	124.3(7)	F(29)-C(29)-C(30)	114.7(8)
Mo(1)-C(3)	2.410(8)	C(37)-C(38)	1.371(16)	C(5)-C(1)-P(1)	128.5(7)	C(28)-C(29)-C(30)	126.3(9)
P(1)-C(6)	1.772(8)	C(38)-C(39)	1.351(13)	C(2)-C(1)-Mo(1)	73.1(4)	F(30)-C(30)-C(31)	122.5(9)
P(1)-C(1)	1.777(8)	C(38)-F(38)	1.360(12)	C(5)-C(1)-Mo(1)	72.3(5)	F(30)-C(30)-C(29)	120.8(9)
P(1)-C(12)	1.779(9)	C(39)-F(39)	1.366(11)	P(1)-C(1)-Mo(1)	127.0(4)	C(31)-C(30)-C(29)	116.6(9)
P(1)-C(18)	1.782(9)	C(40)-C(41)	1.394(11)	C(3)-C(2)-C(1)	108.7(9)	C(30)-C(31)-C(32)	122.8(10)
B(1)-C(22)	1.631(12)	C(40)-C(45)	1.408(11)	C(3)-C(2)-Mo(1)	75.2(5)	C(30)-C(31)-F(31)	119.0(10)
B(1)-C(40)	1.644(12)	C(41)-F(41)	1.338(9)	C(1)-C(2)-Mo(1)	70.7(5)	C(32)-C(31)-F(31)	118.2(10)
B(1)-C(28)	1.661(12)	C(41)-C(42)	1.358(12)	C(4)-C(3)-C(2)	106.1(8)	F(32)-C(32)-C(31)	121.9(10)
B(1)-C(34)	1.668(13)	C(42)-F(42)	1.353(10)	C(4)-C(3)-Mo(1)	70.9(5)	F(32)-C(32)-C(33)	121.2(9)
C(1)-C(2)	1.440(12)	C(42)-C(43)	1.357(13)	C(2)-C(3)-Mo(1)	69.7(5)	C(31)-C(32)-C(33)	116.9(9)
C(1)-C(5)	1.447(13)	C(43)-F(43)	1.348(10)	C(3)-C(4)-C(5)	112.1(9)	F(33)-C(33)-C(32)	113.4(8)
C(2)-C(3)	1.435(12)	C(43)-C(44)	1.359(13)	C(3)-C(4)-Mo(1)	75.3(5)	F(33)-C(33)-C(28)	120.6(8)
C(3)-C(4)	1.390(15)	C(44)-F(44)	1.360(10)	C(5)-C(4)-Mo(1)	71.2(5)	C(32)-C(33)-C(28)	126.0(8)
C(4)-C(5)	1.398(13)	C(44)-C(45)	1.372(11)	C(4)-C(5)-C(1)	106.6(9)	C(35)-C(34)-C(39)	112.1(8)
C(6)-C(11)	1.401(13)	C(45)-F(45)	1.351(9)	C(4)-C(5)-Mo(1)	74.0(5)	C(35)-C(34)-B(1)	129.3(8)
C(6)-C(7)	1.405(12)			C(1)-C(5)-Mo(1)	71.3(5)	C(39)-C(34)-B(1)	118.6(8)
C(7)-C(8)	1.373(13)	C(21)-Mo(1)-C(20)	76.0(4)	C(11)-C(6)-C(7)	119.9(8)	F(35)-C(35)-C(34)	119.9(8)
C(8)-C(9)	1.359(16)	C(21)-Mo(1)-C(19)	79.8(4)	C(11)-C(6)-P(1)	119.4(7)	F(35)-C(35)-C(36)	115.2(9)
C(9)-C(10)	1.361(17)	C(20)-Mo(1)-C(19)	104.3(4)	C(7)-C(6)-P(1)	120.6(7)	C(34)-C(35)-C(36)	124.9(9)
C(10)-C(11)	1.411(15)	C(21)-Mo(1)-C(1)	91.5(3)	C(8)-C(7)-C(6)	120.8(10)	F(36)-C(36)-C(35)	121.7(10)
C(12)-C(17)	1.379(12)	C(20)-Mo(1)-C(1)	145.0(4)	C(9)-C(8)-C(7)	120.0(11)	F(36)-C(36)-C(37)	119.0(10)
C(12)-C(13)	1.409(14)	C(19)-Mo(1)-C(1)	105.4(3)	C(8)-C(9)-C(10)	120.2(11)	C(35)-C(36)-C(37)	119.2(10)
C(13)-C(14)	1.391(15)	C(21)-Mo(1)-C(5)	87.3(4)	C(9)-C(10)-C(11)	122.6(12)	F(37)-C(37)-C(38)	120.8(11)
C(14)-C(15)	1.372(19)	C(20)-Mo(1)-C(5)	109.4(4)	C(6)-C(11)-C(10)	116.4(10)	F(37)-C(37)-C(36)	120.9(12)
C(15)-C(16)	1.34(2)	C(19)-Mo(1)-C(5)	139.7(3)	C(17)-C(12)-C(13)	119.9(9)	C(38)-C(37)-C(36)	118.2(9)
C(16)-C(17)	1.386(17)	C(1)-Mo(1)-C(5)	36.5(3)	C(17)-C(12)-P(1)	121.4(8)	C(39)-C(38)-F(38)	121.7(11)
C(19)-O(1)	1.174(10)	C(21)-Mo(1)-C(2)	125.6(4)	C(13)-C(12)-P(1)	118.6(7)	C(39)-C(38)-C(37)	119.4(10)
C(20)-O(2)	1.182(12)	C(20)-Mo(1)-C(2)	151.6(4)	C(14)-C(13)-C(12)	118.6(11)	F(38)-C(38)-C(37)	118.9(9)
C(21)-O(3)	1.188(11)	C(19)-Mo(1)-C(2)	98.1(4)	C(15)-C(14)-C(13)	119.7(14)	C(38)-C(39)-F(39)	114.4(9)
C(22)-C(27)	1.392(13)	C(1)-Mo(1)-C(2)	36.1(3)	C(16)-C(15)-C(14)	121.7(13)	C(38)-C(39)-C(34)	126.1(10)
C(22)-C(23)	1.411(11)	C(5)-Mo(1)-C(2)	59.6(3)	C(15)-C(16)-C(17)	120.6(13)	F(39)-C(39)-C(34)	119.5(8)
C(23)-F(23)	1.355(9)	C(21)-Mo(1)-C(4)	116.9(4)	C(12)-C(17)-C(16)	119.5(13)	C(41)-C(40)-C(45)	113.2(7)
C(23)-C(24)	1.392(12)	C(20)-Mo(1)-C(4)	97.8(4)	O(1)-C(19)-Mo(1)	175.7(8)	C(41)-C(40)-B(1)	121.2(7)
C(24)-C(25)	1.327(14)	C(19)-Mo(1)-C(4)	155.2(4)	O(2)-C(20)-Mo(1)	172.3(9)	C(45)-C(40)-B(1)	125.3(7)
C(24)-F(24)	1.351(10)	C(1)-Mo(1)-C(4)	58.6(3)	O(3)-C(21)-Mo(1)	177.8(9)	F(41)-C(41)-C(42)	117.3(8)
C(25)-F(25)	1.343(10)	C(5)-Mo(1)-C(4)	34.8(3)	C(27)-C(22)-C(23)	111.4(8)	F(41)-C(41)-C(40)	118.7(7)
C(25)-C(26)	1.362(14)	C(2)-Mo(1)-C(4)	57.5(4)	C(27)-C(22)-B(1)	121.6(7)	C(42)-C(41)-C(40)	123.8(8)
C(26)-F(26)	1.372(10)	C(21)-Mo(1)-C(3)	145.6(4)	C(23)-C(22)-B(1)	126.8(8)	F(42)-C(42)-C(43)	119.2(8)
C(26)-C(27)	1.388(13)	C(20)-Mo(1)-C(3)	116.5(4)	F(23)-C(23)-C(24)	115.7(7)	F(42)-C(42)-C(41)	120.1(9)

C(27)-F(27)	1.345(10)	C(19)-Mo(1)-C(3)	122.9(4)	F(23)-C(23)-C(22)	120.1(7)	C(43)-C(42)-C(41)	120.6(9)
C(28)-C(29)	1.374(12)	C(1)-Mo(1)-C(3)	59.3(3)	C(24)-C(23)-C(22)	124.2(8)	F(43)-C(43)-C(42)	120.5(9)
C(28)-C(33)	1.394(12)	C(5)-Mo(1)-C(3)	58.5(3)	C(25)-C(24)-F(24)	120.8(8)	F(43)-C(43)-C(44)	120.2(8)
C(29)-F(29)	1.356(10)	C(2)-Mo(1)-C(3)	35.1(3)	C(25)-C(24)-C(23)	120.8(8)	C(42)-C(43)-C(44)	119.2(8)
C(29)-C(30)	1.399(13)	C(4)-Mo(1)-C(3)	33.9(4)	F(24)-C(24)-C(23)	118.3(8)	C(43)-C(44)-F(44)	120.3(8)
C(30)-F(30)	1.332(11)	C(6)-P(1)-C(1)	108.0(4)	C(24)-C(25)-F(25)	120.8(9)	C(43)-C(44)-C(45)	120.1(8)
C(30)-C(31)	1.352(15)	C(6)-P(1)-C(12)	110.8(4)	C(24)-C(25)-C(26)	118.7(8)	F(44)-C(44)-C(45)	119.6(8)
C(31)-C(32)	1.354(14)	C(1)-P(1)-C(12)	111.7(4)	F(25)-C(25)-C(26)	120.5(10)	F(45)-C(45)-C(44)	116.1(7)
C(31)-F(31)	1.384(12)	C(6)-P(1)-C(18)	107.3(4)	C(25)-C(26)-F(26)	119.9(9)	F(45)-C(45)-C(40)	120.7(7)
C(32)-F(32)	1.305(11)	C(1)-P(1)-C(18)	107.7(5)	C(25)-C(26)-C(27)	120.6(9)	C(44)-C(45)-C(40)	123.1(8)
C(32)-C(33)	1.388(13)	C(12)-P(1)-C(18)	111.2(5)	F(26)-C(26)-C(27)	119.5(9)		
C(33)-F(33)	1.361(10)	C(22)-B(1)-C(40)	101.5(7)	F(27)-C(27)-C(26)	117.6(9)		

Table 40. Anisotropic displacement parameters ($Å^2 x\ 10^3$)for **$[IV_2][B(C_6F_5)_4]_2$**. The anisotropic displacement factor exponent takes the form: $-2\pi^2[\ h^2a^{*2}U^{11} + ... + 2\ h\ k\ a^*\ b^*\ U^{12}\ ]$

	U^{11}	U^{22}	U^{33}	U^{23}	U^{13}	U^{12}
Mo(1)	35(1)	42(1)	41(1)	-3(1)	4(1)	10(1)
P(1)	33(1)	40(1)	40(1)	-3(1)	3(1)	5(1)
B(1)	28(5)	44(6)	48(6)	3(5)	-3(4)	1(4)
C(1)	28(4)	56(5)	43(5)	-2(4)	5(3)	9(4)
C(2)	44(5)	52(5)	44(5)	-5(4)	6(4)	20(4)
C(3)	42(5)	87(8)	37(5)	-15(5)	-4(4)	27(5)
C(4)	30(5)	108(9)	50(6)	-17(6)	0(4)	-8(6)
C(5)	32(4)	69(7)	50(5)	-7(5)	9(4)	-2(4)
C(6)	39(5)	43(5)	41(5)	6(4)	14(4)	8(4)
C(7)	45(5)	59(6)	60(6)	4(5)	16(4)	9(5)
C(8)	57(7)	84(8)	80(8)	23(7)	30(6)	24(6)
C(9)	92(10)	80(9)	70(8)	2(7)	32(7)	28(7)
C(10)	92(10)	125(12)	53(7)	-31(7)	8(6)	18(8)
C(11)	54(6)	72(7)	65(7)	-20(6)	5(5)	-6(5)
C(12)	31(4)	68(6)	39(5)	-6(4)	4(4)	-5(4)
C(13)	50(6)	67(7)	60(6)	-3(5)	9(5)	-13(5)
C(14)	77(9)	116(11)	73(8)	-15(8)	2(7)	-30(8)
C(15)	44(7)	157(15)	81(9)	-20(10)	2(6)	-22(9)
C(16)	39(7)	177(16)	65(8)	6(9)	-8(5)	5(9)
C(17)	31(5)	107(9)	65(7)	-10(6)	-2(4)	17(5)
C(18)	78(7)	55(6)	48(5)	7(5)	-3(5)	22(5)
C(19)	37(5)	63(6)	43(5)	-4(5)	9(4)	8(5)
C(20)	64(6)	64(7)	48(6)	-3(5)	13(5)	18(5)
C(21)	39(5)	74(7)	56(6)	6(5)	10(4)	16(5)
C(22)	33(4)	44(5)	49(5)	2(4)	-3(4)	9(4)
C(23)	31(4)	48(5)	43(5)	2(4)	0(4)	1(4)
C(24)	33(5)	68(6)	42(5)	1(5)	-4(4)	2(4)
C(25)	52(6)	83(8)	47(6)	22(5)	3(4)	29(6)
C(26)	43(5)	73(7)	62(6)	22(5)	21(5)	-12(5)
C(27)	38(5)	59(6)	53(6)	-12(5)	-1(4)	6(4)
C(28)	34(4)	47(5)	43(5)	6(4)	-6(4)	1(4)
C(29)	45(5)	45(5)	59(6)	0(4)	8(4)	10(4)
C(30)	41(5)	62(7)	80(7)	1(6)	13(5)	3(5)
C(31)	54(6)	74(8)	86(8)	0(6)	17(6)	-12(6)
C(32)	65(7)	40(6)	87(8)	10(5)	-1(6)	4(5)
C(33)	31(4)	55(6)	60(6)	2(4)	-4(4)	3(4)
C(34)	35(4)	55(6)	46(5)	-2(4)	0(4)	6(4)
C(35)	39(5)	58(6)	44(5)	-8(5)	3(4)	9(4)
C(36)	59(6)	62(7)	60(7)	-17(5)	23(5)	-14(5)
C(37)	58(6)	101(9)	45(6)	-31(7)	9(5)	-5(6)
C(38)	50(6)	96(9)	37(5)	-4(6)	-4(4)	0(6)
C(39)	39(5)	76(7)	40(5)	-6(5)	4(4)	10(5)
C(40)	27(4)	47(5)	42(5)	-1(4)	-5(3)	6(4)
C(41)	37(4)	42(5)	49(5)	-8(4)	1(4)	-2(4)
C(42)	59(6)	39(5)	60(6)	-6(5)	4(5)	16(5)
C(43)	47(5)	43(5)	60(6)	-1(4)	13(4)	13(4)
C(44)	36(5)	51(5)	56(6)	9(5)	1(4)	8(4)

C(45)	35(4)	34(5)	53(5)	-9(4)	-5(4)	6(4)
O(1)	46(4)	105(6)	61(4)	-18(4)	9(3)	-13(4)
O(2)	142(8)	48(4)	80(6)	-5(4)	27(5)	13(5)
O(3)	81(5)	102(6)	88(6)	29(5)	10(4)	50(5)
F(23)	45(3)	59(3)	65(3)	6(3)	-17(2)	-11(3)
F(24)	51(3)	116(5)	61(4)	0(4)	-24(3)	3(3)
F(25)	68(4)	97(5)	67(4)	37(3)	5(3)	20(3)
F(26)	67(4)	69(4)	98(5)	25(3)	11(3)	-9(3)
F(27)	50(3)	59(3)	67(3)	-1(3)	-3(3)	-9(3)
F(29)	52(3)	57(3)	87(4)	8(3)	11(3)	16(3)
F(30)	43(3)	102(5)	119(5)	16(4)	22(3)	21(3)
F(31)	74(4)	110(6)	138(7)	20(5)	34(4)	-17(4)
F(32)	87(5)	69(4)	144(7)	51(4)	23(4)	-2(4)
F(33)	57(3)	49(3)	91(4)	17(3)	15(3)	24(3)
F(35)	90(4)	46(3)	68(4)	-4(3)	-7(3)	17(3)
F(36)	112(5)	66(4)	90(5)	-35(4)	26(4)	-2(4)
F(37)	121(6)	116(6)	64(4)	-54(4)	3(4)	-22(5)
F(38)	113(6)	125(6)	49(4)	0(4)	-28(4)	11(5)
F(39)	62(3)	64(4)	58(3)	6(3)	-10(3)	20(3)
F(41)	46(3)	53(3)	74(4)	-18(3)	-7(3)	-8(2)
F(42)	88(5)	63(4)	103(5)	-44(4)	0(4)	1(3)
F(43)	67(4)	72(4)	113(5)	-21(4)	27(4)	30(3)
F(44)	40(3)	70(4)	98(5)	-3(3)	-2(3)	8(3)
F(45)	41(3)	63(3)	66(3)	-21(3)	-10(2)	5(2)

Table 41. Hydrogen coordinates (x 10^4) and isotropic displacement parameters ($Å^2$x 10^3) for **$[IV_2][B(C_6F_5)_4]_2$**.

	x	y	z	U(eq)
H(2A)	4144	7320	10615	56
H(3A)	2929	6196	10147	66
H(4A)	2589	3864	10360	75
H(5A)	3472	3476	10954	60
H(7A)	2579	6231	11321	65
H(8A)	1501	7466	11655	88
H(9A)	2173	8945	12059	96
H(10A)	3901	9056	12172	108
H(11A)	5060	7871	11834	77
H(13A)	5324	8483	11105	71
H(14A)	6888	9540	11015	107
H(15A)	8392	8352	11066	113
H(16A)	8410	6220	11247	113
H(17A)	6887	5120	11348	81
H(18A)	5379	3782	11425	91
H(18B)	4284	3948	11576	91
H(18C)	5249	4568	11776	91

Table 42. Torsion angles [°] for **$[IV_2][B(C_6F_5)_4]_2$**.

C(6)-P(1)-C(1)-C(2)	70.5(7)	C(3)-Mo(1)-C(5)-C(4)	34.5(6)	C(34)-B(1)-C(28)-C(29)	71.2(9)
C(12)-P(1)-C(1)-C(2)	-51.6(8)	C(21)-Mo(1)-C(5)-C(1)	96.2(6)	C(22)-B(1)-C(28)-C(33)	137.1(9)
C(18)-P(1)-C(1)-C(2)	-174.0(7)	C(20)-Mo(1)-C(5)-C(1)	170.4(5)	C(40)-B(1)-C(28)-C(33)	22.1(12)
C(6)-P(1)-C(1)-C(5)	-98.8(8)	C(19)-Mo(1)-C(5)-C(1)	25.4(8)	C(34)-B(1)-C(28)-C(33)	-100.2(10)
C(12)-P(1)-C(1)-C(5)	139.1(7)	C(2)-Mo(1)-C(5)-C(1)	-38.6(5)	C(33)-C(28)-C(29)-F(29)	178.5(8)
C(18)-P(1)-C(1)-C(5)	16.7(9)	C(4)-Mo(1)-C(5)-C(1)	-114.3(9)	B(1)-C(28)-C(29)-F(29)	5.9(13)
C(6)-P(1)-C(1)-Mo(1)	164.7(5)	C(3)-Mo(1)-C(5)-C(1)	-79.8(5)	C(33)-C(28)-C(29)-C(30)	-3.2(14)
C(12)-P(1)-C(1)-Mo(1)	42.6(7)	C(1)-P(1)-C(6)-C(11)	-155.1(8)	B(1)-C(28)-C(29)-C(30)	-175.8(9)
C(18)-P(1)-C(1)-Mo(1)	-79.8(7)	C(12)-P(1)-C(6)-C(11)	-32.4(9)	F(29)-C(29)-C(30)-F(30)	3.5(14)
C(21)-Mo(1)-C(1)-C(2)	162.4(6)	C(18)-P(1)-C(6)-C(11)	89.1(8)	C(28)-C(29)-C(30)-F(30)	-174.9(9)
C(20)-Mo(1)-C(1)-C(2)	-130.2(7)	C(1)-P(1)-C(6)-C(7)	27.7(8)	F(29)-C(29)-C(30)-C(31)	-179.8(9)
C(19)-Mo(1)-C(1)-C(2)	82.5(6)	C(12)-P(1)-C(6)-C(7)	150.4(7)	C(28)-C(29)-C(30)-C(31)	1.8(17)
C(5)-Mo(1)-C(1)-C(2)	-114.2(7)	C(18)-P(1)-C(6)-C(7)	-88.1(8)	F(30)-C(30)-C(31)-C(32)	177.9(11)
C(4)-Mo(1)-C(1)-C(2)	-76.6(6)	C(11)-C(6)-C(7)-C(8)	-0.7(14)	C(29)-C(30)-C(31)-C(32)	1.3(18)
C(3)-Mo(1)-C(1)-C(2)	-36.9(5)	P(1)-C(6)-C(7)-C(8)	176.5(8)	F(30)-C(30)-C(31)-F(31)	-4.0(18)

C(21)-Mo(1)-C(1)-C(5)	-83.4(6)	C(6)-C(7)-C(8)-C(9)	1.3(16)	C(29)-C(30)-C(31)-F(31)	179.3(10)
C(20)-Mo(1)-C(1)-C(5)	-16.0(8)	C(7)-C(8)-C(9)-C(10)	-2.8(18)	C(30)-C(31)-C(32)-F(32)	177.8(11)
C(19)-Mo(1)-C(1)-C(5)	-163.3(5)	C(8)-C(9)-C(10)-C(11)	4(2)	F(31)-C(31)-C(32)-F(32)	-0.3(18)
C(2)-Mo(1)-C(1)-C(5)	114.2(7)	C(7)-C(6)-C(11)-C(10)	1.4(15)	C(30)-C(31)-C(32)-C(33)	-2.4(18)
C(4)-Mo(1)-C(1)-C(5)	37.6(6)	P(1)-C(6)-C(11)-C(10)	-175.8(9)	F(31)-C(31)-C(32)-C(33)	179.5(10)
C(3)-Mo(1)-C(1)-C(5)	77.3(6)	C(9)-C(10)-C(11)-C(6)	-2.9(19)	F(32)-C(32)-C(33)-F(33)	2.2(15)
C(21)-Mo(1)-C(1)-P(1)	41.9(6)	C(6)-P(1)-C(12)-C(17)	138.0(8)	C(31)-C(32)-C(33)-F(33)	-177.5(9)
C(20)-Mo(1)-C(1)-P(1)	109.3(7)	C(1)-P(1)-C(12)-C(17)	-101.5(8)	F(32)-C(32)-C(33)-C(28)	-179.5(10)
C(19)-Mo(1)-C(1)-P(1)	-38.0(7)	C(18)-P(1)-C(12)-C(17)	18.8(9)	C(31)-C(32)-C(33)-C(28)	0.7(16)
C(5)-Mo(1)-C(1)-P(1)	125.3(8)	C(6)-P(1)-C(12)-C(13)	-45.1(8)	C(29)-C(28)-C(33)-F(33)	180.0(8)
C(2)-Mo(1)-C(1)-P(1)	-120.5(9)	C(1)-P(1)-C(12)-C(13)	75.4(8)	B(1)-C(28)-C(33)-F(33)	-7.9(14)
C(4)-Mo(1)-C(1)-P(1)	162.8(8)	C(18)-P(1)-C(12)-C(13)	-164.3(7)	C(29)-C(28)-C(33)-C(32)	1.9(14)
C(3)-Mo(1)-C(1)-P(1)	-157.4(8)	C(17)-C(12)-C(13)-C(14)	-1.4(14)	B(1)-C(28)-C(33)-C(32)	174.0(9)
C(5)-C(1)-C(2)-C(3)	1.2(9)	P(1)-C(12)-C(13)-C(14)	-178.3(8)	C(22)-B(1)-C(34)-C(35)	12.0(13)
P(1)-C(1)-C(2)-C(3)	-170.1(6)	C(12)-C(13)-C(14)-C(15)	2.1(16)	C(40)-B(1)-C(34)-C(35)	128.3(9)
Mo(1)-C(1)-C(2)-C(3)	66.2(6)	C(13)-C(14)-C(15)-C(16)	-2(2)	C(28)-B(1)-C(34)-C(35)	-108.2(10)
C(5)-C(1)-C(2)-Mo(1)	-65.0(5)	C(14)-C(15)-C(16)-C(17)	2(2)	C(22)-B(1)-C(34)-C(39)	-171.0(7)
P(1)-C(1)-C(2)-Mo(1)	123.7(6)	C(13)-C(12)-C(17)-C(16)	0.9(15)	C(40)-B(1)-C(34)-C(39)	-54.7(10)
C(21)-Mo(1)-C(2)-C(3)	-138.1(6)	P(1)-C(12)-C(17)-C(16)	177.7(8)	C(28)-B(1)-C(34)-C(39)	68.8(9)
C(20)-Mo(1)-C(2)-C(3)	-3.5(11)	C(15)-C(16)-C(17)-C(12)	-1.2(19)	C(39)-C(34)-C(35)-F(35)	-176.4(8)
C(19)-Mo(1)-C(2)-C(3)	138.6(6)	C(21)-Mo(1)-C(19)-O(1)	-77(12)	B(1)-C(34)-C(35)-F(35)	0.8(14)
C(1)-Mo(1)-C(2)-C(3)	-116.3(8)	C(20)-Mo(1)-C(19)-O(1)	-149(11)	C(39)-C(34)-C(35)-C(36)	3.8(13)
C(5)-Mo(1)-C(2)-C(3)	-77.4(6)	C(1)-Mo(1)-C(19)-O(1)	12(12)	B(1)-C(34)-C(35)-C(36)	-179.1(8)
C(4)-Mo(1)-C(2)-C(3)	-36.4(6)	C(5)-Mo(1)-C(19)-O(1)	-3(12)	F(35)-C(35)-C(36)-F(36)	-0.3(13)
C(21)-Mo(1)-C(2)-C(1)	-21.8(7)	C(2)-Mo(1)-C(19)-O(1)	48(12)	C(34)-C(35)-C(36)-F(36)	179.6(9)
C(20)-Mo(1)-C(2)-C(1)	112.8(8)	C(4)-Mo(1)-C(19)-O(1)	58(12)	F(35)-C(35)-C(36)-C(37)	176.1(8)
C(19)-Mo(1)-C(2)-C(1)	-105.1(5)	C(3)-Mo(1)-C(19)-O(1)	75(12)	C(34)-C(35)-C(36)-C(37)	-4.1(15)
C(5)-Mo(1)-C(2)-C(1)	38.9(5)	C(21)-Mo(1)-C(20)-O(2)	61(7)	F(36)-C(36)-C(37)-F(37)	-2.4(15)
C(4)-Mo(1)-C(2)-C(1)	79.9(6)	C(19)-Mo(1)-C(20)-O(2)	136(7)	C(35)-C(36)-C(37)-F(37)	-178.8(9)
C(3)-Mo(1)-C(2)-C(1)	116.3(8)	C(1)-Mo(1)-C(20)-O(2)	-11(7)	F(36)-C(36)-C(37)-C(38)	177.8(9)
C(1)-C(2)-C(3)-C(4)	-1.4(9)	C(5)-Mo(1)-C(20)-O(2)	-21(7)	C(35)-C(36)-C(37)-C(38)	1.4(15)
Mo(1)-C(2)-C(3)-C(4)	61.9(6)	C(2)-Mo(1)-C(20)-O(2)	-83(7)	F(37)-C(37)-C(38)-C(39)	-178.7(9)
C(1)-C(2)-C(3)-Mo(1)	-63.3(5)	C(4)-Mo(1)-C(20)-O(2)	-55(7)	C(36)-C(37)-C(38)-C(39)	1.1(15)
C(21)-Mo(1)-C(3)-C(4)	-42.6(9)	C(3)-Mo(1)-C(20)-O(2)	-85(7)	F(37)-C(37)-C(38)-F(38)	1.1(15)
C(20)-Mo(1)-C(3)-C(4)	62.0(7)	C(20)-Mo(1)-C(21)-O(3)	-85(25)	C(36)-C(37)-C(38)-F(38)	-179.1(9)
C(19)-Mo(1)-C(3)-C(4)	-167.4(5)	C(19)-Mo(1)-C(21)-O(3)	167(100)	F(38)-C(38)-C(39)-F(39)	-1.4(13)
C(1)-Mo(1)-C(3)-C(4)	-78.3(6)	C(1)-Mo(1)-C(21)-O(3)	62(25)	C(37)-C(38)-C(39)-F(39)	178.4(9)
C(5)-Mo(1)-C(3)-C(4)	-35.4(5)	C(5)-Mo(1)-C(21)-O(3)	26(25)	F(38)-C(38)-C(39)-C(34)	179.0(9)
C(2)-Mo(1)-C(3)-C(4)	-116.2(8)	C(2)-Mo(1)-C(21)-O(3)	75(25)	C(37)-C(38)-C(39)-C(34)	-1.2(16)
C(21)-Mo(1)-C(3)-C(2)	73.6(10)	C(4)-Mo(1)-C(21)-O(3)	7(25)	C(35)-C(34)-C(39)-C(38)	-1.1(14)
C(20)-Mo(1)-C(3)-C(2)	178.1(6)	C(3)-Mo(1)-C(21)-O(3)	32(25)	B(1)-C(34)-C(39)-C(38)	-178.6(9)
C(19)-Mo(1)-C(3)-C(2)	-51.2(7)	C(40)-B(1)-C(22)-C(27)	-72.8(10)	C(35)-C(34)-C(39)-F(39)	179.3(8)
C(1)-Mo(1)-C(3)-C(2)	37.9(5)	C(28)-B(1)-C(22)-C(27)	163.9(8)	B(1)-C(34)-C(39)-F(39)	1.8(12)
C(5)-Mo(1)-C(3)-C(2)	80.7(6)	C(34)-B(1)-C(22)-C(27)	50.0(11)	C(22)-B(1)-C(40)-C(41)	-71.5(10)
C(4)-Mo(1)-C(3)-C(2)	116.2(8)	C(40)-B(1)-C(22)-C(23)	102.3(9)	C(28)-B(1)-C(40)-C(41)	49.2(11)
C(2)-C(3)-C(4)-C(5)	1.1(10)	C(28)-B(1)-C(22)-C(23)	-20.9(12)	C(34)-B(1)-C(40)-C(41)	164.3(8)
Mo(1)-C(3)-C(4)-C(5)	62.2(7)	C(34)-B(1)-C(22)-C(23)	-134.8(9)	C(22)-B(1)-C(40)-C(45)	101.6(9)
C(2)-C(3)-C(4)-Mo(1)	-61.1(6)	C(27)-C(22)-C(23)-F(23)	176.9(7)	C(28)-B(1)-C(40)-C(45)	-137.6(9)

C(21)-Mo(1)-C(4)-C(3)	154.6(6)	B(1)-C(22)-C(23)-F(23)	1.3(13)	C(34)-B(1)-C(40)-C(45)	-22.5(12)
C(20)-Mo(1)-C(4)-C(3)	-127.1(6)	C(27)-C(22)-C(23)-C(24)	-2.4(12)	C(45)-C(40)-C(41)-F(41)	-176.5(8)
C(19)-Mo(1)-C(4)-C(3)	25.9(11)	B(1)-C(22)-C(23)-C(24)	-177.9(8)	B(1)-C(40)-C(41)-F(41)	-2.5(12)
C(1)-Mo(1)-C(4)-C(3)	80.6(6)	F(23)-C(23)-C(24)-C(25)	-177.7(8)	C(45)-C(40)-C(41)-C(42)	-2.2(13)
C(5)-Mo(1)-C(4)-C(3)	120.0(9)	C(22)-C(23)-C(24)-C(25)	1.5(14)	B(1)-C(40)-C(41)-C(42)	171.7(9)
C(2)-Mo(1)-C(4)-C(3)	37.8(5)	F(23)-C(23)-C(24)-F(24)	-1.5(12)	F(41)-C(41)-C(42)-F(42)	-6.3(13)
C(21)-Mo(1)-C(4)-C(5)	34.6(8)	C(22)-C(23)-C(24)-F(24)	177.7(8)	C(40)-C(41)-C(42)-F(42)	179.3(8)
C(20)-Mo(1)-C(4)-C(5)	112.9(7)	F(24)-C(24)-C(25)-F(25)	3.7(14)	F(41)-C(41)-C(42)-C(43)	177.4(8)
C(19)-Mo(1)-C(4)-C(5)	-94.1(10)	C(23)-C(24)-C(25)-F(25)	179.8(8)	C(40)-C(41)-C(42)-C(43)	3.0(15)
C(1)-Mo(1)-C(4)-C(5)	-39.4(6)	F(24)-C(24)-C(25)-C(26)	-176.9(9)	F(42)-C(42)-C(43)-F(43)	4.7(14)
C(2)-Mo(1)-C(4)-C(5)	-82.2(6)	C(23)-C(24)-C(25)-C(26)	-0.8(15)	C(41)-C(42)-C(43)-F(43)	-179.0(9)
C(3)-Mo(1)-C(4)-C(5)	-120.0(9)	C(24)-C(25)-C(26)-F(26)	-178.8(9)	F(42)-C(42)-C(43)-C(44)	-179.2(8)
C(3)-C(4)-C(5)-C(1)	-0.4(10)	F(25)-C(25)-C(26)-F(26)	0.6(15)	C(41)-C(42)-C(43)-C(44)	-2.8(15)
Mo(1)-C(4)-C(5)-C(1)	64.3(6)	C(24)-C(25)-C(26)-C(27)	1.3(15)	F(43)-C(43)-C(44)-F(44)	-1.9(13)
C(3)-C(4)-C(5)-Mo(1)	-64.6(7)	F(25)-C(25)-C(26)-C(27)	-179.3(9)	C(42)-C(43)-C(44)-F(44)	-178.1(9)
C(2)-C(1)-C(5)-C(4)	-0.5(9)	C(25)-C(26)-C(27)-F(27)	176.2(9)	F(43)-C(43)-C(44)-C(45)	178.3(8)
P(1)-C(1)-C(5)-C(4)	170.3(6)	F(26)-C(26)-C(27)-F(27)	-3.7(13)	C(42)-C(43)-C(44)-C(45)	2.1(14)
Mo(1)-C(1)-C(5)-C(4)	-66.1(6)	C(25)-C(26)-C(27)-C(22)	-2.5(15)	C(43)-C(44)-C(45)-F(45)	-178.1(8)
C(2)-C(1)-C(5)-Mo(1)	65.6(5)	F(26)-C(26)-C(27)-C(22)	177.6(8)	F(44)-C(44)-C(45)-F(45)	2.1(12)
P(1)-C(1)-C(5)-Mo(1)	-123.6(7)	C(23)-C(22)-C(27)-F(27)	-175.9(7)	C(43)-C(44)-C(45)-C(40)	-1.5(14)
C(21)-Mo(1)-C(5)-C(4)	-149.5(7)	B(1)-C(22)-C(27)-F(27)	0.0(12)	F(44)-C(44)-C(45)-C(40)	178.7(8)
C(20)-Mo(1)-C(5)-C(4)	-75.4(7)	C(23)-C(22)-C(27)-C(26)	2.8(13)	C(41)-C(40)-C(45)-F(45)	177.9(8)
C(19)-Mo(1)-C(5)-C(4)	139.6(7)	B(1)-C(22)-C(27)-C(26)	178.7(9)	B(1)-C(40)-C(45)-F(45)	4.3(13)
C(1)-Mo(1)-C(5)-C(4)	114.3(9)	C(22)-B(1)-C(28)-C(29)	-51.5(11)	C(41)-C(40)-C(45)-C(44)	1.4(13)
C(2)-Mo(1)-C(5)-C(4)	75.7(7)	C(40)-B(1)-C(28)-C(29)	-166.5(8)	B(1)-C(40)-C(45)-C(44)	-172.2(8)

Figure 7. The molecular structure of $[IV_2][B(C_6F_5)_4]_2$.

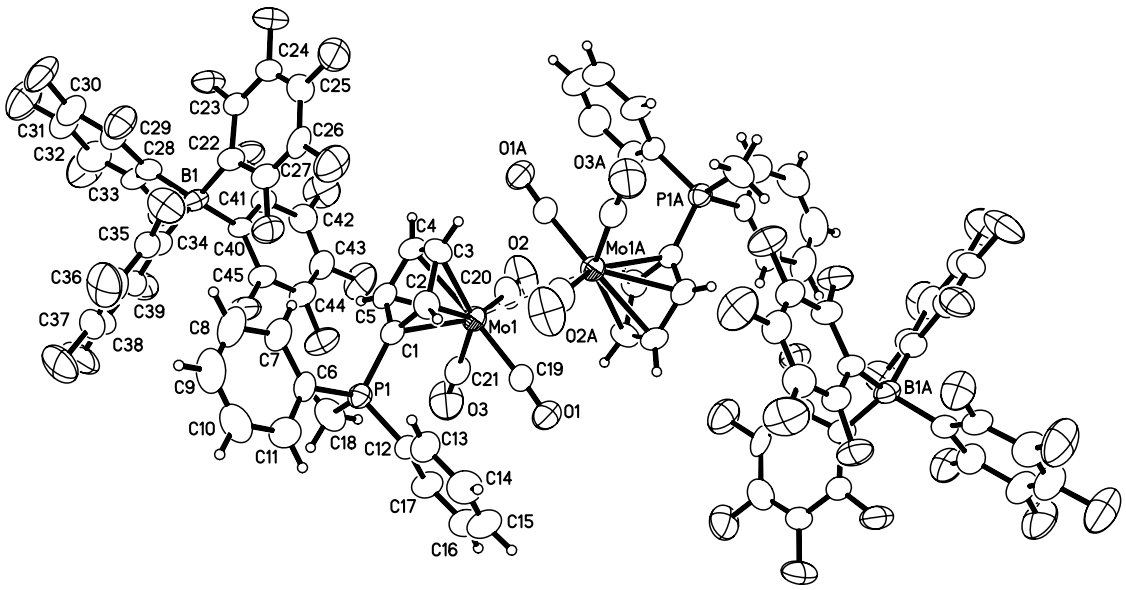

Table 43. Crystal data and structure refinement for **$[V_2][B(C_6F_5)_4]_2$**.

Identification code	**$[V_2][B(C_6F_5)_4]_2$**	
Empirical formula	C102 H58 B2 F40 O9 P2 W2	
Formula weight	2638.74	
Temperature	180(2) K	
Wavelength	0.71073 Å	
Crystal system	Monoclinic	
Space group	P2/n	
Unit cell dimensions	a = 12.9575(7) Å	α= 90°.
	b = 9.9157(6) Å	β= 91.9600(10)°.
	c = 37.847(2) Å	γ = 90°.
Volume	4859.8(5) $Å^3$	
Z	2	
Density (calculated)	1.803 Mg/m^3	
Absorption coefficient	2.535 mm^{-1}	
F(000)	2580	
Crystal size	0.15 x 0.12 x 0.10 mm^3	
Theta range for data collection	1.68 to 25.00°.	
Index ranges	-15<=h<=15, -11<=k<=11, -44<=l<=44	
Reflections collected	44056	
Independent reflections	8569 [R(int) = 0.0418]	
Completeness to theta = 25.00°	99.9 %	
Absorption correction	Multi-scan	
Max. and min. transmission	0.7856 and 0.7023	
Refinement method	Full-matrix least-squares on F^2	
Data / restraints / parameters	8569 / 4 / 729	
Goodness-of-fit on F^2	1.000	
Final R indices [I>2sigma(I)]	R1 = 0.0376, wR2 = 0.1283	
R indices (all data)	R1 = 0.0453, wR2 = 0.1369	
Largest diff. peak and hole	0.852 and -1.104 e.$Å^{-3}$	

Table 44. Atomic coordinates (x 10^4) and equivalent isotropic displacement parameters ($Å^2$x 10^3) for **$[V_2][B(C_6F_5)_4]_2$**. U(eq) is defined as one third of the trace of the orthogonalized U^{ij} tensor.

	x	y	z	U(eq)
W(1)	4862(1)	4605(1)	10413(1)	22(1)
P(1)	4763(1)	5959(1)	11307(1)	16(1)
B(1)	147(4)	2325(6)	11478(1)	17(1)
C(1)	4120(4)	5517(5)	10901(1)	17(1)
C(2)	3904(4)	6441(5)	10611(1)	18(1)
C(3)	3245(4)	5757(6)	10363(1)	25(1)
C(4)	3060(4)	4431(6)	10487(1)	25(1)
C(5)	3585(4)	4278(5)	10813(1)	19(1)
C(6)	3929(4)	7060(5)	11543(1)	18(1)
C(7)	2860(4)	6935(5)	11488(1)	23(1)
C(8)	2206(4)	7682(6)	11689(2)	32(1)
C(9)	2607(5)	8567(6)	11942(2)	39(2)
C(10)	3657(6)	8698(6)	11992(2)	42(2)
C(11)	4325(4)	7936(6)	11797(1)	30(1)
C(12)	5959(4)	6799(5)	11231(1)	21(1)
C(13)	5945(4)	8157(6)	11130(1)	28(1)
C(14)	6884(5)	8789(7)	11059(2)	43(2)
C(15)	7798(5)	8092(8)	11097(2)	47(2)
C(16)	7797(5)	6770(9)	11199(2)	45(2)
C(17)	6888(4)	6106(6)	11267(1)	31(1)
C(18)	4971(4)	4452(5)	11559(1)	26(1)
C(19)	6207(4)	5556(5)	10371(1)	18(1)
C(20)	4984(4)	2936(5)	10121(1)	22(1)
C(21)	5741(4)	3425(5)	10712(1)	25(1)
C(22)	-200(4)	3160(5)	11112(1)	17(1)
C(23)	-1024(4)	2842(5)	10886(1)	19(1)
C(24)	-1268(4)	3535(5)	10573(1)	21(1)
C(25)	-668(4)	4594(5)	10474(1)	25(1)
C(26)	184(4)	4934(6)	10679(2)	25(1)
C(27)	402(4)	4208(5)	10985(1)	19(1)
C(28)	-813(4)	1418(5)	11630(1)	19(1)

C(29)	-1768(4)	2030(5)	11680(1)	23(1)
C(30)	-2604(4)	1398(6)	11815(1)	26(1)
C(31)	-2512(5)	86(7)	11929(2)	34(1)
C(32)	-1584(5)	-572(5)	11892(2)	29(1)
C(33)	-776(4)	82(5)	11745(1)	22(1)
C(34)	459(4)	3276(5)	11826(1)	19(1)
C(35)	302(4)	4648(5)	11870(1)	22(1)
C(36)	576(5)	5361(5)	12176(2)	29(1)
C(37)	1005(5)	4665(6)	12460(2)	30(1)
C(38)	1145(4)	3300(6)	12436(1)	28(1)
C(39)	881(4)	2658(5)	12124(1)	22(1)
C(40)	1148(4)	1445(5)	11343(1)	16(1)
C(41)	1002(4)	389(4)	11100(1)	20(1)
C(42)	1787(4)	-310(5)	10948(1)	22(1)
C(43)	2782(4)	47(5)	11028(2)	25(1)
C(44)	2989(4)	1079(5)	11262(1)	21(1)
C(45)	2181(4)	1755(5)	11411(1)	19(1)
C(46)	2570(7)	526(8)	10020(2)	62(2)
C(47)	1652(7)	124(8)	9787(2)	58(2)
C(48)	972(6)	1311(8)	9810(2)	58(2)
C(49)	1160(5)	1685(7)	10194(2)	44(2)
C(50)	6922(13)	6185(17)	12279(4)	52(4)
C(51)	7884(11)	5927(15)	12509(5)	53(4)
C(52A)	7500(20)	4900(30)	12772(7)	54(6)
C(52B)	7986(19)	4310(20)	12551(10)	54(6)
C(53)	6830(15)	3975(17)	12528(5)	42(4)
O(1)	6980(3)	6126(4)	10373(1)	28(1)
O(2)	5033(3)	1907(4)	9988(1)	36(1)
O(3)	6228(3)	2714(4)	10892(1)	41(1)
O(4)	2212(4)	1427(4)	10285(1)	45(1)
O(5)	6333(7)	4908(10)	12279(2)	44(2)
F(23)	-1664(2)	1805(3)	10955(1)	23(1)
F(24)	-2088(2)	3153(3)	10369(1)	30(1)
F(25)	-906(3)	5270(3)	10173(1)	34(1)
F(26)	800(2)	5955(3)	10585(1)	36(1)
F(27)	1283(2)	4558(3)	11169(1)	26(1)
F(29)	-1915(2)	3336(3)	11582(1)	28(1)
F(30)	-3518(2)	2035(3)	11840(1)	40(1)
F(31)	-3315(3)	-564(4)	12071(1)	51(1)
F(32)	-1484(3)	-1861(3)	11999(1)	45(1)
F(33)	97(2)	-647(3)	11718(1)	28(1)
F(35)	-159(3)	5413(3)	11615(1)	30(1)
F(36)	404(3)	6681(3)	12202(1)	38(1)
F(37)	1282(3)	5329(4)	12760(1)	46(1)
F(38)	1539(3)	2595(4)	12714(1)	40(1)
F(39)	1065(2)	1308(3)	12120(1)	28(1)
F(41)	29(2)	26(3)	11003(1)	25(1)
F(42)	1580(3)	-1312(3)	10719(1)	38(1)
F(43)	3580(3)	-604(3)	10876(1)	38(1)
F(44)	3980(2)	1432(3)	11341(1)	29(1)
F(45)	2467(2)	2792(3)	11624(1)	25(1)

Table 45. Bond lengths [Å] and angles [°] for **$[V_2][B(C_6F_5)_4]_2$**.

W(1)-C(21)	1.965(5)	C(51)-C(52B)#1	1.97(2)	O(1)-C(19)-W(1)	175.0(4)	C(51)#1-C(51)-C(52A)#1	69.9(18)
W(1)-C(19)	1.992(5)	C(51)-C(53)#1	1.98(2)	O(2)-C(20)-W(1)	172.5(4)	C(50)-C(51)-C(52A)#1	58.5(13)
W(1)-C(20)	1.998(5)	C(52A)-C(50)#1	1.49(3)	O(3)-C(21)-W(1)	177.7(5)	C(52A)-C(51)-C(52A)#1	85(2)
W(1)-C(1)	2.298(5)	C(52A)-O(5)#1	1.53(3)	C(23)-C(22)-C(27)	112.8(4)	C(50)#1-C(51)-C(52B)	100(2)
W(1)-C(5)	2.304(5)	C(52A)-C(51)#1	1.54(3)	C(23)-C(22)-B(1)	125.7(4)	C(51)#1-C(51)-C(52B)	94.9(11)
W(1)-C(2)	2.342(5)	C(52A)-C(53)	1.546(19)	C(27)-C(22)-B(1)	121.3(4)	C(50)-C(51)-C(52B)	106.7(15)
W(1)-C(4)	2.367(5)	C(52A)-C(53)#1	1.72(4)	F(23)-C(23)-C(22)	121.3(4)	C(52A)-C(51)-C(52B)	45.5(18)
W(1)-C(3)	2.388(5)	C(52B)-C(53)#1	0.51(4)	F(23)-C(23)-C(24)	114.5(4)	C(52A)#1-C(51)-C(52B)	55.7(18)
P(1)-C(1)	1.777(5)	C(52B)-O(5)#1	1.23(3)	C(22)-C(23)-C(24)	124.1(5)	C(50)#1-C(51)-O(5)#1	64.7(16)
P(1)-C(18)	1.789(5)	C(52B)-C(52B)#1	1.30(5)	F(24)-C(24)-C(25)	120.1(4)	C(51)#1-C(51)-O(5)#1	129.8(16)
P(1)-C(12)	1.791(5)	C(52B)-C(53)	1.534(18)	F(24)-C(24)-C(23)	120.0(5)	C(50)-C(51)-O(5)#1	151.1(14)

P(1)-C(6)	1.796(5)	C(52B)-C(51)#1	1.97(2)	C(25)-C(24)-C(23)	119.9(5)	C(52A)-C(51)-O(5)#1	58.3(15)
B(1)-C(28)	1.653(7)	C(52B)-C(50)#1	1.97(3)	F(25)-C(25)-C(24)	119.9(5)	C(52A)#1-C(51)-O(5)#1	96.4(12)
B(1)-C(40)	1.658(7)	C(53)-C(52B)#1	0.51(4)	F(25)-C(25)-C(26)	121.0(5)	C(52B)-C(51)-O(5)#1	44.5(12)
B(1)-C(34)	1.659(7)	C(53)-O(5)	1.46(2)	C(24)-C(25)-C(26)	119.1(5)	C(50)#1-C(51)-C(52B)#1	119(2)
B(1)-C(22)	1.662(7)	C(53)-C(52A)#1	1.72(4)	F(26)-C(26)-C(25)	120.5(5)	C(51)#1-C(51)-C(52B)#1	54.9(8)
C(1)-C(5)	1.445(7)	C(53)-C(53)#1	1.76(4)	F(26)-C(26)-C(27)	120.5(5)	C(50)-C(51)-C(52B)#1	67.4(13)
C(1)-C(2)	1.451(7)	C(53)-C(51)#1	1.98(2)	C(25)-C(26)-C(27)	119.0(5)	C(52A)-C(51)-C(52B)#1	48.0(16)
C(2)-C(3)	1.419(7)	O(5)-C(52B)#1	1.23(3)	F(27)-C(27)-C(26)	115.9(4)	C(52A)#1-C(51)-C(52B)#1	38.2(16)
C(3)-C(4)	1.418(8)	O(5)-C(52A)#1	1.53(3)	F(27)-C(27)-C(22)	119.0(4)	C(52B)-C(51)-C(52B)#1	41.3(16)
C(4)-C(5)	1.397(7)	O(5)-C(51)#1	1.625(19)	C(26)-C(27)-C(22)	125.1(5)	O(5)#1-C(51)-C(52B)#1	84.0(10)
C(6)-C(11)	1.381(7)			C(33)-C(28)-C(29)	113.0(5)	C(50)#1-C(51)-C(53)#1	107.7(19)
C(6)-C(7)	1.400(7)	C(21)-W(1)-C(19)	80.5(2)	C(33)-C(28)-B(1)	127.4(4)	C(51)#1-C(51)-C(53)#1	100.7(8)
C(7)-C(8)	1.377(7)	C(21)-W(1)-C(20)	76.7(2)	C(29)-C(28)-B(1)	119.4(4)	C(50)-C(51)-C(53)#1	106.1(14)
C(8)-C(9)	1.386(9)	C(19)-W(1)-C(20)	105.2(2)	F(29)-C(29)-C(30)	115.7(4)	C(52A)-C(51)-C(53)#1	57.2(16)
C(9)-C(10)	1.374(10)	C(21)-W(1)-C(1)	91.16(19)	F(29)-C(29)-C(28)	119.6(5)	C(52A)#1-C(51)-C(53)#1	50.3(9)
C(10)-C(11)	1.382(8)	C(19)-W(1)-C(1)	105.53(18)	C(30)-C(29)-C(28)	124.7(5)	C(52B)-C(51)-C(53)#1	11.7(15)
C(12)-C(17)	1.389(7)	C(20)-W(1)-C(1)	144.39(19)	F(30)-C(30)-C(29)	121.4(5)	O(5)#1-C(51)-C(53)#1	46.4(8)
C(12)-C(13)	1.399(8)	C(21)-W(1)-C(5)	87.27(19)	F(30)-C(30)-C(31)	119.3(5)	C(52B)#1-C(51)-C(53)#1	45.8(5)
C(13)-C(14)	1.404(8)	C(19)-W(1)-C(5)	140.18(19)	C(29)-C(30)-C(31)	119.4(5)	C(50)#1-C(52A)-C(51)	33.7(9)
C(14)-C(15)	1.375(10)	C(20)-W(1)-C(5)	108.55(19)	F(31)-C(31)-C(30)	121.1(5)	C(50)#1-C(52A)-O(5)#1	58.5(12)
C(15)-C(16)	1.366(11)	C(1)-W(1)-C(5)	36.60(17)	F(31)-C(31)-C(32)	120.1(6)	C(51)-C(52A)-O(5)#1	64.3(13)
C(16)-C(17)	1.382(9)	C(21)-W(1)-C(2)	125.54(19)	C(30)-C(31)-C(32)	118.8(5)	C(50)#1-C(52A)-C(51)#1	60.0(11)
C(19)-O(1)	1.150(6)	C(19)-W(1)-C(2)	97.58(18)	F(32)-C(32)-C(33)	120.4(5)	C(51)-C(52A)-C(51)#1	38.0(12)
C(20)-O(2)	1.140(6)	C(20)-W(1)-C(2)	150.91(19)	F(32)-C(32)-C(31)	119.6(5)	O(5)#1-C(52A)-C(51)#1	101.9(16)
C(21)-O(3)	1.153(6)	C(1)-W(1)-C(2)	36.42(16)	C(33)-C(32)-C(31)	120.0(5)	C(50)#1-C(52A)-C(53)	134.8(18)
C(22)-C(23)	1.382(7)	C(5)-W(1)-C(2)	59.88(17)	F(33)-C(33)-C(32)	115.6(5)	C(51)-C(52A)-C(53)	101.4(16)
C(22)-C(27)	1.394(7)	C(21)-W(1)-C(4)	116.3(2)	F(33)-C(33)-C(28)	120.3(5)	O(5)#1-C(52A)-C(53)	118(2)
C(23)-F(23)	1.352(6)	C(19)-W(1)-C(4)	155.87(19)	C(32)-C(33)-C(28)	124.0(5)	C(51)#1-C(52A)-C(53)	79.7(15)
C(23)-C(24)	1.395(7)	C(20)-W(1)-C(4)	95.9(2)	C(39)-C(34)-C(35)	113.2(5)	C(50)#1-C(52A)-C(53)#1	95.9(19)
C(24)-F(24)	1.347(6)	C(1)-W(1)-C(4)	59.49(17)	C(39)-C(34)-B(1)	118.4(4)	C(51)-C(52A)-C(53)#1	74.9(16)
C(24)-C(25)	1.368(7)	C(5)-W(1)-C(4)	34.76(18)	C(35)-C(34)-B(1)	128.3(4)	O(5)#1-C(52A)-C(53)#1	52.7(14)
C(25)-F(25)	1.348(6)	C(2)-W(1)-C(4)	58.85(18)	F(35)-C(35)-C(34)	121.9(5)	C(51)#1-C(52A)-C(53)#1	93.2(19)
C(25)-C(26)	1.371(8)	C(21)-W(1)-C(3)	145.06(19)	F(35)-C(35)-C(36)	113.8(4)	C(53)-C(52A)-C(53)#1	64.8(18)
C(26)-F(26)	1.345(6)	C(19)-W(1)-C(3)	122.3(2)	C(34)-C(35)-C(36)	124.3(5)	C(53)#1-C(52B)-O(5)#1	106(5)
C(26)-C(27)	1.385(8)	C(20)-W(1)-C(3)	116.0(2)	F(36)-C(36)-C(37)	119.8(5)	C(53)#1-C(52B)-C(52B)#1	107(6)
C(27)-F(27)	1.360(6)	C(1)-W(1)-C(3)	59.02(17)	F(36)-C(36)-C(35)	121.6(5)	O(5)#1-C(52B)-C(52B)#1	146(3)
C(28)-C(33)	1.395(7)	C(5)-W(1)-C(3)	58.06(18)	C(37)-C(36)-C(35)	118.6(5)	C(53)#1-C(52B)-C(53)	107(5)
C(28)-C(29)	1.397(7)	C(2)-W(1)-C(3)	34.90(18)	F(37)-C(37)-C(38)	120.3(5)	O(5)#1-C(52B)-C(53)	145(3)
C(29)-F(29)	1.359(6)	C(4)-W(1)-C(3)	34.7(2)	F(37)-C(37)-C(36)	120.0(5)	C(52B)#1-C(52B)-C(53)	18.7(18)
C(29)-C(30)	1.366(7)	C(1)-P(1)-C(18)	108.3(2)	C(38)-C(37)-C(36)	119.7(5)	C(53)#1-C(52B)-C(51)	129(5)
C(30)-F(30)	1.348(6)	C(1)-P(1)-C(12)	111.0(2)	F(38)-C(38)-C(37)	120.6(5)	O(5)#1-C(52B)-C(51)	68.2(14)
C(30)-C(31)	1.375(8)	C(18)-P(1)-C(12)	111.0(3)	F(38)-C(38)-C(39)	120.4(5)	C(52B)#1-C(52B)-C(51)	84.0(11)
C(31)-F(31)	1.351(7)	C(1)-P(1)-C(6)	108.0(2)	C(37)-C(38)-C(39)	118.9(5)	C(53)-C(52B)-C(51)	97.8(14)
C(31)-C(32)	1.380(9)	C(18)-P(1)-C(6)	108.9(2)	F(39)-C(39)-C(38)	115.3(5)	C(53)#1-C(52B)-C(51)#1	138(6)
C(32)-F(32)	1.345(6)	C(12)-P(1)-C(6)	109.6(2)	F(39)-C(39)-C(34)	119.5(4)	O(5)#1-C(52B)-C(51)#1	93.9(15)
C(32)-C(33)	1.365(8)	C(28)-B(1)-C(40)	115.2(4)	C(38)-C(39)-C(34)	125.2(5)	C(52B)#1-C(52B)-C(51)#1	54.7(8)
C(33)-F(33)	1.349(6)	C(28)-B(1)-C(34)	101.5(4)	C(45)-C(40)-C(41)	113.2(4)	C(53)-C(52B)-C(51)#1	67.5(12)
C(34)-C(39)	1.379(7)	C(40)-B(1)-C(34)	111.8(4)	C(45)-C(40)-B(1)	125.9(4)	C(51)-C(52B)-C(51)#1	30.3(9)

C(34)-C(35)	1.387(7)	C(28)-B(1)-C(22)	112.0(4)	C(41)-C(40)-B(1)	120.3(4)	C(53)#1-C(52B)-C(50)#1	141(5)
C(35)-F(35)	1.351(6)	C(40)-B(1)-C(22)	101.4(4)	F(41)-C(41)-C(42)	116.7(4)	O(5)#1-C(52B)-C(50)#1	48.7(11)
C(35)-C(36)	1.391(8)	C(34)-B(1)-C(22)	115.5(4)	F(41)-C(41)-C(40)	118.8(4)	C(52B)#1-C(52B)-C(50)#1	98.3(13)
C(36)-F(36)	1.333(6)	C(5)-C(1)-C(2)	106.4(4)	C(42)-C(41)-C(40)	124.5(5)	C(53)-C(52B)-C(50)#1	105.8(16)
C(36)-C(37)	1.378(9)	C(5)-C(1)-P(1)	128.1(4)	F(42)-C(42)-C(43)	120.4(5)	C(51)-C(52B)-C(50)#1	25.9(9)
C(37)-F(37)	1.352(6)	C(2)-C(1)-P(1)	124.9(4)	F(42)-C(42)-C(41)	120.7(5)	C(51)#1-C(52B)-C(50)#1	45.4(8)
C(37)-C(38)	1.368(8)	C(5)-C(1)-W(1)	71.9(3)	C(43)-C(42)-C(41)	118.9(5)	C(52B)#1-C(53)-O(5)	54(4)
C(38)-F(38)	1.350(6)	C(2)-C(1)-W(1)	73.4(3)	C(42)-C(43)-F(43)	120.5(5)	C(52B)#1-C(53)-C(52B)	54(5)
C(38)-C(39)	1.375(7)	P(1)-C(1)-W(1)	126.6(2)	C(42)-C(43)-C(44)	120.1(5)	O(5)-C(53)-C(52B)	107.9(15)
C(39)-F(39)	1.360(6)	C(3)-C(2)-C(1)	107.2(4)	F(43)-C(43)-C(44)	119.4(5)	C(52B)#1-C(53)-C(52A)	72(5)
C(40)-C(45)	1.389(7)	C(3)-C(2)-W(1)	74.3(3)	F(44)-C(44)-C(43)	119.9(5)	O(5)-C(53)-C(52A)	103.6(15)
C(40)-C(41)	1.403(7)	C(1)-C(2)-W(1)	70.1(3)	F(44)-C(44)-C(45)	120.6(5)	C(52B)-C(53)-C(52A)	46.5(18)
C(41)-F(41)	1.350(6)	C(4)-C(3)-C(2)	109.3(5)	C(43)-C(44)-C(45)	119.4(5)	C(52B)#1-C(53)-C(52A)#1	8(4)
C(41)-C(42)	1.374(7)	C(4)-C(3)-W(1)	71.9(3)	F(45)-C(45)-C(44)	114.7(4)	O(5)-C(53)-C(52A)#1	57.0(11)
C(42)-F(42)	1.338(6)	C(2)-C(3)-W(1)	70.8(3)	F(45)-C(45)-C(40)	121.4(4)	C(52B)-C(53)-C(52A)#1	53.5(17)
C(42)-C(43)	1.362(8)	C(5)-C(4)-C(3)	108.0(5)	C(44)-C(45)-C(40)	123.8(5)	C(52A)-C(53)-C(52A)#1	77.9(17)
C(43)-F(43)	1.364(6)	C(5)-C(4)-W(1)	70.1(3)	O(4)-C(46)-C(47)	107.8(7)	C(52B)#1-C(53)-C(53)#1	56(4)
C(43)-C(44)	1.372(8)	C(3)-C(4)-W(1)	73.4(3)	C(48)-C(47)-C(46)	102.4(6)	O(5)-C(53)-C(53)#1	109.8(12)
C(44)-F(44)	1.355(5)	C(4)-C(5)-C(1)	109.1(5)	C(47)-C(48)-C(49)	100.2(7)	C(52B)-C(53)-C(53)#1	16.2(14)
C(44)-C(45)	1.381(7)	C(4)-C(5)-W(1)	75.1(3)	O(4)-C(49)-C(48)	108.1(6)	C(52A)-C(53)-C(53)#1	62.4(17)
C(45)-F(45)	1.349(5)	C(1)-C(5)-W(1)	71.5(3)	C(51)#1-C(50)-O(5)	83.1(17)	C(52A)#1-C(53)-C(53)#1	52.8(10)
C(46)-O(4)	1.431(9)	C(11)-C(6)-C(7)	120.2(5)	C(51)#1-C(50)-C(52A)#1	74.8(17)	C(52B)#1-C(53)-C(51)#1	39(4)
C(46)-C(47)	1.511(13)	C(11)-C(6)-P(1)	120.9(4)	O(5)-C(50)-C(52A)#1	62.1(16)	O(5)-C(53)-C(51)#1	54.0(9)
C(47)-C(48)	1.475(11)	C(7)-C(6)-P(1)	118.7(4)	C(51)#1-C(50)-C(51)	38.4(18)	C(52B)-C(53)-C(51)#1	66.7(11)
C(48)-C(49)	1.511(9)	C(8)-C(7)-C(6)	119.6(5)	O(5)-C(50)-C(51)	105.6(13)	C(52A)-C(53)-C(51)#1	50.0(13)
C(49)-O(4)	1.417(8)	C(7)-C(8)-C(9)	120.1(5)	C(52A)#1-C(50)-C(51)	61.5(14)	C(52A)#1-C(53)-C(51)#1	47.9(8)
C(50)-C(51)#1	0.87(2)	C(10)-C(9)-C(8)	120.0(5)	C(51)#1-C(50)-C(52B)#1	53.8(17)	C(53)#1-C(53)-C(51)#1	78.6(7)
C(50)-O(5)	1.479(17)	C(9)-C(10)-C(11)	120.7(6)	O(5)-C(50)-C(52B)#1	38.5(9)	C(49)-O(4)-C(46)	106.0(5)
C(50)-C(52A)#1	1.49(3)	C(6)-C(11)-C(10)	119.4(6)	C(52A)#1-C(50)-C(52B)#1	38.1(16)	C(52B)#1-O(5)-C(53)	19.8(17)
C(50)-C(51)	1.52(3)	C(17)-C(12)-C(13)	120.4(5)	C(51)-C(50)-C(52B)#1	67.2(11)	C(52B)#1-O(5)-C(50)	92.9(14)
C(50)-C(52B)#1	1.97(3)	C(17)-C(12)-P(1)	120.4(4)	C(50)#1-C(51)-C(51)#1	108(3)	C(53)-O(5)-C(50)	109.1(11)
C(51)-C(50)#1	0.87(2)	C(13)-C(12)-P(1)	119.2(4)	C(50)#1-C(51)-C(50)	133(2)	C(52B)#1-O(5)-C(52A)#1	50.7(18)
C(51)-C(51)#1	0.99(3)	C(12)-C(13)-C(14)	118.6(6)	C(51)#1-C(51)-C(50)	33.1(17)	C(53)-O(5)-C(52A)#1	70.3(12)
C(51)-C(52A)	1.519(19)	C(15)-C(14)-C(13)	120.3(7)	C(50)#1-C(51)-C(52A)	72(2)	C(50)-O(5)-C(52A)#1	59.4(13)
C(51)-C(52A)#1	1.54(3)	C(16)-C(15)-C(14)	120.2(6)	C(51)#1-C(51)-C(52A)	72(2)	C(52B)#1-O(5)-C(51)#1	67.3(11)
C(51)-C(52B)	1.613(19)	C(15)-C(16)-C(17)	121.3(6)	C(50)-C(51)-C(52A)	101.9(15)	C(53)-O(5)-C(51)#1	79.6(11)
C(51)-O(5)#1	1.625(18)	C(16)-C(17)-C(12)	119.2(6)	C(50)#1-C(51)-C(52A)#1	155(2)	C(50)-O(5)-C(51)#1	32.2(7)
						C(52A)#1-O(5)-C(51)#1	57.4(9)

Symmetry transformations used to generate equivalent atoms: #1 -x+3/2,y,-z+5/2

Table 46. Anisotropic displacement parameters ($Å^2 x\ 10^3$)for **$[V_2][B(C_6F_5)_4]_2$**. The anisotropic displacement factor exponent takes the form: $-2\pi^2[\ h^2a^{*2}U^{11} + ... + 2\ h\ k\ a^*\ b^*\ U^{12}\ ]$

	U^{11}	U^{22}	U^{33}	U^{23}	U^{13}	U^{12}
W(1)	21(1)	24(1)	21(1)	-1(1)	0(1)	3(1)
P(1)	14(1)	21(1)	12(1)	0(1)	-1(1)	3(1)
B(1)	18(3)	20(3)	13(3)	-2(2)	-3(2)	2(2)
C(1)	14(2)	19(2)	17(2)	-1(2)	0(2)	4(2)
C(2)	20(2)	19(2)	14(2)	0(2)	0(2)	7(2)

C(3)	19(3)	40(3)	15(3)	-5(2)	2(2)	11(2)
C(4)	16(3)	38(3)	22(3)	-12(2)	1(2)	-5(2)
C(5)	16(2)	22(2)	20(3)	1(2)	7(2)	-1(2)
C(6)	19(2)	20(2)	15(2)	3(2)	5(2)	3(2)
C(7)	23(3)	23(3)	23(3)	4(2)	6(2)	2(2)
C(8)	24(3)	37(3)	37(3)	9(3)	11(2)	11(2)
C(9)	48(4)	33(3)	37(4)	3(3)	25(3)	17(3)
C(10)	66(5)	33(3)	26(3)	-10(3)	3(3)	8(3)
C(11)	31(3)	33(3)	26(3)	-5(2)	3(2)	-1(2)
C(12)	13(2)	37(3)	13(2)	-1(2)	-2(2)	-1(2)
C(13)	25(3)	33(3)	26(3)	-2(2)	1(2)	-10(2)
C(14)	35(4)	50(4)	44(4)	-1(3)	11(3)	-20(3)
C(15)	24(3)	85(6)	33(3)	-16(4)	3(3)	-23(3)
C(16)	18(3)	91(6)	25(3)	-6(3)	0(2)	2(3)
C(17)	17(3)	49(4)	25(3)	-6(3)	-3(2)	6(2)
C(18)	32(3)	25(3)	19(3)	3(2)	-4(2)	7(2)
C(19)	20(3)	20(2)	14(2)	-3(2)	2(2)	7(2)
C(20)	29(3)	25(3)	13(2)	2(2)	2(2)	4(2)
C(21)	23(3)	29(3)	23(3)	1(2)	9(2)	4(2)
C(22)	17(2)	19(2)	16(2)	-2(2)	-3(2)	2(2)
C(23)	16(2)	25(3)	15(2)	0(2)	-3(2)	3(2)
C(24)	16(2)	29(3)	17(2)	-3(2)	-2(2)	7(2)
C(25)	22(3)	35(3)	17(3)	9(2)	6(2)	15(2)
C(26)	21(3)	22(2)	31(3)	2(2)	9(2)	3(2)
C(27)	16(2)	20(2)	19(3)	-2(2)	1(2)	0(2)
C(28)	16(2)	24(3)	16(2)	1(2)	-2(2)	2(2)
C(29)	25(3)	24(3)	20(3)	-1(2)	-1(2)	3(2)
C(30)	18(3)	33(3)	28(3)	-3(2)	1(2)	6(2)
C(31)	28(3)	39(3)	35(4)	1(3)	5(3)	-5(3)
C(32)	30(3)	25(3)	33(3)	7(2)	-1(2)	1(2)
C(33)	19(3)	24(3)	22(3)	4(2)	-3(2)	4(2)
C(34)	11(2)	31(3)	15(2)	-6(2)	1(2)	4(2)
C(35)	17(3)	25(3)	23(3)	-1(2)	-2(2)	3(2)
C(36)	32(3)	28(3)	28(3)	-12(2)	8(3)	-4(2)
C(37)	30(3)	40(4)	19(3)	-14(2)	3(2)	-9(2)
C(38)	24(3)	46(3)	13(3)	-3(2)	-2(2)	2(2)
C(39)	17(2)	31(3)	17(2)	-6(2)	-1(2)	6(2)
C(40)	18(2)	17(2)	11(2)	-1(2)	1(2)	0(2)
C(41)	24(3)	19(3)	17(3)	0(2)	-2(2)	-2(2)
C(42)	28(3)	17(3)	21(3)	-6(2)	0(2)	1(2)
C(43)	26(3)	18(2)	33(3)	2(2)	10(2)	13(2)
C(44)	15(2)	24(3)	22(3)	5(2)	-5(2)	-2(2)
C(45)	21(3)	21(2)	14(2)	2(2)	-4(2)	2(2)
C(46)	59(5)	56(5)	71(6)	-4(4)	20(4)	-1(4)
C(47)	76(6)	48(4)	50(5)	-12(4)	10(4)	-6(4)
C(48)	66(5)	58(5)	49(4)	-7(4)	-1(4)	-22(4)
C(49)	49(4)	42(4)	42(4)	-1(3)	5(3)	-10(3)
C(50)	60(10)	49(9)	46(9)	6(8)	-16(8)	-25(8)
C(51)	37(8)	42(8)	81(12)	12(9)	21(11)	-7(6)
C(52A)	56(16)	52(15)	52(16)	11(12)	-17(12)	5(12)
C(52B)	56(16)	52(15)	52(16)	11(12)	-17(12)	5(12)
O(1)	16(2)	39(2)	28(2)	-7(2)	2(2)	-7(2)
O(2)	54(3)	19(2)	35(2)	-4(2)	9(2)	4(2)
O(3)	42(2)	54(3)	28(2)	15(2)	5(2)	28(2)
O(4)	53(3)	43(3)	38(2)	-7(2)	1(2)	-12(2)
O(5)	44(6)	50(5)	38(5)	12(4)	-19(4)	-17(4)
F(23)	20(2)	27(2)	22(2)	4(1)	-9(1)	-6(1)
F(24)	23(2)	44(2)	20(2)	3(1)	-12(1)	5(1)
F(25)	30(2)	49(2)	25(2)	21(1)	4(1)	13(1)
F(26)	31(2)	36(2)	43(2)	14(2)	9(2)	-6(2)
F(27)	19(2)	31(2)	29(2)	-1(1)	-4(1)	-6(1)
F(29)	26(2)	23(2)	36(2)	4(1)	4(1)	8(1)
F(30)	21(2)	42(2)	58(2)	2(2)	12(2)	7(1)
F(31)	29(2)	52(2)	72(3)	17(2)	17(2)	-7(2)
F(32)	36(2)	34(2)	65(2)	22(2)	12(2)	1(2)
F(33)	24(2)	23(2)	37(2)	9(1)	5(1)	9(1)
F(35)	37(2)	26(2)	28(2)	-2(1)	-6(2)	8(1)
F(36)	47(2)	30(2)	38(2)	-13(2)	9(2)	-1(2)
F(37)	57(2)	61(3)	21(2)	-23(2)	3(2)	-14(2)
F(38)	45(2)	61(2)	13(2)	1(2)	-11(1)	2(2)

F(39)	35(2)	28(2)	20(2)	1(1)	-6(1)	9(1)
F(41)	16(2)	28(2)	31(2)	-7(1)	-6(1)	-6(1)
F(42)	37(2)	28(2)	49(2)	-23(2)	7(2)	-2(1)
F(43)	30(2)	33(2)	53(2)	-12(2)	13(2)	11(1)
F(44)	12(1)	34(2)	41(2)	0(1)	-1(1)	1(1)
F(45)	19(2)	31(2)	25(2)	-12(1)	-6(1)	-1(1)

Table 47. Hydrogen coordinates (x 10^4) and isotropic displacement parameters ($Å^2$x 10^3) for **$[V_2][B(C_6F_5)_4]_2$**.

	x	y	z	U(eq)
H(2A)	4110	7412	10601	21
H(3A)	2938	6157	10141	30
H(4A)	2589	3752	10370	30
H(5A)	3529	3480	10972	23
H(7A)	2587	6337	11312	28
H(8A)	1480	7592	11655	39
H(9A)	2155	9084	12081	47
H(10A)	3927	9319	12163	50
H(11A)	5050	8014	11837	36
H(13A)	5313	8641	11111	34
H(14A)	6888	9703	10983	51
H(15A)	8433	8531	11053	57
H(16A)	8434	6299	11223	53
H(17A)	6898	5187	11337	37
H(18A)	5426	3845	11432	38
H(18B)	4308	4004	11594	38
H(18C)	5294	4681	11789	38
H(46A)	2887	-282	10133	74
H(46B)	3096	978	9878	74
H(47A)	1856	-36	9540	70
H(47B)	1315	-697	9877	70
H(48A)	240	1075	9758	69
H(48B)	1182	2042	9650	69
H(49A)	1001	2651	10230	53
H(49B)	709	1143	10345	53

Table 48. Torsion angles [°] for **$[V_2][B(C_6F_5)_4]_2$**.

C(18)-P(1)-C(1)-C(5)	16.2(5)	F(24)-C(24)-C(25)-F(25)	1.0(7)	C(53)#1-C(51)-C(52A)-C(51)#1	-116(2)
C(12)-P(1)-C(1)-C(5)	138.3(4)	C(23)-C(24)-C(25)-F(25)	-179.6(4)	C(50)#1-C(51)-C(52A)-C(53)	174(3)
C(6)-P(1)-C(1)-C(5)	-101.6(5)	F(24)-C(24)-C(25)-C(26)	-177.7(4)	C(51)#1-C(51)-C(52A)-C(53)	56(2)
C(18)-P(1)-C(1)-C(2)	-173.8(4)	C(23)-C(24)-C(25)-C(26)	1.7(7)	C(50)-C(51)-C(52A)-C(53)	42(2)
C(12)-P(1)-C(1)-C(2)	-51.8(5)	F(25)-C(25)-C(26)-F(26)	0.1(8)	C(52A)#1-C(51)-C(52A)-C(53)	-14.3(15)
C(6)-P(1)-C(1)-C(2)	68.4(5)	C(24)-C(25)-C(26)-F(26)	178.8(5)	C(52B)-C(51)-C(52A)-C(53)	-59.9(16)
C(18)-P(1)-C(1)-W(1)	-79.0(3)	F(25)-C(25)-C(26)-C(27)	-179.7(5)	O(5)#1-C(51)-C(52A)-C(53)	-115(2)
C(12)-P(1)-C(1)-W(1)	43.1(4)	C(24)-C(25)-C(26)-C(27)	-1.0(8)	C(52B)#1-C(51)-C(52A)-C(53)	-2.1(15)
C(6)-P(1)-C(1)-W(1)	163.2(3)	F(26)-C(26)-C(27)-F(27)	-2.6(7)	C(53)#1-C(51)-C(52A)-C(53)	-60(2)
C(21)-W(1)-C(1)-C(5)	-83.8(3)	C(25)-C(26)-C(27)-F(27)	177.2(4)	C(50)#1-C(51)-C(52A)-C(53)#1	-127(2)
C(19)-W(1)-C(1)-C(5)	-164.3(3)	F(26)-C(26)-C(27)-C(22)	178.1(5)	C(51)#1-C(51)-C(52A)-C(53)#1	116(2)
C(20)-W(1)-C(1)-C(5)	-15.4(5)	C(25)-C(26)-C(27)-C(22)	-2.1(8)	C(50)-C(51)-C(52A)-C(53)#1	101.6(18)
C(2)-W(1)-C(1)-C(5)	114.0(4)	C(23)-C(22)-C(27)-F(27)	-175.2(4)	C(52A)#1-C(51)-C(52A)-C(53)#1	45.4(10)
C(4)-W(1)-C(1)-C(5)	36.3(3)	B(1)-C(22)-C(27)-F(27)	-0.8(7)	C(52B)-C(51)-C(52A)-C(53)#1	-0.2(19)
C(3)-W(1)-C(1)-C(5)	76.9(3)	C(23)-C(22)-C(27)-C(26)	4.1(7)	O(5)#1-C(51)-C(52A)-C(53)#1	-55.5(12)
C(21)-W(1)-C(1)-C(2)	162.1(3)	B(1)-C(22)-C(27)-C(26)	178.5(5)	C(52B)#1-C(51)-C(52A)-C(53)#1	57.6(14)
C(19)-W(1)-C(1)-C(2)	81.6(3)	C(40)-B(1)-C(28)-C(33)	18.8(7)	C(50)#1-C(51)-C(52B)-C(53)#1	-130(7)
C(20)-W(1)-C(1)-C(2)	-129.4(4)	C(34)-B(1)-C(28)-C(33)	-102.2(5)	C(51)#1-C(51)-C(52B)-C(53)#1	120(7)
C(5)-W(1)-C(1)-C(2)	-114.0(4)	C(22)-B(1)-C(28)-C(33)	134.0(5)	C(50)-C(51)-C(52B)-C(53)#1	89(7)
C(4)-W(1)-C(1)-C(2)	-77.7(3)	C(40)-B(1)-C(28)-C(29)	-166.7(4)	C(52A)-C(51)-C(52B)-C(53)#1	179(100)
C(3)-W(1)-C(1)-C(2)	-37.1(3)	C(34)-B(1)-C(28)-C(29)	72.3(5)	C(52A)#1-C(51)-C(52B)-C(53)#1	59(7)
C(21)-W(1)-C(1)-P(1)	40.6(3)	C(22)-B(1)-C(28)-C(29)	-51.5(6)	O(5)#1-C(51)-C(52B)-C(53)#1	-94(7)

C(19)-W(1)-C(1)-P(1)	-39.9(3)	C(33)-C(28)-C(29)-F(29)	179.4(4)	C(52B)#1-C(51)-C(52B)-C(53)#1	107(9)
C(20)-W(1)-C(1)-P(1)	109.1(4)	B(1)-C(28)-C(29)-F(29)	4.1(7)	C(50)#1-C(51)-C(52B)-O(5)#1	-36(2)
C(5)-W(1)-C(1)-P(1)	124.5(4)	C(33)-C(28)-C(29)-C(30)	-2.1(7)	C(51)#1-C(51)-C(52B)-O(5)#1	-146(3)
C(2)-W(1)-C(1)-P(1)	-121.5(4)	B(1)-C(28)-C(29)-C(30)	-177.4(5)	C(50)-C(51)-C(52B)-O(5)#1	-177.5(17)
C(4)-W(1)-C(1)-P(1)	160.8(4)	F(29)-C(29)-C(30)-F(30)	1.8(7)	C(52A)-C(51)-C(52B)-O(5)#1	-87(2)
C(3)-W(1)-C(1)-P(1)	-158.6(4)	C(28)-C(29)-C(30)-F(30)	-176.8(5)	C(52A)#1-C(51)-C(52B)-O(5)#1	152(3)
C(5)-C(1)-C(2)-C(3)	0.8(5)	F(29)-C(29)-C(30)-C(31)	-178.3(5)	C(52B)#1-C(51)-C(52B)-O(5)#1	-159(4)
P(1)-C(1)-C(2)-C(3)	-170.9(4)	C(28)-C(29)-C(30)-C(31)	3.2(8)	C(53)#1-C(51)-C(52B)-O(5)#1	94(7)
W(1)-C(1)-C(2)-C(3)	65.7(3)	F(30)-C(30)-C(31)-F(31)	-1.4(9)	C(50)#1-C(51)-C(52B)-C(52B)#1	123(4)
C(5)-C(1)-C(2)-W(1)	-64.8(3)	C(29)-C(30)-C(31)-F(31)	178.7(5)	C(51)#1-C(51)-C(52B)-C(52B)#1	13(4)
P(1)-C(1)-C(2)-W(1)	123.4(4)	F(30)-C(30)-C(31)-C(32)	177.8(5)	C(50)-C(51)-C(52B)-C(52B)#1	-18(4)
C(21)-W(1)-C(2)-C(3)	-137.5(3)	C(29)-C(30)-C(31)-C(32)	-2.1(9)	C(52A)-C(51)-C(52B)-C(52B)#1	72(3)
C(19)-W(1)-C(2)-C(3)	138.8(3)	F(31)-C(31)-C(32)-F(32)	-0.2(9)	C(52A)#1-C(51)-C(52B)-C(52B)#1	-48(3)
C(20)-W(1)-C(2)-C(3)	-2.9(5)	C(30)-C(31)-C(32)-F(32)	-179.4(5)	O(5)#1-C(51)-C(52B)-C(52B)#1	159(4)
C(1)-W(1)-C(2)-C(3)	-115.3(4)	F(31)-C(31)-C(32)-C(33)	179.5(5)	C(53)#1-C(51)-C(52B)-C(52B)#1	-107(9)
C(5)-W(1)-C(2)-C(3)	-76.3(3)	C(30)-C(31)-C(32)-C(33)	0.3(9)	C(50)#1-C(51)-C(52B)-C(53)	110(2)
C(4)-W(1)-C(2)-C(3)	-35.7(3)	F(32)-C(32)-C(33)-F(33)	0.1(8)	C(51)#1-C(51)-C(52B)-C(53)	1(3)
C(21)-W(1)-C(2)-C(1)	-22.2(4)	C(31)-C(32)-C(33)-F(33)	-179.6(5)	C(50)-C(51)-C(52B)-C(53)	-31(2)
C(19)-W(1)-C(2)-C(1)	-105.9(3)	F(32)-C(32)-C(33)-C(28)	-179.6(5)	C(52A)-C(51)-C(52B)-C(53)	59.6(17)
C(20)-W(1)-C(2)-C(1)	112.4(4)	C(31)-C(32)-C(33)-C(28)	0.7(9)	C(52A)#1-C(51)-C(52B)-C(53)	-61(2)
C(5)-W(1)-C(2)-C(1)	39.0(3)	C(29)-C(28)-C(33)-F(33)	-179.5(4)	O(5)#1-C(51)-C(52B)-C(53)	147(3)
C(4)-W(1)-C(2)-C(1)	79.6(3)	B(1)-C(28)-C(33)-F(33)	-4.7(8)	C(52B)#1-C(51)-C(52B)-C(53)	-12.7(19)
C(3)-W(1)-C(2)-C(1)	115.3(4)	C(29)-C(28)-C(33)-C(32)	0.2(8)	C(53)#1-C(51)-C(52B)-C(53)	-120(8)
C(1)-C(2)-C(3)-C(4)	-1.0(5)	B(1)-C(28)-C(33)-C(32)	175.0(5)	C(50)#1-C(51)-C(52B)-C(51)#1	110(3)
W(1)-C(2)-C(3)-C(4)	61.9(4)	C(28)-B(1)-C(34)-C(39)	66.9(5)	C(50)-C(51)-C(52B)-C(51)#1	-31.5(17)
C(1)-C(2)-C(3)-W(1)	-62.9(3)	C(40)-B(1)-C(34)-C(39)	-56.4(6)	C(52A)-C(51)-C(52B)-C(51)#1	59(3)
C(21)-W(1)-C(3)-C(4)	-44.9(5)	C(22)-B(1)-C(34)-C(39)	-171.7(4)	C(52A)#1-C(51)-C(52B)-C(51)#1	-62(3)
C(19)-W(1)-C(3)-C(4)	-169.4(3)	C(28)-B(1)-C(34)-C(35)	-109.3(5)	O(5)#1-C(51)-C(52B)-C(51)#1	146(3)
C(20)-W(1)-C(3)-C(4)	59.6(3)	C(40)-B(1)-C(34)-C(35)	127.4(5)	C(52B)#1-C(51)-C(52B)-C(51)#1	-13(4)
C(1)-W(1)-C(3)-C(4)	-80.0(3)	C(22)-B(1)-C(34)-C(35)	12.1(7)	C(53)#1-C(51)-C(52B)-C(51)#1	-120(7)
C(5)-W(1)-C(3)-C(4)	-36.9(3)	C(39)-C(34)-C(35)-F(35)	-176.2(5)	C(51)#1-C(51)-C(52B)-C(50)#1	-110(3)
C(2)-W(1)-C(3)-C(4)	-118.8(4)	B(1)-C(34)-C(35)-F(35)	0.2(8)	C(50)-C(51)-C(52B)-C(50)#1	-141(2)
C(21)-W(1)-C(3)-C(2)	73.9(5)	C(39)-C(34)-C(35)-C(36)	2.5(8)	C(52A)-C(51)-C(52B)-C(50)#1	-51(2)
C(19)-W(1)-C(3)-C(2)	-50.6(4)	B(1)-C(34)-C(35)-C(36)	178.9(5)	C(52A)#1-C(51)-C(52B)-C(50)#1	-171(3)
C(20)-W(1)-C(3)-C(2)	178.4(3)	F(35)-C(35)-C(36)-F(36)	-1.1(8)	O(5)#1-C(51)-C(52B)-C(50)#1	36(2)
C(1)-W(1)-C(3)-C(2)	38.8(3)	C(34)-C(35)-C(36)-F(36)	-180.0(5)	C(52B)#1-C(51)-C(52B)-C(50)#1	-123(4)
C(5)-W(1)-C(3)-C(2)	82.0(3)	F(35)-C(35)-C(36)-C(37)	176.9(5)	C(53)#1-C(51)-C(52B)-C(50)#1	130(7)
C(4)-W(1)-C(3)-C(2)	118.8(4)	C(34)-C(35)-C(36)-C(37)	-2.0(9)	C(53)#1-C(52B)-C(53)-C(52B)#1	-92(10)
C(2)-C(3)-C(4)-C(5)	0.8(6)	F(36)-C(36)-C(37)-F(37)	-2.2(9)	O(5)#1-C(52B)-C(53)-C(52B)#1	106(3)
W(1)-C(3)-C(4)-C(5)	62.0(4)	C(35)-C(36)-C(37)-F(37)	179.8(5)	C(51)-C(52B)-C(53)-C(52B)#1	43(4)
C(2)-C(3)-C(4)-W(1)	-61.2(3)	F(36)-C(36)-C(37)-C(38)	177.6(5)	C(51)#1-C(52B)-C(53)-C(52B)#1	43(5)
C(21)-W(1)-C(4)-C(5)	36.4(4)	C(35)-C(36)-C(37)-C(38)	-0.4(9)	C(50)#1-C(52B)-C(53)-C(52B)#1	68(4)
C(19)-W(1)-C(4)-C(5)	-94.5(5)	F(37)-C(37)-C(38)-F(38)	1.5(8)	C(53)#1-C(52B)-C(53)-O(5)	-99(5)
C(20)-W(1)-C(4)-C(5)	114.4(3)	C(36)-C(37)-C(38)-F(38)	-178.3(5)	O(5)#1-C(52B)-C(53)-O(5)	98(3)
C(1)-W(1)-C(4)-C(5)	-38.3(3)	F(37)-C(37)-C(38)-C(39)	-178.3(5)	C(52B)#1-C(52B)-C(53)-O(5)	-8(5)
C(2)-W(1)-C(4)-C(5)	-80.9(3)	C(36)-C(37)-C(38)-C(39)	2.0(9)	C(51)-C(52B)-C(53)-O(5)	35(2)
C(3)-W(1)-C(4)-C(5)	-116.8(4)	F(38)-C(38)-C(39)-F(39)	-1.2(7)	C(51)#1-C(52B)-C(53)-O(5)	35.7(13)
C(21)-W(1)-C(4)-C(3)	153.2(3)	C(37)-C(38)-C(39)-F(39)	178.6(5)	C(50)#1-C(52B)-C(53)-O(5)	60.5(18)

C(19)-W(1)-C(4)-C(3)	22.3(6)	F(38)-C(38)-C(39)-C(34)	179.0(5)	C(53)#1-C(52B)-C(53)-C(52A)	169(6)
C(20)-W(1)-C(4)-C(3)	-128.8(3)	C(37)-C(38)-C(39)-C(34)	-1.3(8)	O(5)#1-C(52B)-C(53)-C(52A)	6(3)
C(1)-W(1)-C(4)-C(3)	78.5(3)	C(35)-C(34)-C(39)-F(39)	179.2(4)	C(52B)#1-C(52B)-C(53)-C(52A)	-100(5)
C(5)-W(1)-C(4)-C(3)	116.8(4)	B(1)-C(34)-C(39)-F(39)	2.5(7)	C(51)-C(52B)-C(53)-C(52A)	-56.5(16)
C(2)-W(1)-C(4)-C(3)	35.9(3)	C(35)-C(34)-C(39)-C(38)	-0.9(8)	C(51)#1-C(52B)-C(53)-C(52A)	-56.2(16)
C(3)-C(4)-C(5)-C(1)	-0.2(6)	B(1)-C(34)-C(39)-C(38)	-177.6(5)	C(50)#1-C(52B)-C(53)-C(52A)	-31.4(15)
W(1)-C(4)-C(5)-C(1)	63.9(3)	C(28)-B(1)-C(40)-C(45)	-137.3(5)	C(53)#1-C(52B)-C(53)-C(52A)#1	-81(6)
C(3)-C(4)-C(5)-W(1)	-64.1(4)	C(34)-B(1)-C(40)-C(45)	-22.1(6)	O(5)#1-C(52B)-C(53)-C(52A)#1	116(3)
C(2)-C(1)-C(5)-C(4)	-0.4(5)	C(22)-B(1)-C(40)-C(45)	101.5(5)	C(52B)#1-C(52B)-C(53)-C(52A)#1	10(5)
P(1)-C(1)-C(5)-C(4)	171.0(4)	C(28)-B(1)-C(40)-C(41)	52.1(6)	C(51)-C(52B)-C(53)-C(52A)#1	53.5(16)
W(1)-C(1)-C(5)-C(4)	-66.2(3)	C(34)-B(1)-C(40)-C(41)	167.3(4)	C(51)#1-C(52B)-C(53)-C(52A)#1	53.9(10)
C(2)-C(1)-C(5)-W(1)	65.9(3)	C(22)-B(1)-C(40)-C(41)	-69.1(5)	C(50)#1-C(52B)-C(53)-C(52A)#1	78.7(14)
P(1)-C(1)-C(5)-W(1)	-122.7(4)	C(45)-C(40)-C(41)-F(41)	-177.5(4)	O(5)#1-C(52B)-C(53)-C(53)#1	-162(8)
C(21)-W(1)-C(5)-C(4)	-147.8(3)	B(1)-C(40)-C(41)-F(41)	-5.8(7)	C(52B)#1-C(52B)-C(53)-C(53)#1	92(10)
C(19)-W(1)-C(5)-C(4)	140.5(3)	C(45)-C(40)-C(41)-C(42)	1.7(7)	C(51)-C(52B)-C(53)-C(53)#1	135(6)
C(20)-W(1)-C(5)-C(4)	-72.9(3)	B(1)-C(40)-C(41)-C(42)	173.4(5)	C(51)#1-C(52B)-C(53)-C(53)#1	135(6)
C(1)-W(1)-C(5)-C(4)	116.5(4)	F(41)-C(41)-C(42)-F(42)	-1.1(7)	C(50)#1-C(52B)-C(53)-C(53)#1	160(6)
C(2)-W(1)-C(5)-C(4)	77.7(3)	C(40)-C(41)-C(42)-F(42)	179.5(4)	C(53)#1-C(52B)-C(53)-C(51)#1	-135(6)
C(3)-W(1)-C(5)-C(4)	36.8(3)	F(41)-C(41)-C(42)-C(43)	177.8(5)	O(5)#1-C(52B)-C(53)-C(51)#1	62(3)
C(21)-W(1)-C(5)-C(1)	95.6(3)	C(40)-C(41)-C(42)-C(43)	-1.5(8)	C(52B)#1-C(52B)-C(53)-C(51)#1	-43(5)
C(19)-W(1)-C(5)-C(1)	23.9(4)	F(42)-C(42)-C(43)-F(43)	0.6(8)	C(51)-C(52B)-C(53)-C(51)#1	-0.3(16)
C(20)-W(1)-C(5)-C(1)	170.6(3)	C(41)-C(42)-C(43)-F(43)	-178.4(5)	C(50)#1-C(52B)-C(53)-C(51)#1	24.8(12)
C(2)-W(1)-C(5)-C(1)	-38.8(3)	F(42)-C(42)-C(43)-C(44)	179.7(5)	C(50)#1-C(52A)-C(53)-C(52B)#1	11(6)
C(4)-W(1)-C(5)-C(1)	-116.5(4)	C(41)-C(42)-C(43)-C(44)	0.7(8)	C(51)-C(52A)-C(53)-C(52B)#1	6(4)
C(3)-W(1)-C(5)-C(1)	-79.7(3)	C(42)-C(43)-C(44)-F(44)	-180.0(5)	O(5)#1-C(52A)-C(53)-C(52B)#1	-60(5)
C(1)-P(1)-C(6)-C(11)	-156.8(4)	F(43)-C(43)-C(44)-F(44)	-0.8(7)	C(51)#1-C(52A)-C(53)-C(52B)#1	38(4)
C(18)-P(1)-C(6)-C(11)	85.9(5)	C(42)-C(43)-C(44)-C(45)	-0.5(8)	C(53)#1-C(52A)-C(53)-C(52B)#1	-61(4)
C(12)-P(1)-C(6)-C(11)	-35.8(5)	F(43)-C(43)-C(44)-C(45)	178.7(4)	C(50)#1-C(52A)-C(53)-O(5)	-33(4)
C(1)-P(1)-C(6)-C(7)	28.7(4)	F(44)-C(44)-C(45)-F(45)	2.4(6)	C(51)-C(52A)-C(53)-O(5)	-38(2)
C(18)-P(1)-C(6)-C(7)	-88.7(4)	C(43)-C(44)-C(45)-F(45)	-177.1(4)	O(5)#1-C(52A)-C(53)-O(5)	-105.1(18)
C(12)-P(1)-C(6)-C(7)	149.7(4)	F(44)-C(44)-C(45)-C(40)	-179.6(4)	C(51)#1-C(52A)-C(53)-O(5)	-7.0(18)
C(11)-C(6)-C(7)-C(8)	-0.5(7)	C(43)-C(44)-C(45)-C(40)	0.9(8)	C(53)#1-C(52A)-C(53)-O(5)	-105.5(15)
P(1)-C(6)-C(7)-C(8)	174.1(4)	C(41)-C(40)-C(45)-F(45)	176.4(4)	C(50)#1-C(52A)-C(53)-C(52B)	69(3)
C(6)-C(7)-C(8)-C(9)	0.9(8)	B(1)-C(40)-C(45)-F(45)	5.2(7)	C(51)-C(52A)-C(53)-C(52B)	63.6(18)
C(7)-C(8)-C(9)-C(10)	-0.1(9)	C(41)-C(40)-C(45)-C(44)	-1.4(7)	O(5)#1-C(52A)-C(53)-C(52B)	-3.2(16)
C(8)-C(9)-C(10)-C(11)	-1.2(9)	B(1)-C(40)-C(45)-C(44)	-172.6(4)	C(51)#1-C(52A)-C(53)-C(52B)	94.9(18)
C(7)-C(6)-C(11)-C(10)	-0.8(8)	O(4)-C(46)-C(47)-C(48)	28.8(8)	C(53)#1-C(52A)-C(53)-C(52B)	-3.6(17)
P(1)-C(6)-C(11)-C(10)	-175.3(4)	C(46)-C(47)-C(48)-C(49)	-37.5(8)	C(50)#1-C(52A)-C(53)-C(52A)#1	18(3)
C(9)-C(10)-C(11)-C(6)	1.7(9)	C(47)-C(48)-C(49)-O(4)	36.1(7)	C(51)-C(52A)-C(53)-C(52A)#1	13.0(16)
C(1)-P(1)-C(12)-C(17)	-101.5(4)	C(51)#1-C(50)-C(51)-C(50)#1	-50(4)	O(5)#1-C(52A)-C(53)-C(52A)#1	-53.8(19)
C(18)-P(1)-C(12)-C(17)	18.9(5)	O(5)-C(50)-C(51)-C(50)#1	-106(3)	C(51)#1-C(52A)-C(53)-C(52A)#1	44.4(11)
C(6)-P(1)-C(12)-C(17)	139.3(4)	C(52A)#1-C(50)-C(51)-C(50)#1	-152(4)	C(53)#1-C(52A)-C(53)-C(52A)#1	-54.1(12)
C(1)-P(1)-C(12)-C(13)	77.7(4)	C(52B)#1-C(50)-C(51)-C(50)#1	-110(3)	C(50)#1-C(52A)-C(53)-C(53)#1	72(3)
C(18)-P(1)-C(12)-C(13)	-161.8(4)	O(5)-C(50)-C(51)-C(51)#1	-56.5(17)	C(51)-C(52A)-C(53)-C(53)#1	67.2(18)
C(6)-P(1)-C(12)-C(13)	-41.5(5)	C(52A)#1-C(50)-C(51)-C(51)#1	-102(2)	O(5)#1-C(52A)-C(53)-C(53)#1	0.3(14)
C(17)-C(12)-C(13)-C(14)	1.6(8)	C(52B)#1-C(50)-C(51)-C(51)#1	-59.8(18)	C(51)#1-C(52A)-C(53)-C(53)#1	98.5(16)
P(1)-C(12)-C(13)-C(14)	-177.6(4)	C(51)#1-C(50)-C(51)-C(52A)	26(2)	C(50)#1-C(52A)-C(53)-C(51)#1	-26(3)
C(12)-C(13)-C(14)-C(15)	-2.0(9)	O(5)-C(50)-C(51)-C(52A)	-31(2)	C(51)-C(52A)-C(53)-C(51)#1	-31.3(13)

C(13)-C(14)-C(15)-C(16)	1.3(10)	C(52A)#1-C(50)-C(51)-C(52A)	-76(3)	O(5)#1-C(52A)-C(53)-C(51)#1	-98(2)
C(14)-C(15)-C(16)-C(17)	-0.3(10)	C(52B)#1-C(50)-C(51)-C(52A)	-34(2)	C(53)#1-C(52A)-C(53)-C(51)#1	-98.5(16)
C(15)-C(16)-C(17)-C(12)	0.0(9)	C(51)#1-C(50)-C(51)-C(52A)#1	102(2)	C(48)-C(49)-O(4)-C(46)	-18.6(7)
C(13)-C(12)-C(17)-C(16)	-0.7(8)	O(5)-C(50)-C(51)-C(52A)#1	45.3(18)	C(47)-C(46)-O(4)-C(49)	-6.3(8)
P(1)-C(12)-C(17)-C(16)	178.5(4)	C(52B)#1-C(50)-C(51)-C(52A)#1	42.0(18)	C(52B)-C(53)-O(5)-C(52B)#1	8(5)
C(21)-W(1)-C(19)-O(1)	-66(5)	C(51)#1-C(50)-C(51)-C(52B)	73(2)	C(52A)-C(53)-O(5)-C(52B)#1	56(5)
C(20)-W(1)-C(19)-O(1)	-139(5)	O(5)-C(50)-C(51)-C(52B)	16(2)	C(52A)#1-C(53)-O(5)-C(52B)#1	-10(5)
C(1)-W(1)-C(19)-O(1)	23(5)	C(52A)#1-C(50)-C(51)-C(52B)	-29(2)	C(53)#1-C(53)-O(5)-C(52B)#1	-9(4)
C(5)-W(1)-C(19)-O(1)	8(5)	C(52B)#1-C(50)-C(51)-C(52B)	13(2)	C(51)#1-C(53)-O(5)-C(52B)#1	49(5)
C(2)-W(1)-C(19)-O(1)	59(5)	C(51)#1-C(50)-C(51)-O(5)#1	69(3)	C(52B)#1-C(53)-O(5)-C(50)	-36(5)
C(4)-W(1)-C(19)-O(1)	71(5)	O(5)-C(50)-C(51)-O(5)#1	13(4)	C(52B)-C(53)-O(5)-C(50)	-28.4(19)
C(3)-W(1)-C(19)-O(1)	86(5)	C(52A)#1-C(50)-C(51)-O(5)#1	-33(3)	C(52A)-C(53)-O(5)-C(50)	19.7(19)
C(21)-W(1)-C(20)-O(2)	46(4)	C(52B)#1-C(50)-C(51)-O(5)#1	9(3)	C(52A)#1-C(53)-O(5)-C(50)	-45.8(14)
C(19)-W(1)-C(20)-O(2)	122(4)	C(51)#1-C(50)-C(51)-C(52B)#1	59.8(18)	C(53)#1-C(53)-O(5)-C(50)	-45.4(16)
C(1)-W(1)-C(20)-O(2)	-27(4)	O(5)-C(50)-C(51)-C(52B)#1	3.3(14)	C(51)#1-C(53)-O(5)-C(50)	13.2(11)
C(5)-W(1)-C(20)-O(2)	-37(4)	C(52A)#1-C(50)-C(51)-C(52B)#1	-42.0(18)	C(52B)#1-C(53)-O(5)-C(52A)#1	10(5)
C(2)-W(1)-C(20)-O(2)	-98(4)	C(51)#1-C(50)-C(51)-C(53)#1	84.8(15)	C(52B)-C(53)-O(5)-C(52A)#1	17.3(16)
C(4)-W(1)-C(20)-O(2)	-70(4)	O(5)-C(50)-C(51)-C(53)#1	28.3(16)	C(52A)-C(53)-O(5)-C(52A)#1	65.5(17)
C(3)-W(1)-C(20)-O(2)	-100(4)	C(52A)#1-C(50)-C(51)-C(53)#1	-16.9(17)	C(53)#1-C(53)-O(5)-C(52A)#1	0.3(13)
C(19)-W(1)-C(21)-O(3)	165(100)	C(52B)#1-C(50)-C(51)-C(53)#1	25.0(12)	C(51)#1-C(53)-O(5)-C(52A)#1	58.9(10)
C(20)-W(1)-C(21)-O(3)	-86(12)	C(51)#1-C(51)-C(52A)-C(50)#1	-117(2)	C(52B)#1-C(53)-O(5)-C(51)#1	-49(5)
C(1)-W(1)-C(21)-O(3)	60(12)	C(50)-C(51)-C(52A)-C(50)#1	-132(2)	C(52B)-C(53)-O(5)-C(51)#1	-41.6(16)
C(5)-W(1)-C(21)-O(3)	23(12)	C(52A)#1-C(51)-C(52A)-C(50)#1	172(3)	C(52A)-C(53)-O(5)-C(51)#1	6.6(17)
C(2)-W(1)-C(21)-O(3)	73(13)	C(52B)-C(51)-C(52A)-C(50)#1	126(3)	C(52A)#1-C(53)-O(5)-C(51)#1	-58.9(10)
C(4)-W(1)-C(21)-O(3)	4(13)	O(5)#1-C(51)-C(52A)-C(50)#1	71.1(17)	C(53)#1-C(53)-O(5)-C(51)#1	-58.6(12)
C(3)-W(1)-C(21)-O(3)	30(13)	C(52B)#1-C(51)-C(52A)-C(50)#1	-176(3)	C(51)#1-C(50)-O(5)-C(52B)#1	-36(2)
C(28)-B(1)-C(22)-C(23)	-21.0(7)	C(53)#1-C(51)-C(52A)-C(50)#1	127(2)	C(52A)#1-C(50)-O(5)-C(52B)#1	40.0(19)
C(40)-B(1)-C(22)-C(23)	102.4(5)	C(50)#1-C(51)-C(52A)-O(5)#1	-71.1(17)	C(51)-C(50)-O(5)-C(52B)#1	-5(2)
C(34)-B(1)-C(22)-C(23)	-136.6(5)	C(51)#1-C(51)-C(52A)-O(5)#1	172(2)	C(51)#1-C(50)-O(5)-C(53)	-25(2)
C(28)-B(1)-C(22)-C(27)	165.4(4)	C(50)-C(51)-C(52A)-O(5)#1	157.1(16)	C(52A)#1-C(50)-O(5)-C(53)	51.6(16)
C(40)-B(1)-C(22)-C(27)	-71.2(5)	C(52A)#1-C(51)-C(52A)-O(5)#1	100.9(15)	C(51)-C(50)-O(5)-C(53)	6.7(18)
C(34)-B(1)-C(22)-C(27)	49.8(6)	C(52B)-C(51)-C(52A)-O(5)#1	55.4(18)	C(52B)#1-C(50)-O(5)-C(53)	12(2)
C(27)-C(22)-C(23)-F(23)	176.4(4)	C(52B)#1-C(51)-C(52A)-O(5)#1	113(2)	C(51)#1-C(50)-O(5)-C(52A)#1	-76.4(18)
B(1)-C(22)-C(23)-F(23)	2.4(7)	C(53)#1-C(51)-C(52A)-O(5)#1	55.5(12)	C(51)-C(50)-O(5)-C(52A)#1	-44.9(15)
C(27)-C(22)-C(23)-C(24)	-3.2(7)	C(50)#1-C(51)-C(52A)-C(51)#1	117(2)	C(52B)#1-C(50)-O(5)-C(52A)#1	-40.0(19)
B(1)-C(22)-C(23)-C(24)	-177.3(4)	C(50)-C(51)-C(52A)-C(51)#1	-14.5(15)	C(52A)#1-C(50)-O(5)-C(51)#1	76.4(18)
F(23)-C(23)-C(24)-F(24)	0.3(6)	C(52A)#1-C(51)-C(52A)-C(51)#1	-70.6(19)	C(51)-C(50)-O(5)-C(51)#1	31.5(17)
C(22)-C(23)-C(24)-F(24)	180.0(4)	C(52B)-C(51)-C(52A)-C(51)#1	-116(2)	C(52B)#1-C(50)-O(5)-C(51)#1	36(2)
F(23)-C(23)-C(24)-C(25)	-179.2(4)	O(5)#1-C(51)-C(52A)-C(51)#1	-172(2)		
C(22)-C(23)-C(24)-C(25)	0.5(8)	C(52B)#1-C(51)-C(52A)-C(51)#1	-58(2)		

Symmetry transformations used to generate equivalent atoms: #1 -x+3/2,y,-z+5/2

Figure 8. The molecular structure of $[V_2][B(C_6F_5)_4]_2$.

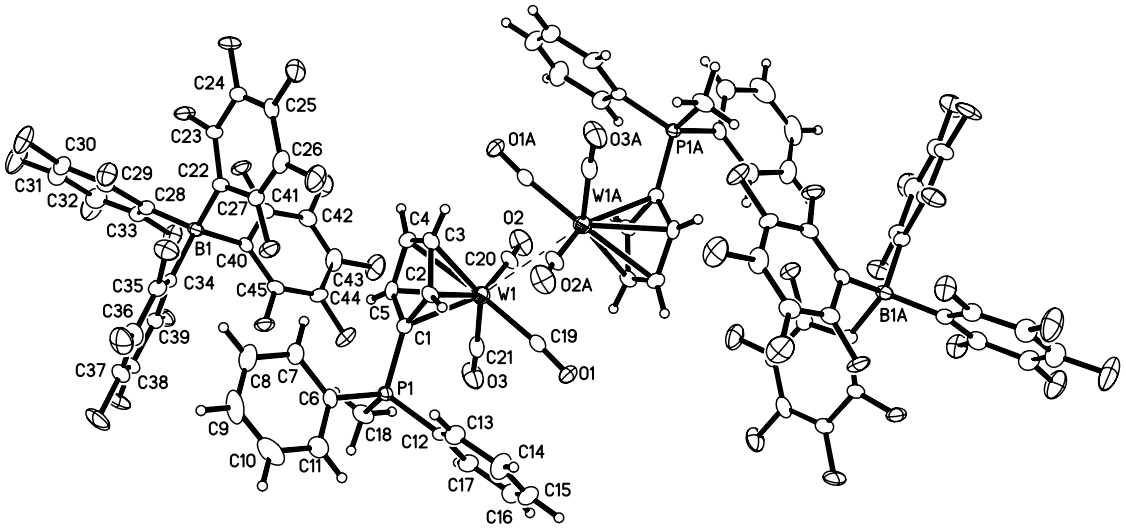

Table 49. Crystal data and structure refinement for **VII**

Identification code	**VII**	
Empirical formula	C22 H19 P	
Formula weight	314.34	
Temperature	180(2) K	
Wavelength	0.71073 Å	
Crystal system	Monoclinic	
Space group	P2(1)/c	
Unit cell dimensions	a = 9.9353(18) Å	α= 90°.
	b = 17.900(3) Å	β= 112.681(4)°.
	c = 10.0935(18) Å	γ = 90°.
Volume	1656.2(5) $Å^3$	
Z	4	
Density (calculated)	1.261 Mg/m^3	
Absorption coefficient	0.163 mm^{-1}	
F(000)	664	
Crystal size	0.40 x 0.06 x 0.04 mm^3	
Theta range for data collection	2.22 to 25.00°.	
Index ranges	-11<=h<=11, -21<=k<=20, -11<=l<=11	
Reflections collected	9436	
Independent reflections	2906 [R(int) = 0.0697]	
Completeness to theta = 25.00°	100.0 %	
Absorption correction	Empirical	
Max. and min. transmission	0.4463 and 0.3000	
Refinement method	Full-matrix least-squares on F^2	
Data / restraints / parameters	2906 / 0 / 208	
Goodness-of-fit on F^2	1.000	
Final R indices [I>2sigma(I)]	R1 = 0.0455, wR2 = 0.0873	
R indices (all data)	R1 = 0.0723, wR2 = 0.0919	
Largest diff. peak and hole	0.393 and -0.332 e.$Å^{-3}$	

Table 50. Atomic coordinates (x 10^4) and equivalent isotropic displacement parameters ($Å^2$x 10^3) for **VII**. U(eq) is defined as one third of the trace of the orthogonalized U^{ij} tensor.

	x	y	z	U(eq)

P(1)	6886(1)	4644(1)	8757(1)	29(1)
C(1)	7372(2)	5419(1)	9830(2)	27(1)
C(2)	8282(2)	5415(1)	11313(2)	30(1)
C(3)	8337(2)	6111(1)	11880(2)	32(1)
C(4)	7464(2)	6596(1)	10764(2)	28(1)
C(5)	6855(2)	6169(1)	9481(2)	28(1)
C(6)	5968(2)	6521(1)	8204(2)	32(1)
C(7)	5695(2)	7271(1)	8206(3)	38(1)
C(8)	6290(3)	7688(1)	9466(3)	40(1)
C(9)	7157(2)	7359(1)	10722(2)	35(1)
C(10)	7399(2)	4689(1)	7234(2)	30(1)
C(11)	7121(2)	4088(1)	6299(2)	41(1)
C(12)	7511(3)	4129(2)	5114(3)	54(1)
C(13)	8140(3)	4774(2)	4876(3)	56(1)
C(14)	8395(3)	5367(2)	5786(3)	48(1)
C(15)	8041(2)	5326(1)	6975(2)	38(1)
C(16)	7739(2)	3849(1)	9799(2)	28(1)
C(17)	7114(2)	3517(1)	10682(3)	38(1)
C(18)	7831(3)	2952(1)	11592(3)	44(1)
C(19)	9158(3)	2698(1)	11646(3)	42(1)
C(20)	9770(2)	3012(1)	10763(2)	38(1)
C(21)	9080(2)	3591(1)	9860(2)	32(1)
C(22)	4957(2)	4499(1)	8030(2)	37(1)

Table 51. Bond lengths [Å] and angles [°] for **VII**.

P(1)-C(1)	1.711(2)	C(17)-C(18)	1.368(3)	C(4)-C(5)-C(1)	107.09(18)
P(1)-C(16)	1.777(2)	C(18)-C(19)	1.375(3)	C(7)-C(6)-C(5)	119.6(2)
P(1)-C(22)	1.787(2)	C(19)-C(20)	1.377(3)	C(6)-C(7)-C(8)	120.8(2)
P(1)-C(10)	1.798(2)	C(20)-C(21)	1.377(3)	C(9)-C(8)-C(7)	120.7(2)
C(1)-C(2)	1.420(3)			C(8)-C(9)-C(4)	120.2(2)
C(1)-C(5)	1.432(3)	C(1)-P(1)-C(16)	108.70(10)	C(15)-C(10)-C(11)	119.8(2)
C(2)-C(3)	1.364(3)	C(1)-P(1)-C(22)	111.90(10)	C(15)-C(10)-P(1)	120.20(17)
C(3)-C(4)	1.421(3)	C(16)-P(1)-C(22)	108.56(10)	C(11)-C(10)-P(1)	119.98(17)
C(4)-C(9)	1.397(3)	C(1)-P(1)-C(10)	113.63(10)	C(10)-C(11)-C(12)	119.7(2)
C(4)-C(5)	1.423(3)	C(16)-P(1)-C(10)	108.33(10)	C(13)-C(12)-C(11)	119.2(3)
C(5)-C(6)	1.400(3)	C(22)-P(1)-C(10)	105.54(10)	C(14)-C(13)-C(12)	121.0(2)
C(6)-C(7)	1.369(3)	C(2)-C(1)-C(5)	106.64(19)	C(13)-C(14)-C(15)	120.2(2)
C(7)-C(8)	1.394(3)	C(2)-C(1)-P(1)	124.94(17)	C(14)-C(15)-C(10)	120.1(2)
C(8)-C(9)	1.362(3)	C(5)-C(1)-P(1)	128.16(16)	C(21)-C(16)-C(17)	118.9(2)
C(10)-C(15)	1.380(3)	C(3)-C(2)-C(1)	110.1(2)	C(21)-C(16)-P(1)	121.48(15)
C(10)-C(11)	1.387(3)	C(2)-C(3)-C(4)	108.2(2)	C(17)-C(16)-P(1)	119.33(16)
C(11)-C(12)	1.394(3)	C(9)-C(4)-C(3)	132.9(2)	C(18)-C(17)-C(16)	119.9(2)
C(12)-C(13)	1.377(4)	C(9)-C(4)-C(5)	119.1(2)	C(17)-C(18)-C(19)	120.9(2)
C(13)-C(14)	1.362(4)	C(3)-C(4)-C(5)	107.96(19)	C(18)-C(19)-C(20)	119.7(2)
C(14)-C(15)	1.377(3)	C(6)-C(5)-C(4)	119.5(2)	C(21)-C(20)-C(19)	120.3(2)
C(16)-C(21)	1.389(3)	C(6)-C(5)-C(1)	133.4(2)	C(20)-C(21)-C(16)	120.25(19)

Table 52. Anisotropic displacement parameters ($Å^2 x\ 10^3$) for **VII**. The anisotropic displacement factor exponent takes the form: $-2\pi^2[\ h^2\ a^{*2}U^{11} + ... + 2\ h\ k\ a^*\ b^*\ U^{12}\ ]$

	U^{11}	U^{22}	U^{33}	U^{23}	U^{13}	U^{12}
P(1)	28(1)	33(1)	28(1)	2(1)	15(1)	1(1)
C(1)	26(1)	31(1)	26(1)	4(1)	13(1)	1(1)
C(2)	25(1)	36(1)	31(1)	7(1)	14(1)	1(1)
C(3)	31(1)	40(2)	28(1)	-3(1)	15(1)	-6(1)
C(4)	28(1)	33(1)	31(1)	0(1)	18(1)	-2(1)
C(5)	26(1)	33(1)	28(1)	2(1)	15(1)	-2(1)
C(6)	32(1)	39(2)	30(1)	3(1)	15(1)	2(1)
C(7)	37(1)	42(2)	38(2)	15(1)	18(1)	11(1)

C(8)	45(2)	31(1)	52(2)	5(1)	26(1)	7(1)
C(9)	37(1)	37(2)	39(2)	-6(1)	23(1)	-3(1)
C(10)	26(1)	40(1)	25(1)	4(1)	11(1)	5(1)
C(11)	39(1)	53(2)	33(2)	-1(1)	15(1)	2(1)
C(12)	47(2)	83(2)	31(2)	-9(2)	14(1)	15(2)
C(13)	40(2)	101(3)	31(2)	19(2)	19(1)	20(2)
C(14)	42(2)	65(2)	44(2)	20(2)	24(1)	10(1)
C(15)	33(1)	49(2)	35(1)	8(1)	17(1)	6(1)
C(16)	31(1)	28(1)	29(1)	0(1)	15(1)	-1(1)
C(17)	36(1)	40(2)	49(2)	11(1)	26(1)	7(1)
C(18)	45(2)	43(2)	56(2)	17(1)	32(1)	6(1)
C(19)	44(2)	39(2)	47(2)	14(1)	21(1)	9(1)
C(20)	34(1)	40(2)	45(2)	8(1)	20(1)	9(1)
C(21)	32(1)	35(1)	34(1)	-1(1)	19(1)	-1(1)
C(22)	32(1)	41(2)	38(2)	-2(1)	15(1)	-1(1)

Table 53. Hydrogen coordinates (x 10^4) and isotropic displacement parameters (Å^{2}x 10^3) for **VII**.

	x	y	z	U(eq)
H(2A)	8781	4989	11835	36
H(3A)	8867	6249	12852	39
H(6A)	5558	6241	7340	39
H(7A)	5092	7509	7339	46
H(8A)	6088	8208	9447	48
H(9A)	7554	7650	11573	42
H(11A)	6667	3651	6465	49
H(12A)	7345	3717	4478	65
H(13A)	8399	4806	4065	67
H(14A)	8818	5810	5599	57
H(15A)	8239	5737	7618	45
H(17A)	6193	3683	10648	46
H(18A)	7407	2731	12196	53
H(19A)	9651	2308	12290	51
H(20A)	10671	2827	10777	46
H(21A)	9523	3816	9276	39
H(22D)	4608	4469	8814	55
H(22A)	4728	4032	7481	55
H(22B)	4476	4917	7396	55

Table 54. Torsion angles [°] for **VII**.

C(16)-P(1)-C(1)-C(2)	-1.2(2)	P(1)-C(1)-C(5)-C(4)	174.13(15)	C(12)-C(13)-C(14)-C(15)	0.8(4)
C(22)-P(1)-C(1)-C(2)	118.68(17)	C(4)-C(5)-C(6)-C(7)	-0.2(3)	C(13)-C(14)-C(15)-C(10)	-1.3(3)
C(10)-P(1)-C(1)-C(2)	-121.90(17)	C(1)-C(5)-C(6)-C(7)	-178.1(2)	C(11)-C(10)-C(15)-C(14)	0.5(3)
C(16)-P(1)-C(1)-C(5)	-174.53(16)	C(5)-C(6)-C(7)-C(8)	0.1(3)	P(1)-C(10)-C(15)-C(14)	-178.15(17)
C(22)-P(1)-C(1)-C(5)	-54.6(2)	C(6)-C(7)-C(8)-C(9)	0.0(3)	C(1)-P(1)-C(16)-C(21)	-93.04(19)
C(10)-P(1)-C(1)-C(5)	64.78(19)	C(7)-C(8)-C(9)-C(4)	0.1(3)	C(22)-P(1)-C(16)-C(21)	145.01(18)
C(5)-C(1)-C(2)-C(3)	0.5(2)	C(3)-C(4)-C(9)-C(8)	178.3(2)	C(10)-P(1)-C(16)-C(21)	30.9(2)
P(1)-C(1)-C(2)-C(3)	-174.07(14)	C(5)-C(4)-C(9)-C(8)	-0.3(3)	C(1)-P(1)-C(16)-C(17)	81.0(2)
C(1)-C(2)-C(3)-C(4)	-0.6(2)	C(1)-P(1)-C(10)-C(15)	-3.7(2)	C(22)-P(1)-C(16)-C(17)	-40.9(2)
C(2)-C(3)-C(4)-C(9)	-178.3(2)	C(16)-P(1)-C(10)-C(15)	-124.58(18)	C(10)-P(1)-C(16)-C(17)	-155.05(18)
C(2)-C(3)-C(4)-C(5)	0.5(2)	C(22)-P(1)-C(10)-C(15)	119.30(18)	C(21)-C(16)-C(17)-C(18)	0.6(3)
C(9)-C(4)-C(5)-C(6)	0.3(3)	C(1)-P(1)-C(10)-C(11)	177.71(17)	P(1)-C(16)-C(17)-C(18)	-173.67(18)
C(3)-C(4)-C(5)-C(6)	-178.59(17)	C(16)-P(1)-C(10)-C(11)	56.8(2)	C(16)-C(17)-C(18)-C(19)	-0.6(4)
C(9)-C(4)-C(5)-C(1)	178.76(17)	C(22)-P(1)-C(10)-C(11)	-59.31(19)	C(17)-C(18)-C(19)-C(20)	-0.6(4)
C(3)-C(4)-C(5)-C(1)	-0.2(2)	C(15)-C(10)-C(11)-C(12)	0.9(3)	C(18)-C(19)-C(20)-C(21)	2.0(4)
C(2)-C(1)-C(5)-C(6)	177.9(2)	P(1)-C(10)-C(11)-C(12)	179.49(18)	C(19)-C(20)-C(21)-C(16)	-2.0(3)
P(1)-C(1)-C(5)-C(6)	-7.8(3)	C(10)-C(11)-C(12)-C(13)	-1.4(4)	C(17)-C(16)-C(21)-C(20)	0.8(3)
C(2)-C(1)-C(5)-C(4)	-0.2(2)	C(11)-C(12)-C(13)-C(14)	0.5(4)	P(1)-C(16)-C(21)-C(20)	174.88(17)

Figure 9. The molecular structure of **VII**.

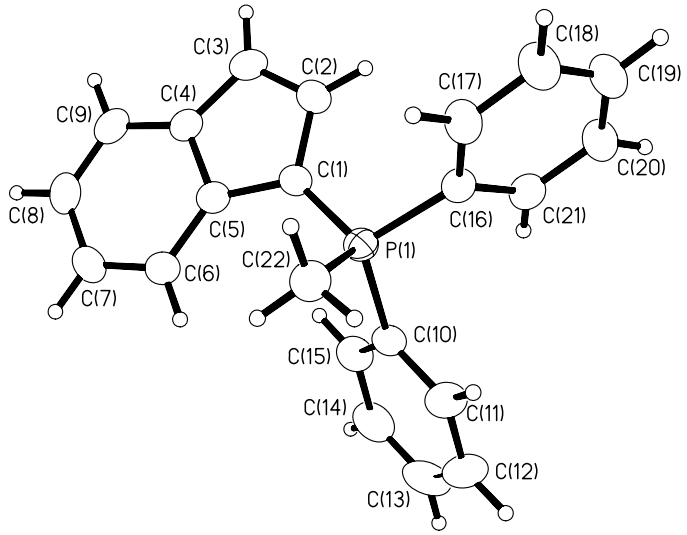

Table 55. Crystal data and structure refinement for **VIII**.

Identification code	**VIII**	
Empirical formula	C25.50 H20 Cl Cr O3 P	
Formula weight	492.84	
Temperature	180(2) K	
Wavelength	0.71073 Å	
Crystal system	Orthorhombic	
Space group	Pna2(1)	
Unit cell dimensions	a = 15.7408(18) Å	α= 90°.
	b = 18.114(2) Å	β= 90°.
	c = 8.5337(10) Å	γ = 90°.
Volume	2433.2(5) $Å^3$	
Z	4	
Density (calculated)	1.345 Mg/m^3	
Absorption coefficient	0.669 mm^{-1}	
F(000)	1012	
Crystal size	0.35 x 0.15 x 0.04 mm^3	
Theta range for data collection	2.25 to 21.75°.	
Index ranges	-16<=h<=16, -18<=k<=18, -8<=l<=8	
Reflections collected	15526	
Independent reflections	2863 [R(int) = 0.0601]	
Completeness to theta = 21.75°	99.7 %	
Absorption correction	Multi-scan	
Max. and min. transmission	0.9737 and 0.7995	
Refinement method	Full-matrix least-squares on F^2	
Data / restraints / parameters	2863 / 1 / 271	
Goodness-of-fit on F^2	1.000	
Final R indices [I>2sigma(I)]	R1 = 0.0421, wR2 = 0.0981	
R indices (all data)	R1 = 0.0528, wR2 = 0.1037	
Absolute structure parameter	0.06(4)	
Largest diff. peak and hole	0.295 and -0.227 $e.Å^{-3}$	

Table 56. Atomic coordinates (x 10^4) and equivalent isotropic displacement parameters ($Å^2$x 10^3) for **VIII**. U(eq) is defined as one third of the trace of the orthogonalized U^{ij} tensor.

	x	y	z	U(eq)
Cr(1)	13686(1)	1976(1)	17324(1)	31(1)
P(1)	12866(1)	2644(1)	20840(2)	31(1)

O(1)	14401(3)	1362(2)	14368(5)	50(1)
O(2)	15315(3)	2593(2)	18522(5)	62(1)
O(3)	13516(3)	3406(2)	15646(5)	59(1)
C(1)	12908(3)	1944(3)	19423(6)	32(1)
C(2)	12371(3)	1932(3)	18053(6)	35(1)
C(3)	12531(3)	1294(3)	17203(8)	39(1)
C(4)	13146(3)	872(3)	18044(6)	35(1)
C(5)	13375(3)	1247(3)	19422(6)	30(1)
C(6)	13988(3)	938(3)	20434(6)	36(1)
C(7)	14317(3)	260(3)	20115(7)	43(1)
C(8)	14081(3)	-125(3)	18771(8)	46(2)
C(9)	13507(3)	157(3)	17730(6)	43(2)
C(10)	12579(3)	3487(3)	19903(6)	34(1)
C(11)	13178(4)	3985(3)	19425(8)	60(2)
C(12)	12956(5)	4625(4)	18660(9)	70(2)
C(13)	12133(5)	4753(4)	18325(8)	69(2)
C(14)	11506(4)	4269(4)	18771(8)	57(2)
C(15)	11729(4)	3635(3)	19570(6)	42(2)
C(16)	12068(3)	2441(3)	22279(7)	31(1)
C(17)	11608(3)	1787(3)	22207(9)	48(2)
C(18)	10997(4)	1626(4)	23297(7)	53(2)
C(19)	10840(4)	2129(4)	24496(7)	51(2)
C(20)	11298(4)	2765(4)	24590(7)	49(2)
C(21)	11899(4)	2924(3)	23468(7)	43(2)
C(22)	13852(3)	2768(3)	21827(7)	42(2)
C(23)	14141(4)	1601(3)	15542(7)	40(1)
C(24)	14680(4)	2340(3)	18060(6)	43(1)
C(25)	13558(3)	2847(3)	16312(6)	36(1)

Table 57. Bond lengths [Å] and angles [°] for **VIII**.

Cr(1)-C(24)	1.810(6)	C(25)-Cr(1)-C(23)	88.3(2)	C(1)-C(2)-Cr(1)	70.8(3)
Cr(1)-C(25)	1.810(6)	C(24)-Cr(1)-C(2)	137.8(2)	C(2)-C(3)-C(4)	107.9(5)
Cr(1)-C(23)	1.813(7)	C(25)-Cr(1)-C(2)	93.6(2)	C(2)-C(3)-Cr(1)	70.0(3)
Cr(1)-C(2)	2.163(5)	C(23)-Cr(1)-C(2)	127.3(2)	C(4)-C(3)-Cr(1)	73.6(3)
Cr(1)-C(1)	2.170(5)	C(24)-Cr(1)-C(1)	102.2(2)	C(5)-C(4)-C(3)	109.6(5)
Cr(1)-C(3)	2.201(5)	C(25)-Cr(1)-C(1)	110.7(2)	C(5)-C(4)-C(9)	119.3(5)
Cr(1)-C(4)	2.259(5)	C(23)-Cr(1)-C(1)	154.8(2)	C(3)-C(4)-C(9)	131.1(5)
Cr(1)-C(5)	2.278(5)	C(2)-Cr(1)-C(1)	38.90(19)	C(5)-C(4)-Cr(1)	72.7(3)
P(1)-C(1)	1.753(5)	C(24)-Cr(1)-C(3)	159.2(2)	C(3)-C(4)-Cr(1)	69.1(3)
P(1)-C(22)	1.781(5)	C(25)-Cr(1)-C(3)	112.0(2)	C(9)-C(4)-Cr(1)	126.7(4)
P(1)-C(10)	1.782(5)	C(23)-Cr(1)-C(3)	94.4(2)	C(4)-C(5)-C(6)	119.8(5)
P(1)-C(16)	1.794(5)	C(2)-Cr(1)-C(3)	37.06(19)	C(4)-C(5)-C(1)	106.8(4)
O(1)-C(23)	1.166(6)	C(1)-Cr(1)-C(3)	63.7(2)	C(6)-C(5)-C(1)	133.3(5)
O(2)-C(24)	1.168(7)	C(24)-Cr(1)-C(4)	123.6(2)	C(4)-C(5)-Cr(1)	71.2(3)
O(3)-C(25)	1.162(6)	C(25)-Cr(1)-C(4)	149.3(2)	C(6)-C(5)-Cr(1)	124.3(4)
C(1)-C(2)	1.443(7)	C(23)-Cr(1)-C(4)	92.6(2)	C(1)-C(5)-Cr(1)	66.9(3)
C(1)-C(5)	1.461(7)	C(2)-Cr(1)-C(4)	61.88(19)	C(7)-C(6)-C(5)	119.7(5)
C(2)-C(3)	1.387(7)	C(1)-Cr(1)-C(4)	62.56(19)	C(6)-C(7)-C(8)	121.1(5)
C(3)-C(4)	1.427(7)	C(3)-Cr(1)-C(4)	37.30(19)	C(9)-C(8)-C(7)	121.6(5)
C(4)-C(5)	1.405(7)	C(24)-Cr(1)-C(5)	97.1(2)	C(8)-C(9)-C(4)	118.5(5)
C(4)-C(9)	1.439(7)	C(25)-Cr(1)-C(5)	148.9(2)	C(11)-C(10)-C(15)	118.4(5)
C(5)-C(6)	1.410(7)	C(23)-Cr(1)-C(5)	121.8(2)	C(11)-C(10)-P(1)	121.6(5)
C(6)-C(7)	1.360(7)	C(2)-Cr(1)-C(5)	63.07(19)	C(15)-C(10)-P(1)	120.0(4)
C(7)-C(8)	1.394(8)	C(1)-Cr(1)-C(5)	38.25(18)	C(10)-C(11)-C(12)	121.4(6)
C(8)-C(9)	1.366(7)	C(3)-Cr(1)-C(5)	62.2(2)	C(13)-C(12)-C(11)	119.4(7)
C(10)-C(11)	1.368(8)	C(4)-Cr(1)-C(5)	36.08(18)	C(12)-C(13)-C(14)	121.5(6)
C(10)-C(15)	1.393(7)	C(1)-P(1)-C(22)	112.6(2)	C(13)-C(14)-C(15)	119.0(6)

C(11)-C(12)	1.376(8)	C(1)-P(1)-C(10)	108.7(2)	C(14)-C(15)-C(10)	120.3(6)
C(12)-C(13)	1.346(9)	C(22)-P(1)-C(10)	109.0(3)	C(21)-C(16)-C(17)	118.5(5)
C(13)-C(14)	1.374(9)	C(1)-P(1)-C(16)	110.5(2)	C(21)-C(16)-P(1)	120.9(4)
C(14)-C(15)	1.381(8)	C(22)-P(1)-C(16)	108.2(3)	C(17)-C(16)-P(1)	120.6(4)
C(16)-C(21)	1.366(7)	C(10)-P(1)-C(16)	107.8(2)	C(18)-C(17)-C(16)	121.2(6)
C(16)-C(17)	1.390(7)	C(2)-C(1)-C(5)	106.4(4)	C(17)-C(18)-C(19)	119.0(6)
C(17)-C(18)	1.369(9)	C(2)-C(1)-P(1)	123.1(4)	C(20)-C(19)-C(18)	120.3(6)
C(18)-C(19)	1.392(8)	C(5)-C(1)-P(1)	130.2(4)	C(19)-C(20)-C(21)	120.0(6)
C(19)-C(20)	1.360(8)	C(2)-C(1)-Cr(1)	70.3(3)	C(16)-C(21)-C(20)	121.1(5)
C(20)-C(21)	1.377(8)	C(5)-C(1)-Cr(1)	74.9(3)	O(1)-C(23)-Cr(1)	177.2(5)
		P(1)-C(1)-Cr(1)	124.8(3)	O(2)-C(24)-Cr(1)	178.2(5)
C(24)-Cr(1)-C(25)	86.8(2)	C(3)-C(2)-C(1)	109.3(5)	O(3)-C(25)-Cr(1)	176.8(5)
C(24)-Cr(1)-C(23)	94.9(2)	C(3)-C(2)-Cr(1)	73.0(3)		

Table 58. Anisotropic displacement parameters ($Å^2 x\ 10^3$)for **VIII**. The anisotropic displacement factor exponent takes the form: $-2\pi^2[\ h^2a^{*2}U^{11} + ... + 2\ h\ k\ a^*\ b^*\ U^{12}\ ]$

	U^{11}	U^{22}	U^{33}	U^{23}	U^{13}	U^{12}
Cr(1)	28(1)	44(1)	22(1)	5(1)	2(1)	5(1)
P(1)	29(1)	40(1)	24(1)	0(1)	1(1)	2(1)
O(1)	60(3)	57(3)	34(3)	1(2)	16(2)	11(2)
O(2)	33(2)	95(3)	59(3)	19(3)	-5(2)	-13(2)
O(3)	78(3)	46(3)	54(3)	19(3)	-7(2)	2(2)
C(1)	22(3)	37(3)	36(3)	2(3)	-2(3)	-3(2)
C(2)	26(3)	48(4)	30(3)	0(3)	0(3)	5(2)
C(3)	35(3)	51(3)	32(3)	-9(3)	9(3)	5(3)
C(4)	33(3)	34(3)	36(3)	-1(3)	6(3)	0(3)
C(5)	25(3)	36(3)	30(3)	-2(3)	9(3)	-3(3)
C(6)	35(3)	51(4)	23(3)	8(3)	2(3)	1(3)
C(7)	40(3)	51(4)	36(4)	11(3)	5(3)	9(3)
C(8)	42(4)	43(4)	53(4)	11(3)	13(3)	11(3)
C(9)	56(4)	40(4)	34(4)	-5(3)	11(3)	1(3)
C(10)	46(4)	37(3)	18(3)	1(3)	-5(3)	3(3)
C(11)	51(4)	54(4)	74(5)	21(4)	-8(4)	-11(3)
C(12)	90(6)	59(5)	63(5)	29(4)	-6(4)	-7(4)
C(13)	103(6)	53(4)	52(4)	7(4)	-8(5)	31(5)
C(14)	57(4)	68(4)	45(4)	5(4)	-7(3)	24(4)
C(15)	40(4)	53(4)	34(4)	-2(3)	-1(3)	4(3)
C(16)	28(3)	42(3)	22(3)	-1(3)	3(3)	4(2)
C(17)	43(3)	48(3)	52(4)	-2(4)	22(4)	1(3)
C(18)	55(4)	58(4)	46(4)	6(3)	22(3)	-7(3)
C(19)	41(4)	74(5)	37(4)	11(4)	16(3)	16(4)
C(20)	43(4)	68(5)	34(4)	-8(3)	10(3)	10(3)
C(21)	52(4)	47(4)	32(4)	-3(3)	-2(3)	3(3)
C(22)	38(3)	45(3)	42(4)	1(3)	-4(3)	0(3)
C(23)	45(4)	43(3)	33(4)	8(3)	-1(3)	4(3)
C(24)	38(4)	63(4)	26(3)	13(3)	3(3)	2(3)
C(25)	38(3)	51(4)	20(3)	-2(3)	-7(3)	2(3)

Table 59. Hydrogen coordinates ($x\ 10^4$) and isotropic displacement parameters ($Å^2 x\ 10^3$) for **VIII**.

	x	y	z	U(eq)
H(2A)	11928	2309	17793	42
H(3A)	12231	1138	16225	47
H(6A)	14171	1203	21334	44
H(7A)	14713	46	20820	51
H(8A)	14325	-596	18573	55
H(9A)	13350	-112	16820	52
H(11A)	13761	3887	19625	72
H(12A)	13378	4974	18371	84
H(13A)	11982	5187	17767	83
H(14A)	10927	4369	18534	68
H(15A)	11301	3298	19895	51
H(17A)	11719	1446	21387	57

H(18A)	10685	1178	23237	63
H(19A)	10412	2028	25251	61
H(20A)	11202	3099	25431	58
H(21A)	12202	3377	23523	52
H(22A)	14297	2880	21060	62
H(22B)	13999	2315	22394	62
H(22C)	13803	3178	22571	62

Table 60. Torsion angles [°] for **VIII**.

C(22)-P(1)-C(1)-C(2)	-152.6(4)	C(5)-Cr(1)-C(3)-C(4)	-35.3(3)	C(4)-Cr(1)-C(5)-C(1)	-118.5(4)
C(10)-P(1)-C(1)-C(2)	-31.8(5)	C(2)-C(3)-C(4)-C(5)	-0.2(6)	C(4)-C(5)-C(6)-C(7)	-3.8(8)
C(16)-P(1)-C(1)-C(2)	86.3(5)	Cr(1)-C(3)-C(4)-C(5)	61.7(4)	C(1)-C(5)-C(6)-C(7)	-179.9(5)
C(22)-P(1)-C(1)-C(5)	35.2(5)	C(2)-C(3)-C(4)-C(9)	177.0(5)	Cr(1)-C(5)-C(6)-C(7)	-90.4(6)
C(10)-P(1)-C(1)-C(5)	156.0(5)	Cr(1)-C(3)-C(4)-C(9)	-121.0(6)	C(5)-C(6)-C(7)-C(8)	2.4(8)
C(16)-P(1)-C(1)-C(5)	-85.9(5)	C(2)-C(3)-C(4)-Cr(1)	-62.0(4)	C(6)-C(7)-C(8)-C(9)	-0.6(8)
C(22)-P(1)-C(1)-Cr(1)	-64.7(4)	C(24)-Cr(1)-C(4)-C(5)	48.8(4)	C(7)-C(8)-C(9)-C(4)	0.2(8)
C(10)-P(1)-C(1)-Cr(1)	56.1(4)	C(25)-Cr(1)-C(4)-C(5)	-122.5(4)	C(5)-C(4)-C(9)-C(8)	-1.6(7)
C(16)-P(1)-C(1)-Cr(1)	174.2(3)	C(23)-Cr(1)-C(4)-C(5)	146.4(3)	C(3)-C(4)-C(9)-C(8)	-178.7(5)
C(24)-Cr(1)-C(1)-C(2)	159.9(3)	C(2)-Cr(1)-C(4)-C(5)	-82.0(3)	Cr(1)-C(4)-C(9)-C(8)	87.9(6)
C(25)-Cr(1)-C(1)-C(2)	68.7(4)	C(1)-Cr(1)-C(4)-C(5)	-37.8(3)	C(1)-P(1)-C(10)-C(11)	-95.4(5)
C(23)-Cr(1)-C(1)-C(2)	-68.3(6)	C(3)-Cr(1)-C(4)-C(5)	-119.7(4)	C(22)-P(1)-C(10)-C(11)	27.6(6)
C(3)-Cr(1)-C(1)-C(2)	-36.3(3)	C(24)-Cr(1)-C(4)-C(3)	168.4(3)	C(16)-P(1)-C(10)-C(11)	144.7(5)
C(4)-Cr(1)-C(1)-C(2)	-78.3(3)	C(25)-Cr(1)-C(4)-C(3)	-2.8(6)	C(1)-P(1)-C(10)-C(15)	81.3(5)
C(5)-Cr(1)-C(1)-C(2)	-114.0(4)	C(23)-Cr(1)-C(4)-C(3)	-93.9(4)	C(22)-P(1)-C(10)-C(15)	-155.7(4)
C(24)-Cr(1)-C(1)-C(5)	-86.1(3)	C(2)-Cr(1)-C(4)-C(3)	37.7(3)	C(16)-P(1)-C(10)-C(15)	-38.5(5)
C(25)-Cr(1)-C(1)-C(5)	-177.3(3)	C(1)-Cr(1)-C(4)-C(3)	81.9(3)	C(15)-C(10)-C(11)-C(12)	1.2(9)
C(23)-Cr(1)-C(1)-C(5)	45.7(6)	C(5)-Cr(1)-C(4)-C(3)	119.7(4)	P(1)-C(10)-C(11)-C(12)	178.0(5)
C(2)-Cr(1)-C(1)-C(5)	114.0(4)	C(24)-Cr(1)-C(4)-C(9)	-65.2(5)	C(10)-C(11)-C(12)-C(13)	-2.4(11)
C(3)-Cr(1)-C(1)-C(5)	77.7(3)	C(25)-Cr(1)-C(4)-C(9)	123.5(5)	C(11)-C(12)-C(13)-C(14)	2.0(11)
C(4)-Cr(1)-C(1)-C(5)	35.7(3)	C(23)-Cr(1)-C(4)-C(9)	32.4(5)	C(12)-C(13)-C(14)-C(15)	-0.5(10)
C(24)-Cr(1)-C(1)-P(1)	42.7(4)	C(2)-Cr(1)-C(4)-C(9)	164.0(5)	C(13)-C(14)-C(15)-C(10)	-0.6(9)
C(25)-Cr(1)-C(1)-P(1)	-48.5(4)	C(1)-Cr(1)-C(4)-C(9)	-151.8(5)	C(11)-C(10)-C(15)-C(14)	0.3(8)
C(23)-Cr(1)-C(1)-P(1)	174.4(4)	C(3)-Cr(1)-C(4)-C(9)	126.3(6)	P(1)-C(10)-C(15)-C(14)	-176.6(4)
C(2)-Cr(1)-C(1)-P(1)	-117.3(5)	C(5)-Cr(1)-C(4)-C(9)	-114.0(6)	C(1)-P(1)-C(16)-C(21)	-177.6(4)
C(3)-Cr(1)-C(1)-P(1)	-153.6(4)	C(3)-C(4)-C(5)-C(6)	-179.0(5)	C(22)-P(1)-C(16)-C(21)	58.7(5)
C(4)-Cr(1)-C(1)-P(1)	164.4(4)	C(9)-C(4)-C(5)-C(6)	3.4(7)	C(10)-P(1)-C(16)-C(21)	-59.0(5)
C(5)-Cr(1)-C(1)-P(1)	128.7(5)	Cr(1)-C(4)-C(5)-C(6)	-119.5(5)	C(1)-P(1)-C(16)-C(17)	2.5(5)
C(5)-C(1)-C(2)-C(3)	-3.5(6)	C(3)-C(4)-C(5)-C(1)	-1.9(6)	C(22)-P(1)-C(16)-C(17)	-121.2(5)
P(1)-C(1)-C(2)-C(3)	-177.4(4)	C(9)-C(4)-C(5)-C(1)	-179.6(4)	C(10)-P(1)-C(16)-C(17)	121.1(5)
Cr(1)-C(1)-C(2)-C(3)	63.3(4)	Cr(1)-C(4)-C(5)-C(1)	57.6(3)	C(21)-C(16)-C(17)-C(18)	0.1(9)
C(5)-C(1)-C(2)-Cr(1)	-66.8(3)	C(3)-C(4)-C(5)-Cr(1)	-59.5(4)	P(1)-C(16)-C(17)-C(18)	-180.0(5)
P(1)-C(1)-C(2)-Cr(1)	119.4(4)	C(9)-C(4)-C(5)-Cr(1)	122.8(5)	C(16)-C(17)-C(18)-C(19)	-0.1(10)
C(24)-Cr(1)-C(2)-C(3)	-148.1(4)	C(2)-C(1)-C(5)-C(4)	3.3(5)	C(17)-C(18)-C(19)-C(20)	-1.0(9)
C(25)-Cr(1)-C(2)-C(3)	122.7(4)	P(1)-C(1)-C(5)-C(4)	176.5(4)	C(18)-C(19)-C(20)-C(21)	2.2(9)
C(23)-Cr(1)-C(2)-C(3)	32.1(4)	Cr(1)-C(1)-C(5)-C(4)	-60.4(3)	C(17)-C(16)-C(21)-C(20)	1.1(8)
C(1)-Cr(1)-C(2)-C(3)	-118.1(5)	C(2)-C(1)-C(5)-C(6)	179.8(6)	P(1)-C(16)-C(21)-C(20)	-178.9(4)
C(4)-Cr(1)-C(2)-C(3)	-37.9(3)	P(1)-C(1)-C(5)-C(6)	-7.0(9)	C(19)-C(20)-C(21)-C(16)	-2.2(9)
C(5)-Cr(1)-C(2)-C(3)	-78.8(4)	Cr(1)-C(1)-C(5)-C(6)	116.1(6)	C(24)-Cr(1)-C(23)-O(1)	-154(10)
C(24)-Cr(1)-C(2)-C(1)	-30.0(5)	C(2)-C(1)-C(5)-Cr(1)	63.6(3)	C(25)-Cr(1)-C(23)-O(1)	-68(10)
C(25)-Cr(1)-C(2)-C(1)	-119.2(3)	P(1)-C(1)-C(5)-Cr(1)	-123.1(4)	C(2)-Cr(1)-C(23)-O(1)	26(10)

C(23)-Cr(1)-C(2)-C(1)	150.2(3)	C(24)-Cr(1)-C(5)-C(4)	-140.9(3)	C(1)-Cr(1)-C(23)-O(1)	73(10)
C(3)-Cr(1)-C(2)-C(1)	118.1(5)	C(25)-Cr(1)-C(5)-C(4)	123.4(4)	C(3)-Cr(1)-C(23)-O(1)	44(10)
C(4)-Cr(1)-C(2)-C(1)	80.2(3)	C(23)-Cr(1)-C(5)-C(4)	-40.5(4)	C(4)-Cr(1)-C(23)-O(1)	82(10)
C(5)-Cr(1)-C(2)-C(1)	39.4(3)	C(2)-Cr(1)-C(5)-C(4)	78.4(3)	C(5)-Cr(1)-C(23)-O(1)	104(10)
C(1)-C(2)-C(3)-C(4)	2.4(6)	C(1)-Cr(1)-C(5)-C(4)	118.5(4)	C(25)-Cr(1)-C(24)-O(2)	14(16)
Cr(1)-C(2)-C(3)-C(4)	64.3(4)	C(3)-Cr(1)-C(5)-C(4)	36.5(3)	C(23)-Cr(1)-C(24)-O(2)	103(16)
C(1)-C(2)-C(3)-Cr(1)	-61.9(4)	C(24)-Cr(1)-C(5)-C(6)	-27.1(5)	C(2)-Cr(1)-C(24)-O(2)	-77(16)
C(24)-Cr(1)-C(3)-C(2)	88.6(7)	C(25)-Cr(1)-C(5)-C(6)	-122.8(5)	C(1)-Cr(1)-C(24)-O(2)	-96(16)
C(25)-Cr(1)-C(3)-C(2)	-65.0(4)	C(23)-Cr(1)-C(5)-C(6)	73.3(5)	C(3)-Cr(1)-C(24)-O(2)	-141(16)
C(23)-Cr(1)-C(3)-C(2)	-154.9(4)	C(2)-Cr(1)-C(5)-C(6)	-167.8(5)	C(4)-Cr(1)-C(24)-O(2)	-161(16)
C(1)-Cr(1)-C(3)-C(2)	38.1(3)	C(1)-Cr(1)-C(5)-C(6)	-127.7(6)	C(5)-Cr(1)-C(24)-O(2)	-135(16)
C(4)-Cr(1)-C(3)-C(2)	116.6(5)	C(3)-Cr(1)-C(5)-C(6)	150.3(5)	C(24)-Cr(1)-C(25)-O(3)	40(8)
C(5)-Cr(1)-C(3)-C(2)	81.3(4)	C(4)-Cr(1)-C(5)-C(6)	113.8(6)	C(23)-Cr(1)-C(25)-O(3)	-55(8)
C(24)-Cr(1)-C(3)-C(4)	-28.0(8)	C(24)-Cr(1)-C(5)-C(1)	100.7(3)	C(2)-Cr(1)-C(25)-O(3)	178(100)
C(25)-Cr(1)-C(3)-C(4)	178.5(3)	C(25)-Cr(1)-C(5)-C(1)	4.9(5)	C(1)-Cr(1)-C(25)-O(3)	142(8)
C(23)-Cr(1)-C(3)-C(4)	88.5(3)	C(23)-Cr(1)-C(5)-C(1)	-159.0(3)	C(3)-Cr(1)-C(25)-O(3)	-149(8)
C(2)-Cr(1)-C(3)-C(4)	-116.6(5)	C(2)-Cr(1)-C(5)-C(1)	-40.0(3)	C(4)-Cr(1)-C(25)-O(3)	-147(8)
C(1)-Cr(1)-C(3)-C(4)	-78.5(3)	C(3)-Cr(1)-C(5)-C(1)	-82.0(3)	C(5)-Cr(1)-C(25)-O(3)	139(8)

Figure 10. The molecular structure of **VIII**.